UNIVERSITÀ
DEGLI STUDI
DI PADOVA

Sede Amministrativa: Università degli Studi di Padova

Dipartimento di Ingegneria Civile, Edile ed Ambientale

SCUOLA DI DOTTORATO DI RICERCA IN:
STUDIO E CONSERVAZIONE DEI BENI ARCHEOLOGICI E ARCHITETTONICI

CICLO XXVII

Seismic Behaviour of Post-Installed Anchors: Non-Structural Components and Art Objects Fastening

Direttore della Scuola
Ch.mo Prof. Giuseppe Salemi

Supervisore
Ch.mo Prof. Claudio Modena

Dottorando
Ing. Marco Abate

ABSTRACT

The damage observation in recent seismic events (L'Aquila 2009, Chile 2010, Christchurch 2011, Tohoku 2011, Emilia 2012) helps in the identification of the critical aspects related to the response to earthquake of non-structural components (Miranda et al. 2012). Generally these elements are included in buildings and may belong to the architectural system, to the utility system or to the building content. The failure of the non-structural components can represent a significant danger for life safety and leads to relevant economic losses and this also contributes in amounting to a severe impact for the society (Miranda et al. 2012).

This thesis contains the results of an experimental campaign which had the aim of evaluating different typologies of post-installed anchors under seismic actions.

The mentioned topic is considered of importance for the central role of these devices in anchoring non-structural elements in order to avoid failures and damages which can cause danger for life safety, huge economic loss and lack of functionality in a building after an earthquake occurs. (Taghavi and Miranda 2003; ATC 69 2008).

During an earthquake the non-structural components should withstand to relevant inertial forces, transferred through the connection to the structural elements (beams, slabs, columns, walls) or often to other non-structural elements, such as infill walls. In many cases those connections are realized by means of post-installed anchors which should be designed properly in order to ensure a good behaviour to the seismic actions (Makris and Black 2001; Naumoski et al. 2002; Solomos and Berra 2006; Hoehler et al. 2011). Among all the requirements the reliability in terms of failure modes and strength of post-installed anchors results to be fundamental to obtain a valid design in the dynamic field. For instance the design of fire protection systems in schools, medical equipment in hospitals, masterpieces displayed in museums need an in-depth knowledge on the performance of anchors to use. Such knowledge should cover both the resistance for life safety limit state and the admissible displacements that allow the element functionality for serviceability limit state.

The purpose of the experimental campaign presented within this research is to study the seismic behaviour of various anchoring systems through shaking table tests.

Two cross-shaped structures were built at full scale, one consisted of concrete walls and one of a RC framed structure with masonry infill panels. Two different conditions were investigated in the case of fasteners installed in concrete, namely non-cracked and cracked support. Poroton® hollow bricks were used to build the specimen with masonry infill walls.

Tri-axial shaking table tests were designed on the basis of the standard AC156 (2010) which provides a test setup for the seismic certification of non-structural components by shaking table tests. The experiments were realized by subsequent signals scaled at a growing ZPA (Zero Period Acceleration) to study the effects induced on the specimens at increasing seismic intensity.

The results allowed the overall seismic behaviour of each fastening element to be investigated, especially in terms of failure mode, maximum sustained acceleration and anchor slippage from support. The influence of cracks on these aspects was also deepened for the concrete structural unit. The test plan also allowed a complete comparison among different anchoring methodologies, such as mechanical, chemical and undercut anchors.

Some recent studies (Rieder 2009; Watkins 2011; Mahrenholtz et al. 2012) focused on the seismic assessment of metal anchors in concrete by means of shake-table testing,

whereas the use of fasteners in masonry and the behaviour of plastic anchors in general were not exhaustively investigated until now (Algin 2007; Sinica et al. 2010). Nevertheless these are two fields of interest because of their widespread presence in constructions. Therefore during the experimental study a particular attention has been paid to the issues of plastic anchors and installations in masonry.

SOMMARIO

L'osservazione del danno nei recenti eventi sismici (L'Aquila 2009, Chile 2010, Christchurch 2011, Tohoku 2011, Emilia 2012) aiuta nell'identificazione delle criticità legate alla risposta al terremoto degli elementi non strutturali (Miranda et al. 2012). Generalmente tali elementi sono parte dei fabbricati e possono appartenere al sistema architettonico, al sistema impiantistico o al contenuto. La rottura degli elementi non strutturali può rappresentare un pericolo rilevante per la salvaguardia della vita umana e porta perdite di grande valore, nonché contribuisce all'impatto gravoso del sisma per la società (Miranda et al. 2012).

Questa tesi contiene i risultati di una campagna sperimentale di ricerca che si poneva lo scopo di valutare diverse tipologie di ancoranti post installati sotto azione sismica.

L'argomento appena menzionato è considerato di grande importanza per il ruolo centrale di questi dispositivi nell'ancoraggio di elementi non strutturali per evitare rotture e danneggiamenti che possano causare pericolo per le persone, grosse perdite economiche e interruzione dell'operatività di un edificio nelle settimane o mesi nel seguito di un terremoto (Taghavi and Miranda 2003; ATC 69 2008).

Durante un terremoto gli elementi non strutturali dovrebbero resistere ad elevate forze d'inerzia, trasferite attraverso la connessione agli elementi strutturali (travi, solai, pilastri, pareti) o spesso ad altri elementi non strutturali, come le pareti di tamponamento. In molti casi questi punti di connessione sono realizzati con l'uso di ancoranti post installati i quali dovrebbero essere adeguatamente progettati per assicurare un buon comportamento alle azioni sismiche (Makris and Black 2001; Naumoski et al. 2002; Solomos and Berra 2006; Hoehler et al. 2011). Tra tutti i requisiti, quello della affidabilità in termini di modalità di rottura e valore di resistenza risulta fondamentale per ottenere un progetto degli ancoranti post installati che sia valido in campo dinamico. Ad esempio, progetti di sistemi antincendio nelle scuole, di attrezzature mediche negli ospedali, di oggetti d'arte esposti nei musei necessitano di una buona conoscenza della prestazione dei sistemi di ancoraggio da impiegare. Tale conoscenza deve coprire sia la resistenza, per lo stato limite di salvaguardia della vita (SLV), che gli spostamenti in grado di permettere la funzionalità dell'elemento non strutturale, per lo stato limite di esercizio (SLE).

Lo scopo della campagna sperimentale presentata all'interno di questo lavoro di ricerca è lo studio del comportamento sismico di diversi sistemi di ancoraggio attraverso prove su tavola vibrante.

Due strutture con pianta a croce sono state costruite a scala reale, una consisteva di pareti in calcestruzzo e una di un telaio in calcestruzzo armato con pareti di tamponamento in muratura. Due condizioni differenti sono state studiate nel caso di ancoranti installati in calcestruzzo, ovvero supporto non fessurato e fessurato. Mattoni forati Poroton® sono stati utilizzati per costruire il campione con pareti di tamponamento in muratura.

Le prove triassiali sono state progettate sulla base dello standard AC156 (2010) che fornisce delle impostazioni di prova per la certificazione sismica di elementi non strutturali da prove su tavola vibrante. Gli esperimenti sono stati realizzati con l'applicazione alla

tavola di segnali scalati a ZPA (Zero Period Acceleration) crescenti per studiare gli effetti indotti sui campioni all'aumentare dell'intensità dell'azione sismica.

I risultati hanno permesso di studiare il comportamento sismico generale di ciacun fissaggio, specialmente in termini di modalità di rottura, massimo carico dinamico sopportato e sfilamento del campione dal supporto.

Anche l'influenza delle fessure per questi parametri è stata aprofondita per l'unità strutturale di calcestruzzo. Il programma di prova ha anche permesso un confronto completo tra diverse metodologie di ancoraggio, come gli ancoranti ad espansione, chimici o a sottosquadro.

Recenti studi (Rieder 2009; Watkins 2011; Mahrenholtz et al. 2012) si sono concentrati sulla valutazione sismica di ancoranti metallici in calcestruzzo attraverso prove su tavola vibrante, invece il comportamento di sistemi di fissaggio impiegati in muratura e di ancoranti plastici in generale non sono stati investigati in modo esaustivo fino ad ora (Algin 2007; Sinica et al. 2010). Ciononostante queste applicazioni appena citate sono di elevato interesse per la loro presenza diffusa nelle costruzioni. Quindi durante lo studio sperimentale una particolare attenzione è stata data alle questioni riguardanti gli ancoranti plastici e le installazioni in muratura.

ACKNOWLEDGEMENTS

First and foremost I want to thank my advisor Professor Claudio Modena. It has been an honour to be his doctoral candidate. It has been always illuminating to deal with such a great brilliant and professional person. I am particularly grateful to him for allowing me to grow as a research scientist as well as an independent professional at the same time. By means of his example he taught me important expertise as setting priority objectives and overachieving in working and life. My greatest and sincere gratitude goes to post-doctoral fellow, eng. Nicola Mazzon, who patiently and wisely look after my experimental and analytic work. His preparation, constancy, attention to detail and terrific methodology have sure allowed me to become a more independent researcher and a better professional. No doubt on that. Beyond the scientific mate, Nicola has been also a great person to spend time with, some of the experiences we passed through I am sure I will never forget for the rest of my life. I would also like to thank Ass. Prof. Francesca da Porto and eng. Matteo Panizza, inside the Department of Civil, Environmental and Architectural Engineering. The former for having inspired and pushed me to work hardly following a personal passion and the latter for the having always helped me in solving formal and technical problems.

In addition to that I want to express my gratitude ITW Construction Products Italy srl for having entrusted me with great responsibility and confidence. I am also grateful for the possibility I have always received patiently by ITW to care about all the complex aspects of a doctoral training programme. I appreciated it so much. In particular I would like to thank the persons -and great professionals- of Simone, Michele and Andrea Santini.

I would also like to mention that I am thankful to a couple of research professionals, namely Prof. Lucia Regolin and Andrea Berti, who I had the pleasure to work with dealing with some inspiring projects. They contributed to make me find my way.

My most intense thoughts go to my family as they have always supported me following my experience from the right distance, closer in times of troubles further as I needed more space. Mostly I am thankful to my parents for having taught me the right values, which have been essential to make me overcome a doctoral path. My mother has showed me in her life how to face troubles with unbelievable strength and dignity. My father provided me with intellectual coherence and a fine sense of humour. My brother, as in all of my life main events, has played a fundamental role, namely making me prioritize my needs and my duties.

Finally the best, I want to thank Eli for the joy she has brought into my life and for the support to my choices she has always demonstrated.

Marco Abate
Pordenone, December 2014

CONTENTS

LIST OF TABLES

LIST OF FIGURES

FOREWORD: PROJECT EXPLANATION

The work presented in this document is included in a wider research project as a result of a partnership between the Department of Civil, Environmental and Architectural Engineering at University of Padua and the manufacturing company ITW Construction Products Italy srl. The main objective of this experimental study related to an Industrial Doctoral programme is to carry out a Research and Development project able to bring knowledge and innovation in both scientific community and private company in a sensitive field as is earthquake engineering. The study focuses on the seismic behaviour of post-installed anchors with regards to the installation of non-structural elements. Applicative cases on relevant non-structural elements are also presented. The reliability of the connection of these elements highly affects the safety of a built environment and their strength influences the functionality of strategic buildings.

Therefore this research programme should be seen as part of an applicative industrial project in which also technical and commercial issues are addressed. The scientific research represents the core of the project since it can have provided so far the company with remarkable outcomes on how its products may behave when a seismic event occurs. Hence the research allowed an increased knowledge to be achieved and technical suggestions in new product development and prototyping to be collected and put into practice. The activity of comparison with the thresholds given by relevant seismic assessment standards allowed to deepen and anticipate the product compliance from one side and to refer to recognized technical benchmarks from the other.

It is clear how the investments in the experimental research within the industrial project can lead to innovation in the particular field of post-installed anchors for use in seismic hazard regions. The higher specific requirements which came out in the study reflect in a better performance of future products. Besides thanks to the experimental discoveries a correct support in using the current available products is also an asset to be taken into account.

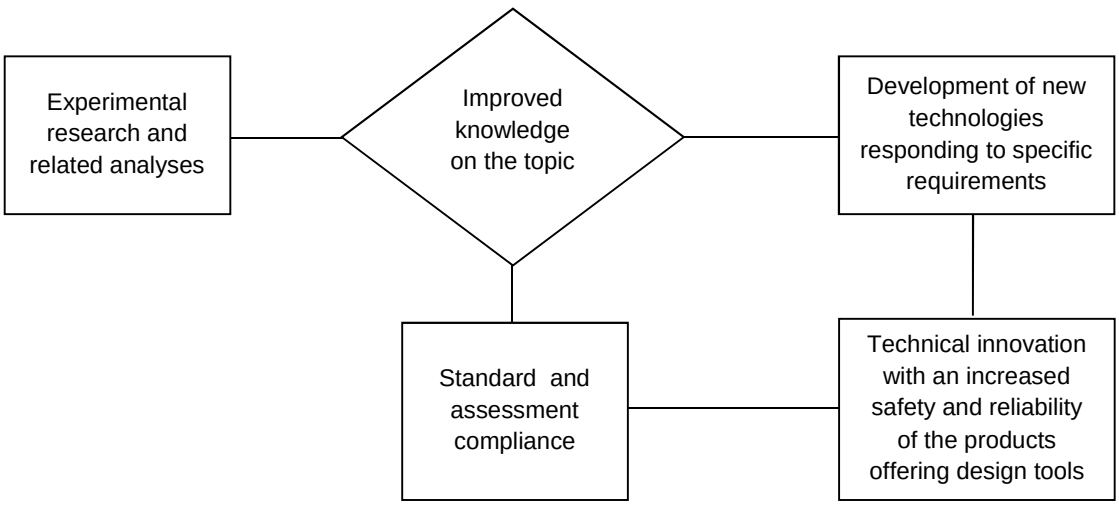

Figure 0.1 The methodology of the industrial project

According to the collected information on the use of post-installed anchors in seismic application and the relevant codes and guidelines, the current research has been developed within fields of application not covered by any regulation and by the scientific literature so far. From the very beginning plastic anchors in all base materials and anchors in masonry installations were the main focus of this work. Nevertheless also other common anchor typologies and base materials were investigated within the experimental campaign.

This document, as well as the work that is presented within, follows a subsequent order of explanation starting from the seismic characterisation of the anchoring system passing through a data processing and finally to the study of applicative cases of importance. In the following the contents of the various sections are briefly presented in order to make the thesis structure clear.

Chapter §1 contains a state-of-art related to the behaviour of both anchoring systems and non-structural elements under seismic actions. For the latter aspect a particular attention has been given to components of strategic buildings such as art objects and fire safety equipment.

After the mentioned introductive section the core of the experimental study is presented, where the chosen methodology of the seismic characterisation for post-installed anchors and the experiments are described. In particular the work of designing the test setup and the structural units is reported in §2 as well as the definition of the synthetic input signal and the features of the shake-table testing system.

The two subsequent chapters present the execution of the experimental campaign distinguished for the base material of the structural unit walls. Section §3 deals with the testing of specimens installed in concrete, cracked and non-cracked, and section §4 deals with the testing of specimens installed in lightweight brick masonry. In the presentation of the experimental part also the instrumentation, the testing plan, the experimental observations and the captured data processing are widely reported. In the respective section also the test results for both the structural units are shown in these chapters.

In chapter §5 the outcomes of the shake-table testing campaign are summarized in order to highlight the data used when studying an applicative case such as the anchoring of a non-structural element which might undergo seismic actions. Relevant applicative case studies are also included in this part of the document. In particular the two following deepening paragraphs focus on applications considered critical and of high importance, namely art objects and fire safety equipment. It is presented how post-installed anchors are involved to ensure a reduction of damage from earthquakes for such strategic buildings, respectively like museums and school or hospitals.

A conclusive chapter reports the remarks for each aspect faced in the research project as the seismic characterisation of the anchors, the experimental procedure and the case studies. The future developments also for the industrial project are presented then.

The aim of the work is to develop the matter of anchoring systems in order to flank the knowledge of specific topics to construction products manufacturing, in the case of this project the behaviour under seismic actions. An improvement in the development of product and useful information on the performance of the already existing ones are researched. As a consequence of such a research there is the objective to make the built environment more safe and to reduce the damages to buildings and the related costs.

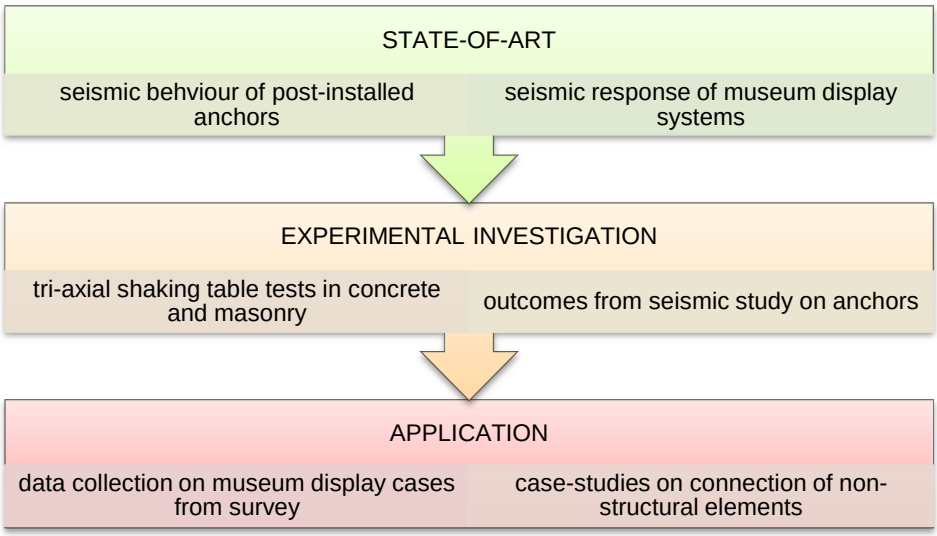

Figure 0.2 Outline structure of the thesis work

There are various possibilities to deepen the study on the seismic application of both light-duty and heavy-duty fastenings. A particular attention is required for the study of the behaviour of these systems during an earthquake. From past seismic events life safety can be jeopardized also for damages to non-structural elements or even pieces of furniture. Latest anchoring systems cover the needs of new additional technical requirements as the use under fatigue loading, the cracked concrete condition and the design under seismic actions. For the future reliable and economic solutions with the above mentioned directions are to be developed.

The general scope of the work of research is to find outcomes and new knowledge out of the assessment procedures according to existing standards. For this reason an experimental campaign on shaking table with a realistic configuration was carried out in order to observe the behaviour of non-structural elements attached to different supports.

1. STATE-OF-ART

In this chapter a state-of-art of fastening for non-structural elements under seismic actions is reported. To do so means that indications both on the seismic behaviour of post-installed anchors and on seismic response of non-structural elements should be collected and analysed before starting an experimental programme in that field.

1.1. SEISMIC APPLICATION OF POST-INSTALLED ANCHORS

The anchorage is a complex system which includes interactions between at least three types of different materials, the base material consists of the support element to which the load is wanted to be transferred from the fixture by means of the connection made by a single post-installed anchor or a group of anchors. Therefore the anchor duty is to transfer the load from a relatively deformable material, that is steel, to a low deformability material, namely concrete or masonry.

The function of anchors, especially those for non-structural application, was often left out from the scientific literature and the worldwide technical standards. Nevertheless it is becoming more and more recognized the importance given to fasteners since a large use of these connectors is done within the construction of new buildings. As an example one can think about the anchorages of curtain walls and claddings, for internal stairs, traditional systems of lighting, electrical and mechanical equipment. Post-installed anchors are used in any type of civil construction and their reliability and performance are needed to know for a correct design. For a good result in the wide use of such construction products a collaboration between the interested figures, namely the manufacturer, the designer and the end-user, is also needed. This kind of cooperation takes place through a continue communication between the three players allowing the installed fastening to be done with the best quality. In particular the manufacturer is in charge of the quality and the efficiency of the products, the professional indicates the right fastener for each application through the knowledge of design methods and finally the end-user has to ensure a correct installation of the product, according to what declared by the manufacturer. Various companies manufacture different typologies of anchoring systems and since their installation and performance products can vary largely it is of importance to face the design according to the technical standards and to realize the installation following the recommendations provided by the manufacturer.

1.1.1. Anchor Typologies

A large variety of anchor types has been developed by manufacturers to meet several different needs of constructors, normative bodies and designers. Nevertheless with the current demand of attributing such systems to common regulations in order to proof the

functionality and the quality, it is convenient to subdivide the anchors into various classifications.

There are different parameters to take into account in order to classify the fastening systems. The most common ways to distinguish them are according to the application field, whether it is structural or non-structural, the installation technique, the load transfer principle, the adaptation to specific base materials, the constitutive material. In the following paragraph some of them are presented.

A first subdivision among fastenings can be done according to the mode they transfer the load from the fixture to the base material. Generally there are three possible mechanisms, namely mechanical interlock, friction and bond. A fastening system can work by one of the following mechanisms or a combination of these.

Mechanical interlock means a direct exchange of tensions between anchor and base material surfaces when a part of the anchor has a shape so that the slipping is prevented. Besides the anchor works by friction whether its geometry is able to generate a pressure towards the base material surfaces inside the hole. Such pressure should withstand the load pattern applied to the anchoring point. Finally the fastening by bonding operates through chemical blocking achieved from a reaction between base material, resin and steel stud.

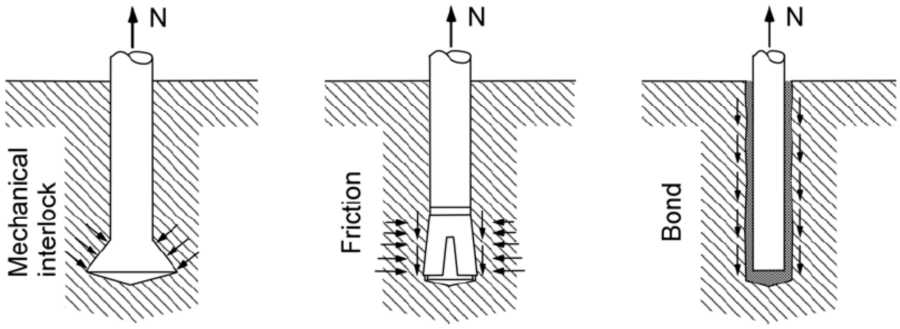

Figure 1.1 Load transfer mechanisms for post-installed anchors (Eligehausen 2006)

In the case of applications in concrete it is possible to differ the anchor depending on the installation timing, namely if that is done previously or after the concrete pouring and curing. The cast-in-place fasteners are ensured to the formwork before the concrete pouring, whereas the post-installed anchors are installed in the hardened material. The cast-in-place anchors have a good performance in cracked and non-cracked concrete. The disadvantages include low flexibility in adjusting the realization from the design stage and the need of an extremely accurate installation. For the above mentioned reasons that type is not so widespread anymore, in favour of the easier and more flexible installation represented by post-installed anchors. The post-installed anchors usually are inserted into a pre-drilled hole subsequently to concrete curing.

As shown in Figure 1.2 the post-installation can be done in-place through the fixture, with a pre-positioned fastener or stand-off at a certain distance from the support surface.

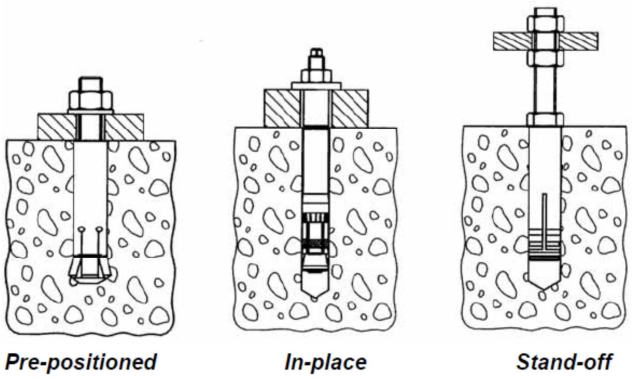

Figure 1.2 Setting configurations for post-installed anchors (Eligehausen 2006)

The post-installed anchors include those working by mechanical expansion, undercut or chemical bond. These anchor typologies are described in the following paragraphs.

Among the anchors with an easy installation, there are those included in the expansion type, working by friction: the expanding element of the anchor (e.g. a sleeve) applies pressure to the hole sides. This type can subdivided into two groups according to their activation method:

- Torque-controlled; in this case the friction is generated through an expansion cone which pushes a sleeve against the hole sides after the application of a tightening torque. In this class a sleeve-type and a bolt-type can be recognized. The former is composed by a screw or a threaded bar with nut and washer, a spacer, an expanding sleeve and a cone at the end. The latter consists of a bolt which has the end shaped as a cone with an expanding clamp just over the final part of the fastener.
  These anchors usually have a sleeve thick enough to transmit efficiently high expanding forces preventing the slipping from the support. Hence they are loaded and fixed as they are installed in the base material allowing a good reserve of expansion and a high tension resistance to be shown.

- Deformation-controlled or displacement-controlled; in this case the friction is activated by the expansion achieved through the insertion of a cone or a stud in a sleeve by means of specific setting tools, a hammer or a screwdriver.
  In these group of anchors the expansion remains constant after the installation, without any reserve. Among the deformation-controlled there can be distinguish the following types:
  cone-down (drop-in)
  shank-down (stud anchor)
  sleeve-down
  sleeve-down (stud version)

  In addition it can be underlined that these anchors are quite sensitive to the setting, in particular attention has to be paid to the drilling precision. Moreover it is not possible to measure the expansion of the anchor while it is installed without breaking it. As a consequence of that generally they are not used for fastening structural elements neither for cracked condition supports. However whether it is properly installed this type can be even more efficacious than the previous one.

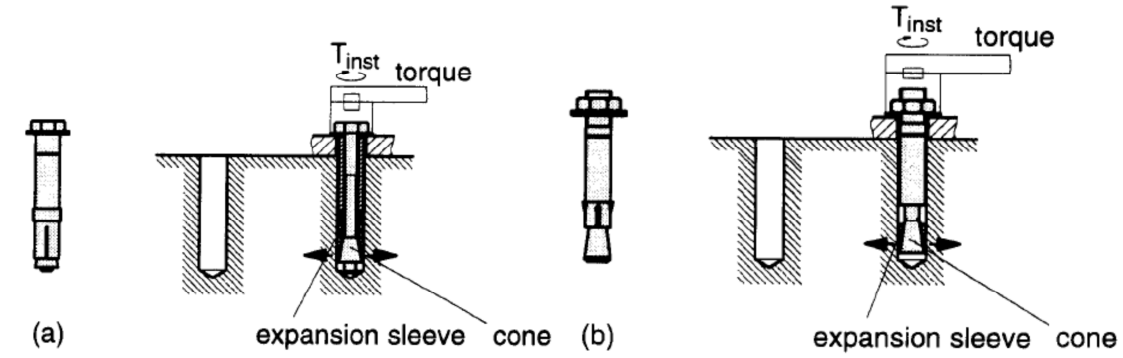

Figure 1.3 (a) Shell-type. (b) Bolt-type. (ETAG 001 2013)

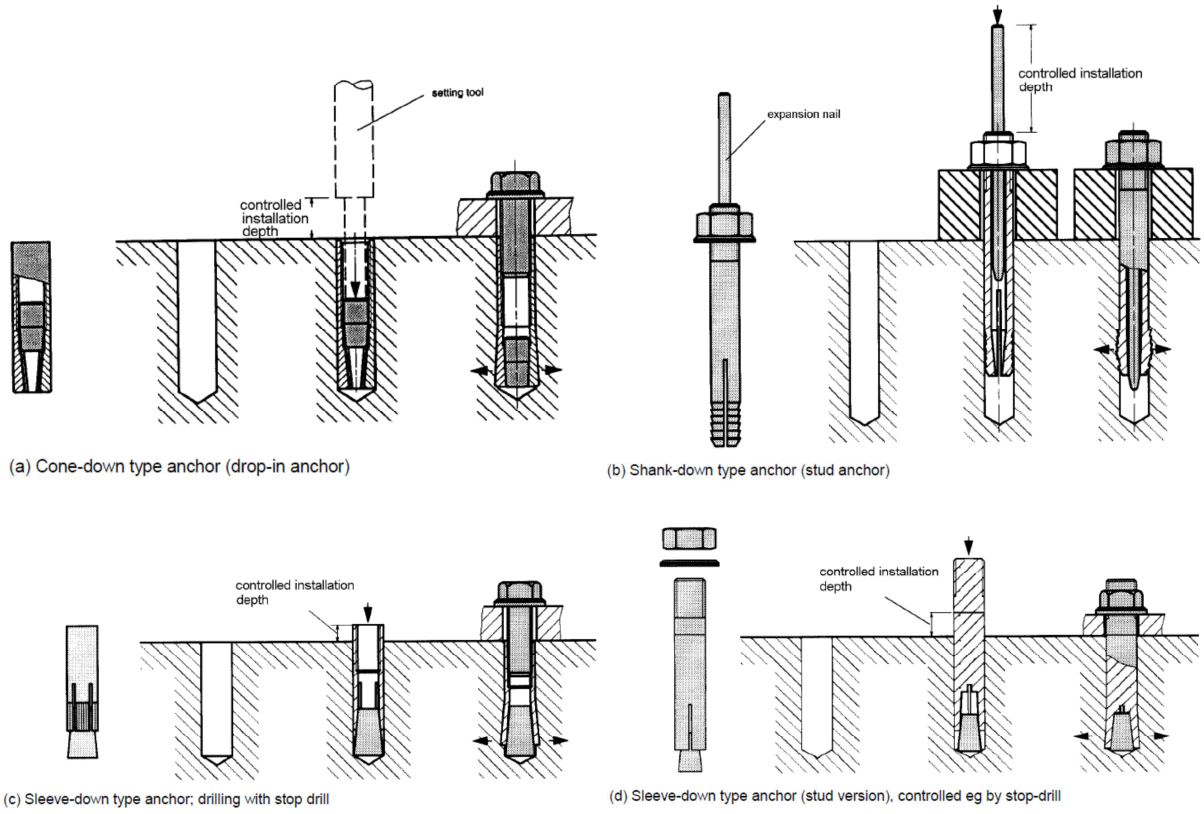

Figure 1.4 Typologies of deformation-controlled expansion anchor (ETAG 001 2013)

Undercut anchors use mechanical interlock by means of an enlargement of the fastener section on the final part of it in order to withstand the loading. The undercut can be obtained with the following techniques.

- Displacement-controlled installations. In one case the undercut can be drilled before the anchor installation and the interlock is made by hammering the sleeve onto the cone, hammering the expansion element into the sleeve or torqueing the nut and pulling the cone inside the sleeve. This type of anchors needs a double drilling.
  Alternatively the undercut can be made during the setting of the anchor, that is cutting the base material in the hole surfaces. For instance self-cutting concrete screws are included in this type of anchors. Installation for this type is easier as for an expansion anchor.
- Torque-controlled installations. A tightening torque is applied to the anchor screwing it into a pre-drilled and shaped hole, the particular sleeve opens against the hole sides inducing mechanical interlock.

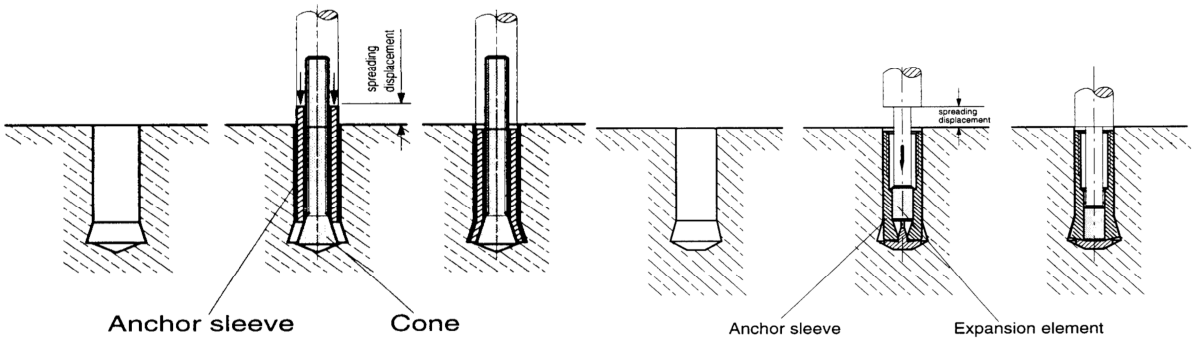

Figure 1.5 Displacement-controlled undercut anchors (technique a), hammering of the anchor onto the cone (left) and in the sleeve (right) (ETAG 001 2013)

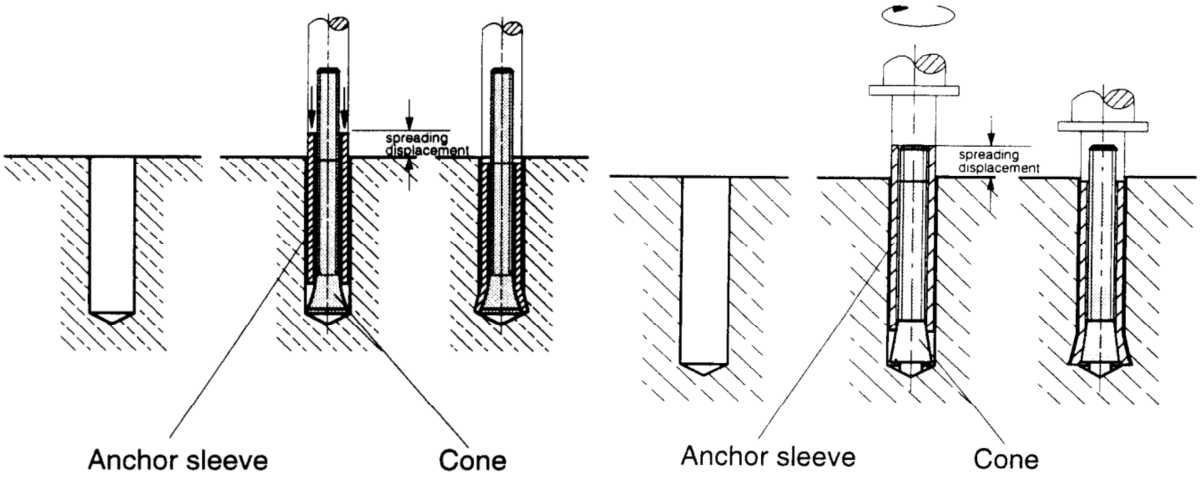

Figure 1.6 Displacement-controlled undercut anchors (technique b), hammering of the sleeve over the cone (left) or application of tightening torque to anchor bolt (ETAG 001 2013)

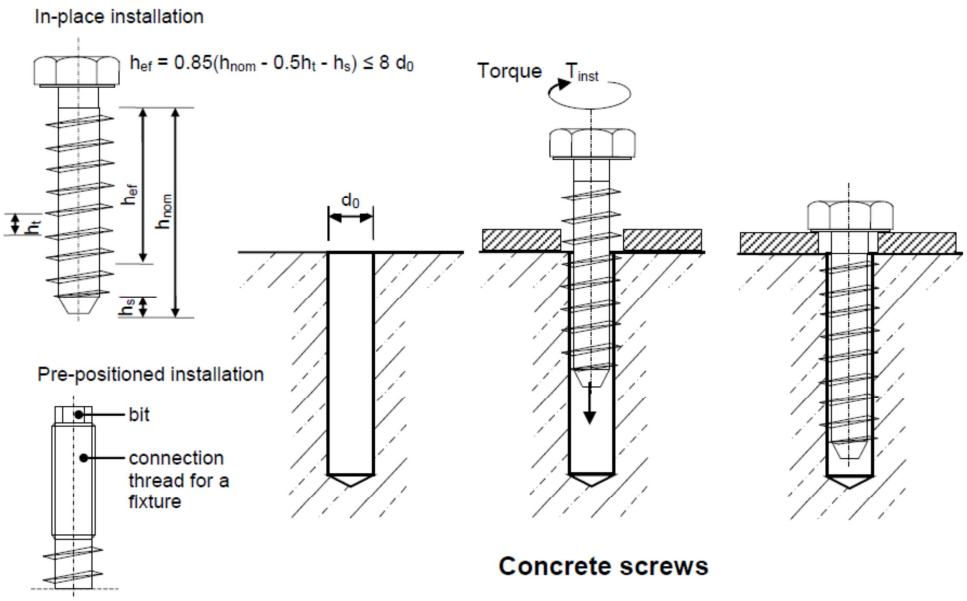

Figure 1.7 Displacement-controlled undercut anchors (technique c), insertion of a special threaded screw cutting the base material (ETAG 001 2013)

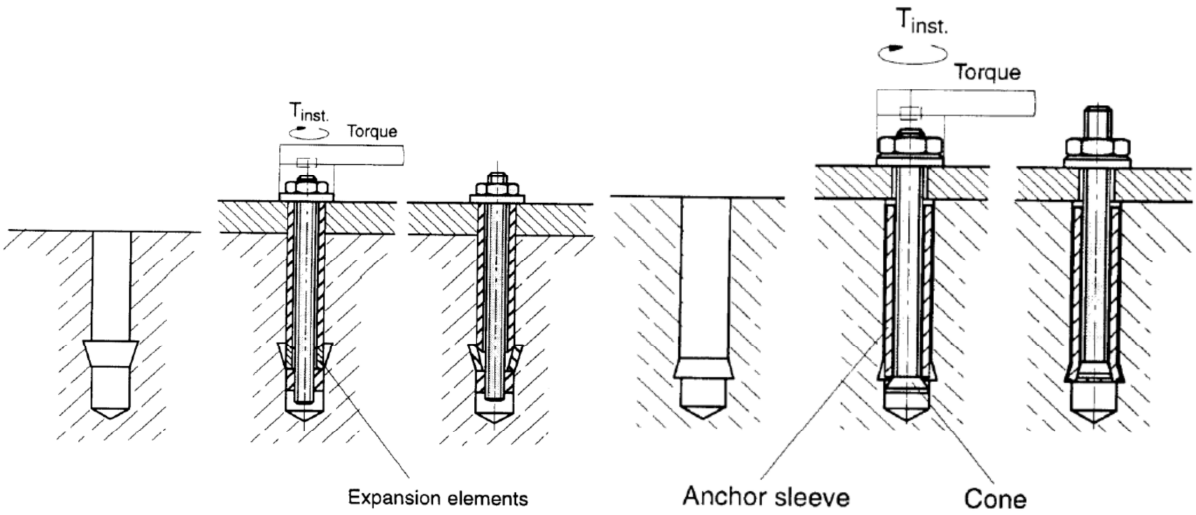

Figure 1.8 Torque-controlled undercut anchors (technique a), opening of the sleeve through the application of a certain tightening torque to the anchor bolt (ETAG 001 2013)

Chemical anchors are set inside drilled holes and fixed by the bonding, obtained through an adhesive mixture, between metal parts and the internal surface of the hole. The axial loading are transferred to the base material through the double interface bar-resin and resin-base material. These anchors are used also in structural elements fastening and are useful in proximity of support edges where the expansion pressure cannot be tolerated. The most important setting phases are the mingling and the hole cleaning. The loading to a chemical anchor can be applied only after the curing time passed, which depends on the resin, the environmental and base material temperature, so that to obtain the highest bonding resistance. Within this category four groups can be distinguished by functioning principle:

- Chemically bonded anchors
- Chemically bonded undercut anchors; there is a combination of adhesion and mechanical interlock.
- Chemically bonded torque-controlled anchors; there is a combination of adhesion and expansion pressure
- Chemically bonded rebars; reinforcement bars to strengthen structures or enlarge them.

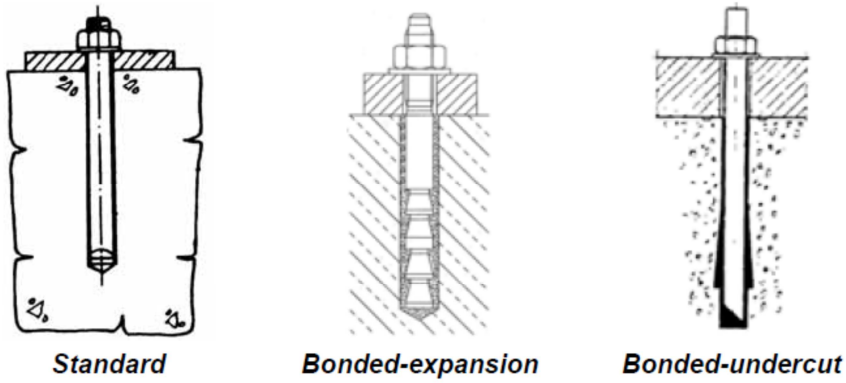

Figure 1.9 Typical chemically bonded metal anchors (Eligehausen 2006)

As adhesive material various chemical blends and cementitious grouts can be used. Chemical resins are not suitable for high temperature applications, while cementitious grout works better in such conditions. Though the latter type needs a longer time to

harden without being loaded. Several setup ways do exist for the blends: breaking a capsule inserted in the hole by directly screwing in the steel bar, injecting from a cartridge before screwing the bar or pouring the bonding material in the hole. With the commonly used method of capsule inserting the resistance value can vary depending on the steel bar type and the hardening can occur faster than the epoxy mixtures.

As regards the resin injection from cartridges, the setting and the curing phases highly depend on the bonding material selected. Epoxy and acrylic are two type examples.

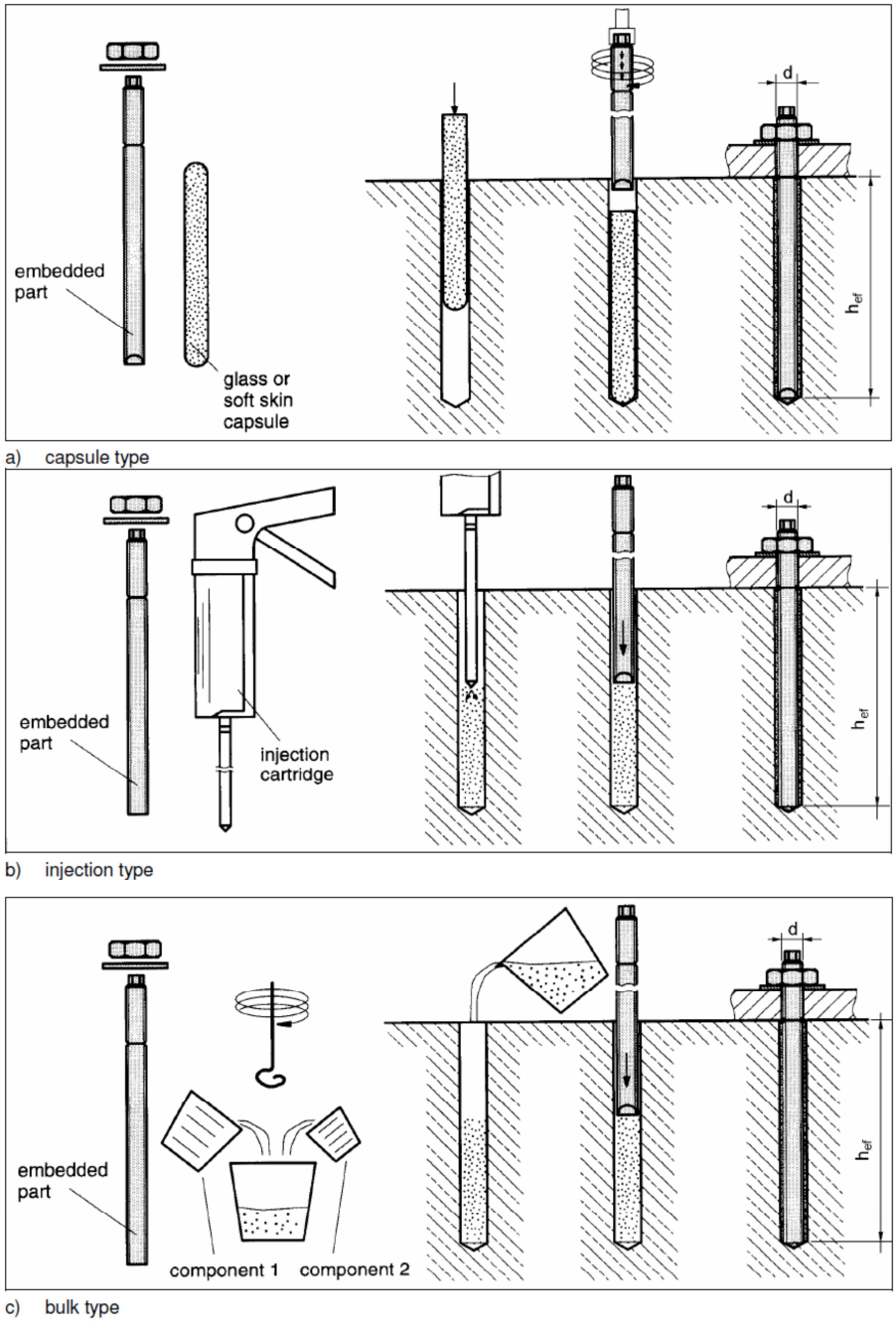

Figure 1.10 Installation methodologies for chemically bonded anchors (ETAG 001 2013)

To conclude the overview on anchor typologies several light-duty fastening systems can be considered. An instance of this class are the plastic expansion anchors which consist of an expansion element, namely a nail or a screw, and a plastic sleeve. These components are of the same length. The expansion, with the consequent pressure on the hole sides, can be achieved through the hammering of a nail or the screwing in of a

screw. The polymeric materials commonly used for the sleeve are the polyamide PA6 and PA6.6, the polyethylene PE or polypropylene PP. The installation of these anchors is generally quick and easy to realize in various base materials.

This class of anchor has a growing importance in the research because it allows the fastening of the building content, i.e. the furniture, and also of the false ceiling and piping equipment.

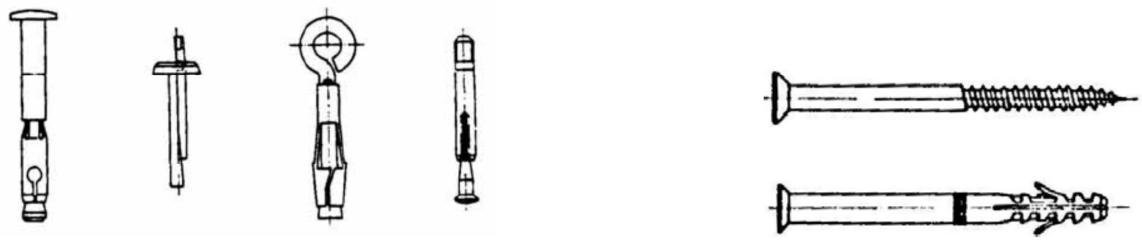

Figure 1.11 Typical light-duty anchors (Eligehausen 2006)

1.1.2. Forces Acting On Anchors And Failure Modes

Load bearing capacity of a heavy-duty anchor is driven by several factors which have to be considered during the design phase. These factors are the base material resistance, the bolt diameter, the embedment depth in the base material, the spacing with adjacent anchors, and the distance from support edges.

The anchoring points, as shown in Figure 1.12, can be subjected to tension, shear, shear combined with tension, bending moment. As a consequence of the above mentioned loading patterns, various failure modes for the fastening systems - which are presented at a later stage - can occur.

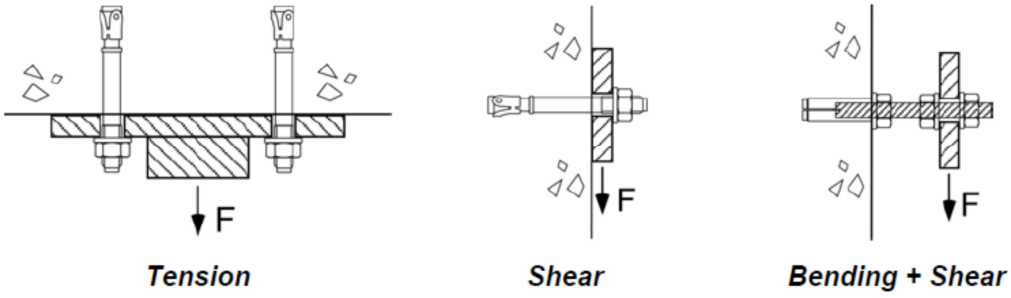

Figure 1.12 Loads acting on fastening systems (Eligehausen 2006)

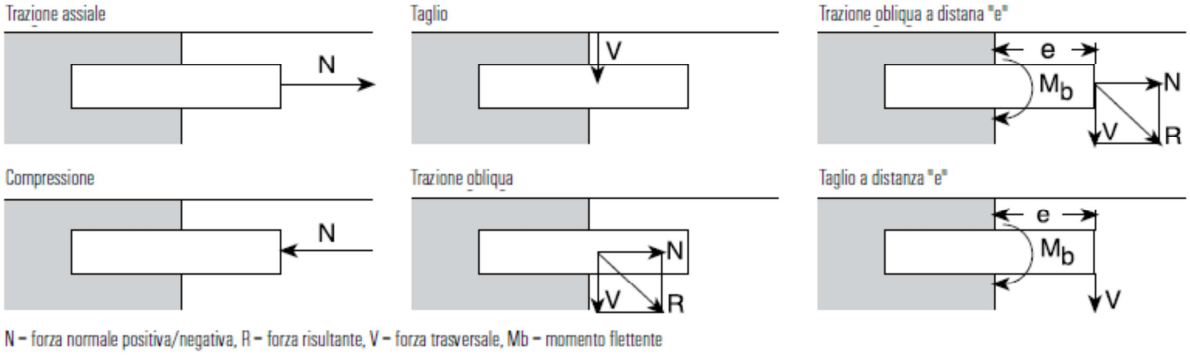

Figure 1.13 Strain types affecting the fastening systems

Anchorage failure modes can be distinguished according to the cause, namely the loading conditions to which the anchoring point is subjected. Factors affecting the failure of a fastening system are the base material features, the material and diameter of the bolts, the spacing between anchors, the distance to support edges, the embedment depth.

As the force acting on the fastening point is mainly represented by tension there can be recognized five general failure modes. The reference for the failure modes is those occurring in the concrete as base material.

- Steel failure; fastening maximum capacity is driven by the failure related to the yielding of the steel of the bolt.
- Pull-out and pull-through; Under tension loading mechanical fasteners can be subjected to the extraction from the hole (pull-out), in the areas where the base material is damaged. This rupture occurs only if the expansion force and the bearing area are enough low, for expansion anchor and undercut anchors respectively. In the pull-out failure the resistance depends on base material compression under the fastener head. The pull-through occurs only for torque-controlled expansion anchors when the expansion cone is pulled through the expanding sleeve.
- Concrete cone failure; the most common failure mode is the expulsion of a concrete cone around the fastening point, though in the case of edges presence the cone is cut by those. According to this failure mode the CCD method can be adopted in order to evaluate the resistance (Fuchs et al. 1995). In group of anchors the expulsion cones of material can overlap. This rupture is the consequence of the low concrete elements resistance to tension actions.
- Splitting of support element; this failure modes can occur when the anchor setting is made in low thickness supports or in the vicinity of support edges.
- Blow-out; in the case of fasteners installed near the edges of a support element can occur that, due to the high pressure applied, a blow-out of base material from the side of the element can be induced.

Concerning the reference failure modes of fastenings under shear loading there can be recognized four types presented in the following.

- Steel failure; the bolt steel failure occurs with damages to the base material in the direction of the shear load.
- Base material failure; if the lateral shear action affects an anchor positioned near edges or a corner of the support element an expulsion of the external base material can occur similarly to the concrete cone failure in tension.
- Pry-out; this failure consists of the expulsion of base material semi cone in the side where the shear action is applied, because of the lever effect induced by the fastener. This type depends on an inadequate embedment depth.
- Pull-out; if the tension strength is not sufficient to withstand the axial component of the shear force a pull-out failure can occur.

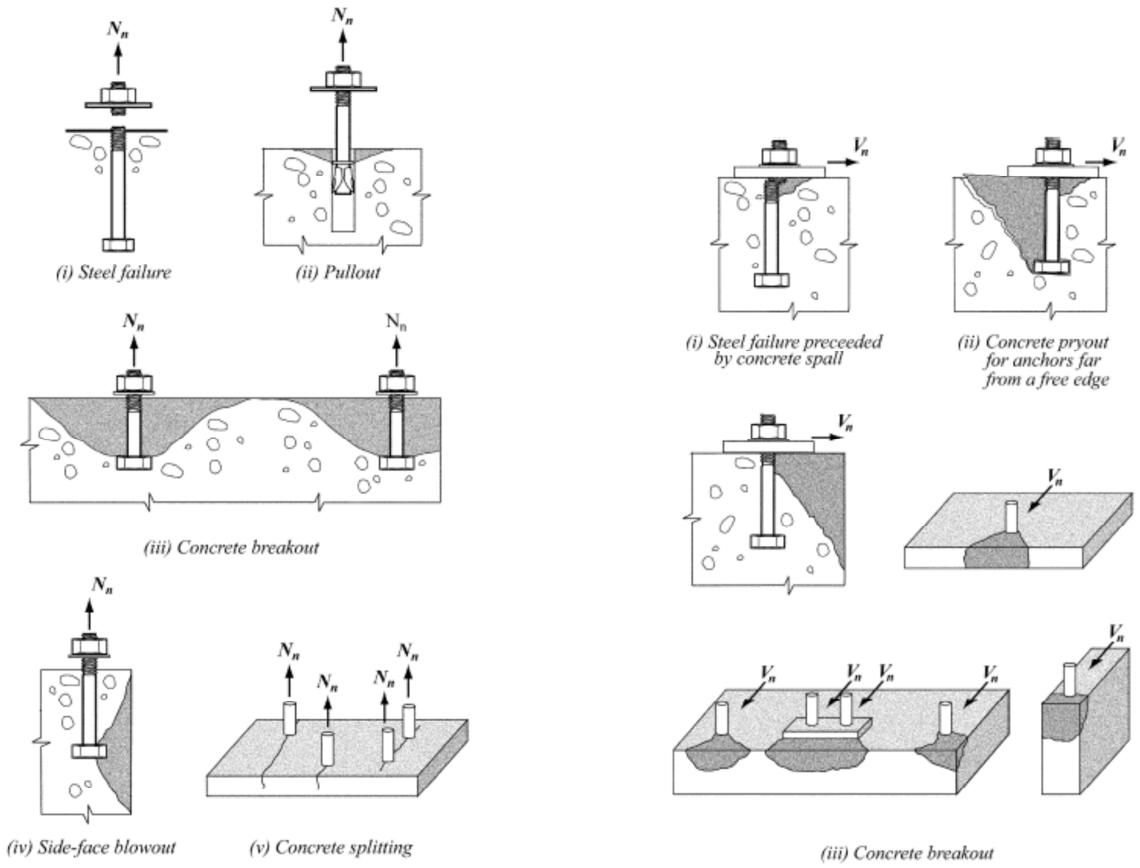

Figure 1.14 Anchors failure modes in concrete under tension (left) and shear loading (right) (ACI 318 2005)

For an evaluation of the static behaviour of the post-installed anchors the load-displacement graphs can be analysed in the cases of both tension and shear actions. In Figure 1.15 the curves under monotonic loading can be observed for tension failure modes. In the failure modes driven by base material, as for pull-out and pull-through failure, after the peak the load decreases. The different curves for pull-out failures correspond to different types of tested anchors, namely expansion deformation-controlled ($a_{1,1}$) and torque-controlled ($a_{1,2}$ and $a_{1,3}$ if the applied pressure is not fully developed during the setting phase), undercut ($a_{1,4}$). From the plots it is clear that base material (i.e. concrete) cone failure and splitting occur at an intermediate stage of loading but with restricted displacements. Whereas the maximum capacity of the fastening system is represented by steel failure in displacements, because of material ductility, and in ultimate load.

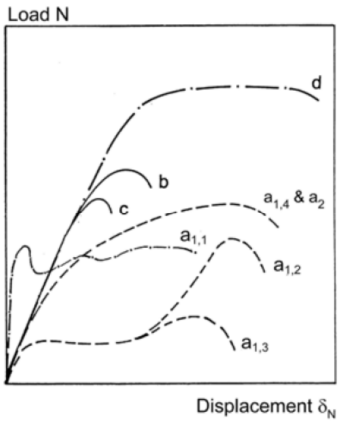

Figure 1.15 Load-displacement graph for tension loading. Failure mode curves: $a_{1,n}$) pull-out; a_2) pull-through; b) concrete cone; c) splitting; d) steel failure (Hoehler 2006)

In the same graph referred to shear actions (Figure 1.16) the displacement values are larger than those obtained for axial load of the same anchor. At first the shear action is transferred from the fixture to base material through friction generated by pre-load. When friction resistance is overtook the fixture slides until the space between anchor and the hole in the fixture. Whether the anchor is embedded deeply in the base material the bolt can withstand up to steel failure. In the case of installation close to support edges the ultimate load is driven by the expulsion of base material in the weak side of the fastening point.

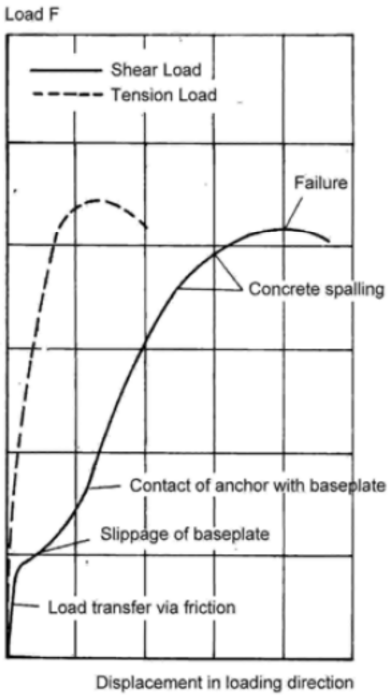

Figure 1.16 Comparison of load-displacements curves for an anchor under shear and tension loading (Hoehler 2006)

For the design of anchoring points in concrete is important to know the relevant differences between cracked and non-cracked conditions. When installed in non-cracked concrete the fastening system works for the balance of the stress allocated radially around its axis. Cracks interrupt the stress transfer towards the surrounding area of anchor installation, jeopardizing the bearing mechanism. Amongst the two different conditions change in stiffness, in ultimate load capacity and failure modes can be observed. Cracks occur diffusely in concrete due to structural response to tension loading and due to deformation shrinkage. If the concrete element has a propensity for cracking it is likely that cracks occur where the anchor installation holes were drilled.

As shown in Figure 1.17 not all the anchors are suitable for the use in cracked concrete with a good response although a reduced performance is expected. The anchor type and the design, the crack position, the applied load and the crack width are all critical factors to determine the influence of cracks in the fastening behaviour. Also in presence of limited crack width (Δw = 0.3mm) many tension tests demonstrated a significant reduction in anchor bearing capacity.

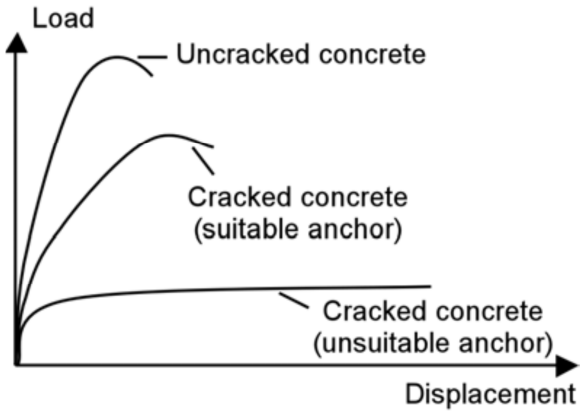

Figure 1.17 Load-displacement plots for a torque-controlled expansion anchor under tension in cracked and non-cracked concrete (Hoehler 2006)

An estimation of crack width in a concrete element is possible to be made, according to Eurocode 2, considering that as a product of calculated crack spacing and the mean difference between steel strain and concrete strain. The key parameters are the reinforcement ratio with respect to concrete area, the number and the diameter of rebars, the neutral axis height, the concrete cover. Generally the factor that affects the most the anchor behaviour is neutral axis height.

A separate issue is the behaviour of plastic anchors in both cracked and non-cracked concrete. Indeed the ultimate resistance to tension and shear for this particular type of anchor, composed by plastic sleeve and complementary steel or plastic screw, is influenced by many factors.

Among these the humidity ratio contained in the polyamide sleeve, the stiffness of the sleeve and temperature at which the installation is realized are important. Typically the humidity ratio contained in hygroscopic plastic anchors in stable conditions (23°C – 50% RH) is on the average of 2.5%. The increase of absorbed humidity can lead to reduction of stiffness for the engineering plastics, resulting in a decrease of ultimate bearable load. On the contrary, the decrease of humidity in the anchor leads to a rise in the stiffness and a consequent increase in the strength. Also the stiffness of the plastic used to manufacture the sleeve influences the global resistance of the anchoring system. Softer materials, like polyethylene, show lower maximum loads than more rigid materials, like polyamide. A similar effect is brought by thermal variations. An increase in temperature causes a drop in strength, while a decrease in temperature results in a rise of ultimate bearable load.

Concerning cracked concrete opening and closing cracks within a range of 0.1 and 0.2mm do not represent a critical issue for plastic anchors.

A building can respond to horizontal actions as a frame which represents a brittle system or a ductile system. In a brittle system as in Figure 1.18 displacements occurring to the structure in only one storey are too large to be withstood given the weight of upper storeys. Displacements are not distributed among all building storeys, but they are fully absorbed by the first level with only four points of rotation and therefore of energy dissipation, namely plastic hinges.

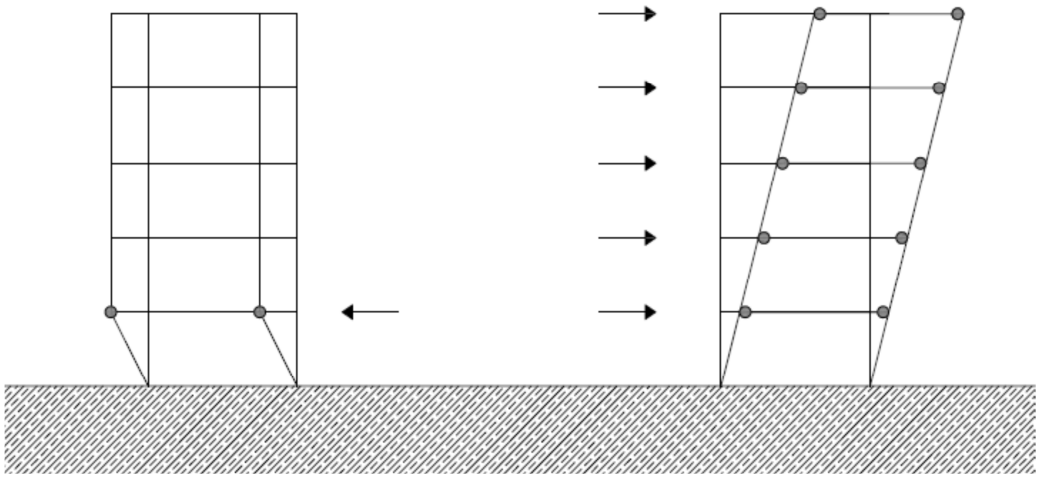

Figure 1.18 Difference in a brittle (left) or ductile (right) seismic response of a building structure

If the building responded to earthquake with a perfect elastic behaviour that would continue rocking to infinity. Energy dissipators are necessary in order to damp the motion. Such behaviour is ensured if some parts of the structure assume a plastic attitude allowing local rotations, and small displacements, which if added together let the structure withstand the seismic acceleration.

On the basis of ductility class chosen by the designer a ductile structural behaviour can be ensured allowing large deformations and displacements without collapse occurrence. In that way human life is protected, but after a seismic event even of small intensity, the structure may face widespread damages and the building has to be demolish or rehabilitate. That is the reason why ductility class selection is also an economic issue which involves the client and the contractor.

Plastic hinges are to be designed to occur on the beam ends and not on the columns in order to avoid structure collapse. The designer indeed should oversize the columns increasing the reinforcement stirrups in the vicinity of the node. The ductile attitude of the steel, greater than concrete's, has to be used.

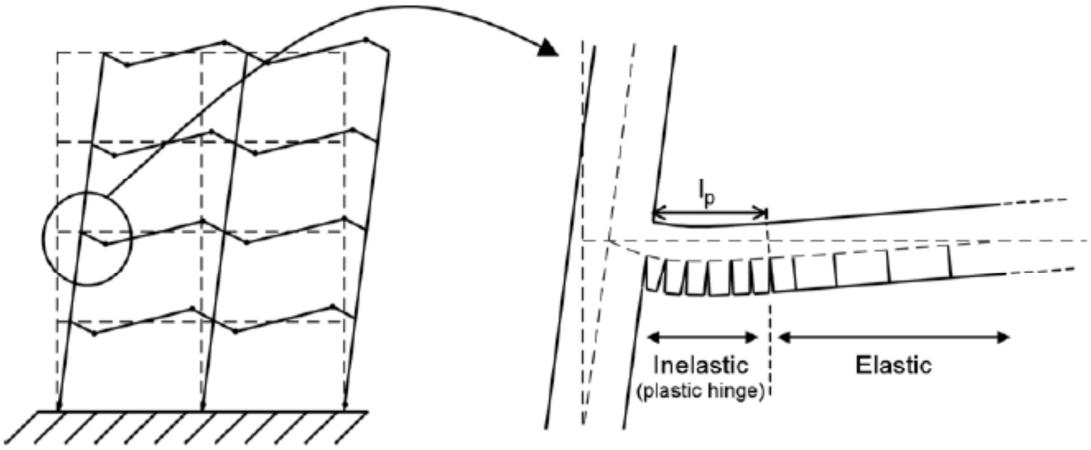

Figure 1.19 Structural mechanism to dissipate the energy related to horizontal motion through the beam deformation close to the node; l_p = plastic hinge length (Hoehler 2006)

The structural factor q, included between 1.5 and 6, is an index of the ductility capacity of a structure and represents the value to divide the design seismic action, considered in terms of acceleration. Hence the value of q depends only by the structure type and can vary by four times the effects of the design seismic action on a building. That factor is given according to building typologies, materials, nodes and joints realization.

Connections at this point become of high importance in order to provide the structural node with a ductile behaviour. For instance in the case of industrial structures built with pre-cast elements the connections are realized through fastening systems. Through the anchorage properties and the quality of nodes installation, the structural factor q can be of 1.5, 2 or 2.5 leading to more or less expensive works.

Different type of actions can affect the building and the civil engineering. Actions can be static, if constant, or dynamic if vary in time. The remarkable difference between the two mentioned loading conditions is the presence of inertial and damping forces in the latter case. Earthquakes generate variable transient dynamic actions, as shown in Figure 1.20.

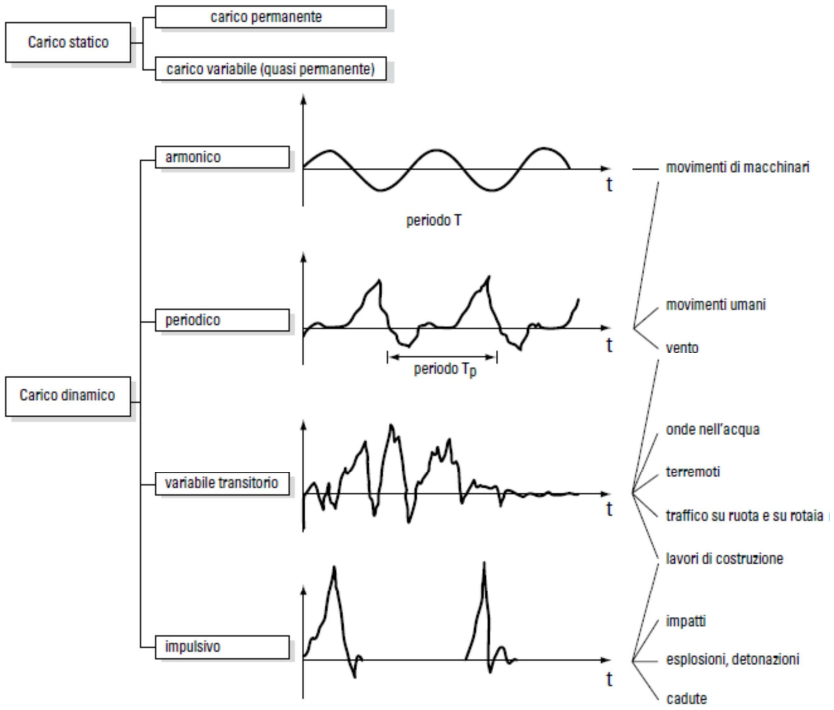

Figure 1.20 Classification of action types according to period intensity

Seismic events generate actions, with a strong demand of horizontal resistance and displacements, in building structural and non-structural elements. Many factors contribute to that process as a direct ground acceleration transfer, soil liquefaction with foundation differential subsidence, lateral and vertical displacements in the vicinity of fracture lines. In the structural design the acceleration of the building, induced by ground motion, is taken into account.

Seismic actions vary in time and are classified as dynamic forces. Differently from quasi static actions, in which the load varies slowly and inertial forces and damping can be neglected, seismic actions vary quickly and cannot be considered piecewise constant. Axial or shear dynamic forces can be considered pulsating or alternate. For axial forces there can be only pulsating tension in tension or in compression.

The main cause for anchoring system failure is the deformation imposed by such a severe type of action, since many fasteners are not developed to withstand large deformations. Therefore it is necessary to focus on the responses of the different types of anchor and their proper functioning in particular conditions as the hole enlargement is.

During an earthquake the acceleration diffuses from the ground, through the foundations, to the structure. These dynamic inputs bring as a consequence various

responses of structural frame according to event characteristics (i.e. magnitude, frequency, duration), the interface soil-structure and the dynamic properties of the structure. With the seismic action a fastening system is subjected to a combination of cyclic tension and shear forces. Moreover it is likely that the anchor is located close to an existing crack or a crack opened by the ongoing quake. Typically the crack width vary during the earthquake, namely it closes and opens many times as a result of the displacement of the structural elements where the anchor is installed.

According to the state-of-art literature the seismic behaviour of fastening systems depends on several parameters, presented in the following.

- The amplitude, the sequence and the number of cycles of seismic actions, the applied forces direction, namely whether one among shear and tension is prevalent.
- The presence of cracks in surrounding base material, the crack movement during the earthquake, the cracks orientation with respect to anchor axis.
- The quantity and the pattern of reinforcement bars close to the anchorage point.
- Anchor and setting features, namely the load transfer mechanism, material properties, diameter and embedment depth.

Therefore some important parameters depending on time can be distinguished, e.g. number of cycles, dynamic action peak values and their subsequence in time, the strain on anchor and base material, the likelihood for an earthquake to occur in the mean life of an anchor.

When a connection is loaded repeatedly it can fail at a loading level which is lower than that under monotonic condition, even ten times lower. The fatigue failure for anchors is driven directly by the steel behaviour of anchor bolts with no influence of load transfer mechanism.

The fatigue phenomenon depends on the range amplitude to which the anchor is subjected. Stainless steel can undergo to 10^7 cycles if the strain range is enough low. The transient non-periodic forces show a limited number of loading cycles but of growing amplitude. Cycles number, in the case of earthquakes, goes from 10 to 10^3 and the subsequent failure, due to low cycle fatigue, can occur with anchor large deformations or base material failure.

During an earthquake alternate horizontal displacements affect structural elements causing both axial and shear opposite deformations in the fastening system. This topic has been deepened since the 80's with experimental studies (Usami et al. 1980, Klingner and Mendonca 1982, Collins et al. 1989). The analysis of hysteretic curves is important to evaluate the connection loss of stiffness. In the case of tension loading tests with a short embedment depth the anchor showed a concrete cone failure, whereas with greater depth a pull-out was observed. The testing results demonstrated that under cyclic combined forces, i.e. shear and tension, the anchor failure is generally linked to tension failure modes.

The ductility of a structural element depends on the context it is part of, thus it is not needed a design of singly ductile elements but they have to be considered together. It is not possible to consider brittle or ductile the anchor behaviour in advance.

Usually steel failure is related to ductility but it can happen if only the all fastening system is adequately designed. The anchor design strength should be driven by the yielding of attached elements or of the fixture. When the failure mode involves the yielding ot the anchor itself, the resultant mechanism is not ductile, but is brittle as the failure mode activated is sudden pull-out or pull-through failure.

In (Nuti 2008) a design of the attached element in order to yield for loading levels lower than the anchor is proposed. In codes and guidelines in general ductile failure modes are required by considering the capacity design seismic resistance of anchors.

From laboratory tests on connections composed by anchor groups some significant and basic notions concerning the seismic behaviour of post-installed anchors.

- Connections made of group of anchors and designed for a ductile behaviour in non-cracked concrete subjected to static loading, will keep a ductile attitude in cracked concrete under dynamic loading.
- Singly tested anchors which show a bas performance are likely to show a bad performance also when set in a group under seismic actions.
- The dynamic cycle does not influence significantly the load-displacement behaviour of a group of anchors.
- In cracked and non-cracked concrete fastening systems subjected to a load applied with an eccentricity greater than 300mm reach steel failure. In cracked concrete a greater deformation and a lower capacity with respect to non-cracked conditions is observed.

1.1.3. Codes And Guidelines

Currently as regards the European regulations of mechanical anchors for both structural and non-structural application there is a phase of constant development and updating. At the moment the codes provide only requirements for the anchor design in concrete by a technical specification of Eurocode 2. Guidelines issued by EOTA[1] instead deal with both the design and the qualification of fastening. A technical report of ETAG 001 (TR 045 2013) includes information about the seismic design of metal anchors in concrete. Each ETAG[2] contains an evaluation testing programme in order to assess one type of anchors for a specific intended usage. That programme will lead to the achievement of an ETA[3] for the anchor object of the test procedures. Annexes of ETAGs provide testing setup and procedures for manufacturers, furthermore they provide design principles. So far the resistance verification in the anchors design regarded only static or quasi-static actions. In fact though testing procedures used to concern anchor behaviour in cracked concrete, there was nothing specific for the seismic response of fastening in terms of dynamic loading. Recently an ETAG 001 annex (Annex E) was issued to consider the assessment under seismic action of anchors. Such assessment procedure is recalled in design recommendations included in TR 045 since July of 2013.

[1] European Organisation for Technical Assessment
[2] European Technical Approval Guideline
[3] European Technical Assessment

Table 1.1 Summary of the evolution of European regulations for anchors

	Design	Assessment
PAST (from 1997)	ETAG 001-Annex C 1997	ETAG 001 1997
PRESENT	TR 045*; ETAG 001 (mechanical); TR029 (chemical).	ETAG 001 2013
FUTURE	EN 1992-4*	ETAG 001+Annex E*

*seismic provisions included

All ETAGs concerning qualification and/or deign of different types of fasteners are summarized in the following table. All of them refer to static or quasi-static actions and contain the procedures to assess an intended use for a particular fastener.

Table 1.2 Guidelines concerning fastening issued by EOTA

Object	Base material	Application	Document
Metal anchors	Concrete	Structural/Non-structural	(ETAG 001)
Plastic anchors	Insulation panels	Non-structural	(ETAG 014)
Plastic anchors	Concrete and masonry	Non-structural	(ETAG 020)
Metal anchors for injection	Masonry	Structural/Non-structural	(ETAG 029)
Anchors resistance under fire	Concrete	Structural/Non-structural	(TR 020)
Post-installed rebars	Concrete	Structural	(TR 023)
Adhesive anchors design	Concrete	Structural/Non-structural	(TR 029)
Metal anchors	Concrete	Structural/Non-structural	(TR 045)

Seismic Design Standards

As regards fasteners used to transmit seismic actions between connected structural elements or between structural elements and non-structural attachments provisions are given in addition to the design basis for static loads (according to EN 1992-4).

First of all, as it is to be determined the design resistance, the concrete where fastening is installed shall be assumed as cracked. It's important to consider that the seismic design cannot be applied where concrete spalling or excessive cracking may occur: thus plastic hinges regions are excluded from the fixing. Their critical length l_{cr} is regulated in EN 1998-1, where also seismic actions (E_d) calculation can be found. Moreover to determine the distribution of forces acting on single anchors of a group, fixture stiffness and its ability to redistribute loads to other fasteners beyond yield shall be taken into account. Annular gaps between the fastener and the fixture should be avoided. With attachments of large importance or dangerous nature it is recommended to account for the displacement of the anchor by engineers calculation. The seismic design resistance of a fastening is obtained by means of following relation with α_{eq} equals to 0.75 for concrete failure modes and

equals to 1 for steel failure, $R_{k,eq}$ which is the characteristic seismic resistance for a given failure mode.

$$R_{d,eq} = \alpha_{eq} \cdot \frac{R_{k,eq}}{\gamma_M} \quad \text{Eq. 1.1}$$

The design of fastening shall prevent a fragile collapse ensuring a ductile behaviour instead, or making sure that the fastening will not experience overloading.

There are different possibilities to approach the seismic design of fastening. Indeed one among the following conditions shall be satisfied:

1. Design for the minimum of these force values:
   - Force corresponding to yield of a ductile steel component (in attached element or in baseplate) considering over-strength.
   - Maximum force that can be transferred to the connection by the attachment or the structural system, depending on fixture capacity.

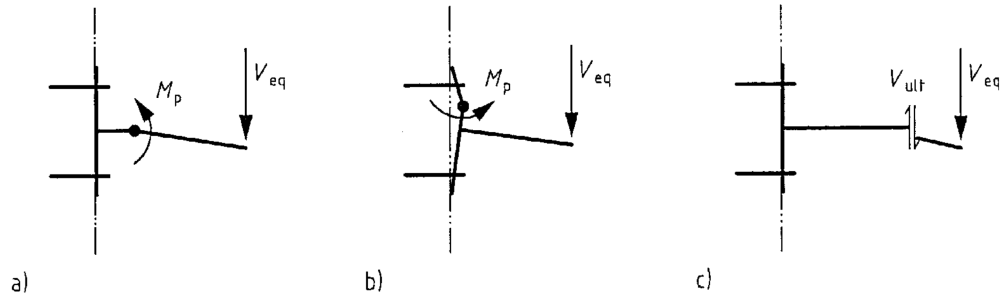

Figure 1.21 a) yielding in the attached element; b) yielding in baseplate; c) capacity of attached element (TR 045 2013)

2. The anchorage is designed for a steel ductile failure. This alternative provides to ensure the ductile failure by satisfying the following condition with $R_{k,s,eq}$ as the seismic characteristic resistance for steel failure, $R_{k,conc,eq}$ as the seismic characteristic resistance for concrete failure modes:

$$R_{k,s,eq} \leq 0{,}6 \cdot \frac{R_{k,conc,eq}}{\gamma_{inst}} \quad \text{Eq. 1.2}$$

3. Only for non-structural elements application it is possible to design for a fragile failure of the fastening only if the seismic design resistance $R_{d,eq}$ is taken as at least 2,5 times the effect of seismic action E_d applied on the attached non-structural element.

$$2{,}5 \cdot E_d \leq \alpha_{eq} \cdot \frac{R_{k,eq}}{\gamma_M} \quad \text{Eq. 1.3}$$

First two options exclude the yielding of fasteners thanks to the designed capacity. Last option provides that design resistance of the anchor shall assure an elastic behaviour of the fastening. Besides the third possibility can go against the new codes dispositions for seismic zones, in which negative aspects of connector yielding are presented because it doesn't lead to a response in terms of plastic cycle.

The interaction between tension and shear forces is determined according to the following linear relation, unless different product specific interaction relations are provided

for seismic applications. Maximum values of ratios corresponding to the failure modes shall be used in this inequality.

$$\frac{N_{Sd,eq}}{N_{Rd,eq}} + \frac{V_{Sd,eq}}{V_{Rd,eq}} \leq 1 \qquad \text{Eq. 1.4}$$

In the United States the main code concerning the design of metal anchors installed in concrete is ACI 318 Appendix D which includes a part (D3.3.1 to D3.3.5) dedicated to seismic loads and the testing qualification references in such cases.

"Post-installed structural anchors are required to be qualified for moderate or high seismic risk zone usage by demonstrating the capacity to undergo large displacements through several cycles as specified in the seismic simulation tests of ACI 355.2. Because ACI 355.2 excludes plastic hinge zones, Appendix D is not applicable to the design of anchors in plastic hinge zones under seismic loads. In addition, the design of anchors in zones of moderate or high seismic risk is based on a more conservative approach by the introduction of 0.75 factor on the design strength φN_n and φV_n, and by requiring the system to have adequate ductility. Anchorage capacity should be governed by ductile yielding of a steel element.

If the anchor cannot meet these ductility requirements, then the attachment is required to be designed so as to yield at a load well below the anchor capacity. In designing attachments for adequate ductility, the ratio of yield to ultimate load capacity should be considered. A connection element could yield only to result in a secondary failure as one or more elements strain harden and fail if the ultimate load capacity is excessive when compared to the yield capacity.

Seismic Qualification Standards

As regards European regulations, ETAG 001 annexes present testing requirements for tension, shear and combined actions, crack cycling tests, repeated load tests, sustained load tests, tests with anchor in contact with reinforcement, tests varying distance to edges and spacing between anchors, torsion tests. In these years a new document was issued by EOTA with a testing procedure able to assess the metal anchors for the use in high risk seismic regions. Indeed the Annex E of ETAG001 was issued in addition of assessment provisions in ETAG 001. These new testing requirements go beyond the qualification standards that already exist in the United States (Seismic Simulation Tests ACI355.2 2007), as they contain a more extensive and restrictive evaluation programme. The seismic problem is presented deeply by means of references to Eurocode 8. Furthermore the carrying out of seven tests is provided, two of them are similar to those included in ACI355.2 and the others show more severe parameters concerning the cracks width and the entity of cyclic load histories. Seismic evaluation tests are divided into two main groups of anchor seismic performance by three factors: seismic activity, building importance class and the ductility class of the structure. For all of these factors tables in Eurocode 8 (EN 1998-1, §3.2.1, §5.2.1 and §4.2.5) shall be considered. C1 category represents a small seismic activity or a medium-high seismic activity only in the case of building belonging to 1st importance class. The C2 category on the other hand is provided for medium-high seismic activity for those buildings belonging to 2nd,3rd and 4th importance class with the ductility of the structure that cannot be taken as low level by the designer. First category is composed by two tests, C1.1 functioning under pulsating tension load and C1.2 functioning under alternating shear load. In both the test setups crack width is fixed at 0.5mm. Additional tests for C2 category include:

- Two reference tension and shear tests (C2.1 and C2.2 respectively) with 0.8mm crack width of the concrete;

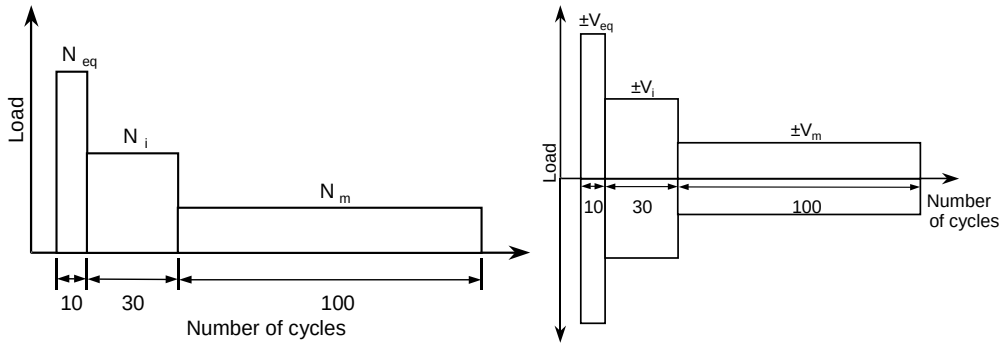

Figure 1.22 Load histories required for C1.1 and C1.2 testing (ETAG001 Annex E)

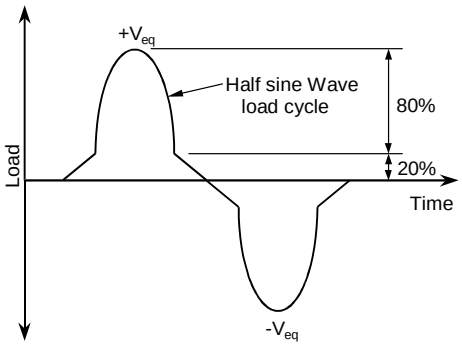

Figure 1.23 Admissible approximation for shear cyclic load regarding C1.2 testing (ETAG001 Annex E)

- Two functioning tests of pulsating tension load and alternating shear load (C2.3 and C2.4 respectively) with crack width varied from 0.5 to 0.8mm at a half of the load history for the first type of tests and fixed at 0.8mm for second tests;

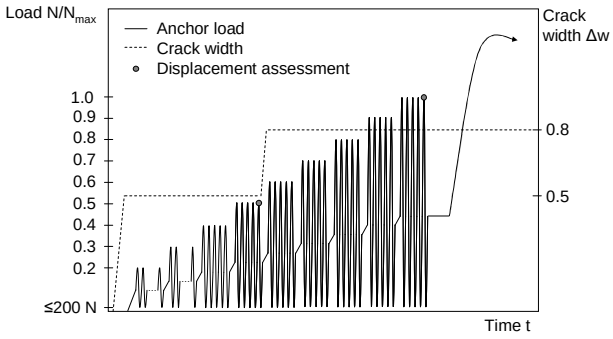

N/N_{max}	Number of cycles	Crack width Δw [mm]
0,2	25	0,5
0,3	15	0,5
0,4	5	0,5
0,5	5	0,5
0,6	5	0,8
0,7	5	0,8
0,8	5	0,8
0,9	5	0,8
1	5	0,8
SUM	75	

Figure 1.24 Required load history and crack width for C2.3 testing series (ETAG001 Annex E)

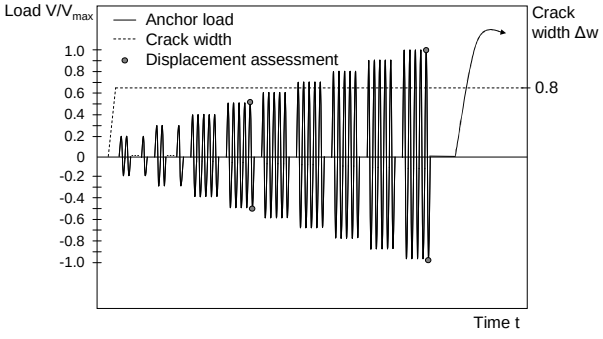

$\pm V/V_{max}$	Number of cycles	Crack width Δw [mm]
0,2	25	0,8
0,3	15	0,8
0,4	5	0,8
0,5	5	0,8
0,6	5	0,8
0,7	5	0,8
0,8	5	0,8
0,9	5	0,8
1	5	0,8
SUM	75	

Figure 1.25 Required load history and crack width for C2.4 testing series (ETAG001 Annex E)

- A functioning tests under tension load with variation of crack width from Δw_1 = 0.0mm to Δw_2 = 0.8mm (C2.5).

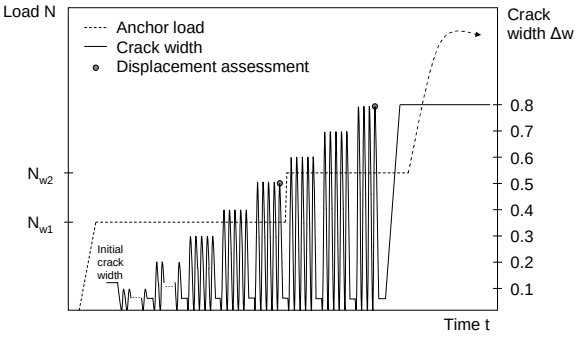

Crack width Δw [mm]	Number of cycles	Anchor load
0,1	20	N_{w1}
0,2	10	N_{w1}
0,3	5	N_{w1}
0,4	5	N_{w1}
0,5	5	N_{w1}
0,6	5	N_{w2}
0,7	5	N_{w2}
0,8	4	N_{w2}
SUM	59	

Figure 1.26 Required load history and crack width for C2.5 testing series (ETAG001 Annex E)

In the United States ACI 318 Appendix D states that "in regions of moderate to high seismic risk, or for structures assigned to intermediate or high seismic performance or design categories, post-installed structural anchors shall have passed Simulated Seismic Tests of ACI 355.2".

ACI 355.2 provides evaluation criteria and methods for post-installed mechanical anchors in order to assess their use in concrete. Qualification programme establishes the assessment by the following four experimental steps:

1) Identification tests to find out possible critical characteristics.

2) Capacity reference tests in both cracked and uncracked concrete (Δw = 0.3mm); such testing consists in monotonic tension tests on low (from 17 to 28 MPa) or high (from 46 to 60MPa) concrete strength; fasteners shall perform tension tests installed in 0.5mm wide cracks.

3) Reliability tests to establish the performance in adverse conditions; in cracked concrete (Δw=0.3mm) a constant tension of 30% of mean resistance shall be applied; 1000 cycles of opening and closing cracks starting from, respectively, w_1 = 0.3 mm and w_2 = 0.1 mm shall be performed. During the testing the closing width can increase provided that w_1-w_2 is larger than 0.1 mm. To be accepted the anchor displacement shall be smaller than 2 mm after 20 cycles and smaller than 3mm after 1000 cycles. After the test the residual resistance shall be larger than 90% of the initial mean resistance. This evaluation procedure does not match the cyclic effects due to real seismic events, but the purpose is to simulate the service conditions cycling.

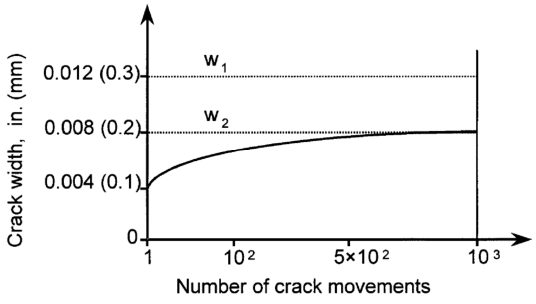

Figure 1.27 Requirements for crack width in cyclic tests (ACI 355.2 2007)

4) Tests to evaluate the service conditions of anchors group, close to the edges in cracked concrete (w = 0.5mm) under simulated seismic action. Load cycles of pulsating tension and alternating shear are performed with frequency range within 0.1 and 2Hz, after that the fastener shall be loaded monotonically to collapse with a starting crack width at least as the one resulted from cyclic action. The test is considered successful only if collapse during load cycles is avoided and if, after the cycle its-self the residual capacity maintains at 80% of initial capacity. These tests are optional.

Load level	N_{eq}	N_i	N_m
Number of cycles	10	30	100

Load level	$\pm V_{eq}$	$\pm V_i$	$\pm V_m$
Number of cycles	10	30	100

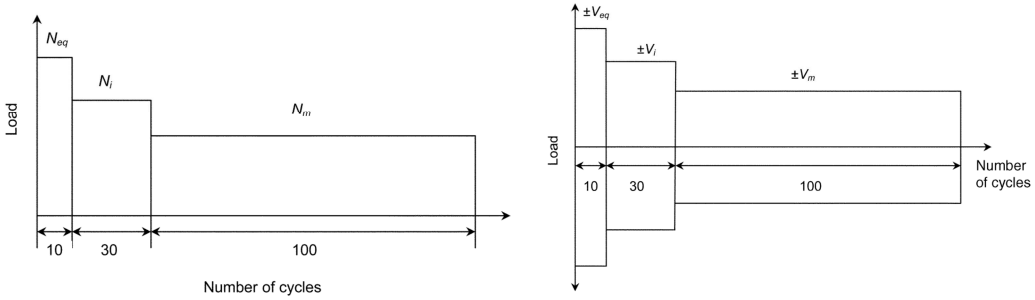

Figure 1.28 Load histories for tension and shear simulated seismic test (ACI 355.2 2007)

Table 1.3 Testing programme for anchors qualification in cracked concrete according to ACI 355.2 (2007)

Test number	Section	Purpose	Description	Crack opening width w, in. (mm)	Concrete strength	Member thickness	Drill bit diameter	Minimum sample size* n
Reference tests								
1	7.2	Reference test in uncracked low-strength concrete	Tension—single anchor with no edge influence	—	Low	$\geq h_{min}$	d_m	5
2	7.2	Reference test in uncracked high-strength concrete	Tension—single anchor with no edge influence	—	High	$\geq h_{min}$	d_m	5
3	7.2	Reference test in low-strength, cracked concrete	Tension—single anchor with no edge influence	0.012 (0.3)	Low	$\geq h_{min}$	d_m	5
4	7.2	Reference test in high-strength, cracked concrete	Tension—single anchor with no edge influence	0.012 (0.3)	High	$\geq h_{min}$	d_m	5
Reliability tests								
5	8.2	Sensitivity to reduced installation effort	Tension—single anchor with no edge influence	0.012 (0.3)	Varies with anchor type	$\geq h_{min}$	d_m †	5
6	8.3	Sensitivity to crack width and large hole diameter	Tension—single anchor with no edge influence	0.020 (0.5)	Low	$\geq h_{min}$	d_{max}	5
7	8.4	Sensitivity to crack width and small hole diameter	Tension—single anchor with no edge influence	0.020 (0.5)	High	$\geq h_{min}$	d_{min}	5
8	8.6	Test in cracks whose opening width is cycled	Sustained tension—single anchor with no edge influence, residual capacity	0.004 to 0.012 (0.1 to 0.3)	Low	$\geq h_{min}$	d_{max} ‡	5
Service-condition tests								
9	9.2	Verification of full concrete capacity in corner with two edges located at $1.5h_{ef}$	Tension—single anchor in corner with two edges located at $1.5h_{ef}$	—	Low	h_{min}	d_m	4
10	9.3	Minimum spacing and edge distance to preclude splitting on installation in uncracked concrete	High installation tension (torque or direct)—two anchors near edge	—	Low	h_{min}	d_m	5
11	9.4	Shear capacity of anchor steel§	Shear—single anchor with no edge influence	—	Low	$\geq h_{min}$	d_m	5
12‖	9.5	Seismic tension	Pulsating tension, single anchor, with no edge influence	0.020 (0.5)	Low	$\geq h_{min}$	d_m	5
13‖	9.6	Seismic shear	Alternating shear, single anchor, with no edge influence	0.020 (0.5)	Low	$\geq h_{min}$	d_m	5

*Minimum sample size for each anchor diameter, unless otherwise noted.
†Drilling diameters for undercuts are specified in Table 5.6.
‡Test of undercut anchors use d_m.
§Required only for anchors whose cross-sectional area, within five anchor diameters for the shear failure plane, is less than that of a threaded bolt of the same nominal diameter as the anchor, or for sleeved anchors when shear capacity of the sleeve will be considered.
‖These tests are optional.

The table above shows all the tests to be performed to achieve the assessment of a fastener, including the reference tests. All the assessment criteria, with the exception of reliability tests on cycling cracks, are based on resistance, with no regards to displacement behaviour of the fastener. In ACI 355.4 a similar procedure is given for what it concerns the qualification of post-installed adhesive anchors in concrete.

Acceptance criteria issued by ICC-ES (International Code Council – Evaluation Service) refer to standard test methods in order to release the assessment for use of different types of anchors in various applications. For example in AC193, seismic evaluation is beyond the scope of the report and it is to be find out from ACI 355.2.

Table 1.4 List of Acceptance Criteria involving fastening issued by ICC-ES (Hoehler 2006)

	Document Title	Anchor Type	Base Materials	Design Basis [a,b,c,d]	Seismic	Cracked Concrete
AC01 (2005)	Expansion Anchors in Concrete and Masonry Elements	Mechanical	Concrete or new masonry	ASD $R_{u,m}/4 \geq WL$	Optional[e]	Not permitted
AC58 (2005)	Adhesive Anchors in Concrete and Masonry Elements	Bonded	Concrete or new masonry	ASD $R_{u,m}/4 \geq WL$	Optional[e]	Not permitted
AC60 (2005)	Anchors in Unreinforced Masonry Elements	Bonded	Existing unreinforced masonry	ASD[f] $R_{u,m}/5 \geq WL$	Mandatory	Not applicable
AC106 (2005)	Predrilled Fasteners (Screw Anchors) in Concrete and Masonry	Screw anchors	Concrete or new masonry	ASD $R_{u,m}/4 \geq WL$	Optional[e]	Not permitted
AC193 (2005)	Mechanical Expansion Anchors in Concrete Elements	Mechanical	Concrete	Strength design per ACI 318 Appendix D	Optional	Optional
AC308 (2005)	Adhesive Anchors in Concrete Elements	Bonded	Concrete	Strength design per ACI 318 Appendix D[g]	Optional	Optional

[a] Assumes on-site inspection of anchor installation.
[b] Allowable Stress Design (ASD).
[c] $R_{u,m}$ = mean ultimate test load.
[d] WL = working load or service load (unfactored).
[e] 1/3 increase in allowable loads permitted.
[f] Capacity limits defined in criteria may result in larger safety factors.
[g] Strength design amended for standard bonded anchors.

As it is noticeable from the table shown above only AC60 has a mandatory consideration of seismic actions. The scope of this document is limited to adhesively bonded anchors used to attach building components to unreinforced masonry walls. The anchors strengthen the walls to resist short-term loads imposed by wind and earthquake and are limited to three applications:

1. Embedded bent anchors resisting tension and shear loads;
2. Embedded anchors resisting shear loads;
3. Through-wall anchors resisting tension and shear loads.

Furthermore ASTM E488-96 (2003) is a generic document that gives standard test methods for evaluation of strength of anchors in concrete and masonry. It contains information about specimens, test rigs, duration, temperature conditions etc.

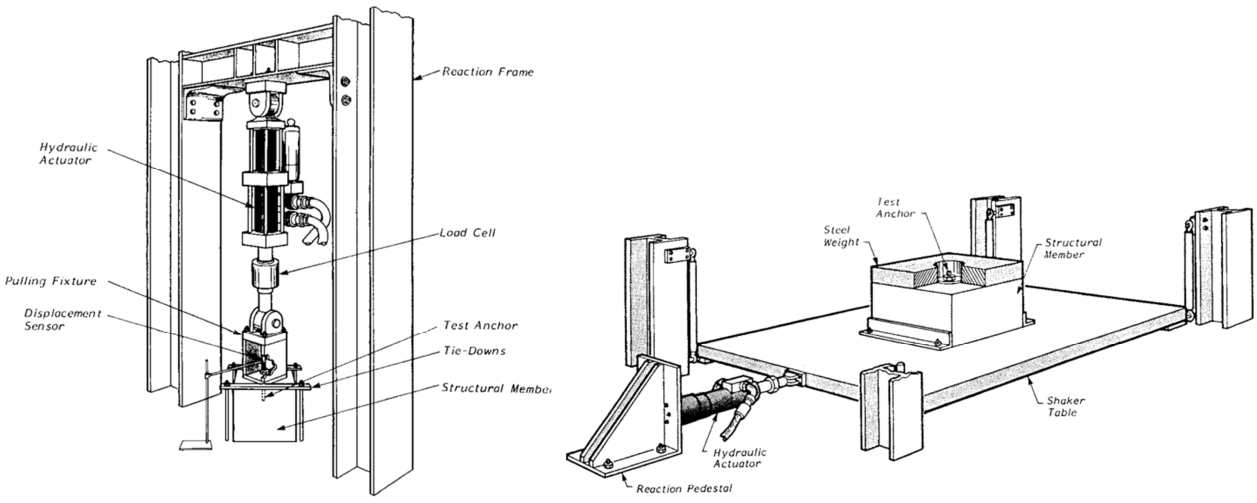

Figure 1.29 Typical seismic tension (left) and shear (right- indirect loading method) arrangement (ASTM E488 2003)

Table 1.5 Summary of seismic qualification tests in the United States and Europe

Source	Purpose	Description	Crack width	Min. sample size	Number of cycles	Max. Frequency
ACI 355.2 Reference	Reference test in low-strength, cracked concrete	Tension-single anchor with no edge influence	0.3 mm	5	/	/
ACI 355.2 Reference	Reference test in high-strength, cracked concrete	Tension-single anchor with no edge influence	0.3 mm	5	/	/
ACI 355.2 Reliability	Test in cracks whose opening width is cycled	Sustained tension-single anchor with no edge influence, residual capacity	0.1 to 0.3 mm	5	1000	0.2 Hz
ACI 355.2 Service-condition	Seismic tension	Pulsating tension, single anchor, with no edge influence	0.5 mm	5	10+30+100	0.1 to 2 Hz
ACI 355.2 Service-condition	Seismic shear	Alternating shear, single anchor, with no edge influence	0.5 mm	5	10+30+100	0.1 to 2 Hz
ETAG001 Suitability	Functioning in low strength concrete		0.5 mm		/	/
ETAG001 Suitability	Functioning in high strength concrete		0.5 mm		/	/
ETAG001 Suitability	Functioning in crack movements		0.1 to 0.3 mm		1000	0.2 Hz
ETAG001 Suitability	Functioning under repeated loads		0 mm		100000	6 Hz
ACI 355.2 Reliability	Reliability under repeated load	Repeated tension-single anchor with no edge influence, residual capacity	0 mm	5	100000	6 Hz
Annex E ETAG001	C1.1 Functioning under pulsating tension load		0.5 mm	5	10+30+100	0.1 to 2 Hz
Annex E ETAG001	C1.2 Functioning under alternating shear load		0.5 mm	5	10+30+100	0.1 to 2 Hz
Annex E ETAG001	C2.1 Reference tests tension load		0.8 mm	5	/	/
Annex E ETAG001	C2.2 Reference tests shear load		0.8 mm	5	/	/
Annex E ETAG001	C2.3 Functioning under pulsating tension load		0.5 mm ($\leq 0.5 \cdot N/N_{max}$) 0.8 mm ($>0.5 \cdot N/N_{max}$)	5	75	<0.5 Hz
Annex E ETAG001	C2.4 Functioning under alternating shear load		0.8 mm	5	75	<0.5 Hz
Annex E ETAG001	C2.5 Functioning with tension load under varying crack width		Δw_1 = 0.0 mm Δw_2 = 0.8 mm	5	59	<0.5 Hz

1.1.4. Reference Testing Experiences

The aim is to define different types of testing in order to evaluate existing ways to assess the reliability and the performance of a fastening system. By observing the current state of the subject it's possible to recognize some researches which in terms of setups and goals are close to codes prescriptions and can be define as "standard" testing. Other campaigns are focused on pure research –not according to approvals provisions- with new purposes to investigate over specific application conditions and to improve particular skills. First type, which is the more widespread in scientific literature, sometimes can go further with reviews and comparisons in the carrying out of assessment testing, whereas in other cases experiments are performed in order to anticipate the drafting or the updating of a guideline. In the latter situation according to a seismic qualification document it is possible to vary only few parameters to study the anchor behaviour in worse conditions than the ones required by code, or to propose a completely new testing methodology but with the definition of a setup such that it could be taken as a reference in the future for the evaluation of a performance. For execution easiness, repeatability and costs saving all the research related to the seismic standard evaluation provide for the application of a monotonic or cyclic load to the specimen. On the other hand in the second group of experiences the more deep and innovative campaigns used a shake-table system with motion in one, two or three among the principal directions, as the purpose was to study the most realistic fastening behaviour. Moreover in such studies an interest has been given to the applications and therefore to the dynamic characteristics of the fixture in terms of accelerations, relative displacement, restraint, natural frequencies (also of base material to which the component is attached).

The laboratory experiences evidenced that most common failure causes for anchorage systems are deformations imposed by seismic action, because often fasteners are not designed to tolerate large deformations. Therefore it is necessary to focus on the behaviour of different typologies of anchors and on the possibility to guarantee enough thrust to base material surfaces in spite of a big hole dilatation. During an earthquake the ground acceleration is transferred to the structure through the foundation: these dynamic inputs lead to different structural responses depending on seismic features (magnitude, frequency and duration), on efficiency of ground-structure interface and on dynamic characteristics of the building. When an earthquake occurs fasteners receive a combination of cyclic tension and shear. More it is likely that the anchor is placed where a crack developed. Typically crack width vary –closing and opening- during an earthquake as a result of structural deformation. Seismic behaviour of fastenings depends on several parameters, listed below.

- The amplitude, the sequence and the number of cycles of seismic actions; direction of load application, that is if act on connector tension, shear or combined load.
- The cracking of surrounding concrete, cracks behaviour during ground shaking, cracks orientation in respect to anchor longitudinal axis.
- Amount and disposition of reinforcing steel close to an anchorage.

Monotonic and Cyclic Testing

First experience to take into account is (Ghobarah and Aziz 2004). In this case the procedure follows the requirements provided by Canadian codes for anchors to use inside nuclear plants. The aim is to extend the knowledge of testing procedure for that specific

use (both static and dynamic tests) to all the critical applications in building such as seismic action. Tests, performed on single anchors, proved the differences between four different anchor types among the most used in nuclear industry. Specimens consist of simple concrete blocks, and the test rig consists in a load cell with the possibility to perform tension and shear tests. Each anchor type experienced four tests: tension static, shear static, tension dynamic and shear dynamic. Each size and load setup has been performed three times in order to obtain statistically valid data. As a result of the research it has been discuss if products achieved the assess for seismic qualification. As told above this kind of test provides a correct procedure and experimental interpretation of test to carry out for the qualification fulfilment, following details given by CSA N287.2 1998. Besides considerations about failure modes and ductility of the failure related to the functioning principle are presented.

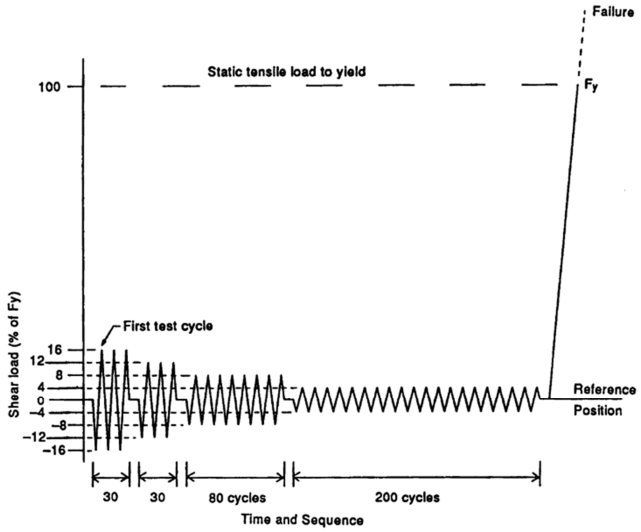

Figure 1.30 Dynamic load according to CSA N287.2 (1998) (Ghobarah and Aziz 2004)

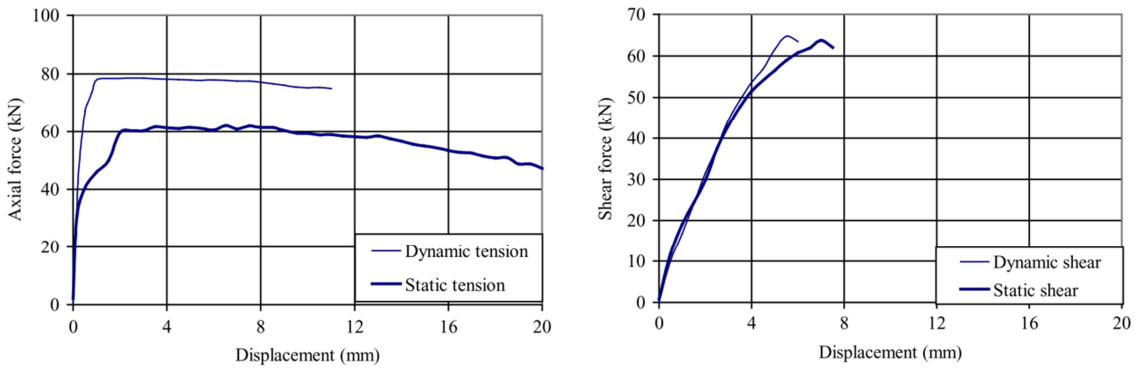

Figure 1.31 Load-displacement behaviour of failure tests before and after dynamic cycles in case of tension (left) and shear (right) for a M16 expansion anchor (Ghobarah and Aziz 2004)

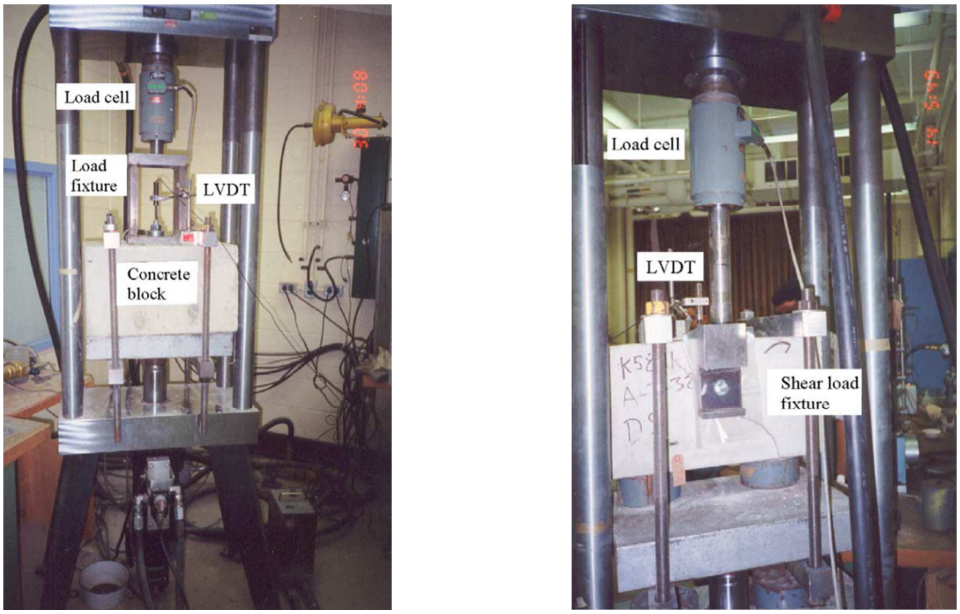

Figure 1.32 Tests rig for dynamic tension (left) and shear (right) (Ghobarah and Aziz 2004)

A case-study which has the intent to update the assessment criteria for seismic qualification of anchors is (Hoehler 2006). In the choice of cracks width, which had to open in a cyclic way as was required by ACI355.2, the upper bound has been brought to 0.8mm instead of 0.5mm. The research item is to study the fastener behaviour according to the crack width in which it is embedded. In this experimental study new test setups have been developed in order to compare the performance of different types of anchors loaded with monotonic constant tension of $N_w = 0.4 \cdot N_{u,m}$ (defined according to design loading levels for seismic actions prescribed in ACI 318 2005) subjected to ten crack cycles between $w_1 = 0.8\,mm$ and $w_2 = 0.0\,mm$. Specific attention has been paid to the failure mode of different anchor types. Moreover it is interesting to observe their different residual strength over the initial ultimate strength and the displacement capacity in case of such cracked concrete installations. As anchor suitability indicator it is usual to consider the load-displacement curve growing in a linear way or in a digressive way: a progressive increase of displacement warns of forthcoming failure. As a consequence of the testing is important to note that many factors affect the displacement trend as the anchor type, the failure mode, opening and closing crack width, number of cycles and the fastener bearing pressure.

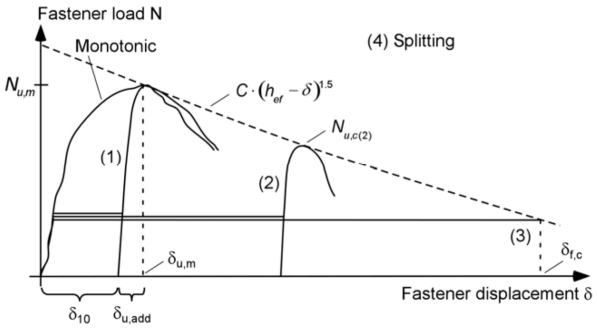

Figure 1.33 Load-displacement curves for cyclic crack testing in the case of concrete cone failure (1) $\boldsymbol{\delta_{10} < \delta_{u,m}}$; (2) $\boldsymbol{\delta_{u,m} \leq \delta_{10} < \delta_{f,c}}$; (3)) $\boldsymbol{\delta_{10} = \delta_{f,c}}$ (Hoehler 2006)

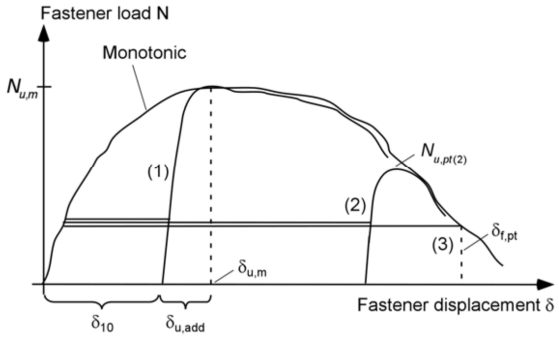

Figure 1.34 Load-displacement curves for cyclic crack testing in the case of pull-through failure (1) $\boldsymbol{\delta_{10} < \delta_{u,m}}$; (2) $\boldsymbol{\delta_{u,m} \leq \delta_{10} < \delta_{f,pt}}$; (3)) $\boldsymbol{\delta_{10} = \delta_{f,pt}}$ (Hoehler 2006)

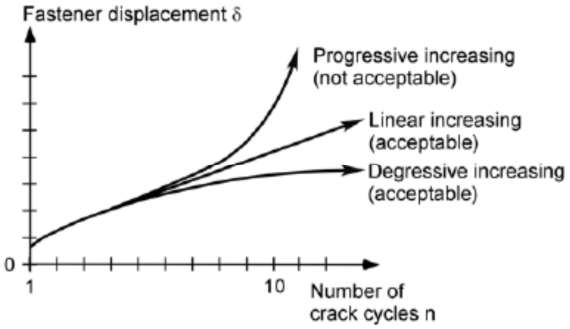

Figure 1.35 Synthetic displacement curves of anchor for low cyclic crack testing (<100) of relatively wide gap width ($\boldsymbol{w_1 - w_2 \geq 0.5\ mm}$) (Hoehler 2006)

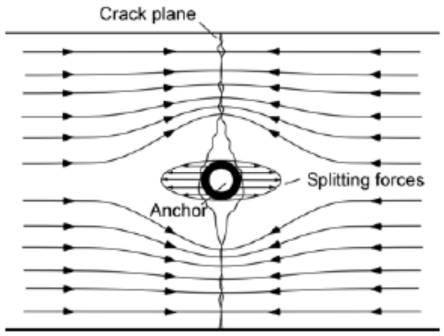

Figure 1.36 Compression load transfer around the anchor (plan view) (Hoehler 2006)

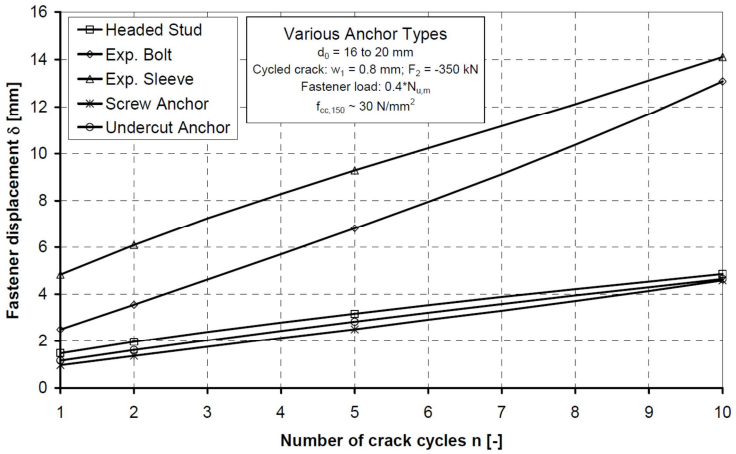

Figure 1.37 Fastener displacement as function of number of crack cycles (Hoehler 2006)

In (Hoehler 2006) there are also cyclic loading tests in which fasteners were post-installed in cracks cyclically varied with remarkable gap width (Δw = 0.8mm). Here is presented as failure indicator the crossing of ultimate load displacement in the

corresponding monotonic test. The research again focuses on failure modes and the performance under cyclic loads related to the ultimate static load among different types of anchor.

It is important to note that for tested anchors there is absence of hysteretic behaviour even with the failure due to steel rupture. Frequencies of load cycles applied to the fastener is usually included between 0.1 and 2Hz according to existing seismic qualification tests. Frequencies up to 10 Hz should be taken into account for seismic application of the anchor. However an increase to 5Hz in the frequency of the load history does not affect residual strength in a negative way because anchor displacement would be widely reduced, not depending on the failure modes.

The requirements of steel ductile failure found in design methods shall be coupled to a specific strain length (≥ 5·*d* according to CEN TS 1992-4-1:2009) to reach large deformation capacity. In any case it is necessary for the yielding to occur along the anchor equally. Finally some ideas for the future and recommendations are given.

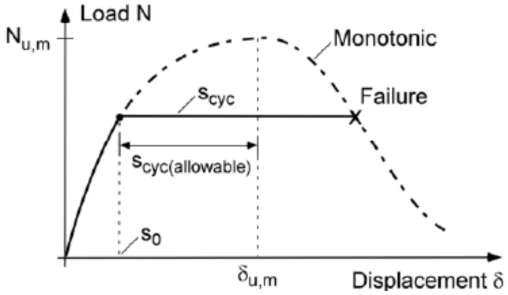

Figure 1.38 Synthetic load-displacement curves for tension cyclic loads for concrete failure indicating admissible displacement before the collapse (Hoehler 2006)

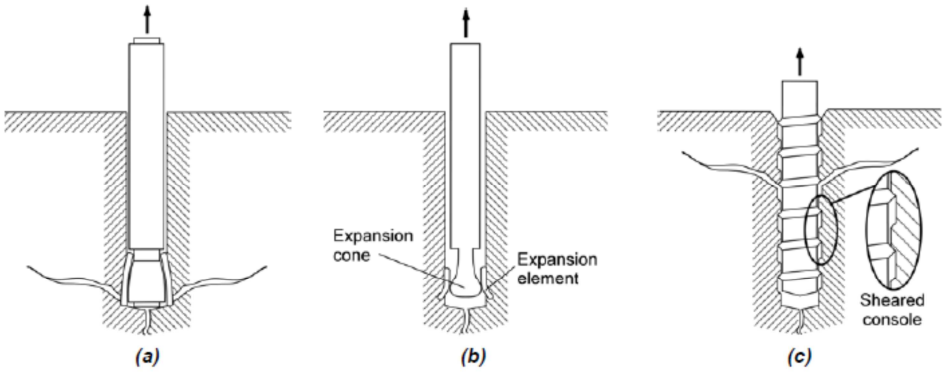

Figure 1.39 Failure modes: (a) sleeve-type expansion anchor (concrete cone); (b) bolt-type expansion anchor (pull-through); (c) screw anchor (pull-out/concrete cone) (Hoehler 2006)

Shake-Table Tests

Some of the experimental campaigns presented below are interested only in strength values of anchors, whereas others look –more in general- at the fastening behaviour inside a representative application system.

(Rieder 2009) shows further and specific investigations about fastening seismic behaviour. Test system consists in a shake-table and the motion is applied in all of the

three principal direction according to the IEEE693[4] standard. The target of the research is to compare different types of heavy-duty anchors: undercut anchor, expansion anchor and adhesive anchor. For each anchor the test has been performed twice. Base material consists of a cracked concrete specimen and the component attached are made of steel plates adequately designed (~300 kg per mass). Therefore the intent is to observe the strain acting on the fastener induced by following steps of seismic level as well as the failure modes for different anchor types.

Figure 1.40 Shake table testing of three anchor types (Rieder 2009)

Inside (Hoehler et al. 2009) the shake-table testing of piping system attached to different levels of a seven-storey RC-framed building is presented. The pipes are attached to 20 cm thick concrete slabs by two types of anchors and a seismic bracing system. On 16 anchors out of the 39 used for the entire equipment fixing axial strain gages were mounted. More than 600 sensors have been used in order to measure the dynamic response of the structure through the testing. The aim of the research is to consider the seismic behaviour under increasing states of damage of an high-rise building located in Southern California for anchors designed to attach important non-structural components (i.e. they have to remain operational during and after an earthquake occurs).

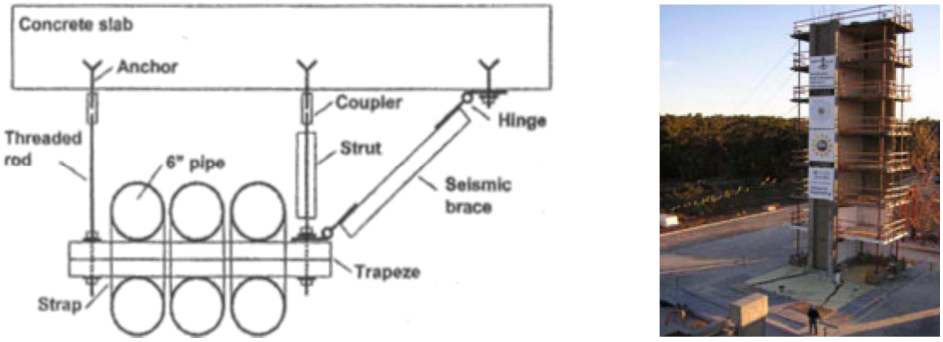

Figure 1.41 Shake-table testing of piping system in a seven-storey building (Hoehler et al. 2009)

(Watkins 2011) is an in-depth research that deals with the seismic behaviour of anchors connecting in four points a steel structure –representative of a non-structural hospital component- to a 25cm thick concrete slab. The motion is given in only one

[4] IEEE 693 Standard. Recommended Practice For Seismic Design Of Substations. IEEE, 2005

direction (out-of-plane) and the purpose of the study is to find out the strength of different anchors and the failure modes under seismic action. Two layout versions of the specimen have been performed, one rigid (borne at the top with a mass of 390kg) and one flexible (borne at the top with a mass of 1160kg) to better consider the influence of the vibration period of the non-structural component (T_{rig}=0.10sec, T_{flex}=0.25sec).

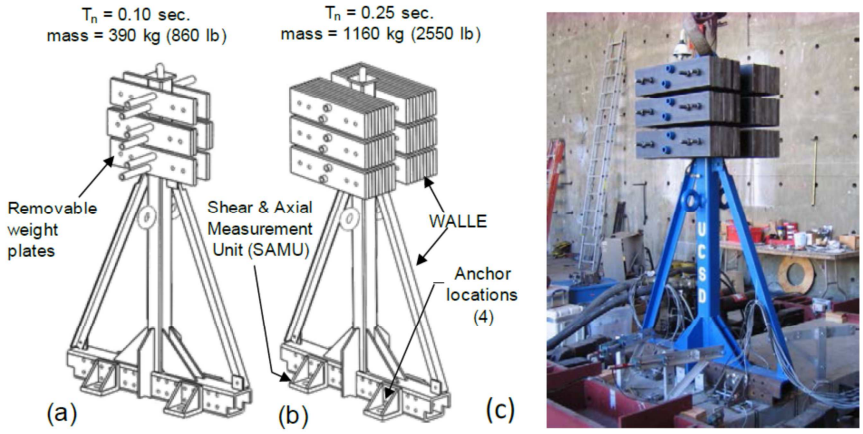

Figure 1.42 Shake-table testing of a steel system anchored to concrete slab (Watkins 2011)

In the experimental study shown in (Scheidel 2011) the attention is focused on the shear behaviour of a group of anchors under seismic action represented by a one-direction motion of shaking-table. The attached element is a typical non-structural component (e.g. HVAC) with a mass of about 2515kg. Testing results report differences among the anchors used in terms of ultimate strength and of failure modes.

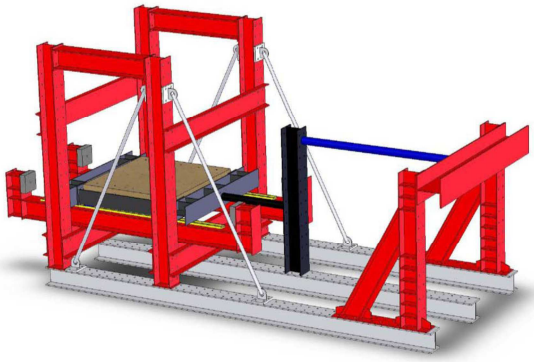

Figure 1.43 Shear behaviour of anchors in an unidirectional shake-table testing (Scheidel 2011)

1.2. Seismic Response of Non-Structural Elements

The non-structural elements placed inside buildings can be subdivided in various categories such as architectural components (e.g. infill walls, cladding panels, suspended ceilings), utility systems (e.g. electrical and mechanical equipment, water heaters, HVAC systems, elevators) and all the contents (e.g. computers, communication systems, furniture,…). According to the experience of recent earthquakes (L'Aquila 2009, Chile 2010, Christchurch 2011, Tohoku 2011, Emilia 2012) it is understood that these components are extremely sensitive to dynamic loading caused by the occurrence of an earthquake. The seismic actions are affected by several factors related to both the structure of the building itself and the construction site characteristics (type of soil and location).

In this paragraph a state-of-art on the response to earthquake of high importance non-structural elements is reported. Also an overview among the codes and the guidelines which regulate this subject are summarized. Moreover some significant reference testing experiences regarding the seismic evaluation of non-structural elements are described in the final part.

1.2.1. Non-Structural Elements Typologies

Non-structural components could be further divided into two principal classes, depending on the predominance of their critical sensitivity, namely whether to acceleration or displacement effects. The first group mainly includes elements with relevant mass and lead to the activation of inertial forces (e.g. water heaters and HVAC systems). The latter case represents a higher vulnerability as a consequence of the large deformations of the structure (e.g. infill walls and piping suffer the drifts of parts of the structure they are fixed to).

Hence preventing the possible collapse of component or its damage is of primary importance mainly for the human life safety but also for the huge social and economic loss (Taghavi and Miranda 2002, Figure 1.44) in relation to the period with the lack of functionality of a building, especially in the case of relevant structures (e.g. hospitals, schools, police and fire stations). Moreover the most recent regulations and guidelines require to guarantee the functioning of non-structural components of high importance, such as fire systems and medical equipment, also in the post-earthquake phase also providing recommendations for their seismic assessment and mitigation (ASCE 7-10 2010, FEMA E-74 2011).

The Figure 1.44 highlight the evident prevalence of the non-structural elements costs out of the entire construction value, thus the economic impact due to widespread damages to non-structural elements becomes clearer.

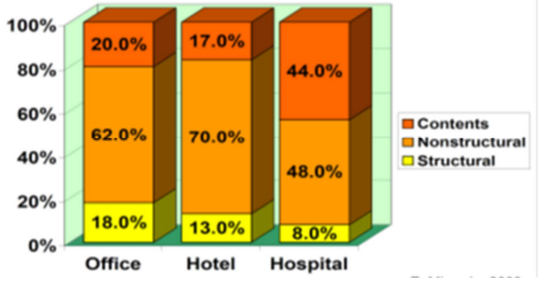

Figure 1.44 Construction costs partition into structural elements, non-structural elements and building content (Miranda et al. 2003)

Some instances of relevant non-structural elements are presented in the following paragraphs in order to describe which kind of issues can affect the seismic response of these components of high importance included in buildings. In particular strategic utility system equipment attached in strategic buildings and art objects displayed inside museums are reported as examples.

1.2.1.1. Utility System Components

Utility system components are the built-in elements which form part of the building and cover the fundamental functions to make a construction operative. Important components are included within this category such as mechanical and electrical equipment, distribution systems, water, gas, electric piping and conduits, elevators or escalators, HVAC systems and roof-mounted solar panels (Retamales et al. 2011). Besides the higher is the importance of a building the more complex and numerous are the utility systems. For instance fire suppression system is a very critical components to stay operational during and after an earthquake because of the common relation between seismic actions and fire. Fire safety system indeed has to withstand the earthquake for two main reasons. One is to be ready in case of a subsequent fire to suppress it and second is that a failure in the piping system can cause flooding inside a building. The latter case is the demonstration of how only one damage, even as a consequence of small quakes, can interrupt the activity of a building and more, cause huge economic losses as all the building contents can experience damages by water.

Many strategic buildings are affected by damages and economic losses when an earthquake occurs because of several utility system components. Therefore there is a need of an harmonisation of structural and non-structural components in the seismic design of a building otherwise the scope to ensure safety and functionality cannot be complied. For instance the failure of non-structural elements can impede people to evacuate or rescuing operations. Moreover in past events economic losses by non-structural damage often exceeded losses from structural elements.

Concerning non-structural components there is a lack of information available and only limited basic researches were carried out, therefore an effective method to understand the issue is to observe the good and bad practices from past events and try to prevent the same mistakes (Retamales et al. 2011).

From Chilean recent earthquake of Maule in 2010, damages to the utility systems were evident at Santiago and Concepcion International Airports (Figure 1.45), in many hospitals and industries as reported by (Miranda et al. 2012). Due to the lack of functionality of the buildings two thirds of the air traffic stuck and the cost for repairing non-structural components damage reached 40 million US$ only for SCL Airport (Aon Benfield 2010). Concerning effects on hospitals, the Ministry of Health of Chile estimated around 2.8 billion US$ to repair non-structural damages.

Also Christchurch earthquakes of 2010 and 2011 brought massive economic losses, approximately 17 billion US$, especially considering the relative population and the magnitude of the events.

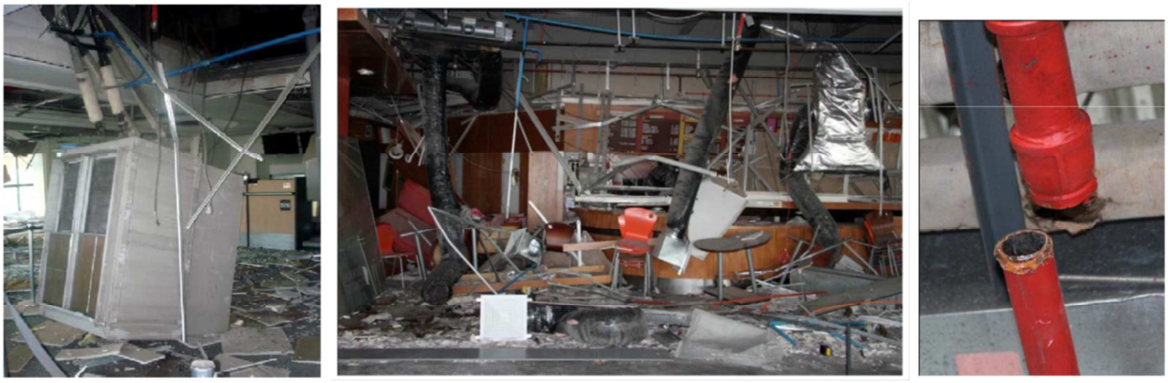

Figure 1.45 damages to utility system components at Santiago Airport (Miranda et al. 2012)

Considering the recent strongest seismic events a series of remarks can be pointed out. They all occurred in countries with long time tradition in earthquake engineering, furthermore in recently designed structures the damage to structural parts was relatively small compared to large amounts of damage to non-structural components. In all the cases such damage leaded to relevant impacts on facilities and society, therefore economic losses and downtime for function recovery are definitely to be taken into account in a performance based design. Often the failure of non-structural elements occurred as a consequence of a bad or missing anchorage and bracing to the structure. The interaction between components was one of the main causes of heavy damage.

Multiple factors affect the seismic behaviour of non-structural components. Among them some influence the structural response, namely the regional seismicity, proximity to an active fault, local soil conditions, the dynamic characteristics of a structure. Some others are additional factors which influence the non-structural response, namely the dynamic characteristics of the non-structural element, the element bracing and restraint to the structure, the location inside building, the facility function and the role of the component to that operation.

The primary responses to earthquake of non-structural components are inertial effects, distortions imposed by structural swaying, separation or pounding between adjacent structures and non-structural interaction. The inertial forces depend on different accelerations at various storeys in the structures and cause overturning or sliding according to the slenderness of the element and its friction coefficient. The distortions of a building, namely inter-storey drifts, affect the displacement-sensitive components. The pounding of adjacent structures cause damages to all the components which are located across the separation. The interaction between non-structural elements can occur when several systems are set closely one to the other with different dynamic characteristics and dimensions. An usual example is the ceiling plenum where, above the suspended ceiling, the utility systems are often installed.

1.2.1.2. Art Objects

Museums are the buildings with the function of keeping the art and culture forms of a society ensuring their passing down from generation to generation. The museum content represents an inestimable heritage for a Country which has to pay attention in the conservation through the best protection techniques. One of the highest risks for art objects displayed in museums is the response of this type of non-structural elements to seismic actions. By shape, mass and material composition, museum assets show high susceptibility to inertial forces generated by earthquakes.

Besides often the building itself cannot withstand properly the seismic action. Therefore the possible interaction of the building should be taken into account when evaluating the seismic vulnerability of the displayed art objects.

Since the 1980s many researches focused on studying the seismic response of art objects by first distinguishing different typologies and behaviour categories (Agbabian et al. 1988, Augusti and Ciampoli 1996). In particular the classification of the object type and support system helped in understanding the related response behaviour and damage mechanisms. As effects of seismic actions applied on art objects there can be recognized joined motion, sliding and rocking. Such response modes lead some specific respective damages to occur due to high internal stress, excessive displacements, repeated impacts and overturning.

With the purpose to categorize the displayed non-structural elements by damage mechanisms in order to reduce the seismic vulnerability it is first of all needed a classification by art object typology. This subdivision into classes takes into account the object shape and dimensions allowing the field of possible related support and fastening systems to be restricted. The identified element typologies are presented in Table 1.6.

Table 1.6 Classification of art objects typologies according to (Augusti and Ciampoli 1996, Liberatore 2000)

Category	*Object description*	*Reference*	*Examples*
T1	Small flat-bottomed objects	VASE	Small vases, ceramic ware, glasses
T2	Small not flat-bottomed objects	BUST	Busts, jewels, grave goods
T3	Large objects	STAT	Statues and sculptures, large vases, stone plates, columns and capitals, wood furniture
T4	Paintings and panels in general	QUAD	Paintings on canvas or wood
T5	Objects attached to the ceiling	LAMP	Chandeliers and suspended objects
T6	Others	MISC	All what is not included in T1-T5

With a similar methodology of the previous classification a further subdivision by support system typologies can be made. The aim of this second passage is to collect data on the constraint level and the geometry of support displaying element. The so obtained indications are useful to identify the possible object motion activated by the occurrence of an earthquake. The support typologies are presented within the Table 1.7.

Table 1.7 Classification of art objects support systems according to (Augusti and Ciampoli 1996, Liberatore 2000)

Group	*Category*	*Description*	*Possible related types*
Objects supported on a flat plane	A1	On the floor	T1, T2, T3,T6
	A2	On a pedestal	T1, T2, T3,T6
	A3	In display cases	T1, T2, T6
	A4	On cantilever or in wall cases	T1, T2, T6
Objects fixed on a flat plane or a pedestal	B	Objects fixed on a flat plane or a pedestal	T1, T2, T3,T6
Suspended/ hanging objects	C1	Suspended on a wall	T4, T6
	C2	Hanging from the ceiling	T5, T6

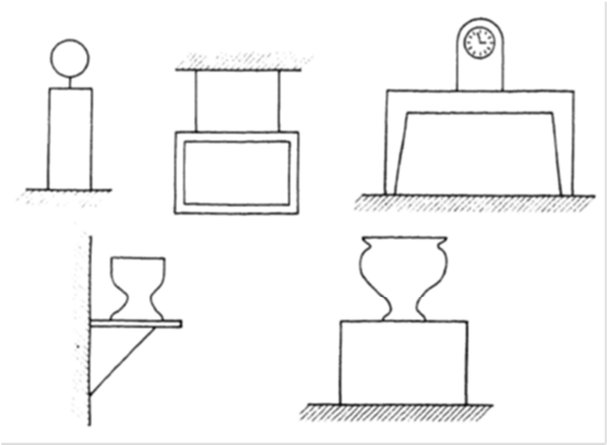

Figure 1.46 Examples of art objects support systems (Agbabian et al. 1988)

In (Agbabian et al. 1988, Augusti and Ciampoli 1996) the identified art objects response categories are presented. Some among them, namely rocking or sliding, stress failure at the base and internal stress failure, describe the behaviour of rigid bodies. Other categories include non-rigid responses, which can be represented by 1 or 2 DOF pendulum, a dynamic stress failure at the base or a dynamic internal stress failure. The dynamic responses and damage mechanisms are presented in detail in Table 1.8.

The laws that govern whether the object is expected to undergo one of the different dynamic responses have been investigated in many works dealing with overturning of rigid bodies. That is because the greatest part of art objects consists of rigid bodies. (Ishiyama 1983) and (Housner 1963) include in-depth studies on rigid bodies rocking and overturning with several sample cases. From the above mentioned studies the main parameters that affect the dynamic response of an art object, namely its slenderness and the friction coefficient between the surfaces, are described and related together. The equations to consider as criteria for understanding the object failure stages at a certain horizontal motion are also synthetically stated in the experimental study of (Spyrakos et al. 2008) and reported in the following. The thresholds of facing possible mechanisms are also summarized graphically in the Figure 1.46.

$$\frac{A}{g} \geq \frac{B}{H'} \qquad \text{Eq. 1.5}$$

$$V \geq 10\frac{B}{\sqrt{H'}} \qquad \text{Eq. 1.6}$$

$$\frac{A}{g} \geq C \qquad \text{Eq. 1.7}$$

In the relations from Eq. 1.5 to Eq. 1.7, A and V are the peak horizontal acceleration and velocity at the base of the rigid body and B is the base width of the art object, C is the friction coefficient and H' can be assumed as the centre of gravity height. From such relations the limit values of acceleration and velocity that can cause failure are identified.

The work of (Augusti and Ciampoli 1996) provides also a list of check and interventions for easily reducing the risk of damages according to the identified mechanisms.

Table 1.8 Art object seismic response according to their classification in typology and support system

Support category	*Dynamic response*	*Damage/failure mechanism*	*Reference*	*Possible related types*
A	Stick motion	Excessive stress	R1	T1, T2, T3, T6
	Sliding motion	Excessive displacements	R2	T1, T2, T3, T6
	Rocking	Repeated impacts	R3	T1, T2, T3, T6
	Rocking	Overturning	R4	T1, T2, T3, T6
B	Stick motion	Excessive stress	R1	T1, T2, T3, T6
C	Sliding motion	Excessive displacements	R5	T4, T6
	Rocking	Excessive displacements	R6	T5, T6

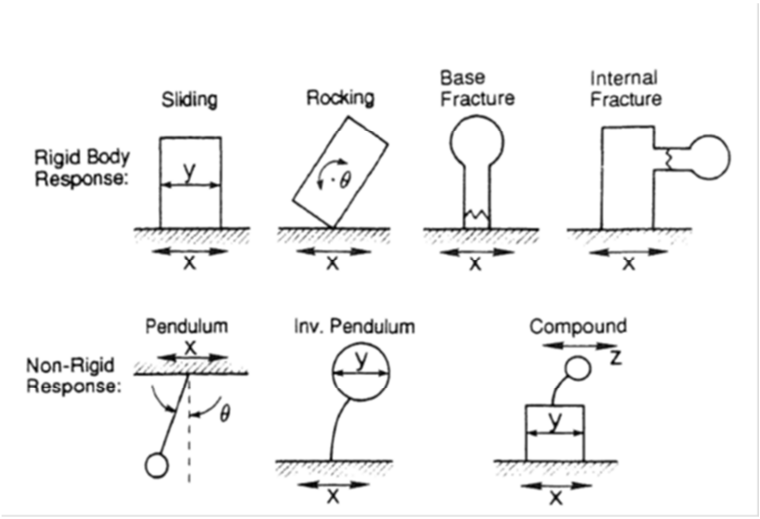

Figure 1.47 Analytical models for categorizing art objects response behaviour (Agbabian et al. 1988)

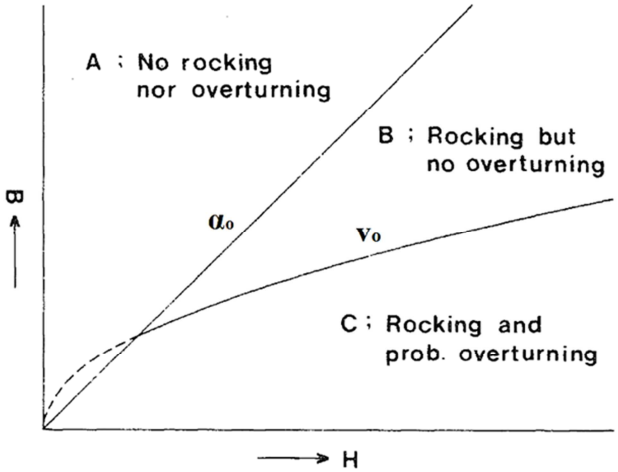

Figure 1.48 Dynamic response regions of a rigid body affected by earthquake motion (Ishiyama 1983)

As a consequence of the studies mentioned above various solutions to reduce the seismic risk of art objects were developed in the last decades, in order to make museums safer places to preserve their important contents. Some examples in particular earthquake sensitive areas can be counted and are reported in various scientific works.

(Lowry et al. 2007) presents many different technical solutions designed to provide an earthquake protection to J. Paul Getty Museum assets in Los Angeles (Figure 1.49). The

reported work was developed by Lindvall, Richter & Associates. A more recent study (Berto et al. 2011) proposes other specific types of seismic restraints to avoid the overturning for small statues in Galleria dei Prigioni, Florence (Figure 1.50).

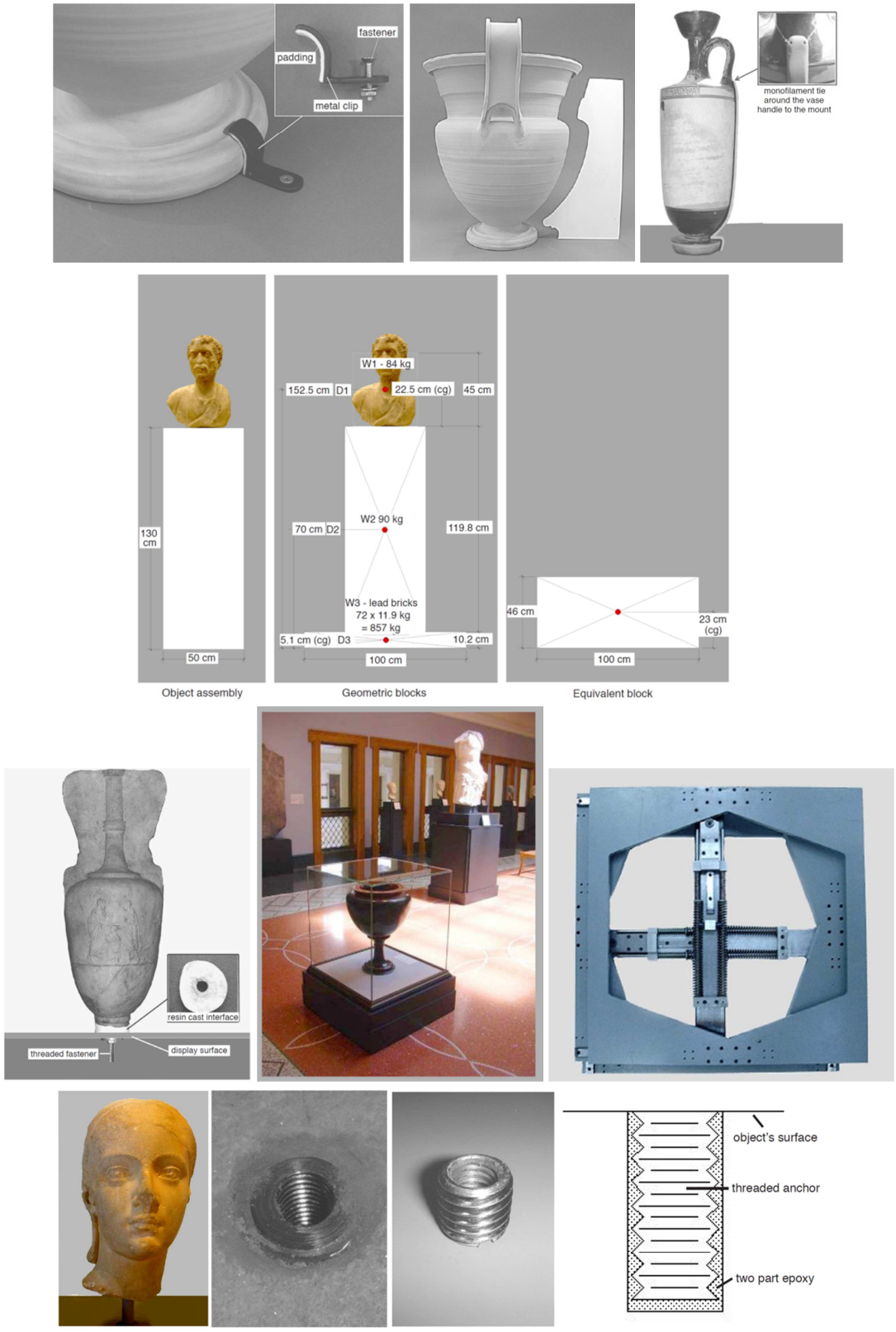

Figure 1.49 Technical solutions developed to protect Getty Museum collections to earthquake (Lowry et al. 2007)

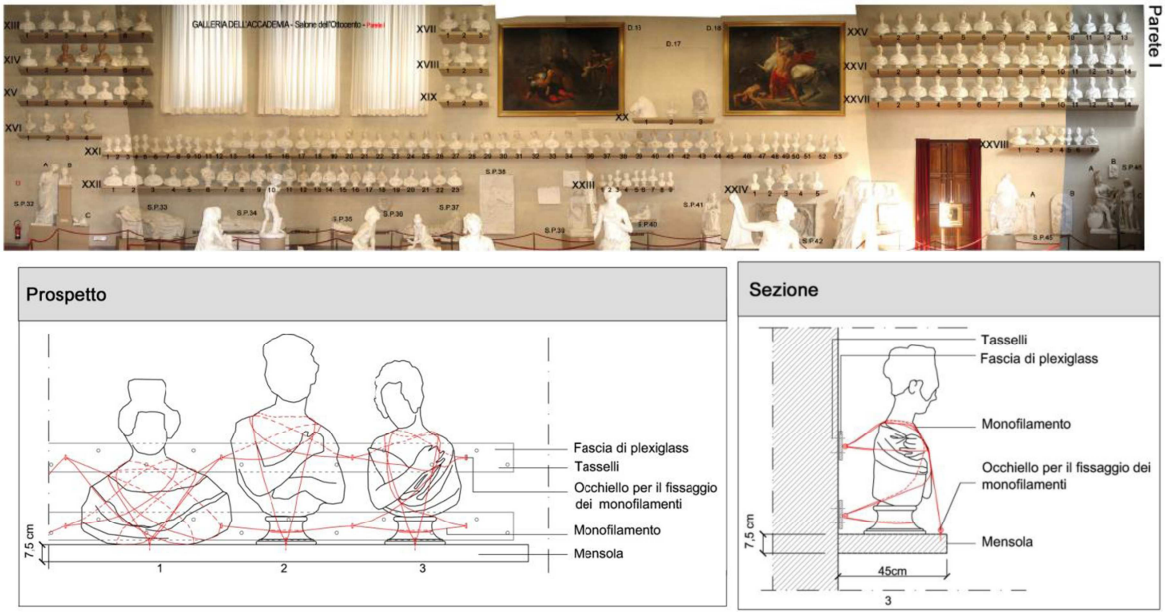

Figure 1.50 Systems to prevent rocking and protect the statues in Galleria dei Prigioni in Florence from impact and overturning (Berto et al. 2011)

1.2.2. Codes And Guidelines

In last decades an increasing effort was registered by normative bodies and agencies, as well as industry groups, in developing guidelines and standards for the seismic design and assessment of non-structural elements. The main purpose of such activity has been to avoid life safety hazards due to non-structural damage by limiting large displacements and by anchoring the elements to the structure. The assumption made was that these components are dynamically independent from structures more they should be evaluated through a cascading method in which the Floor Response Spectra (FRS) are calculated previously.

The common criteria in the so far issued codes are to calculate equivalent static design horizontal and vertical forces applied to the centre of mass of a component, to multiply them by an importance factor (≥ 1) and to divide the terms by a response modification factor (≥ 1) to account for the over-strength and non-linear behaviour of components. Furthermore the reaction of the support elements has to be evaluated before designing properly the component, together with anchorage and bracing, in order to withstand the seismic actions.

The peak acceleration to be considered for a component is related to the floor spectrum response of the floor it is located at. The peak floor acceleration profile usually grows from a PGA basis at increasing heights of the building due to the structural amplification. The acceleration acting at the centre of mass of non-structural element is obtained multiplying floor acceleration by a further component amplification factor. Whether it is anchored to the structure then the component is considered rigid and the factor is equal to 1. Otherwise the component is flexible and it can show larger factors.

In United States standard ASCE 7-10 referred to also by International Building Code, chapter 13 provides a procedure for the seismic design of non-structural elements. The seismic action is calculated through the equivalent static force according to the equations below. In addition for some critical cases limited relative displacements and seismic qualification of components are required.

$$F_{ph} = \frac{0.4\, a_p S_{DS}}{\left(\frac{R_p}{I_p}\right)}\left(1 + 2\frac{z}{h}\right) W_p \qquad \text{Eq. 1.8}$$

$$F_{pv} = \pm\, 0.2\, S_{DS}\, W_p \qquad \text{Eq. 1.9}$$

Where:

a_p	component amplification factor (from 1 to 2.5),
S_{DS}	design earthquake spectral response acceleration at short period,
R_p	component response modification factor (from 1 to 12),
I_p	component importance factor (1 or 1.5),
z	height of the structure the component is located at,
h	average roof height from the base,
W_p	weight of non-structural component.

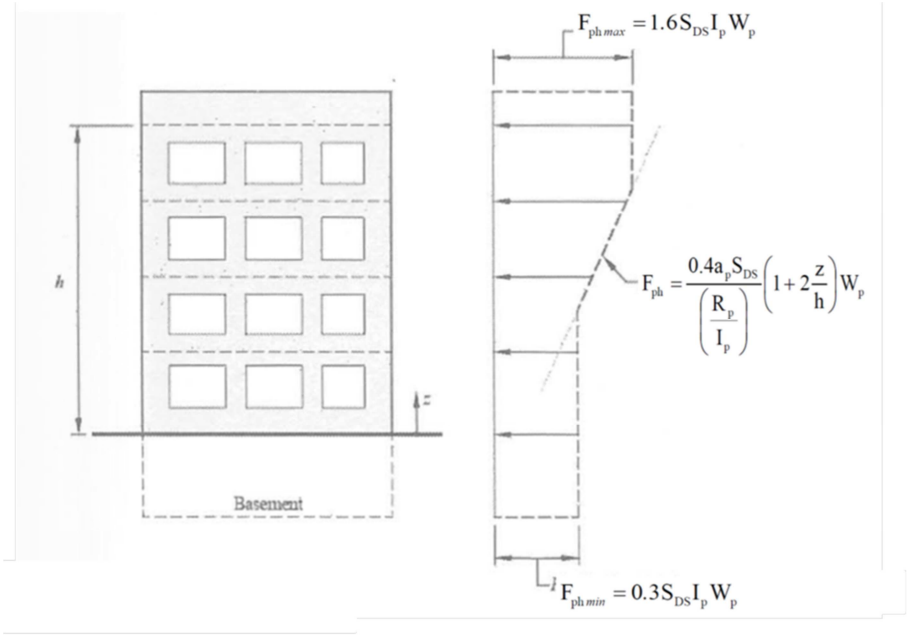

Figure 1.51 Amplification floor peak acceleration with building height (Retamales et al. 2011)

Components with importance factor of 1.5 are required to remain operational after a design earthquake, therefore they also may be subjected of seismic qualification procedures to demonstrate they are suitable when working under seismic actions. It is also required to evaluate the anchor displacements to evaluate the connection to the structural system. Furthermore detailing requirements are also provided for such components of importance according to what included in industry standards.

In section §4.3.5 of Eurocode 8 the relations to calculate the equivalent static design forces are reported, as in equations below.

$$F_a = \frac{S_a\, W_a \gamma_a}{q_a} \qquad \text{Eq. 1.10}$$

Where:

W_a	weight of the element,
S_a	seismic coefficient which includes acceleration,
γ_a	importance factor of the element (1 or 1.5),
q_a	behaviour factor of the element (1 or 2).

$$S_a = \alpha\, S \left[3 \frac{\left(1 + \frac{z}{H}\right)}{\left(1 + \left(1 - \frac{T_a}{T_1}\right)^2\right)} - 0.5 \right] \qquad \text{Eq. 1.11}$$

Where:

α	ground acceleration on type A soil over g,
S	soil factor,
z	height of the non-structural element in the structure,
H	height of the structure from the foundations,
T_a	fundamental vibration period of the component,
T_1	fundamental vibration period of the structure in the relevant direction.

In Eurocode 8 the importance factor is equal to 1.5 for anchorage elements of machinery and equipment included in systems covering a life safety function and for tanks with dangerous substances. For a comparison among the above presented standards the different nature of basic seismic parameters has to be taken into account. However the two formulations lead to a very similar result in the evaluation of the expected action applied to the component.

A fundamental guideline which it worth to be mentioned is FEMA E-74 as it includes a state-of-art report on seismic behaviour of almost every non-structural element type and it also provides practical solutions to reduce the risk which the components are typically exposed to. Some examples of technical solutions for a reduction of seismic damage to non-structural component are shown in Figure 1.52 and Figure 1.53.

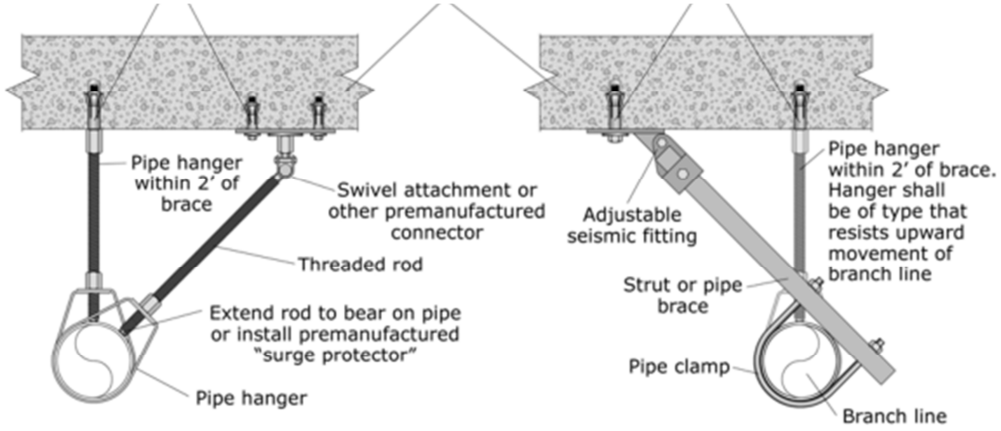

Figure 1.52 Systems for seismic damage reduction to fire suppression piping (FEMA E-74)

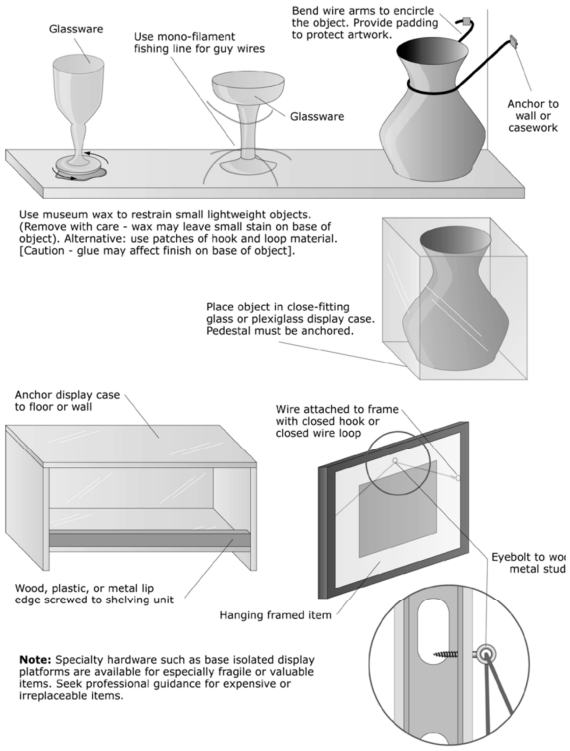

Figure 1.53 Systems for seismic damage reduction to art objects (FEMA E-74)

1.2.3. Reference Testing Experiences

As a consequence of the increased attention given to the non-structural components by lessons learned from recent events and of assessment procedure requirements indicated by standards, several experimental studies to evaluate the seismic behaviour of non-structural components were performed. In particular in the following some of the most significant are reported.

A first example of dynamic testing on non-structural components is presented in (Retamales et al. 2011) with a focus on pressurized fire suppression piping, i.e. sprinkler systems (Figure 1.54). Analyses on different damage levels, from leakage to failure, according to a shaking table test performed in University of Buffalo are reported. First leakage fragility curves, hysteretic models developed for moment-rotation response of tee joints and numerical modelling of seismic response were delivered as outcomes.

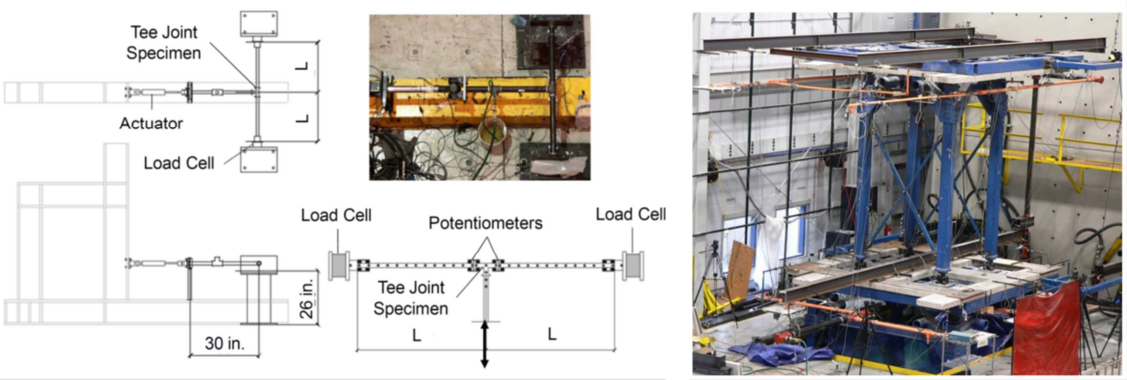

Figure 1.54 Dynamic experimental campaign on sprinkler system at Buffalo University (Retamales et al. 2011)

An in-depth experimental study on the seismic vulnerability of art objects and display cases was carried out in (Neurohr 2007) at McGill University of Montreal (Figure 1.55). In that research different museum display cases with various floor surfaces, in order to simulate the sliding or rocking behaviour, were tested under seismic condition. Before that a background work in the classification of art objects and in the generation of building floor spectra to use as table input signals were presented.

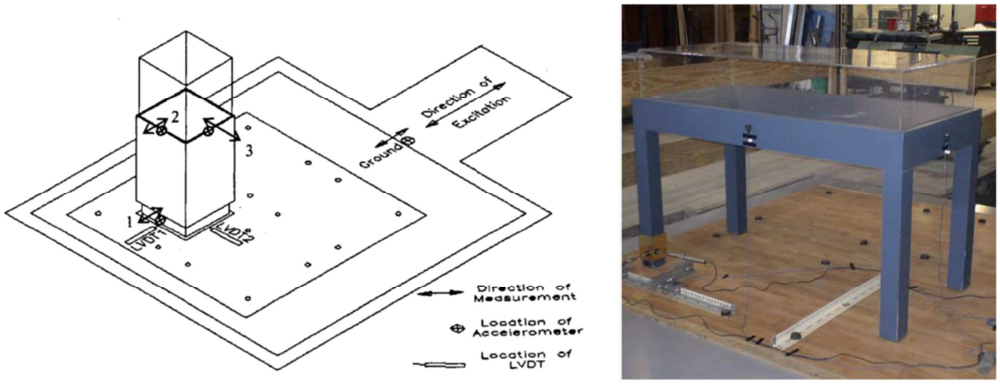

Figure 1.55 Shaking table testing on museum display cases (Neurohr and McClure 2008)

Another research taken into account for the implementation of the current work is that included in (Di Sarno et al. 2014). The work dealt with a study on the seismic response of hospital equipment by means of 63 shaking table tests (Figure 1.56). The units under testing were representative configurations of examination rooms equipped with various susceptible elements. The peak floor accelerations related to the rocking and the overturning of the cabinets were recorded respectively as values from 0.37g to 0.61g for the former and slightly over 1.00g for the latter.

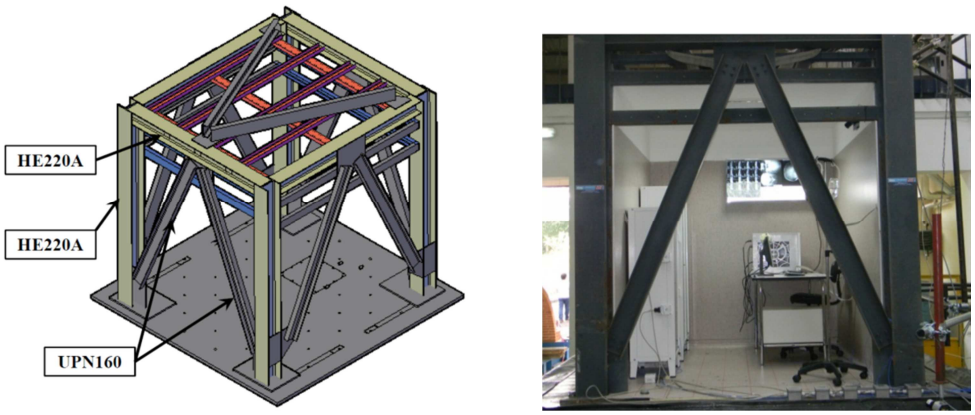

Figure 1.56 Shaking table tests on hospital equipment (Di Sarno et al. 2014)

In (Badillo-Almaraz 2003) various laboratory experiences developed at University of California on the seismic behaviour of suspended ceiling were reported. The presence and the lack of connections and bracing of the sustaining system and the undersizing or oversizing of the fastening were used as variables. The testing layout showed a support represented by a steel frame attached to the simulation table. Six different testing configurations were used.

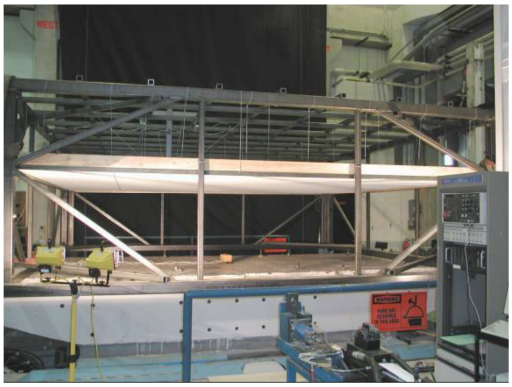

Figure 1.57 Dynamic testing on suspended ceiling panels anchored to a steel frame (Badillo-Almaraz 2003)

In (Comerio 2005) a bi-axial shaking table experimental campaigned carried out at UC Irvine on office equipment seismic response is described. Office desks and shelves were included in the configuration under testing represented by wood panels supported by a steel frame. Displacements and accelerations were recorded by means of a spatial positioning system driven by a special camera.

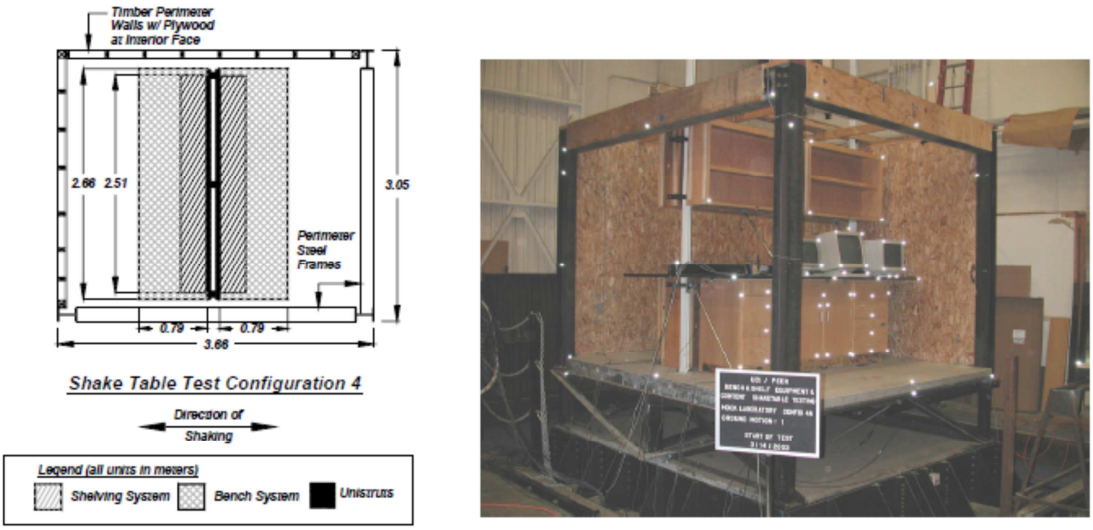

Figure 1.58 Dynamic testing on office equipment (Comerio 2005)

2. SEISMIC EXPERIMENTAL CAMPAIGN

This second section includes all the work faced in the design of a shaking table experimental campaign focused on investigating the seismic behaviour of post-installed anchors. In particular the test setup parameters selected before to carry out the testing are reported here in the following. Among all, the acceleration time histories and the design of the structural units and the fastened elements under testing were the most crucial issues.

2.1. TESTING SCOPE

The scope of the presented experimental campaign is a study on the seismic behaviour of post-installed anchors. In particular the purpose of a dynamic testing rather than a quasi-static or cyclic testing was to reproduce a real installation case of non-structural elements inside a multi-storey building. Also the choice of the reference target spectrum was related to the will of considering the structural units under testing like a portion of a building. The design target spectrum indeed included the floor spectra up to an amplification of three times of the Zero Period Acceleration, namely the peak acceleration of a rigid structure with a motion linked to the ground motion. That allowed the attached components to be thought as they were located at the top floor of a building, e.g. mechanical, hydraulic or electrical equipment in a strategic building and art objects displayed in a multi-storey museum.

Moreover the experimental study was focused on the non-structural elements fastening in the most widespread support conditions in the built environments. As a consequence of that a necessity of indications over all the different typologies of post-installed anchors and installations in different base materials was recognized. Therefore an in-depth knowledge was sought on a field of application which is not covered by any seismic assessment procedure, which currently exist only for metal anchors in concrete support. Hence also for the latter reason it was necessary to choose a dynamic and realistic testing as the best to provide some development directions, reliability judgement, design tools concerning the tested anchoring systems.

2.2. EXPERIMENTAL PROGRAMME

In this paragraph the test setup is reported, namely all the various aspects of designing a such complex experimental study. In particular the type of post-installed anchors to undergo the testing, the design of the structural units, the design of the non-structural elements, the data acquisition systems are presented here in the following.

2.2.1. Specimens Features

The whole campaign involved six products each one representing a different typology of anchor. The choice has been made taking into account the manufacturing material, the functioning principle and the resistance to static loading. A total of 38 anchor specimens, among which there are both mechanical and chemical ones, have been tested. Within the total number of anchors 23 were installed on the concrete walls and 15 on the masonry infill walls. Among the mechanical fasteners one is an undercut anchor (i.e. functioning through mechanical interlock) and a second type is represented by a metal expansion fastener. These two typologies have been both tested only on concrete.

Other two fasteners, installed both on concrete and masonry supports, are plastic expansion anchors. The first fastening element consists of a plastic sleeve passing through the fixture thickness, whereas the second one is a plastic anchor not passing through the fixture. For the chemically bonded systems one type for concrete and one for masonry applications (with the addition of a dedicated plastic sleeve) have been selected. In Table 2.1 the products under testing and their installation characteristics are summarized.

Figure 2.1 Anchoring systems under testing (ITW Construction 2013)

Table 2.1 Installation properties of anchors under testing: d0=nominal diameter; hef=effective embedment depth; dh=hole diameter

Support	Type	d_0 [mm]	h_{ef} [mm]	d_h [mm]	T_{inst} [Nm]
Concrete	Undercut	M10	60	14	40
Concrete	Metal expansion	M12	80	18	80
Concrete	Plastic expansion	10	50	10	15
Masonry	Plastic expansion	10	50	10	7
Concrete	Plastic-fibre expansion	8	50	8	3.5
Masonry	Plastic-fibre expansion	8	50	8	3
Concrete	Chemical	M16	85	18	60
Masonry	Chemical	M10	85	15	20

The mass values for the attached components are summarizes in Table 2.2 in relation to both anchor product and base material. The steel plates (i.e. masses) were fixed to the walls by means of a single anchor located in the centre.

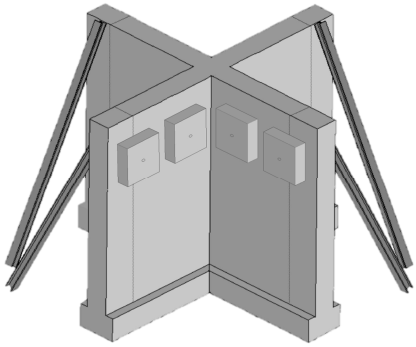

Figure 2.2 View of the concrete structural unit and location of attached components

Table 2.2 Application details for each anchor typology

Anchor Type	Base Material	Support Condition	Mass [kg]
Undercut	Concrete	Uncracked	400
		Cracked	400
Metal expansion	Concrete	Uncracked	400
		Cracked	400
Plastic expansion A	Concrete	Uncracked	200 (test1, 2) 250 (test3)
		Cracked	200 (test1, 2) 250 (test3)
Plastic expansion B	Concrete	Uncracked	85
		Cracked	85
Chemical	Concrete	Uncracked	400
		Cracked	400
Plastic expansion A	Masonry	-	85
Plastic expansion B	Masonry	-	50
Chemical	Masonry	-	200

2.2.2. Layout of Structural Units

The two structural units have been designed with a similar geometrical configuration: a cross-shaped plan with an overall length of walls of 3.75m and a height of 2.80m. The purpose has been to choose a layout that could simulate the behaviour of a portion of a building.

The concrete unit has been designed in order to allow at least two flanked fastening points to be realized on each of the four panels. On the external part of each wall a crack was induced as previously designed. This allowed the installation of the same anchor on non-cracked and cracked conditions for each wall, facilitating the direct comparison between the two cases.

The cracks on the base materials have been induced through some flat jacks placed in predefined sections in combination with conveniently shaped 3mm thick metal sheets. The

latter provision has been taken in order to reduce the RC section resistance and to drive the direction of crack opening.

As a consequence of various recommendations included in the ETAGs, cracks have been opened after the complete installation of the anchor specimens. The adopted opening values have been equal to 0.35mm and 0.80mm, respectively for plastic and metal anchors. Figure 2.3 shows the two designed structural units.

On the basis of the considered testing configuration some FE models have been developed (see §2.2.4) in order to assess the response of both structural units and anchor specimens to be tested (Mazzon et al. 2013b).

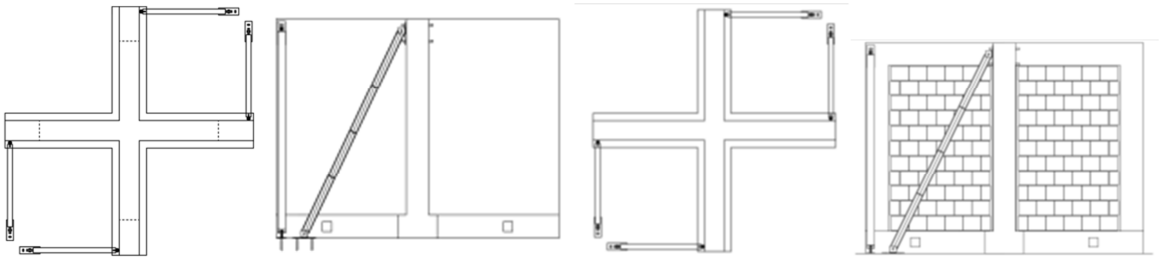

Figure 2.3 Design views of structural unit layouts under testing, see Annex A for a quoted drawing

2.2.3. Structural Design

Both the structural units which represented the support of the anchoring systems were designed according to Eurocode 8 and the current Italian standard, namely NTC 2008. In the concrete structure as in the RC frame with masonry infill walls all the verifications were done in order to allow the units uplift and repositioning onto the table and the testing sessions realization to take place without any damage which could modify the behaviour of the support walls. Moreover the oversizing for the walls reinforcements as for some of the other structural elements is justified by the need to observe clearly the specimens behaviour without the influence of structural elements damage. The structural design covered also the steel elements used in the laboratory for the moving of the structural units and the pieces which addressed the fixing of the units to the table.

Operatively some FE analyses were run to the find the design actions for both the uplift of the units (Figure 2.4), i.e. static analyses, and the seismic signals of the testing sessions, i.e. dynamic analyses (see §2.2.4). Once found the required design values several usual verifications were accomplished and the critical issues are listed in the following.

In particular for the base beams a static verification for uplift by four nodes was realized, taking into account the bending and the shear actions. The location of the lifting points was also found and the lifting steel beams were sized. Besides the dynamic verification was carried out, with regard to bending and shear actions, for the base beams as for the top beams.

Concerning the steel bracings, which were designed to stiffen the units and to fix them to the table, verifications to tension and compression and shear actions were realized. Moreover the truss buckling was checked. Finally the bolted joints and the steel structure-work were all checked by shear and bearing strength.

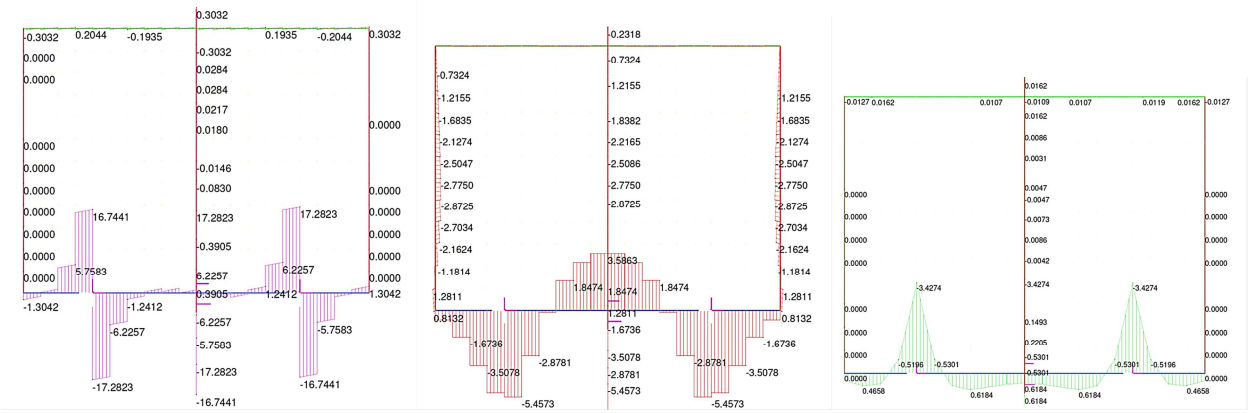

Figure 2.4 Examples of strain analyses for the verification of RC frame to the unit uplift in four points

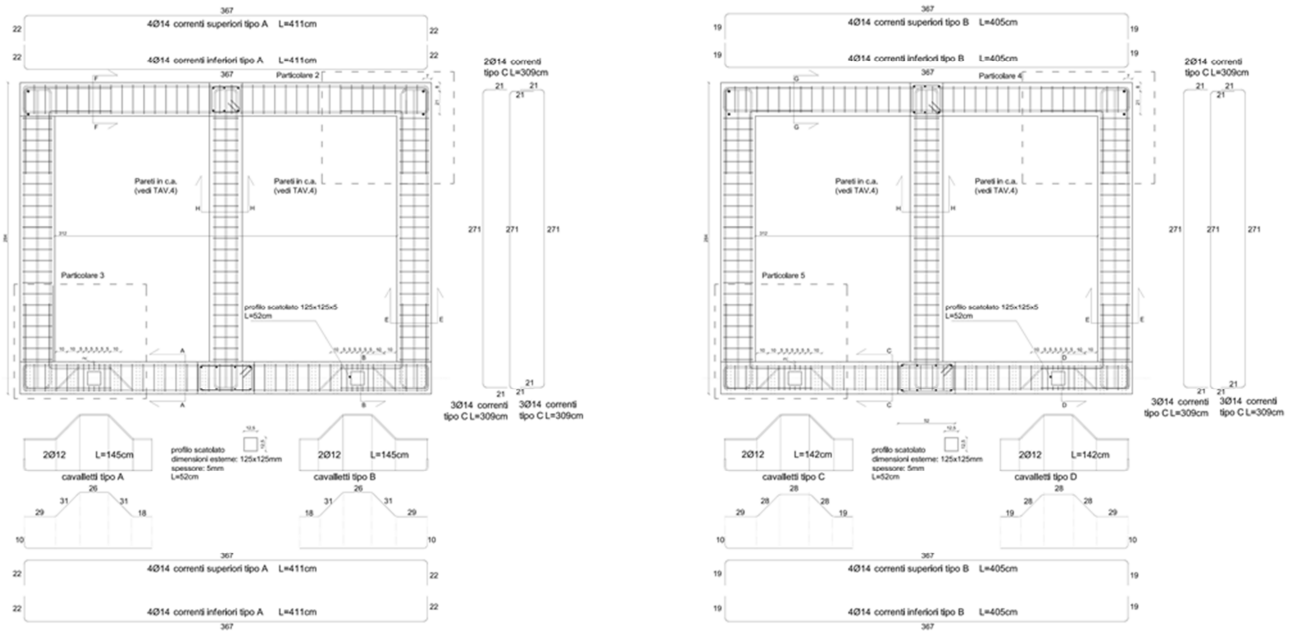

Figure 2.5 Front structural layout of the concrete unit structure

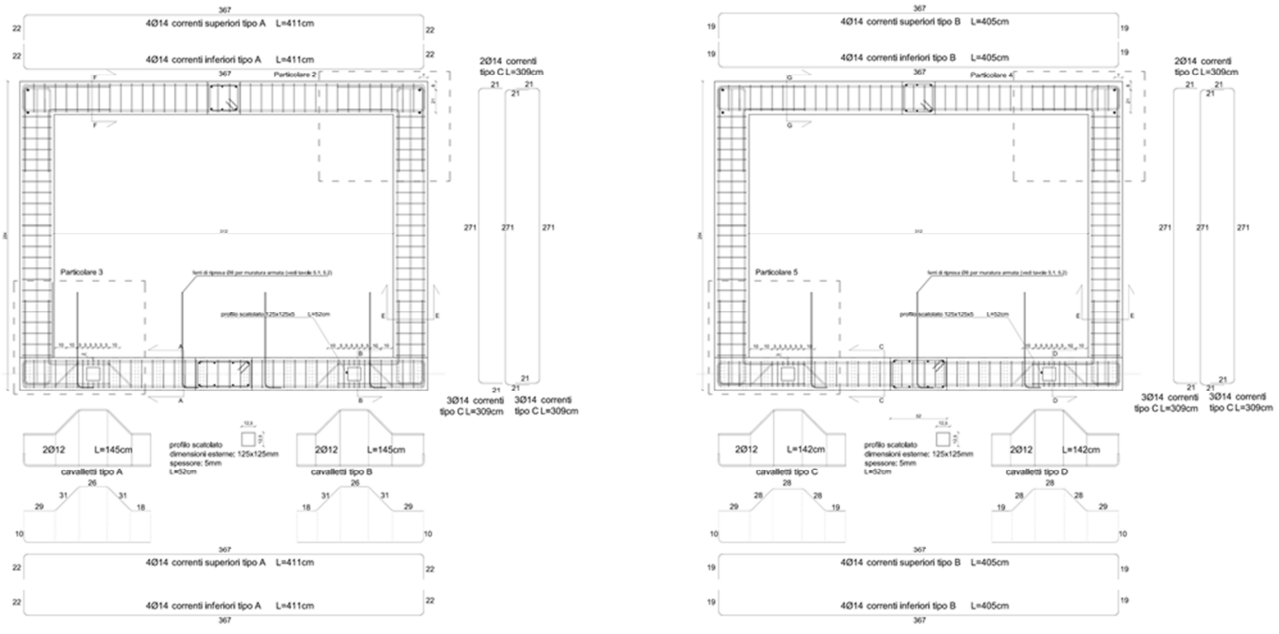

Figure 2.6 Front structural layout of the masonry infill wall unit

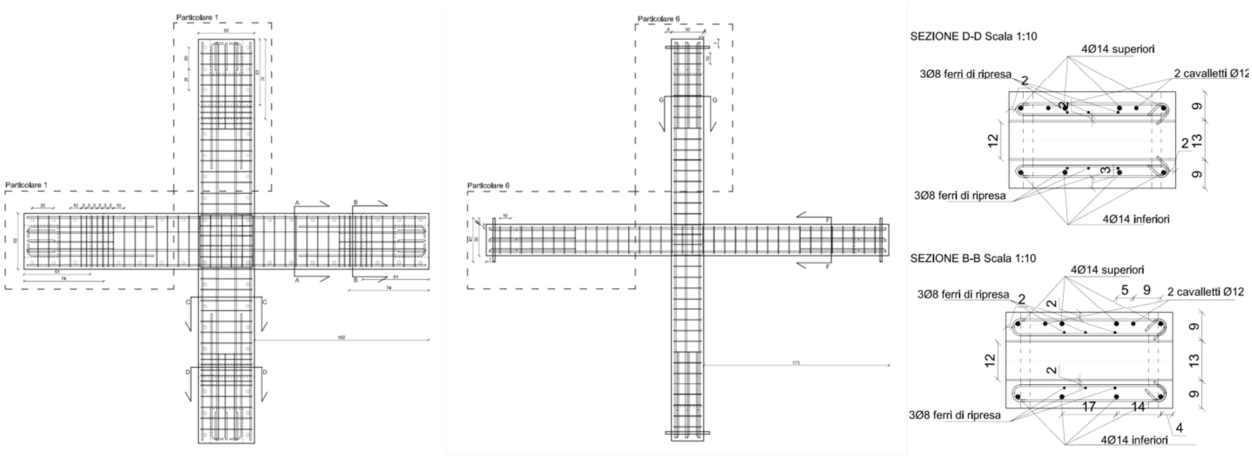

Figure 2.7 From left to right: base structural plan, top beams structural plan, sections with lifting points. These patterns were common of both the structural units

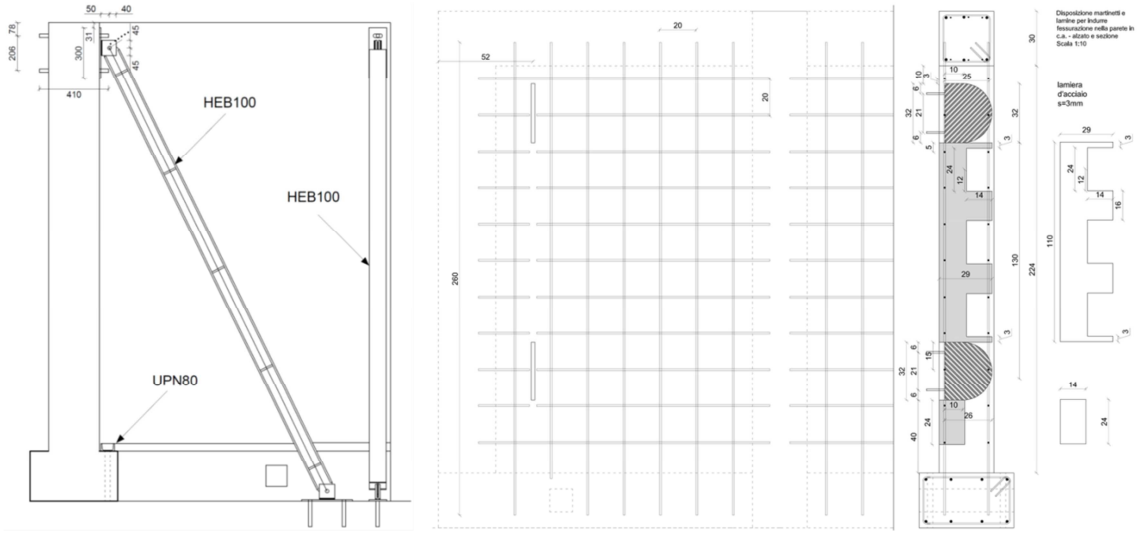

Figure 2.8 Steel bracings used to stiffen the structural unit (left); crack inducing system within concrete walls (right)

2.2.4. Modelling

The use of a finite element model in order to predict the behaviour of the testing frame has imposed the need to preliminarily evaluate the reliability of the model itself (Hoehler et al. 2009, Zienkievicz and Taylor 1989). For this purpose, different numerical simulations with a gradually increasing complexity were developed to obtain the final model, used to design the structure considered in the experimental campaign. All the numerical analyses were performed using the software Straus7[5]. This process allowed the reliability of the more basic models to be verified comparing the obtained results in terms of frequencies and mode shapes. The most important features of the structure are essentially the natural frequencies of vibration and the vibration modes that depends on the stiffness of the frame (Mazzon et al. 2013a, Chaudhuri and Hutchinson 2004). The four considered

[5] Straus7 rel. 2.3.3, G+DComputing HSH – Padova – Italy. Online: www.straus7.com

models are presented in Figure 2.9 to Figure 2.12 respectively and they are characterized by an increasing complexity.

The complete FE model consists of 3608 plates to represent the walls and 4 truss elements to simulate the influence of braces. Each steel element, fixed to the structure through the selected anchors, is modelled using a nodes with an assigned mass, positioned in the centre of gravity of the steel block, and 8 beam elements to connect these nodal masses with the surface of the support. The beam elements have been preferred to the link elements since a well calibrated stiffness do not affect the behaviour of the structure and it allows the stress in the connected nodes to be investigated.

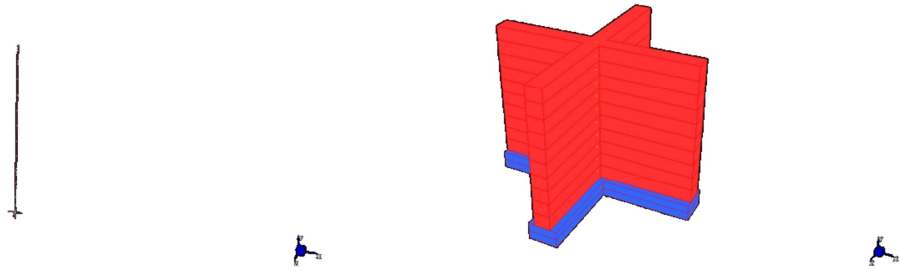

Figure 2.9 Single beam model, wireframe and solid views

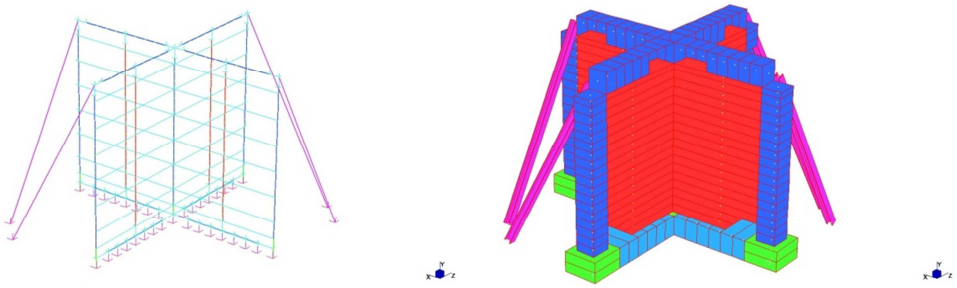

Figure 2.10 Multi beams model, wireframe and solid views

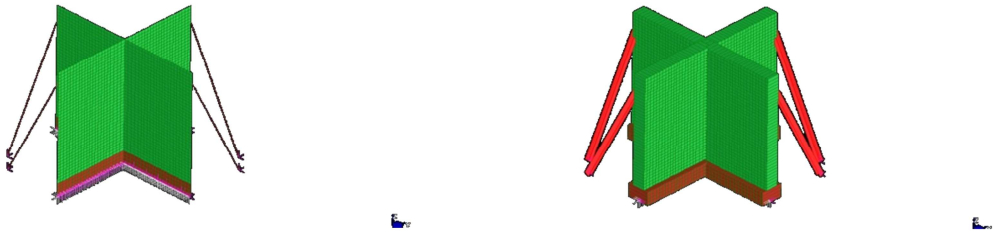

Figure 2.11 Plate model, wireframe and solid views

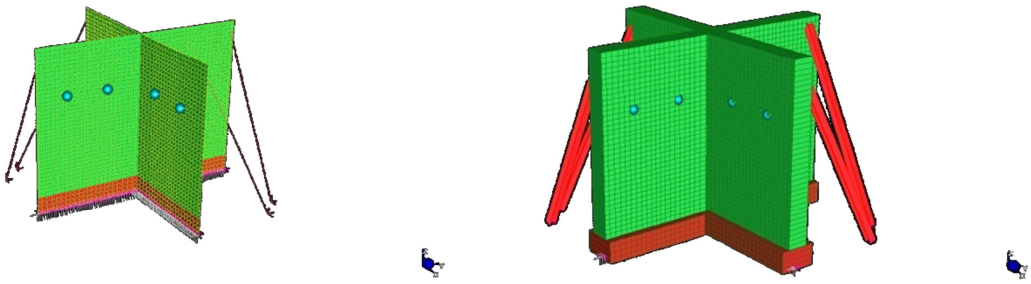

Figure 2.12 Plate model with adjunctive masses, wireframe and solid views

The first three models were considered to determine the stiffness of the structure. As Table 2.3 shows, the natural frequencies obtained from different numerical analyses are very close to each other. In this sense the more refined numerical simulation shows overall characteristics, especially in terms of stiffness, similar to those of the less complex models, so this was used for the subsequent analyses.

Table 2.3 Natural frequencies of different macro models

Mode	Single Beam Model [Hz]	Beam Model [Hz]	Plate Model [Hz]
1	35.34	58.13	59.61
2	105.19	75.49	75.38
3	125.49	77.62	78.50
4	125.49	78.89	81.01

The first design phase of the experimental campaign aimed at calibrating the values of mass to be anchored on the structure. This allowed the stress of the fastening systems to be maximized in compliance with the operating limits of the shaking table. The first considered approach was to fix the mass value for each anchor and to determine the maximum achievable level of acceleration. The computed load acting on each block was compared to the related anchor resistance, under dynamic conditions. These data allowed the verification of the fastening systems through the following normalized formulation:

$$F_{eq,adim} = \frac{N_{tot}}{N_R} + \frac{T_{xz}}{T_R} + \frac{T_{xy}}{T_R} \qquad \text{Eq. 2.1}$$

Where:

N_{tot} is the total axial force, which is the sum of: $N_{tot} = N + \frac{M_{xz}}{b_{xz}} + \frac{M_{xy}}{b_{xy}}$ with M_{xz} and M_{xy} principal moments, and b_{xz} e b_{xy} distances between the anchor and the contact point of steel block with the wall in horizontal and vertical directions;

T_{xz} is the shear force acting on the x-z plane;

T_{xy} is the shear force acting on the x-y plane;

N_R is the tensile resistance for dynamic loading;

T_R is the shear resistance for dynamic loading.

The second procedure considers the maximization of the load acting on the anchor increasing the hanged mass and allowing a reduction of the maximum attained acceleration. Comparing the results obtained from the various tests, the second approach has provided the best result.

Table 2.4 summarizes the value of hanged masses depending on each anchor type. The corresponding maximum normalized stresses are presented on the last column.

When the factor $F_{eq,\ adim}$, computed as presented in Eq. 2.1, attains the unit the maximum resistance in the element is achieved thus this corresponds to its failure. The maximum normalized stress on anchors of different types, evaluated with the global model, results less than the resistance. However this simplified model neglects some details to contain the computational effort of the FE models. In this case the strength of the anchoring systems was estimated applying an appropriate reduction factor to the static resistance. On these bases the anchors can be supposed to be failed also for ratios lower than the unit. In this sense the results presented on Table 2.4 can be considered to identify the failure of the fastenings.

Subsequently to the calibration of the anchored masses, all testing steps have been numerically simulated considering increasing levels of ZPA. As an example, Figure 2.13 shows the results obtained for a plastic expansion anchor for a ZPA equal to 0.9 g.

Furthermore, this model allowed to study the effective seismic signal acting on each anchor. Indeed the structure filters the dynamic input and this could induce some modifications on the dynamic properties of the selected time history.

Different macro models aimed at simulating the overall behaviour of a concrete structure upon which 8 steel masses are fixed with four different anchoring systems. These FE models allowed the calibration of the mass levels to be considered in the experimental program. Furthermore these analyses allowed to study the modification of the input signal from the base of the structure up to the fastening point, highlighting as any significant variation can be observed.

Table 2.4 Values of masses fixed to the structure and normalized load-strength ratios

Anchor Typology	Steel Plate [kg]	$F_{eq,adim}$ [-]
Expansion (plastic)	300	0.98
Under-cut	500	0.75
Expansion (metallic)	700	0.86
Bond	900	0.90

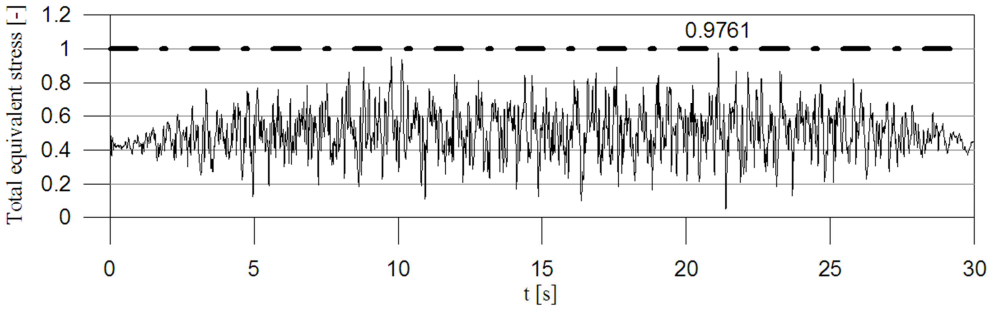

Figure 2.13 Total equivalent stress in the plastic expansion anchor for a test with a ZPA of 0.9 g

2.2.5. Anchored Elements Design

In the table below items to be tested are summarized for the two shake-table tests. Mechanical and adhesive anchors will be adopted for the test on the concrete structure. Among the mechanical fasteners one metal expansion anchor and one plastic expansion anchor –both functioning by friction-, and an undercut anchor -functioning by geometrical interlock- will be under testing. For the second test different types of plastic expansion fasteners and a chemical anchor will be tested. The size of connection elements is chosen in order to obtain similar resistance levels, considering also the possibility to change the embedment depth.

Once defined geometric and mechanical characteristics of fasteners to be tested, it is necessary to find out the correct weight of the attached elements. Maximum values will come up after the calculation of seismic actions affecting the connections by going backwards into standards relations. Indeed the upper bound of mass for each fastening system that satisfy tension, shear and combined loads verification will be found out.

Typical applications for the chosen fasteners are from furniture elements to rack structures (shelves) or structural nodes. The testing masses will be made of steel plates in order to investigate the effective strength of anchors , avoiding damages to the connections because of a weakness on the anchoring point in the attachment.

Considerations after testing will be made about relating the results to real typical applications. The relations proposed in the Eurocode 8 have been used in order to calculate the force acting on an attached element at a certain height of the building, which is similar to what is presented in ASCE 7-10 (§13.3.1). Hence the dimensions of the masses are established by using the relation for calculation of seismic actions applied to the attachment according to §4.3.5 in Eurocode 8 (and Italian NTC 2008, §7.2.3), as reported in §1.2.2 of this document. Where F_a is the horizontal force acting on the centre of mass of each non-structural component, W_a is the component weight and S_a is the maximum acceleration amplified by the structure when an earthquake occurs according to the considered limit state. Partial safety factors q are not used in this study because the scope is to manage the ultimate strength. In a real condition, the acceleration acting on the attachment depends on its location –in terms of height- inside the building, the seismic hazard of the area and the ratio between the period of attachment over the period of the structure. It shall be calculate by the following relation.

As shown in the table below the strength verifications are according to TR 045 assuming that $\frac{N_{sd}}{N_R} + \frac{V_{sd}}{V_R} = 1$ in order to find out the weights of masses to be attached.

Table 2.5 An example of anchorage calculation for a given acceleration level according to regulations

ANCHORAGE DESIGN					ENEA shake-table test							
Norme Tecniche per le Costruzioni 2008 - Calcolo dell'accelerazione spettrale per elementi non strutturali												
place:		soil:	$F_a = (S_a \cdot W_a)/q_a$							*vibration periods*		
ag	0.35	g		**Sa**	0.673504	g		*non-structural component*	Ta	0		
S	1							*building*	T1	1		
z/h	0.6161972	m	$S_a = \alpha \cdot S \cdot \left[\frac{3 \cdot (1 + Z/H)}{1 + (1 - \frac{T_a}{T_1})^2} - 0{,}5\right]$									
z	1.75	m										
h	2.84	m										
U.S. standards on non-structural components												
IEEE 693				*damping*	5	%						
ag	0.5	g	*high required RS*	**Sa,max**	1.25	g				ag	0.269404	g
β	0.9999916		*moderate required RS*	**Sa,max**	0.624995	g				Sa	0.673504	g
IEEE 693				*damping*	2	%				ag	0.208111	g
ag	0.5	g	*high required RS*	**Sa,max**	1.62	g				Sa	0.673504	g
β	1.2945074		*moderate required RS*	**Sa,max**	0.809067	g						
AC 156												
ag	0.2694014	g										
Sa	0.6735035	g										
anchor capacity			anchor type: expansion **T101 PIOVRA**	**M10**								
Nuk	11.11	kN		**Wa**	300	kg						
Vuk	14.11	kN		**Forizz**	1.981313	kN		*Forizz out-of-plane*	Vtot	4.52685	kN	
seismic reduction factor	0.75			**Fvert**	1.58505	kN		*Forizz in-plane*	Vmax	4.941454	kN	
Nuk,dyn	8.3333333	kN	*tensile/shear combination*	**T**	0.704814	<1		**PASS**				
Vuk,dyn	10.58	kN	*tension*	**N**	0.237758	<1		**PASS**				
			shear	**V**	0.467056	<1		**PASS**				
anchor capacity			anchor type: expansion **FIX Z**	**M10**								
Nuk	10.67	kN		**Wa**	300	kg						
Vuk	12.00	kN		**Forizz**	1.981313	kN		*Forizz out-of-plane*	Vtot	4.52685	kN	
seismic reduction factor	0.75			**Fvert**	1.58505	kN		*Forizz in-plane*	Vmax	4.941454	kN	
Nuk,dyn	8	kN	*tensile/shear combination*	**T**	0.796715	<1		**PASS**				
Vuk,dyn	9	kN	*tension*	**N**	0.247664	<1		**PASS**				
			shear	**V**	0.54905	<1		**PASS**				
anchor capacity			anchor type: expansion **TRIGA Z**	**M10**								
Nuk	10.67	kN		**Wa**	300	kg						
Vuk	18.56	kN		**Forizz**	1.981313	kN		*Forizz out-of-plane*	Vtot	4.52685	kN	
seismic reduction factor	0.75			**Fvert**	1.58505	kN		*Forizz in-plane*	Vmax	4.941454	kN	
Nuk,dyn	8	kN	*tensile/shear combination*	**T**	0.602654	<1		**PASS**				
Vuk,dyn	13.92	kN	*tension*	**N**	0.247664	<1		**PASS**				
			shear	**V**	0.35499	<1		**PASS**				
anchor capacity			anchor type: adhesive **EPCON C8**	**M16**								
Nuk	13.04	kN		**Wa**	300	kg						
Vuk	15.65	kN		**Forizz**	1.981313	kN		*Forizz out-of-plane*	Vtot	4.52685	kN	
seismic reduction factor	0.75			**Fvert**	1.58505	kN		*Forizz in-plane*	Vmax	4.941454	kN	
Nuk,dyn	9.7791667	kN	*tensile/shear combination*	**T**	0.623692	<1		**PASS**				
Vuk,dyn	11.735	kN	*tension*	**N**	0.202605	<1		**PASS**				
			shear	**V**	0.421087	<1		**PASS**				

2.2.6. Data Acquisition Systems

Two equipment were adopted to monitor the relevant quantities during the test campaign and they are presented in the following. A first acquisition system recorded data from traditional sensors (accelerometers and displacement sensors) while a second innovative optical equipment monitored the displacements of significant points.

The first acquisition system monitored the following quantities in order to establish the damage increment and the failure modes of fastenings by evaluating the dynamic properties of fixtures. Two quantities were monitored with different aims:

- Displacements (Figure 2.14 and Figure 2.15): slipping of the fastener from the base material; crack opening (on concrete structure only); overall movements of the structure.
- Accelerations in all the principal directions with three unidirectional accelerometers (Figure 2.14 and Figure 2.16) for each survey point; this allows to compute the loads acting on the anchors and to identify the dynamic properties of both the structure and the fixtures after every seismic step. Moreover the acceleration at the table level was recorded to define the real dynamic input.

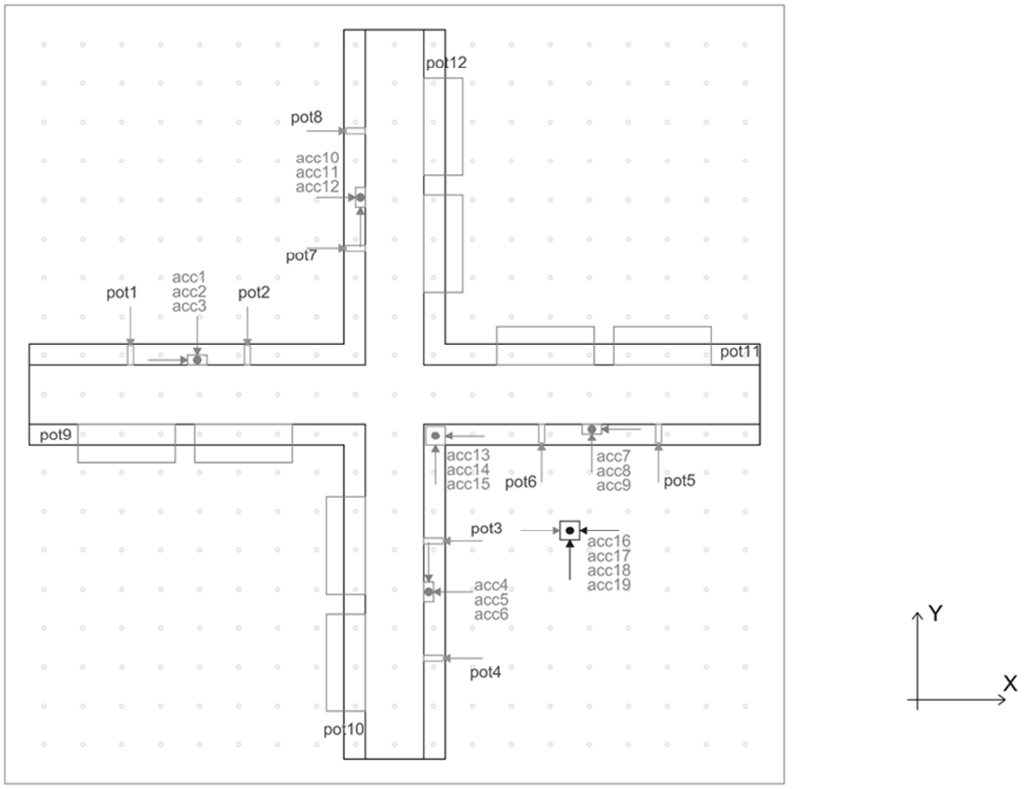

Figure 2.14 Acquisition system 1: Example of the setup (see §3.1.1 and §4.1.1)

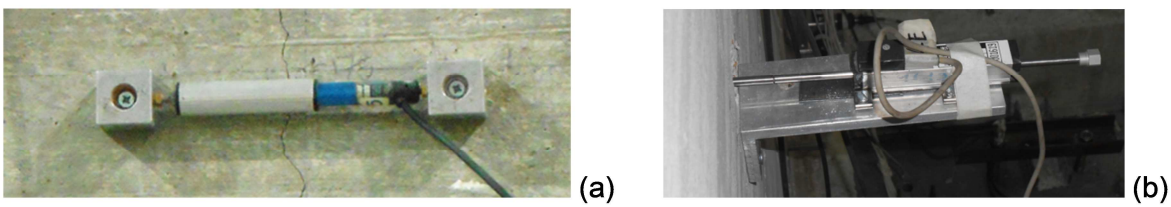

Figure 2.15 Examples of displacement sensors to monitor the crack opening (a) and the slip of anchors (b)

Figure 2.16 Example of acceleration sensors installed on the wall surface opposite to that of anchor installation

Table 2.6 Instrumentation in test session 2 (devices for other test sessions are listed in §3.1.1 and §4.1.1 of this document)

No.	Name	Captured quantity	Units	Specimen	Wall	Measurement range	Manufacturer
1	acc1	-Z_Acceleration	g	MEC	8	0.50g	PCB Piezotronics
2	acc2	+X_Acceleration	g	MEC	8	0.50g	PCB Piezotronics
3	acc3	-Y_Acceleration	g	MEC	8	0.50g	PCB Piezotronics
4	acc4	-Z_Acceleration	g	AC	3	0.50g	PCB Piezotronics
5	acc5	-Y_Acceleration	g	AC	3	0.50g	PCB Piezotronics
6	acc6	-X_Acceleration	g	AC	3	0.50g	PCB Piezotronics
7	acc7	-Z_Acceleration	g	UC	4	0.50g	PCB Piezotronics
8	acc8	-X_Acceleration	g	UC	4	0.50g	PCB Piezotronics
9	acc9	+Y_Acceleration	g	UC	4	0.50g	PCB Piezotronics
10	acc10	-Z_Acceleration	g	PEC	7	0.50g	PCB Piezotronics
11	acc11	+Y_Acceleration	g	PEC	7	0.50g	PCB Piezotronics
12	acc12	+X_Acceleration	g	PEC	7	0.50g	PCB Piezotronics
13	acc13	-Z_Acceleration	g	-	base	0.50g	PCB Piezotronics
14	acc14	-X_Acceleration	g	-	base	0.50g	PCB Piezotronics
15	acc15	+Y_Acceleration	g	-	base	0.50g	PCB Piezotronics
16	acc16	-X_Acceleration	g	-	Table	0.50g	PCB Piezotronics
17	acc17	+X_Acceleration	g	-	Table	2.50g	PCB Piezotronics
18	acc18	+Y_Acceleration	g	-	Table	2.50g	PCB Piezotronics
19	acc19	-Z_Acceleration	g	-	Table	2.50g	PCB Piezotronics
20	pot1	-Y_Displacement	mm	MEC4	8	50mm	**novo**technik
21	pot2	-Y_Displacement	mm	MEC3	8	50mm	**novo**technik
22	pot3	-X_Displacement	mm	AC3	3	50mm	**novo**technik
23	pot4	-X_Displacement	mm	AC4	3	50mm	**novo**technik
24	pot5	+Y_Displacement	mm	UC4	4	50mm	**novo**technik
25	pot6	+Y_Displacement	mm	UC3	4	50mm	**novo**technik
26	pot7	+X_Displacement	mm	PEC3	7	50mm	**novo**technik
27	pot8	+X_Displacement	mm	PEC4	7	50mm	**novo**technik
28	pot9	-X_Displacement	mm	crack1	1	25mm	penny&gilles
29	pot10	+Y_Displacement	mm	crack2	2	25mm	penny&gilles
30	pot11	-X_Displacement	mm	crack3	5	25mm	penny&gilles
31	pot12	-Y_Displacement	mm	crack4	6	25mm	penny&gilles

The second equipment has consisted of an optical system (*3D-Vision*) which allowed the displacement of about 80 points to be monitored. As a general layout each steel mass was monitored through four markers placed at the corners. This allowed the overall displacement and the rotation of the plates to be recorded and computed. An additional marker was fixed in the centre as an indicator of the anchor slip. Two more markers were installed on the support over the plates. In the cases of anchors installed on cracked support these two markers were installed over the crack to monitor its opening variation as well as the displacement of the support.

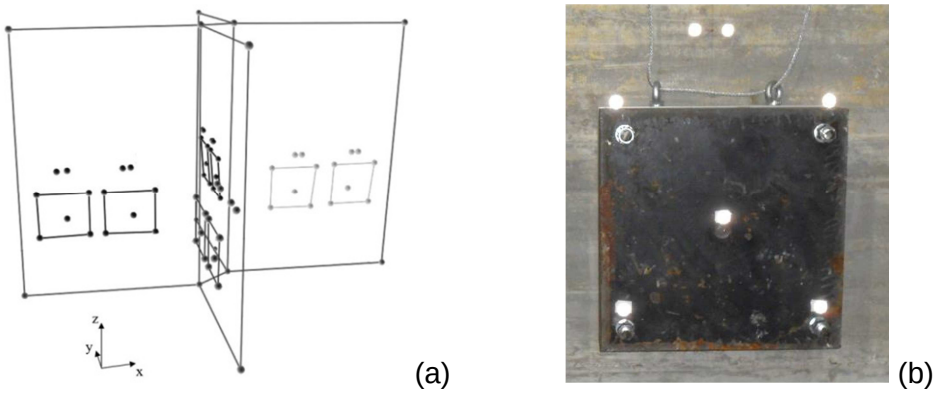

(a) (b)

Figure 2.17 General view of the testing layout through the optical spatial positioning system *3D-Vision* (a) and example of marker disposal for each mass (b)

Figure 2.18 Marker location in the concrete testing configuration

2.3. INPUT SIGNAL

The state-of-art presented on previous chapters highlights as there is no normative issue that provides either requirements or recommendation specifically for testing anchors on shaking table. As a consequence some other standards are taken into account. The norms which may be considered to mainly concern the scope of this experimental campaign is issued by ICC-ES and deals with the dynamic certification of non-structural components (AC156 2010). These Acceptance Criteria consist in procedures of mandatory assessment by shake table testing for specific important equipment according to ASCE7-10 (§13.3.1) (likely widespread in large importance buildings as nuclear plants, hospitals, museums, etc.). A tri-axial input is required, provided that it had been generated on the basis of a synthetic response spectrum, with a frequency content between 1.3Hz and 33.3 Hz. The signal shall represent a build-hold and decay curve in order to simulate the non-stationary feature of earthquakes and this reflects in an overall duration of 30 seconds composed by at least 20 seconds of strong motion. To create the RRS (Required Response Spectrum) it is necessary to respect the following relations according to section §6.5 of the document.

$$F_{ph} = \frac{0.4\, a_p S_{DS}}{\left(\frac{R_p}{I_p}\right)}\left(1 + 2\frac{z}{h}\right) W_p \qquad \text{Eq. 2.2}$$

$$A_{FLX-H} = S_{DS}\left(1 + 2\frac{z}{h}\right) \qquad A_{RIG-H} = 0.4 S_{DS}\left(1 + 2\frac{z}{h}\right) \qquad \text{Eq. 2.3}$$

$$A_{FLX-V} = 0.67 S_{DS} \qquad A_{RIG-V} = 0.27 S_{DS} \qquad \text{Eq. 2.4}$$

With:

R_p/I_p = 1; $0 < z/h < 1$; $1 < a_p < 2.50$;

$S_{DS} = 2/3 * S_{MS}$; $S_{MS} = Fa * S_S$ (values from ASCE7-10).

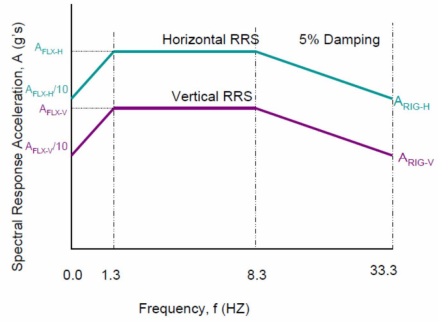

Figure 2.19 Required Response Spectrum provided by AC156 2010

The dynamic loading of the test will be applied as an acceleration signal generated by the software SIMQKE (NISEE 1976) from a target spectrum to choose among standards. The input time history will be scaled on the basis of its PGA (Peak Ground Acceleration, or the spectral acceleration at short period, namely T < 0.2s) in order to evaluate specimens under increasing steps of seismic amplitude so that it becomes easy to recognize the level which lead to failure. Besides performing the test in such a way allows to observe different damages and the displacement of the anchorage relating to the shaking level.

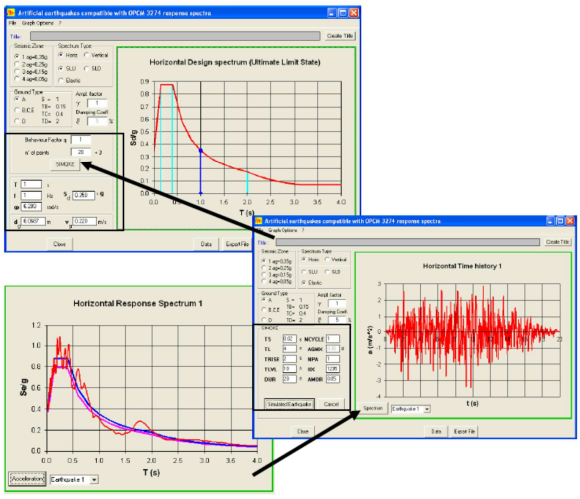

Figure 2.20 SIMQKE interface (NISEE 1976)

Considering that a tri-axial motion will be input to the table (two horizontal components and the vertical one) by means of time histories with 20 seconds of strong motion, it will be quite severe for the whole system under testing, including fastenings.

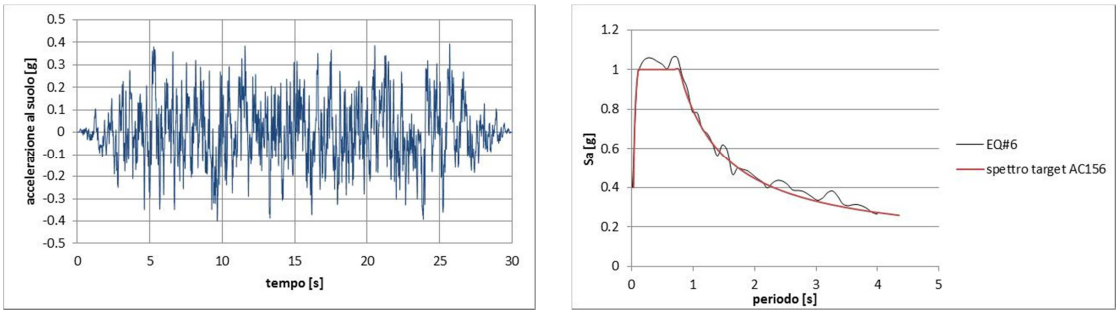

Figure 2.21 Time history (left); generated acceleration spectrum versus target spectrum (right)

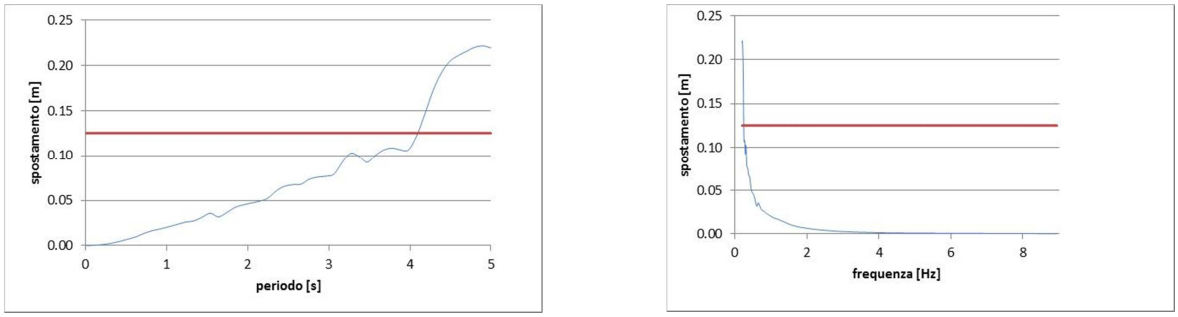

Figure 2.22 Displacement spectra over period (left) and frequency (right)

The signal that will be applied to the shaking table has been generated with SIMQKE matching the spectrum obtained according to requirements of AC156. The figures below show the time history scaled to a PGA of 0.4g for all the three direction of motion referring to both acceleration and displacement.

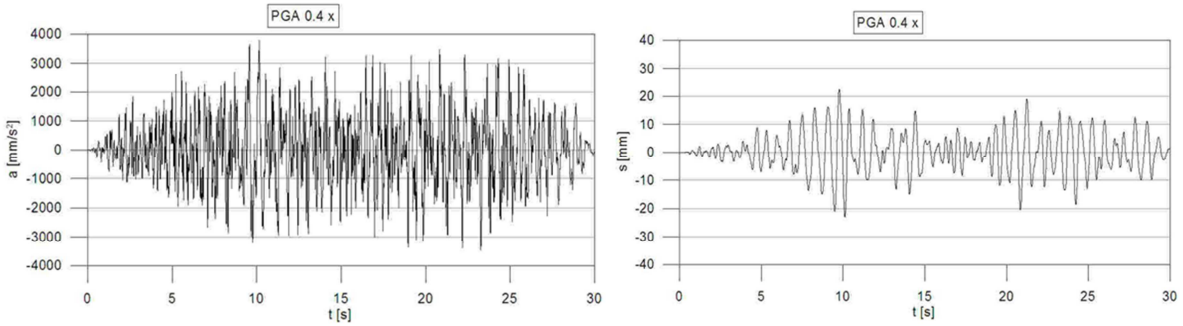

Figure 2.23 Time history for acceleration and displacement in X-direction scaled with a PGA of 0.4g

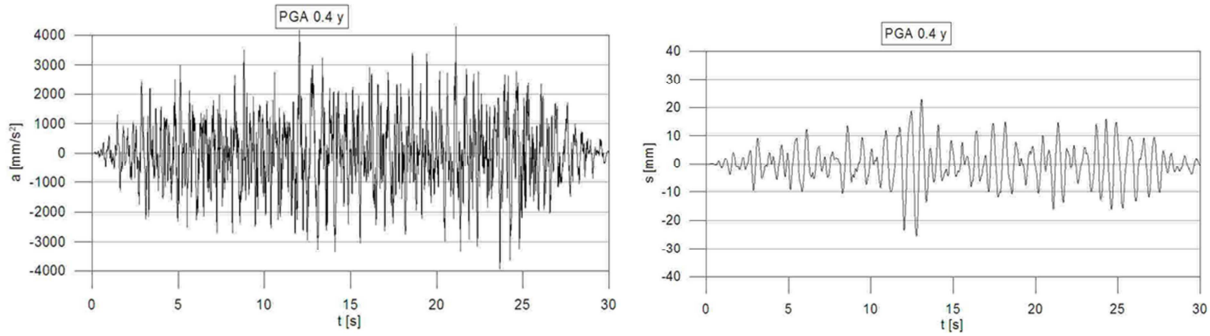

Figure 2.24 Time history for acceleration and displacement in Y-direction scaled with a PGA of 0.4g

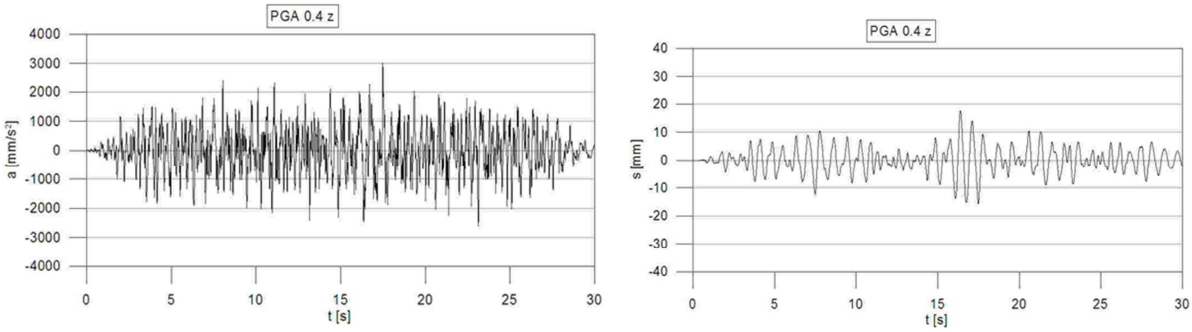

Figure 2.25 Time history for acceleration and displacement in Z-direction scaled with a PGA of 0.4g

The generation of seismic signal to be adopted as input motion for the shake table testing has been based on the requirements included in the US standard issued by ICC-ES for the seismic qualification of non-structural elements (AC156 2010). This standard has been chosen considering the absence of specific regulations and guidelines for the seismic assessment of anchors through shake-table and its remarkable closeness to the dealt topic. According to the above mentioned document a tri-axial shake-table testing has been designed, with the generation of three incoherent artificial acceleration signals in relation to both horizontal (*x*, *y*) and vertical directions (*z*). The installation of the specimens has been made according to EOTA guidelines for metal anchors (ETAG 001 2013), for plastic anchors (ETAG 020 2012) in concrete and for adhesive anchors in masonry (ETAG 029 2013).

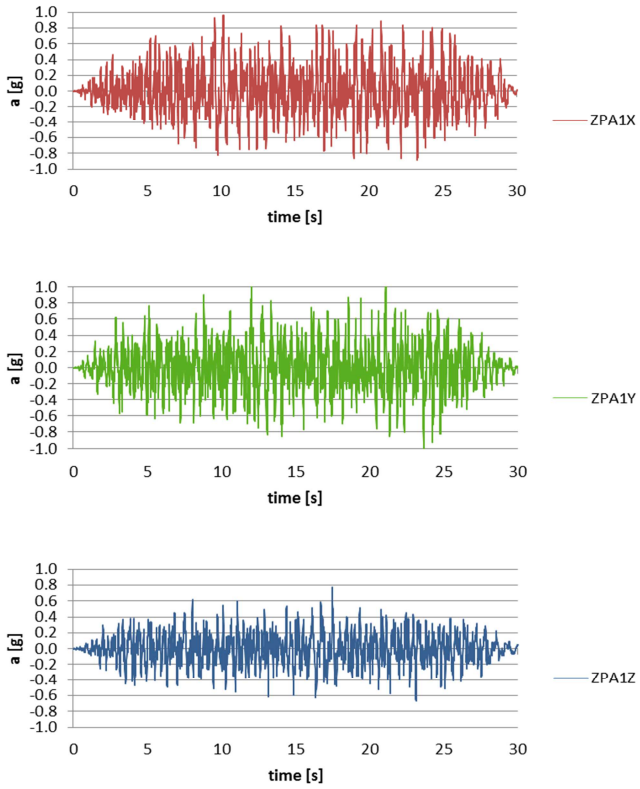

Figure 2.26 Input time histories generated according to AC156 (2010) in the three main axes

Some comparison analyses among the generated time histories and the related response spectra, according to different generation software and reference standards, were carried out before selecting the time history input signal of the testing. It was important to notice that signals generated through SIMQKE software had the higher

matching between RRS and TRS. Moreover AC156 allows the achieved spectrum to match with a larger tolerance around the indicated reference curve than other standard taken into account.

Other considered programmes, Belfagor and RSCTH, demonstrated to be able to reproduce signals more adherent to the real earthquake records. That came out from the observation of the elastic spectrum and from the trend of ground motion energy, i.e. Arias intensity. Although it was difficult to obtain time histories able to match the target spectrum of standards.

Attention had to be paid in the parameters selection for the programmes in order to generate accelerograms with admissible features according to reference standards.

For this research project it was chosen to use SIMQKE, considering the limit PGA value which matches precisely the reference prescriptions. Besides that is the only software which shows a signal outline subdivided into build, hold and decay phases as required by the AC156 standard.

2.4. TESTING FACILITY

The main purpose of this testing campaign is to evaluate the dynamic behaviour of post-installed fasteners in terms of mechanical resistance and failure modes for application on both masonry and concrete elements (cracked and non-cracked). The experimental study will be performed in the larger among the two shake-table of the laboratory. The features of the test rig are presented in Table 2.7 and the limitations imposed to specimens in terms of geometry and weight.

The testing system used for the here presented experimental campaign is the greater shaking table among the two included in the Laboratory of Structural Dynamics and Vibration Monitoring at ENEA Research Centre in Casaccia, Rome. The system characteristics determined the limits for the design of the structural units and the mass of the anchored elements under testing. Considering the Table 2.7 the geometrical limits and the maximum structural units weights were easily found.

It was of importance to focus on the maximum overturning moment and the maximum vertical load bearable by the table. On the basis of the selected mass of the attached elements and the centre of gravity height of the structural member, the maximum peak acceleration to apply was defined.

The vertical capacity of the table is about 20 tons, hence it was decided to limit the overall weight of the concrete structural unit to undergo the dynamic testing sessions to 15 tons and taking into account the maximum overturning moment of the table. This latter value was calculated equal to 300 kNm, which can be exemplified as a 10 tons weight with the centre of gravity located at a one meter height with a peak acceleration of 3g.

Plan dimensions of the table are 4m x 4m. Considering the necessity to fix the structure to the steel plate of the table with an efficacious blocking system, the structural units were designed to stay fully inside the cut-out of the table. Structural units were thought to be fixed to the table in order to reproduce a joint condition and transfer completely the input signals to the structure.

Table 2.7 Shake-table testing system characteristics

A.10.3. Shaking table description

Type of Shaking Table

	Longitud. X	Lateral Y	Vertical Z	Pitch	Roll	Yaw
Uniaxial						
Biaxial						
Multiaxial	**YES**	**YES**	**YES**	**YES**	**YES**	**YES**

Characteristics of the Platform

Size (m×m) : **4×4** Weight (kN) : **100** Material : **Aluminium**

Type of Actuation

Characteristics of the Actuators

	Manufacturer	Total Force (kN)	Number of units
Horizontal	**MTS**	**640 + 640**	**2 (X) + 2 (Y)**
Vertical	**MTS**	**1460**	**4**

Shaking Table Performances

Frequency Range			Hz	**0÷50**
Stroke	Horizontal		mm_{pp}	**250**
	Vertical		mm_{pp}	**250**
Max Velocity	Horizontal		m/s	**0,78**
	Vertical		m/s	**0,78**
Max Acceleration at bare table	Horizontal	harmonic	m/s^2	**49**
		impulse	m/s^2	**78**
	Vertical	harmonic	m/s^2	**49**
		impulse	m/s^2	**78**
Yaw	Rotation degrees		°	**±4,70**
	Velocity		rad/s	**±0,3**
Pitch/Roll	Rotation degrees		°	**±4,70**
	Velocity		rad/s	**±0,3**
Max Overturning Moment			kN×m	**450**
Max Specimen Dead Weight			kN	**300**
Max Compensated Dead Weight			kN	**300**

A.10.4. Characteristics of the Control System

Type of Control

Analogue	Digital	**Mixed**

Characteristics of the Analogue Part

Manufacturer	**MTS**
Type	**469a**

Characteristics of the Digital Part

Hardware	Computer	**Compaq**
	D/A Channels	**6 channels**
	A/D Channels	**32 channels**
Software	Designer	**STEX-MTS**

Controlled motions	Sinusoidal	Random	Shock	Seismic
Controlled Channels	**6**	**6**	**6**	**6**
Acquisition Channels	**32**	**32**	**32**	**32**

A.10.5. Complementary facilities

Floating Foundation

Dimensions (m×m)	**8×8**
Weight (kN)	**10200**
Natural Freq. (Hz)	**0,5**

Hydraulic System

Electric Power (kW)	**950**
Flow Rate (l/min)	**670**
Pressure (MPa)	**21**

Bridge Cranes Capacity

No. of Cranes	**2**
Max Load (kN)	**100**
Useful Height (m)	**9,0**

	MASTER	CHILD
Dimensioni	4m x 4m	2m x 2m
Gradi di Libertà	6	6
Frequenza	0-50 Hz	0-100 Hz
Accelerazione	3g Peak	5g Peak
Velocità	0.5 m/s (0-Peak)	1 m/s (0-Peak)
Spostamento	0.25 m (0-Peak)	0.30 m (0-Peak)
Peso Campione Overturning	10 ton (3g peak) 300 KN x m	1 ton (5g peak) 50 KN x m
Potenza Installata Portata Pressione	950 KW 670 l/min 210 Mpa	

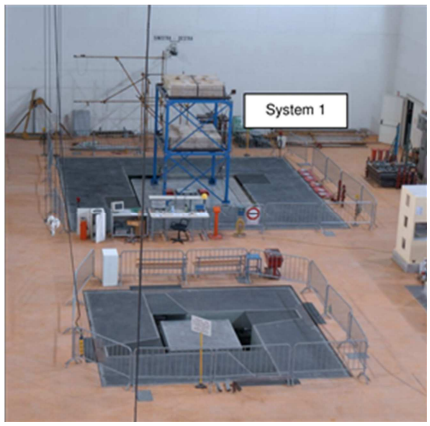

Figure 2.27 Shaking-table facility at ENEA labs, Rome (Italy)

3. SHAKING TABLE TESTS IN CONCRETE

In this chapter the shaking table tests results of post-installed anchors installed in non-cracked and cracked concrete are presented (Figure 3.1). First facts about the test setup for the concrete structural unit are reported. Subsequently, the testing sessions realization and the data processing analyses are described. Finally the test results divided by specimens are listed in the last part of the section.

Figure 3.1 Views of the concrete structural unit under testing

3.1. TEST SETUP

The instrumentation patterns for the three test sessions and the testing plan, namely a list of all the input signals given to the table in the test sessions for the concrete structural unit are presented within this paragraph.

3.1.1. Instrumentation

In the concrete test sessions the structural unit walls, the anchor specimens and the cracks were instrumented through the data acquisition systems presented in §2.2.6. Accelerations and displacements were monitored in order to register the dynamic behaviour of the attached components as well as the structural parts and the anchoring systems under testing. The seismic loading, namely a combination of shear and tension forces, referred to the relative slipping of the specimens would allowed an evaluation of their behaviour in critical conditions.

In test session 1 as shown in Figure 3.2 and Table 3.1, a total of fifteen unidirectional accelerometers was mounted, among which three were placed on the table and the remaining were installed on the walls. Moreover twelve potentiometers were used to measure displacements of each specimen and the crack width on the four walls.

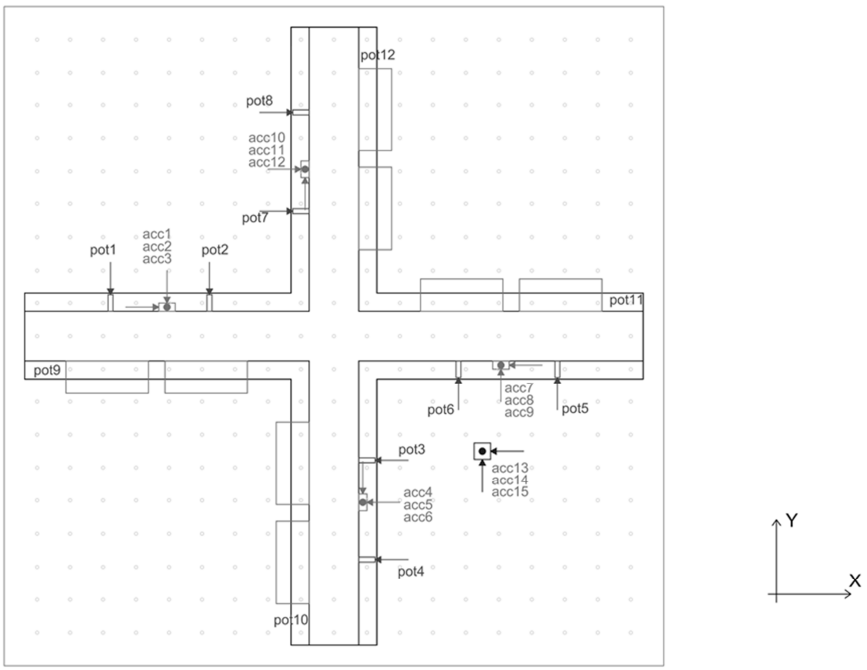

Figure 3.2 Setup instrumentation for TS1; system 1

Table 3.1 Instrumentation adopted in test session 1

No.	Name	Captured quantity	Units	Specimen	Wall	Measurement range	Manufacturer
1	acc1	-Z_Acceleration	g	MEC	8	0.50g	PCB Piezotronics
2	acc2	+X_Acceleration	g	MEC	8	0.50g	PCB Piezotronics
3	acc3	-Y_Acceleration	g	MEC	8	0.50g	PCB Piezotronics
4	acc4	-Z_Acceleration	g	AC	3	0.50g	PCB Piezotronics
5	acc5	-Y_Acceleration	g	AC	3	0.50g	PCB Piezotronics
6	acc6	-X_Acceleration	g	AC	3	0.50g	PCB Piezotronics
7	acc7	-Z_Acceleration	g	UC	4	0.50g	PCB Piezotronics
8	acc8	-X_Acceleration	g	UC	4	0.50g	PCB Piezotronics
9	acc9	+Y_Acceleration	g	UC	4	0.50g	PCB Piezotronics
10	acc10	-Z_Acceleration	g	PEC	7	0.50g	PCB Piezotronics
11	acc11	+Y_Acceleration	g	PEC	7	0.50g	PCB Piezotronics
12	acc12	+X_Acceleration	g	PEC	7	0.50g	PCB Piezotronics
13	acc13	-Z_Acceleration	g	-	Table	0.50g	PCB Piezotronics
14	acc14	-X_Acceleration	g	-	Table	0.50g	PCB Piezotronics
15	acc15	+Y_Acceleration	g	-	Table	0.50g	PCB Piezotronics
16	pot1	-Y_Displacement	mm	MEC2	8	50mm	**novo**technik
17	pot2	-Y_Displacement	mm	MEC1	8	50mm	**novo**technik
18	pot3	-X_Displacement	mm	AC1	3	50mm	**novo**technik
19	pot4	-X_Displacement	mm	AC2	3	50mm	**novo**technik
20	pot5	+Y_Displacement	mm	UC2	4	50mm	**novo**technik
21	pot6	+Y_Displacement	mm	UC1	4	50mm	**novo**technik
22	pot7	+X_Displacement	mm	PEC1	7	50mm	**novo**technik
23	pot8	+X_Displacement	mm	PEC2	7	50mm	**novo**technik
24	pot9	-X_Displacement	mm	crack1	1	25mm	penny&gilles
25	pot10	+Y_Displacement	mm	crack2	2	25mm	penny&gilles
26	pot11	-X_Displacement	mm	crack3	5	25mm	penny&gilles
27	pot12	-Y_Displacement	mm	crack4	6	25mm	penny&gilles

In test session 2, as shown in Figure 3.3 and Table 3.2, the instrumentation layout was similar to the previous session, it was only increased the number of accelerometers to measure unidirectional acceleration at the base of the structure and on the table. This setup was selected to check correspondence and synchronization of the used data acquisition system and some redundant quantities were captured. The potentiometers were mounted with the same layout of the previous session.

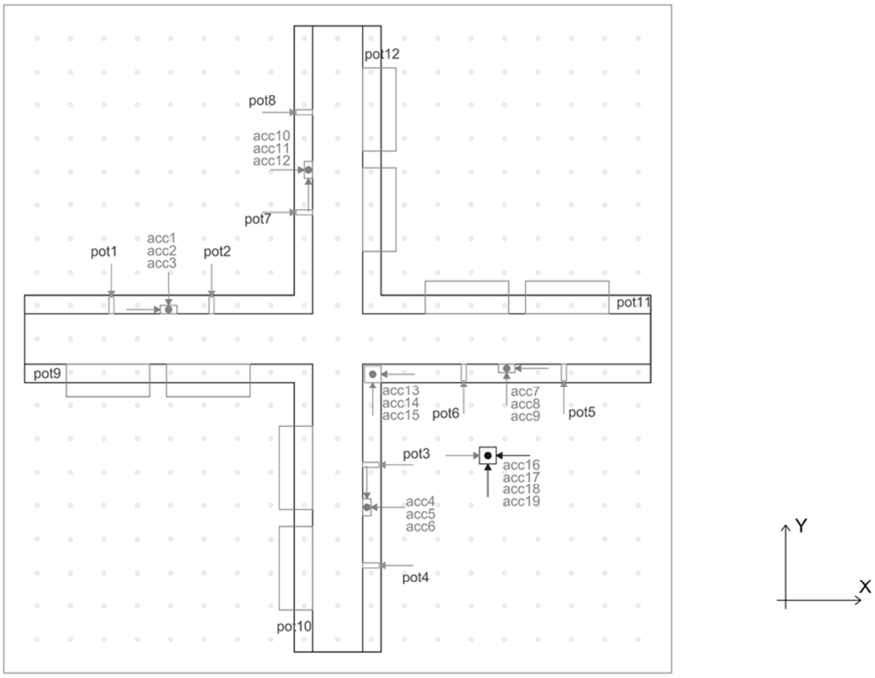

Figure 3.3 Setup instrumentation for TS2; system 1

Table 3.2 Instrumentation adopted for test session 2

No.	Name	Captured quantity	Units	Specimen	Wall	Measurement range	Manufacturer
1	acc1	-Z_Acceleration	g	MEC	8	0.50g	PCB Piezotronics
2	acc2	+X_Acceleration	g	MEC	8	0.50g	PCB Piezotronics
3	acc3	-Y_Acceleration	g	MEC	8	0.50g	PCB Piezotronics
4	acc4	-Z_Acceleration	g	AC	3	0.50g	PCB Piezotronics
5	acc5	-Y_Acceleration	g	AC	3	0.50g	PCB Piezotronics
6	acc6	-X_Acceleration	g	AC	3	0.50g	PCB Piezotronics
7	acc7	-Z_Acceleration	g	UC	4	0.50g	PCB Piezotronics
8	acc8	-X_Acceleration	g	UC	4	0.50g	PCB Piezotronics
9	acc9	+Y_Acceleration	g	UC	4	0.50g	PCB Piezotronics
10	acc10	-Z_Acceleration	g	PEC	7	0.50g	PCB Piezotronics
11	acc11	+Y_Acceleration	g	PEC	7	0.50g	PCB Piezotronics
12	acc12	+X_Acceleration	g	PEC	7	0.50g	PCB Piezotronics
13	acc13	-Z_Acceleration	g	-	base	0.50g	PCB Piezotronics
14	acc14	-X_Acceleration	g	-	base	0.50g	PCB Piezotronics
15	acc15	+Y_Acceleration	g	-	base	0.50g	PCB Piezotronics
16	acc16	-X_Acceleration	g	-	Table	0.50g	PCB Piezotronics
17	acc17	+X_Acceleration	g	-	Table	2.50g	PCB Piezotronics
18	acc18	+Y_Acceleration	g	-	Table	2.50g	PCB Piezotronics
19	acc19	-Z_Acceleration	g	-	Table	2.50g	PCB Piezotronics
20	pot1	-Y_Displacement	mm	MEC4	8	50mm	**novo**technik
21	pot2	-Y_Displacement	mm	MEC3	8	50mm	**novo**technik
22	pot3	-X_Displacement	mm	AC3	3	50mm	**novo**technik
23	pot4	-X_Displacement	mm	AC4	3	50mm	**novo**technik
24	pot5	+Y_Displacement	mm	UC4	4	50mm	**novo**technik
25	pot6	+Y_Displacement	mm	UC3	4	50mm	**novo**technik
26	pot7	+X_Displacement	mm	PEC3	7	50mm	**novo**technik
27	pot8	+X_Displacement	mm	PEC4	7	50mm	**novo**technik
28	pot9	-X_Displacement	mm	crack1	1	25mm	penny&gilles
29	pot10	+Y_Displacement	mm	crack2	2	25mm	penny&gilles
30	pot11	-X_Displacement	mm	crack3	5	25mm	penny&gilles
31	pot12	-Y_Displacement	mm	crack4	6	25mm	penny&gilles

In test session 3, as shown in Figure 3.4 and Table 3.3, the instrumentation layout was almost the same of the previous test session. Compared to test session 2 only the potentiometer pot11 was missing because in the wall number 5 no anchor specimen was installed in the crack as that wall was used to attach real non-structural components, namely a monitor and a water heater.

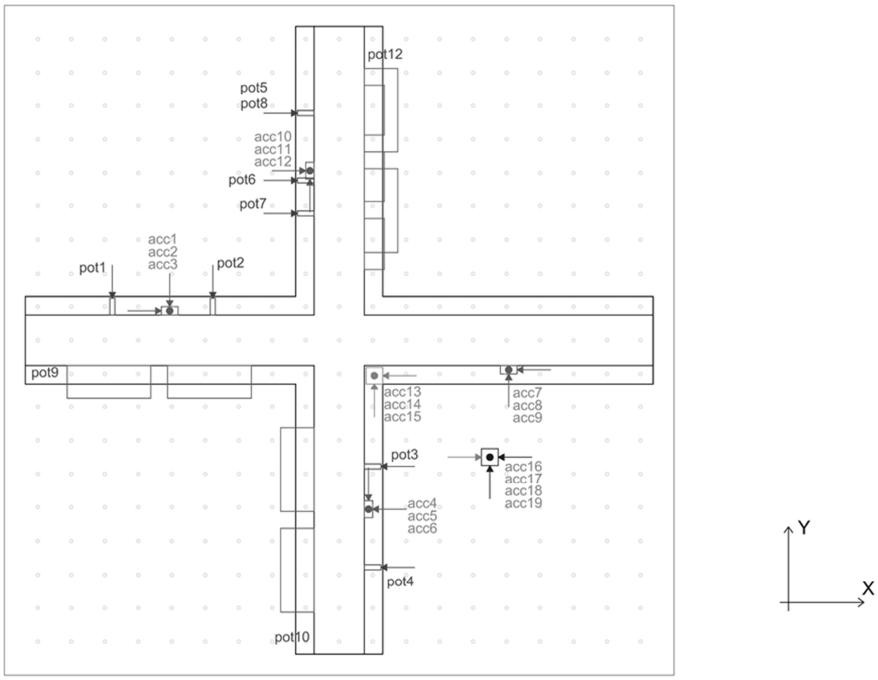

Figure 3.4 Setup instrumentation for TS3; system 1

Table 3.3 Instrumentation adopted for test session 3

No.	Name	Captured quantity	Units	Specimen	Wall	Measurement range	Manufacturer
1	acc1	-Z_Acceleration	g	MEC	8	0.50g	PCB Piezotronics
2	acc2	+X_Acceleration	g	MEC	8	0.50g	PCB Piezotronics
3	acc3	-Y_Acceleration	g	MEC	8	0.50g	PCB Piezotronics
4	acc4	-Z_Acceleration	g	AC	3	0.50g	PCB Piezotronics
5	acc5	-Y_Acceleration	g	AC	3	0.50g	PCB Piezotronics
6	acc6	-X_Acceleration	g	AC	3	0.50g	PCB Piezotronics
7	acc7	-Z_Acceleration	g	heater_monitor	4	0.50g	PCB Piezotronics
8	acc8	-X_Acceleration	g	heater_monitor	4	0.50g	PCB Piezotronics
9	acc9	+Y_Acceleration	g	heater_monitor	4	0.50g	PCB Piezotronics
10	acc10	-Z_Acceleration	g	PEC	7	0.50g	PCB Piezotronics
11	acc11	+Y_Acceleration	g	PEC	7	0.50g	PCB Piezotronics
12	acc12	+X_Acceleration	g	PEC	7	0.50g	PCB Piezotronics
13	acc13	-Z_Acceleration	g	-	base	0.50g	PCB Piezotronics
14	acc14	-X_Acceleration	g	-	base	0.50g	PCB Piezotronics
15	acc15	+Y_Acceleration	g	-	base	0.50g	PCB Piezotronics
16	acc16	-X_Acceleration	g	-	Table	0.50g	PCB Piezotronics
17	acc17	+X_Acceleration	g	-	Table	2.50g	PCB Piezotronics
18	acc18	+Y_Acceleration	g	-	Table	2.50g	PCB Piezotronics
19	acc19	-Z_Acceleration	g	-	Table	2.50g	PCB Piezotronics
17	pot1	-Y_Displacement	mm	MEC6	8	50mm	**novo**technik
18	pot2	-Y_Displacement	mm	MEC5	8	50mm	**novo**technik
19	pot3	-X_Displacement	mm	AmC5	3	50mm	**novo**technik
20	pot4	-X_Displacement	mm	AmC6	3	50mm	**novo**technik
21	pot5	+Y_Displacement	mm	PFEC3	7D	50mm	**novo**technik
22	pot6	+Y_Displacement	mm	PFEC1	7D	50mm	**novo**technik
23	pot7	+X_Displacement	mm	PEC5	7U	50mm	**novo**technik
24	pot8	+X_Displacement	mm	PEC6	7U	50mm	**novo**technik
25	pot9	+X_Displacement	mm	crack1	1	25mm	penny&gilles
26	pot10	+Y_Displacement	mm	crack2	2	25mm	penny&gilles
27	pot12	-Y_Displacement	mm	crack4	6	25mm	penny&gilles

3.1.2. Testing Plan

The experimental campaign has been developed in five subsequent sessions, each one corresponding to an independent load history related to specimens and structural units behaviour. Every test session has consisted of successive steps with a nominal increased peak of 0.05g. The first three test sessions have been performed on the concrete structure while the remaining two on the RC frame with masonry infill walls. A full list of the performed steps for each session is reported in Table 3.5. The maximum attained nominal acceleration is listed in Table 3.4.

Table 3.4 Test sessions features

Session	Base material	ZPA[3] max
TEST SESSION 1	UC[1]/CC[2]	1.10g
TEST SESSION 2	UC[1]/CC[2]	1.00g
TEST SESSION 3	UC[1]/CC[2]	1.10g

[1]UC = Uncracked concrete;
[2]CC = Cracked concrete;
[3]ZPA = Zero Period Acceleration (AC156 2010).

The ZPA could be considered as the acceleration to which the non-structural component was subjected being filtered by the structure, according to its dynamic properties. Moreover this acceleration depends on the location of the fixed component inside the building, especially in terms of ratio between height of installation point and total height.

Table 3.5 List of performed steps for each test session

No.	Test 1	Test 2	Test 3
1	0.05g	0.05g	0.05g
2	0.10g	0.10g	0.10g
3	0.15g	0.15g	0.15g
4	0.20g	0.20g	0.20g
5	0.25g	0.25g	0.25g
6	0.30g	0.30g	0.30g
7	0.35g	0.35g	0.35g
8	0.40g	0.40g	0.40g
9	0.45g	0.45g	0.45g
10	0.50g	0.50g	0.50g
11	0.55g	0.55g	0.55g
12	0.60g	0.60g	0.60g
13	0.65g	0.60g	0.65g
14	0.70g	0.65g	0.70g
15	0.75g	0.70g	0.75g
16	0.80g	0.75g	0.80g

17	0.40g	0.80g	0.90g
18	0.45g	0.80g	0.90g
19	0.50g	0.90g	1.00g
20	0.55g	1.00g	1.10g
21	0.60g	-	-
22	0.65g	-	-
23	0.70g	-	-
24	0.75g	-	-
25	0.80g	-	-
26	0.90g	-	-
27	1.00g	-	-
28	1.10g	-	-

3.2. EXPERIMENTAL OBSERVATIONS

The description of the realization of the testing can be useful to understand the immediate facts on the seismic behaviour of the anchor specimens. In particular a direct comparison could be made for the differences in the response of the same anchor type for specimens installed in non-cracked concrete and cracked concrete, which were located on the same support wall.

In the three test sessions of the concrete structural unit, during the subsequent input signals induced to the table, the damages occurring to the structure as to the connection of the attached components were registered. As a primary evaluation and comparison, the nominal peak accelerations at which the specimens failure modes occurred were recorded (Table 3.6). Besides the damages subjected by anchor specimens and base material surface around the installation points were reported.

In general a progressive slipping of the concrete specimens was observed with a different largeness depending on the functioning principle of the anchor type. At the end of the testing an extensive damage to the concrete surface was noted.

Some specimens did not reach failure after the test sessions they underwent, especially for the cases of installation in non-cracked concrete support. In the cases when a specimen reached collapse different failure modes were shown, as a consequence of the combination of axial and shear actions. Concerning the chemical anchor installed in non-cracked and cracked concrete a substantial difference has to be reported. As demonstrated by various studies (Hoehler 2006, Rieder 2009, Watkins 2011) that typology presents indeed has a larger difference in the behaviour of the two support conditions than other types. Metal expansion anchor for example maintains a good expansion reserve which contributes to its friction functioning also when installed in an opening crack.

The stress responses related to the three components of acceleration applied to the table were different according to the anchor type. Typical failure modes that occurred to the specimens were recognized in relation to the anchors under study. The damages occurred to the various parts of the anchorage and of the support surface helped in the definition of each specimen response to dynamic loading.

The metal expansion anchor never reached failure in non-cracked concrete neither in cracked concrete, as it overtook in the three test sessions all the applied signals up to the maximum ZPA given by the table. Nevertheless that anchor type showed in both support conditions noticeable shear deformation of the threaded bar and a crushing of the external sleeve. Moreover a concrete detachment was observed in the support surface below the installation hole. The damage patterns were more perceptible in the specimens installed in cracked concrete. An enlargement of the hole due to the dynamic loading acting on the fastening point was also noted.

The chemical anchor experienced different effects depending on the support condition. In non-cracked concrete damages to the bar and to the base material, as well as a possible slipping of the stud, were totally absent after two test sessions with no failure reached. On the other hand the installation in the crack showed a pull-out failure with a concrete 4cm deep cone detachment. Also a slight shear deformation of the stud was noticed. Crack width for chemical anchor is a crucial point to be deepen, especially for this particular type of anchor. This parameter influences considerably the final performance of the system and has to be monitored.

Undercut anchor specimens never reached failure in both non-cracked and cracked concrete. Large shear deformations of the bar and an enlargement of the external sleeve were reported. Besides the base material around the hole showed an evident damage.

The type A plastic expansion anchor installed in non-cracked concrete showed failure only in one case out of three due to shear steel failure of the screw. While in the other two cases it withstood the entire sequence of acceleration time histories. Concerning installations in cracks with a Δw of 0.35mm, the specimens always reached failure due to screw slipping or to screw shear collapse. Also some secondary failure mechanisms were observed as plastic failure or slipping of the whole anchor. Specimens in both concrete conditions produced damages on the base material surface around the installation point.

The type B plastic expansion anchor, in one specimen in non-cracked and one in cracked concrete, showed a slipping of the plastic sleeve as a secondary mechanism, but the principal mode was the screw shear collapse. In the third specimen, the second installation on non-cracked concrete, the specimen did not reach failure but showed a slipping of about 2mm.

A direct comparison was done among the different anchor typologies in terms of reduction resistance between installations in cracked and non-cracked concrete. Among the five anchor types under testing, three of different diameter were used to fix a same mass, thus were expected to experience a similar stress. The observed behaviours among these types were different. For mechanical anchors, namely metal expansion and undercut, no differences could have been recorded regarding the ultimate resistance. Whereas for the chemical anchor installed in the crack, as mentioned above, failure was reached at a lower level of nominal peak acceleration.

For plastic anchors an immediate evaluation can be realized since nominal peak accelerations related to failure for specimens installed in both non-cracked and cracked concrete could be observed.

Table 3.6 Nominal peak accelerations related to specimens failure (*no failure occurred)

Non-Str. Comp.	Anchor type	Δw [mm]	Nominal failure ZPA
A1	metal expansion	0.8	1.10g*
A2	metal expansion	0.8	1.00g*
A3	metal expansion	0.8	1.10g*
B1	metal expansion	UC	1.10g*
B2	metal expansion	UC	1.00g*
B3	metal expansion	UC	1.10g*
C1	adhesive	UC	1.10g*
C2	adhesive	UC	1.00g*
D1	adhesive	0.8	0.55g
D2	adhesive	0.8	0.60g
E1	undercut	0.8	1.10g*
E2	undercut	0.8	1.00g*
E3	plastic expansion (B)	0.35	0.75g
F1	undercut	UC	1.10g*
F2	undercut	UC	1.00g*
F3	plastic expansion (B)	UC	1.10g
G1	plastic expansion (A)	UC	1.10g*
G2	plastic expansion (A)	UC	1.00g*
G3	plastic expansion (A)	UC	1.00g
H1	plastic expansion (A)	0.35	0.90g
H2	plastic expansion (A)	0.35	1.00g*
H3	plastic expansion (A)	0.35	0.90g
I3	plastic expansion (B)	UC	1.10g*

3.3. DATA PROCESSING

A first evaluation considers the comparison between accelerations captured directly by the accelerometers and those computed from the displacements recorded through the spatial positioning system. The values of the acceleration measures at the ground level allow a verification of the input signal while those from sensors fixed at a certain height provide information on the structural units response. The values recorded on the masses give an indication on the dynamic behaviour of different fixtures. These values mainly depend on the connection condition which developed during the testing. Therefore indirectly it is possible to observe the behaviour of post-installed anchor specimens in addition to the immediate experimental observations, i.e. specimens failure modes and maximum peak acceleration suffered.

The considered tri-axial accelerations refer: (1) to the sensors for the control of the testing system, (2) to accelerometers attached to the shaking table and (3) to the accelerometers fixed to the walls at the fixtures height, in addition to (4) to the acceleration values obtained from the displacement of markers. The most relevant ones are those installed at the base beam of the structures and those on the steel masses.

The aim of this first processing phase was to go backward to the design stage of the experimental campaign evaluating and discussing the setup decisions and validating the assumptions considered previous to the testing.

3.3.1. Analysis of Accelerations

The analysis of the structural units response subjected to the input signal is a preliminary fundamental consideration to be developed for a complete understanding of the connection trend behaviour. The purpose is to verify the amplification which the anchored elements were subjected to during the shaking as well as to verify the results about the amplification ratio between base and anchoring height obtained from the design of the experimental campaign.

3.3.1.1. Comparison of Measures

Two FE Models were created in order to predict the stiffness of both structures and thus the foresee accelerations acting at the wall fixing height (Mazzon et al. 2013b). It is therefore needed to validate the designed testing layout according to the expected accelerations at different heights. The amplification acceleration ratio allows the influence of the structure and its filtering action to be evaluated.

The Figure 3.5 shows the trend of the measured accelerations with reference to the nominal step for the case of a test session in the concrete structural unit. The charts underline as the input ("achieved" signal) and the values recorded on the shaking table ("Table" signal) substantially agree along the whole test except for the last steps on some sessions.

A more noticeable difference can be noticed if the input/table signal and the valued recorded on the support at the fixing points ("wall" signal) are compared. In that case the influence of the structure can be clearly identified and in general this induces an amplification of accelerations and a modification of frequencies.

In the case of the concrete unit a substantial difference between the overall trend of accelerations at the base and fixing levels becomes evident only at the higher steps.

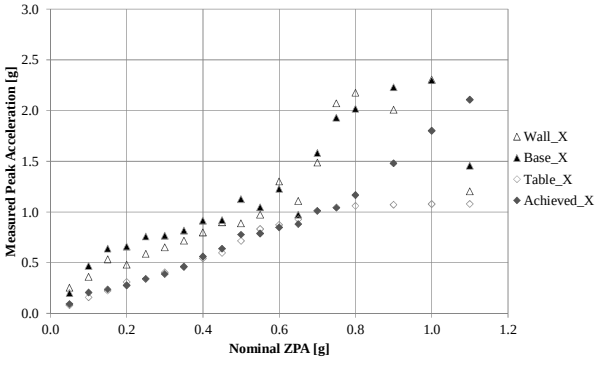

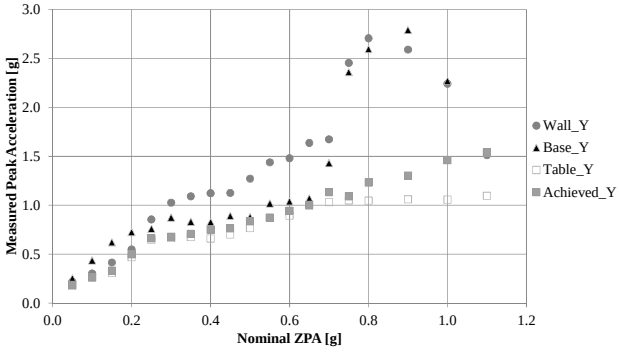

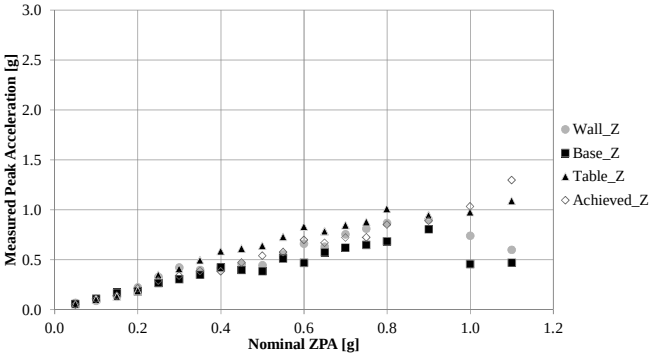

Figure 3.5 Example of measured peak accelerations for the concrete unit (test session 3)

In this section a study on the relation between accelerations measured on the structural unit walls, at fixing height, and on the fixtures is presented. This kind of investigation allows the presence of variation of trend behaviour of specimens to be recognized, i.e. whether after a certain number of testing steps the specimen behaviour modified depending on the decreasing of stiffness, that is related to the progressive damage of the fastening system. Such finding leads to get information on where a discontinuity point, related to specimen slipping from the base material surface, can be found.

Concerning the testing in concrete the general behaviour manifested by all the specimens is linear (Figure 3.6) with almost no differences between those installed in uncracked (B, C, F, G) and cracked concrete (A, D, E, H). A slightly evident trend of decreasing in fixture acceleration in relation to the highest ZPA steps of support acceleration can be also noticed.

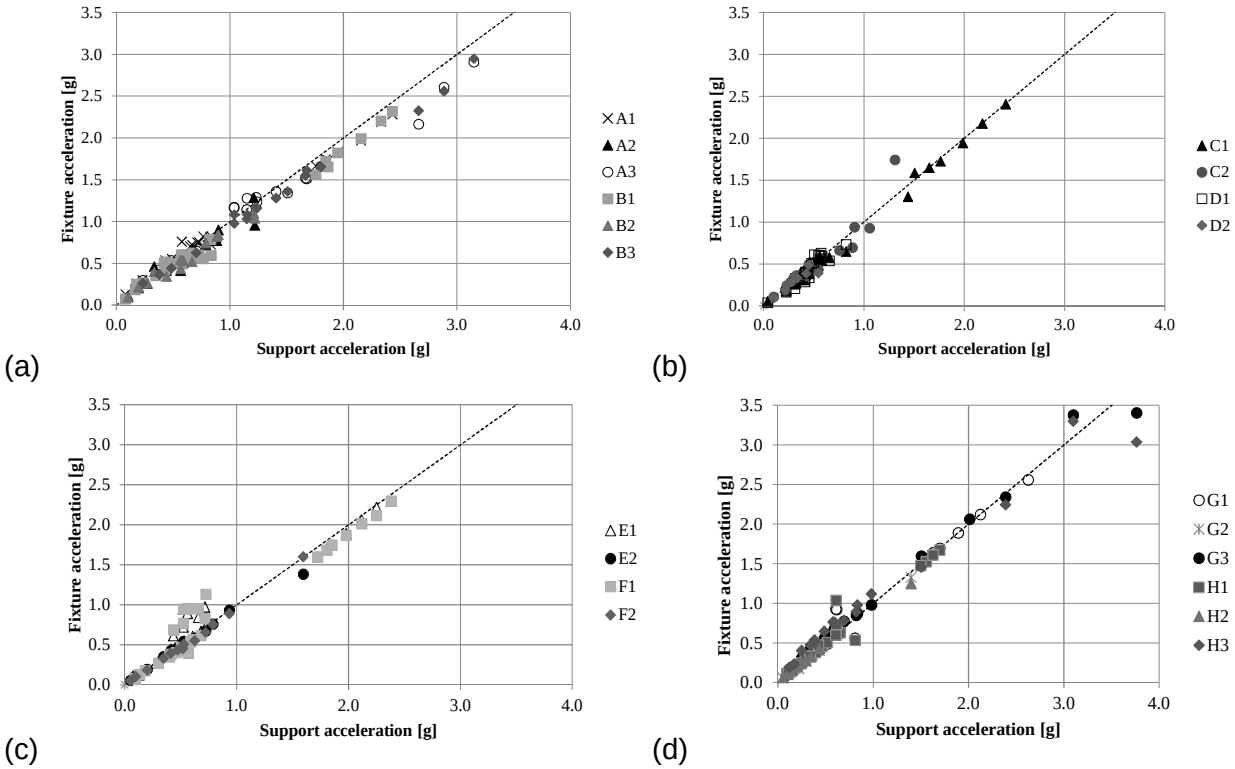

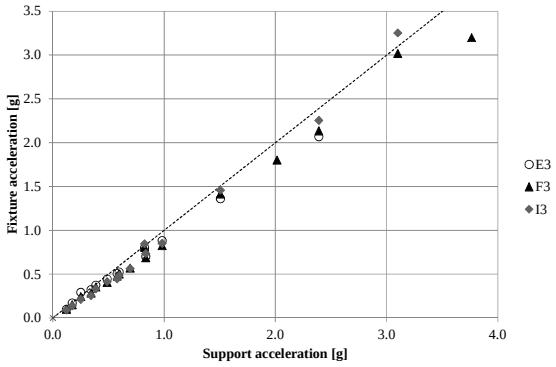

(e)

Figure 3.6 Maximum recorded acceleration on the fixture versus maximum recorded acceleration on the support at each testing step for concrete application of metal expansion anchor (a), chemical anchor (b), undercut anchor (c), plastic expansion anchor type A (d) and plastic expansion anchor type B (e)

3.3.1.2. Conclusive Remarks

The preliminary analyses of accelerations after the shake-table testing of post-installed anchors reveal the progressive damage of the structural units. In the concrete unit a slightly variation of the acceleration ratio among the considered structural elements can be recognized.

The linear trend observed on the acceleration ratio between mass and support underlines as the anchor specimens were able to transfer the whole acceleration from the structure to the fixture. This was analysed in terms of peak measured acceleration, up to almost the last testing steps. The trend among the measured accelerations was indeed mainly linear for the concrete structural unit.

The presented analyses also allow a difference in the behaviour of different anchor typologies to be studied. While the anchors installed in concrete manifested in most cases an overall linear trend, the plastic expansion anchors showed a variation on their overall behaviour.

The above presented analyses of acceleration are a fundamental step for the computation of loads acting on the different anchor typologies. In the case of fastenings that manifested an overall linear trend the possible relative acceleration will not have a relevant influence on the computation of the acting load. Differently the relative acceleration should be taken into account when the ratio deviates from the linear trend.

3.3.1.3. Calculation of Actions on Anchors

Three different approaches were considered to compute the forces acting on the tested anchors. The tensile extraction force (N) and the shear loads (V) were calculated from the computed accelerations. The calculation methodologies are briefly presented in the following with the relevant formulations. The accelerations considered in the calculations are those computed from data measured with markers.

The first approach was that adopted by (Rieder 2009; Figure 3.7) and the related equations are presented in the following (from Eq. 3.1 to Eq. 3.4). In the vertical direction the combined effect of the gravity and of the induced acceleration was considered (V_z) while the additional horizontal shear effect (V_y) was only due to the dynamic input. The tensile extraction force (N) was computed considering both the direct effect due to the out-of-plane acceleration applied to the mass and the indirect effect of shear actions (the

vertical and horizontal ones). This second contribution takes into account the effective application point of the force and thus of its lever arm (Eq. 3.4).

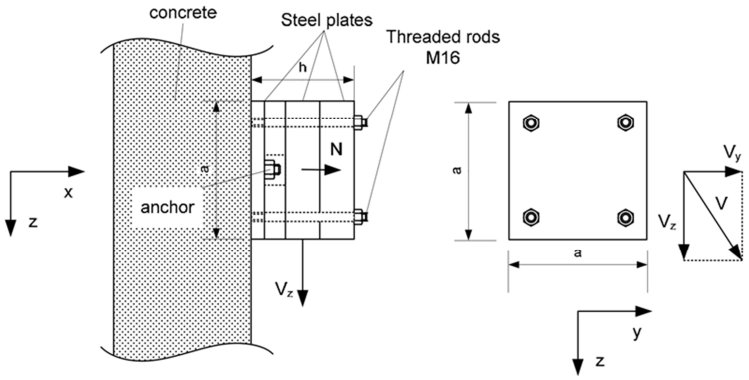

Figure 3.7. Scheme of the first calculation approach (Rieder 2009).

$$V_z = m \cdot g + m \cdot a_z \quad \text{Eq. 3.1}$$

$$V_y = m \cdot a_y \quad \text{Eq. 3.2}$$

$$V = \sqrt{{V_y}^2 + {V_z}^2} \quad \text{Eq. 3.3}$$

$$N = \frac{h}{a} \cdot V + m \cdot a_x, \quad a_x \geq 0 \quad \text{Eq. 3.4}$$

With:

a_x, a_y, a_z	measured acceleration in each relevant direction,
V_y, V_z	shear load on the relevant direction,
m	mass of the anchored steel plate,
a	side length of the steel plate,
h	thickness of the steel plate,
V	resulting shear force in kN,
N	resulting tension force in kN.

A refinement of this method was developed with a modification of the Eq. 3.4. The effects of the two shear components (V_y and V_z) were considered separately and thus two different lever arms were computed, one for each acting shear force.

The third approach considers the acceleration of both the anchored mass and the support. The adopted equations are presented in the following (from Eq. 3.5 to Eq. 3.7, the adopted symbols are analogous to those presented on the first approach). In all the formulations the vectorial combination of accelerations was adopted in order to consider the relative behaviour between the structure ($a_{support}$) and the steel plates (a_{mass}). To solve this problem a calculation algorithm was expressly developed in MATLAB® and different formulations were defined to take into account all possible cases of relative acceleration and accordance or discordance of the mass acceleration with the out-of-plane unit vector. As on the second calculation methodology the effect of shear loads were considered to be uncoupled (Eq. 3.7).

A comparisons among the results obtained from the three above described methods show an analogous trend, confirming the reliability of computed values of forces acting on the anchors. Among all, the last methodology highlights higher values of loads. The

results presented in the following chapters were obtained from the application of the last presented calculation approach.

$$\boldsymbol{V}_z = m \cdot \boldsymbol{g} + m \cdot \left(\boldsymbol{a}_{z,mass} + \boldsymbol{a}_{z,support}\right) \quad \text{Eq. 3.5}$$

$$\boldsymbol{V}_y = m \cdot \left(\boldsymbol{a}_{y,mass} + \boldsymbol{a}_{y,support}\right) \quad \text{Eq. 3.6}$$

$$\boldsymbol{N} = \frac{h_z}{a} \cdot \boldsymbol{V}_z + \frac{h_y}{a} \cdot \boldsymbol{V}_y + m \cdot \left(\boldsymbol{a}_{x,mass} + \boldsymbol{a}_{x,support}\right) \quad \text{Eq. 3.7}$$

3.4. TEST RESULTS

In the following section the experimental outcomes of the testing, the results of data analyses and a general comment on the seismic behaviour of various anchor types are reported with a recurrent order. Paragraphs distinguish for anchor type and include test results and observations for each specimen. The relevant aspects taken into account for the different specimens are the load history related to the maximum action withstood by the specimen in the test session, the failure mode and the slipping vs load plot. Moreover after all the specimens are presented separately, at the end of every paragraph, a summarizing part with a comparison among the specimens and the base material conditions is presented. In particular the maximum forces for every anchor specimen are reported in a table together with the slipping related to maximum load and the maximum slipping. Such general information is also provided graphically with the load-slip curves for all the specimens. Hence it is of importance to find out the influence of cracks in the seismic behaviour as the dynamic resistance level for the anchor.

Table 3.7 Anchor types under dynamic testing in concrete

Anchor type	Tested specimens	Type reference
Metal Expansion	6	MEC
Undercut	4	UC
Chemical	4	AC
Plastic Expansion	6	PEC
Plastic Fibre Expansion	3	PFEC

The load-slip curves for each specimen consider the maximum values for both quantities for each step. Nevertheless in some cases the loads acting on the anchored masses showed spike values. This behaviour was observed to be in correspondence to the failure of some anchor specimens. The observed peak values could be then the consequence of the impact with the support. In this case those spikes were neglected for the computation of the acting loads.

3.4.1. Metal Expansion Anchor (ME)

This paragraph includes the results of the metal expansion anchor ME M12 in non-cracked and cracked concrete. A total of 6 specimens were tested in the 3 test sessions with the concrete structural unit. Three of them were installed in a 0.80mm wide crack. The component fixed with MEC specimens consisted in a 400kg steel plate.

Figure 3.8 View of metal expansion anchor MEC M12

Table 3.8 Installation features for metal expansion anchor specimens

Specimen reference	Test session	Component reference	Mass [kg]	Height from table [cm]	Crack	Measured crack width [mm]
MEC1	TS1	B1	400	115	No	-
MEC2	TS1	A1	400	115	Yes	0.798
MEC3	TS2	B2	400	155	No	-
MEC4	TS2	A2	400	155	Yes	0.802
MEC5	TS3	B3	400	195	No	-
MEC6	TS3	A3	400	195	Yes	0.812

3.4.1.1. MEC specimen 1

Specimen 1 of metal expansion anchor was installed in uncracked support. It didn't reach failure after having withstood all of the testing steps in test session 1. No damages on the anchor were observed at the end of the testing. The progressive slippage of the anchor is mainly caused by axial forces acting on the fixing point instead. The base material has manifested no damages due to the installation in uncracked support.

Among all the experimental steps, the maximum dynamic loads -related to the instant of peak normalized force, namely 0.50- acting on the specimen, consisted of almost 8kN in tension and 6.5kN in shear.

The measured slipping of the anchor during the test session 1 increased with an inflected curve up to 0.3mm. In this case the maximum slip value for the specimen is that related to the experimental step of maximum loading.

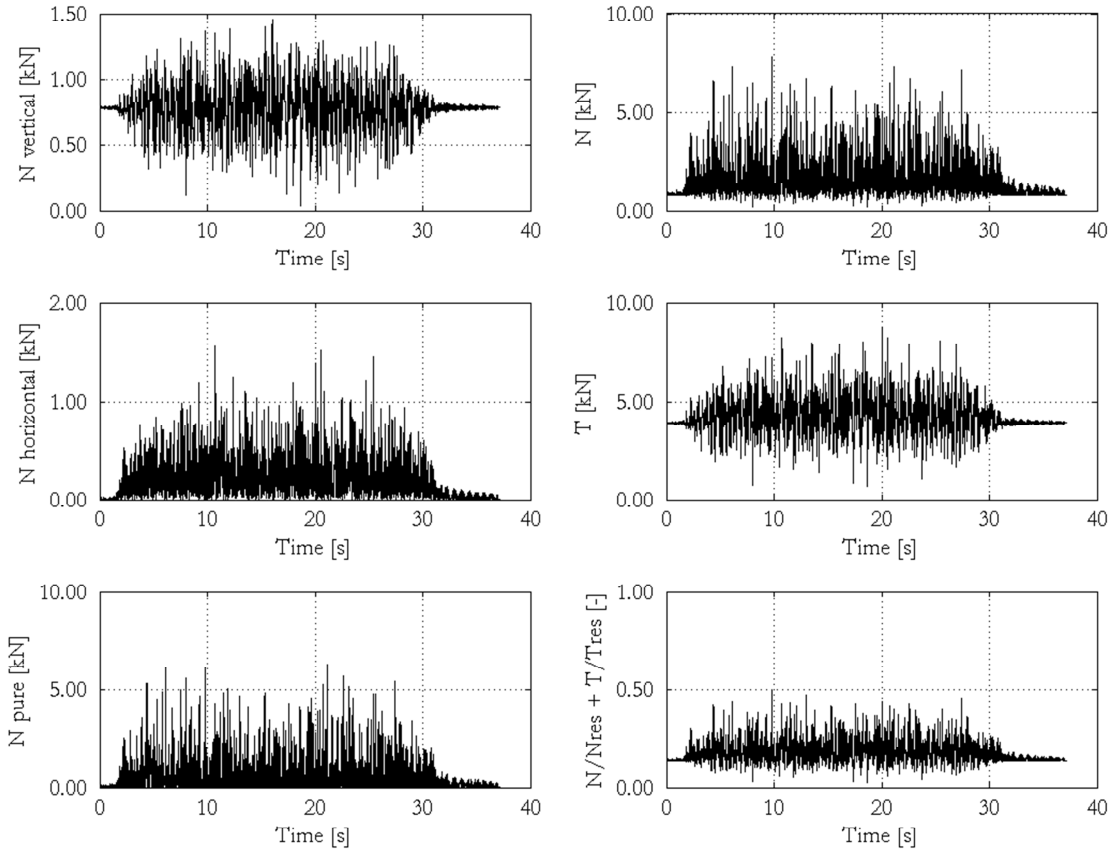

Figure 3.9 Loads acting on MEC1 specimen in test session 1 – 1.10g of ZPA testing step; N = axial load, T = shear load, N/Nres+T/Tres = normalized force for design load combination

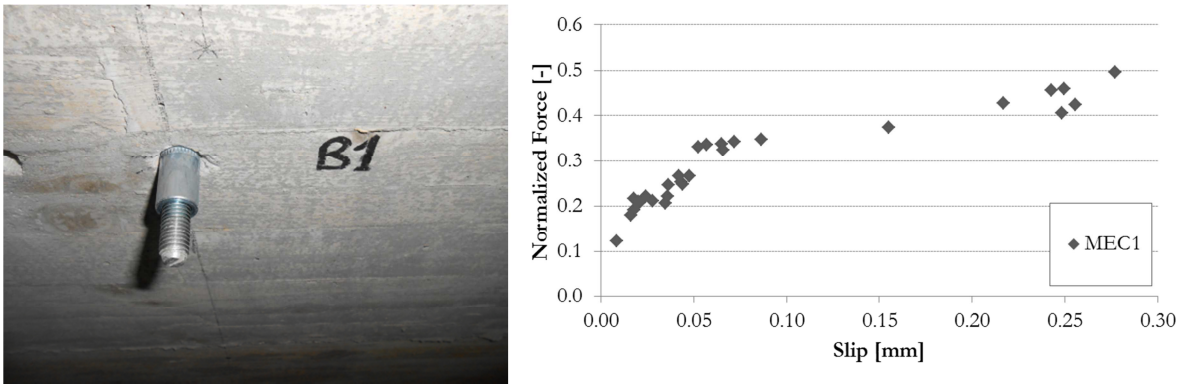

Figure 3.10 View of MEC1 specimen of after test session 1. Load vs displacement graph for MEC1

3.4.1.2. MEC specimen 2

Specimen 2 of metal expansion anchor was installed in the crack. It didn't reach failure after having withstood all of the testing steps in test session 1. The large shear deformation of the threaded stud and the flattening of a small part of the sleeve indicate the predominance of shear actions in the plane of the wall. The progressive slippage of the anchor is mainly caused by axial forces acting on the fixing point instead. The base material has manifested an evident damage state due to the installation in cracked support. A concrete detachment of 3x3x1.5cm was observed indeed below the anchoring

point. The hole enlarged because of cyclic displacement of the specimen being affected by dynamic loading.

Among all the experimental steps, the maximum dynamic loads -related to the instant of peak normalized force, namely 0.65- acting on the specimen, consisted of more than 7kN in tension and 8.7kN in shear.

The measured slipping of the anchor during the test session 1 increased with an inflected curve up to 2.4mm. In this case the maximum slip value for the specimen is that related to the experimental step of maximum loading.

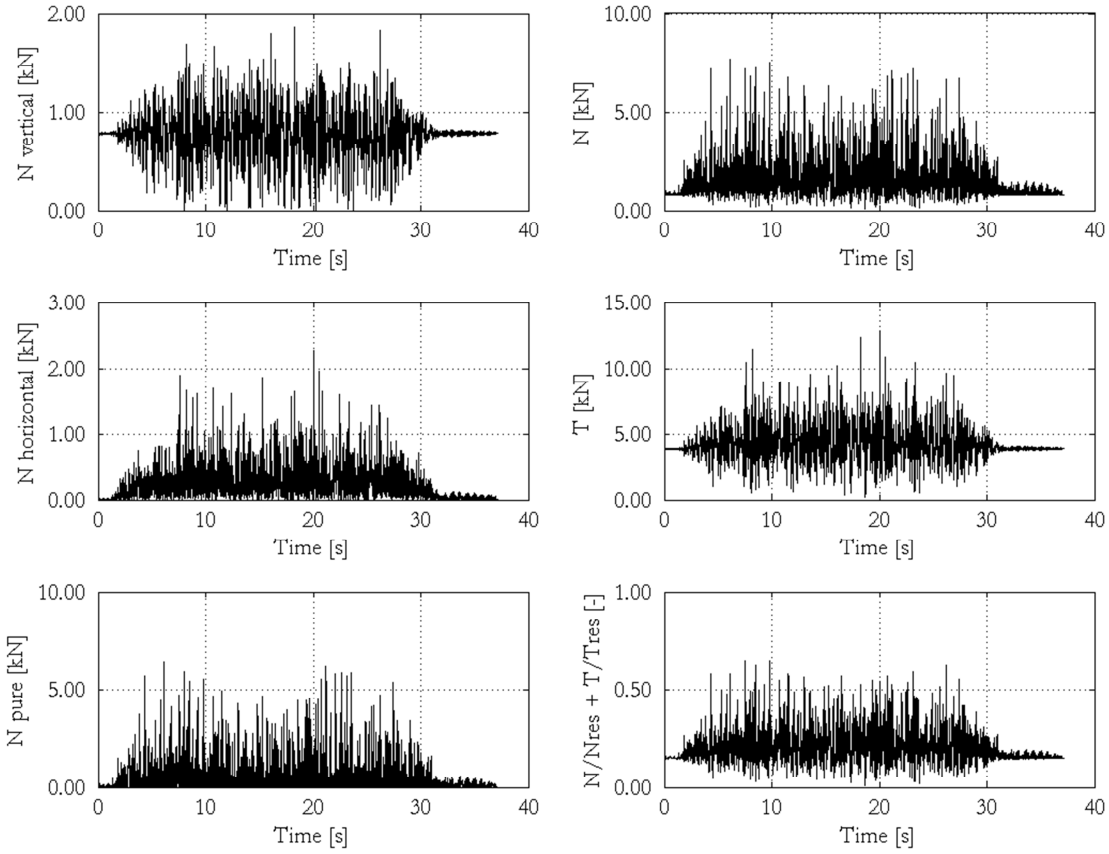

Figure 3.11 Loads acting on MEC2 specimen in test session 1 – 1.10g of ZPA testing step; N = axial load, T = shear load, N/Nres+T/Tres = normalized force for design load combination

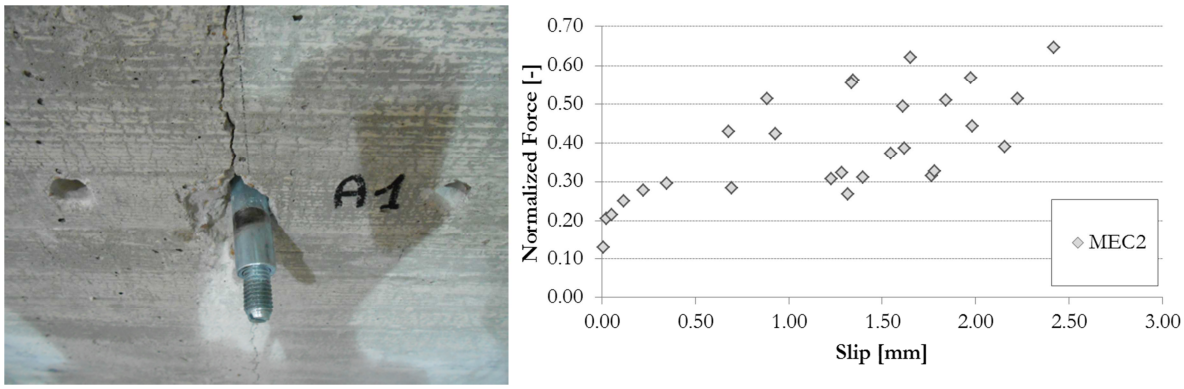

Figure 3.12 View of MEC2 specimen after test session 1. Load vs displacement graph for MEC2

3.4.1.3. MEC specimen 3

Specimen 3 of metal expansion anchor was installed in uncracked support. It did not reach failure after having withstood all of the testing steps in test session 2. A light shear deformation occurred to the stud and the external sleeve was slightly flattened at the end of the testing. The progressive slippage of the anchor is mainly caused by axial forces acting on the fixing point instead. The base material has manifested no damages due to the installation in uncracked support. A concrete detachment of 3x3x1cm was observed indeed below the anchoring point.

Among all the experimental steps, the maximum dynamic loads -related to the instant of peak normalized force, namely 0.60- acting on the specimen, consisted of almost 9.5kN in tension and 7.8kN in shear.

The measured slipping of the anchor during the test session 2 increased with an inflected curve up to 0.8mm. In this case the maximum slip value for the specimen is that related to the experimental step of maximum loading.

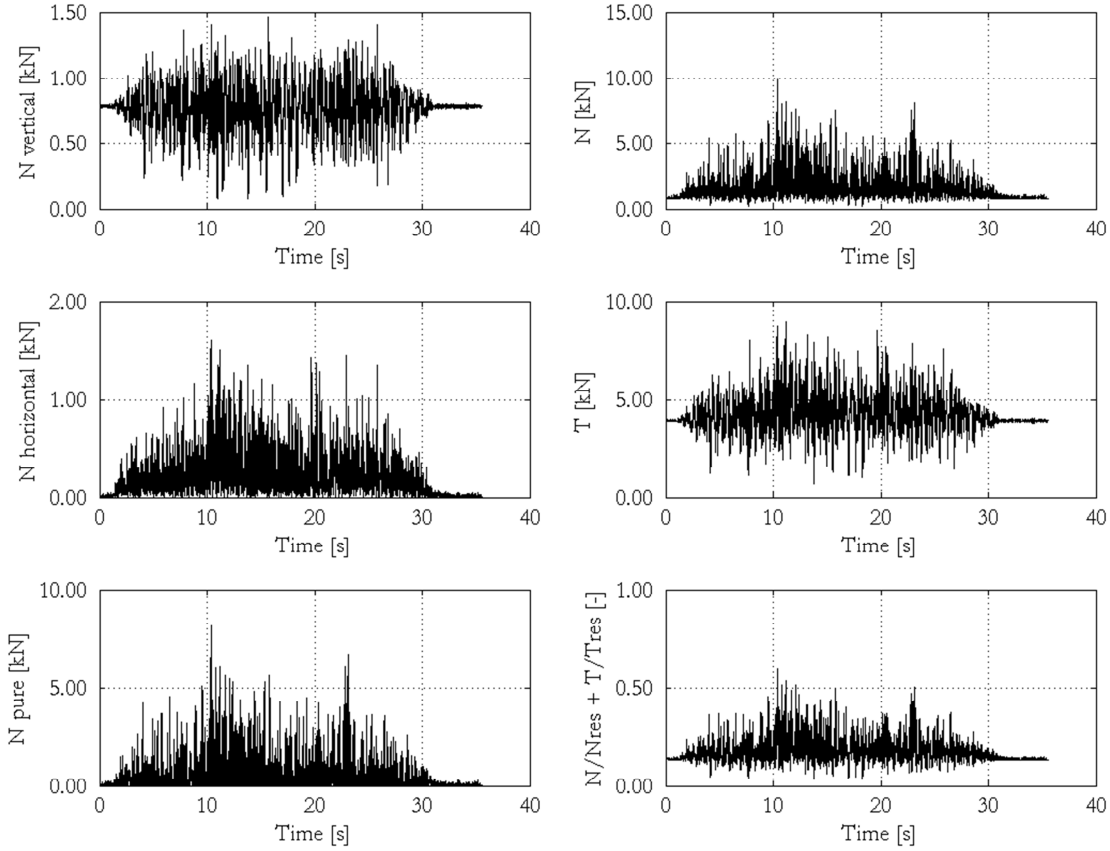

Figure 3.13 Loads acting on MEC3 specimen in test session 2 – 0.90g of ZPA testing step; N = axial load, T = shear load, N/Nres+T/Tres = normalized force for design load combination

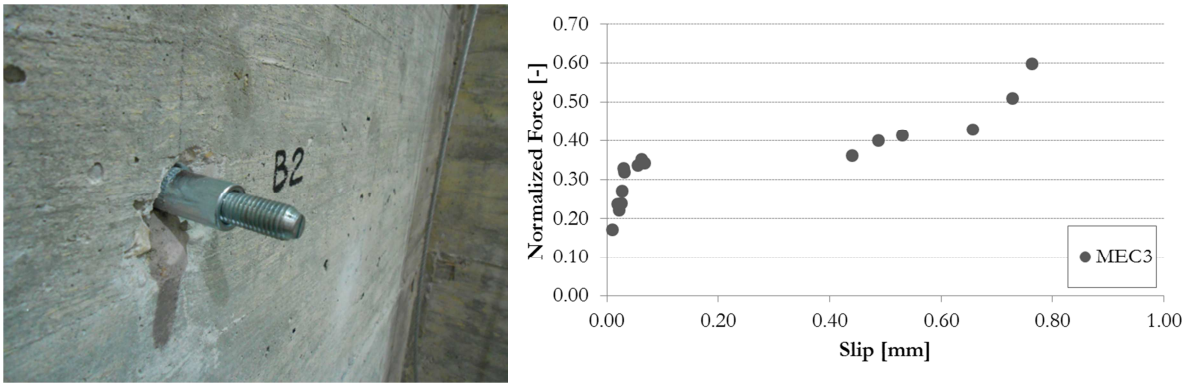

Figure 3.14 View of MEC3 specimen after test session 2. Load vs displacement graph for MEC3

3.4.1.4. MEC specimen 4

Specimen 4 of metal expansion anchor was installed in the crack. It did not reach failure after having withstood all of the testing steps in test session 2. The large shear deformation of the threaded stud and the flattening of a small part of the sleeve indicate the predominance of shear actions in the plane of the wall. The progressive slippage of the anchor is mainly caused by axial forces acting on the fixing point instead. The base material has manifested an evident damage state due to the installation in cracked support. A concrete detachment of 5x7x2cm was observed indeed below the anchoring point. The hole enlarged because of cyclic displacement of the specimen being affected by dynamic loading.

Among all the experimental steps, the maximum dynamic loads -related to the instant of peak normalized force, namely 0.75- acting on the specimen, consisted of almost 8kN in tension and 10.9kN in shear.

The measured slipping of the anchor during the test session 2 increased with an linear curve up to 2.3mm. In this case the maximum slip value for the specimen is that related to the experimental step of maximum loading.

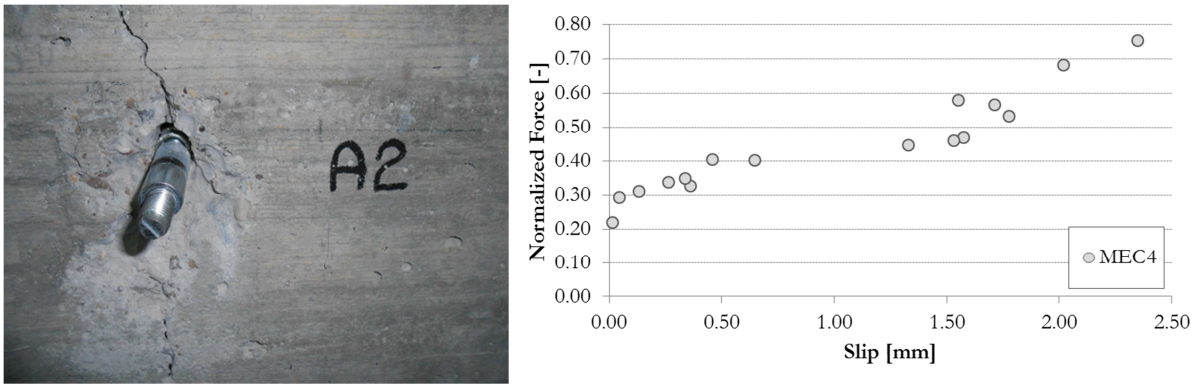

Figure 3.15 View of MEC4 specimen after test session 2. Load vs displacement graph for MEC4

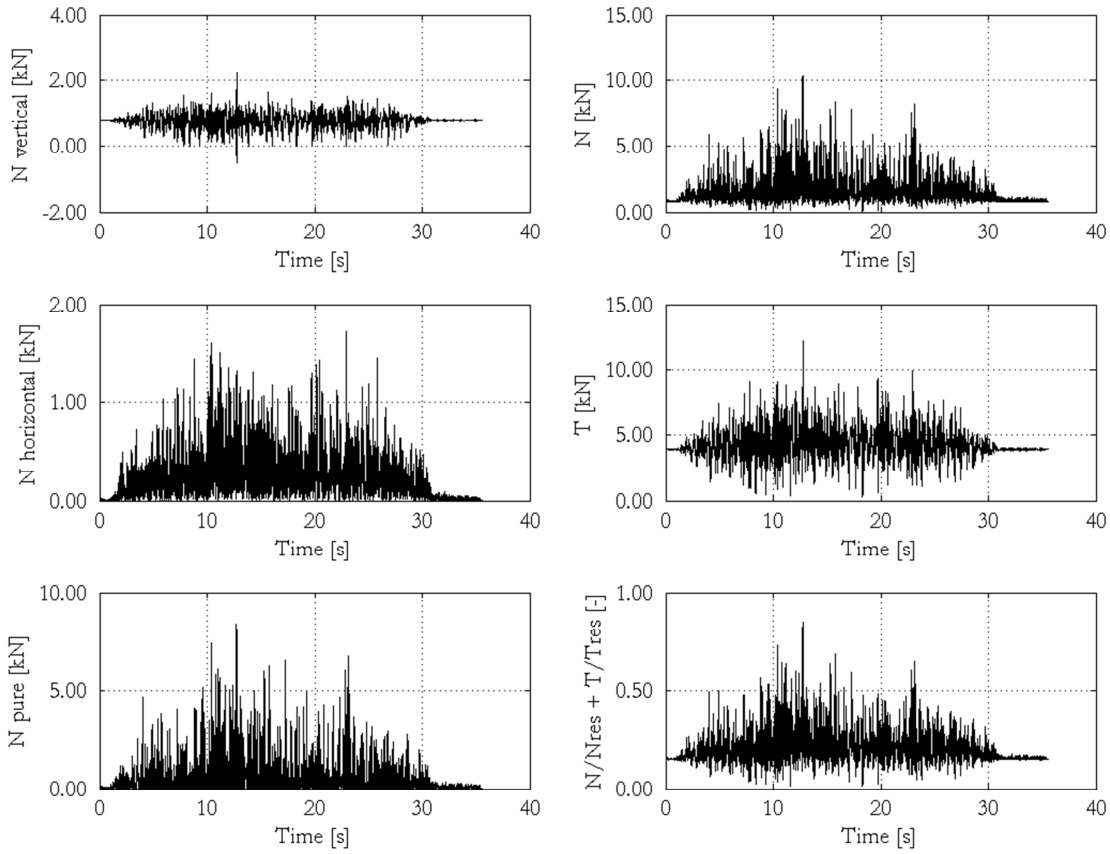

Figure 3.16 Loads acting on MEC4 specimen in test session 2 – 0.90g of ZPA testing step; N = axial load, T = shear load, N/Nres+T/Tres = normalized force for design load combination

3.4.1.5. MEC specimen 5

Specimen 5 of metal expansion anchor was installed in uncracked support. It didn't reach failure after having withstood all of the testing steps in test session 3. A light shear deformation occurred to the stud and the external sleeve was slightly flattened at the end of the testing. The progressive slippage of the anchor is mainly caused by axial forces acting on the fixing point instead. The base material has manifested no damages due to the installation in uncracked support. A concrete detachment of 3x2x1cm was observed indeed below the anchoring point. The hole slightly enlarged because of cyclic displacement of the specimen being affected by dynamic loading.

Among all the experimental steps, the maximum dynamic loads -related to the instant of peak normalized force, namely 0.78- acting on the specimen, consisted of more 12.4kN in tension and 10kN in shear.

The measured slipping of the anchor during the test session 3 increased with an inflected curve up to 1.5mm. In this case the maximum slip value for the specimen is different from that related to the experimental step of maximum loading, which was of 1.1mm.

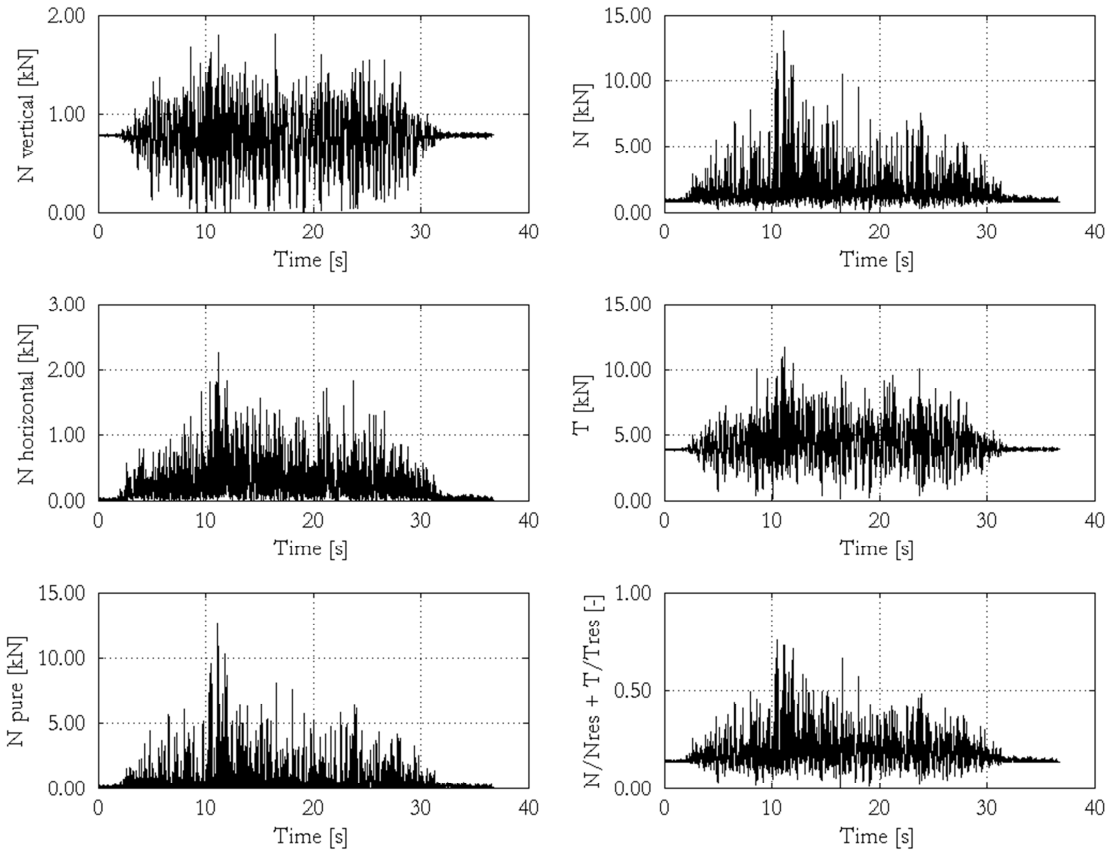

Figure 3.17 Loads acting on MEC5 specimen in test session 3 – 1.10g of ZPA testing step; N = axial load, T = shear load, N/Nres+T/Tres = normalized force for design load combination

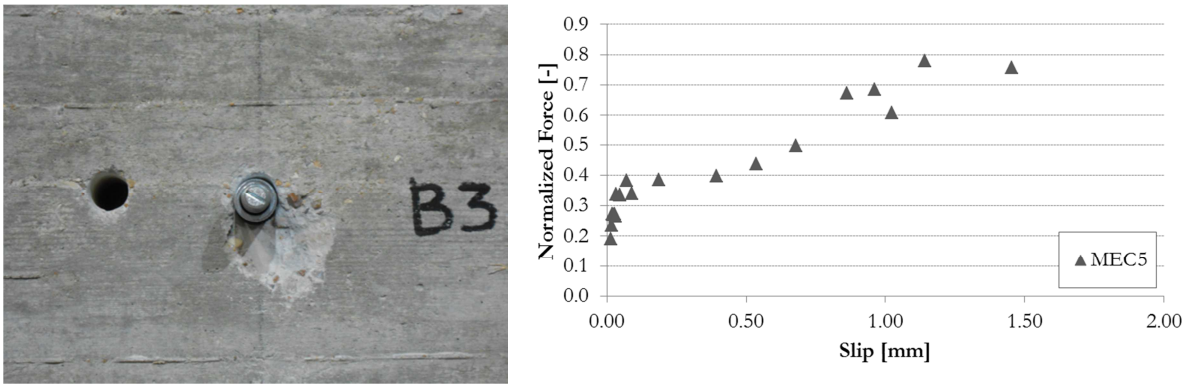

Figure 3.18 View of MEC5 specimen after test session 3. Load vs displacement graph for MEC5

3.4.1.6. MEC specimen 6

Specimen 6 of metal expansion anchor was installed in the crack. It didn't reach failure after having withstood all of the testing steps in test session 3. The large shear deformation of the threaded stud and the flattening of a small part of the sleeve indicate the predominance of shear actions in the plane of the wall. The progressive slippage of the anchor is mainly caused by axial forces acting on the fixing point instead. The base material has manifested an evident damage state due to the installation in cracked support. A concrete detachment of 3x3x2cm was observed indeed below the anchoring point. The hole enlarged because of cyclic displacement of the specimen being affected by dynamic loading.

Among all the experimental steps, the maximum dynamic loads -related to the instant of peak normalized force, namely 1.08 - acting on the specimen, consisted of almost 14kN in tension and 10.1kN in shear.

The measured slipping of the anchor during the test session 3 increased with an inflected curve up to 4.9mm. In this case the maximum slip value for the specimen is that related to the experimental step of maximum loading.

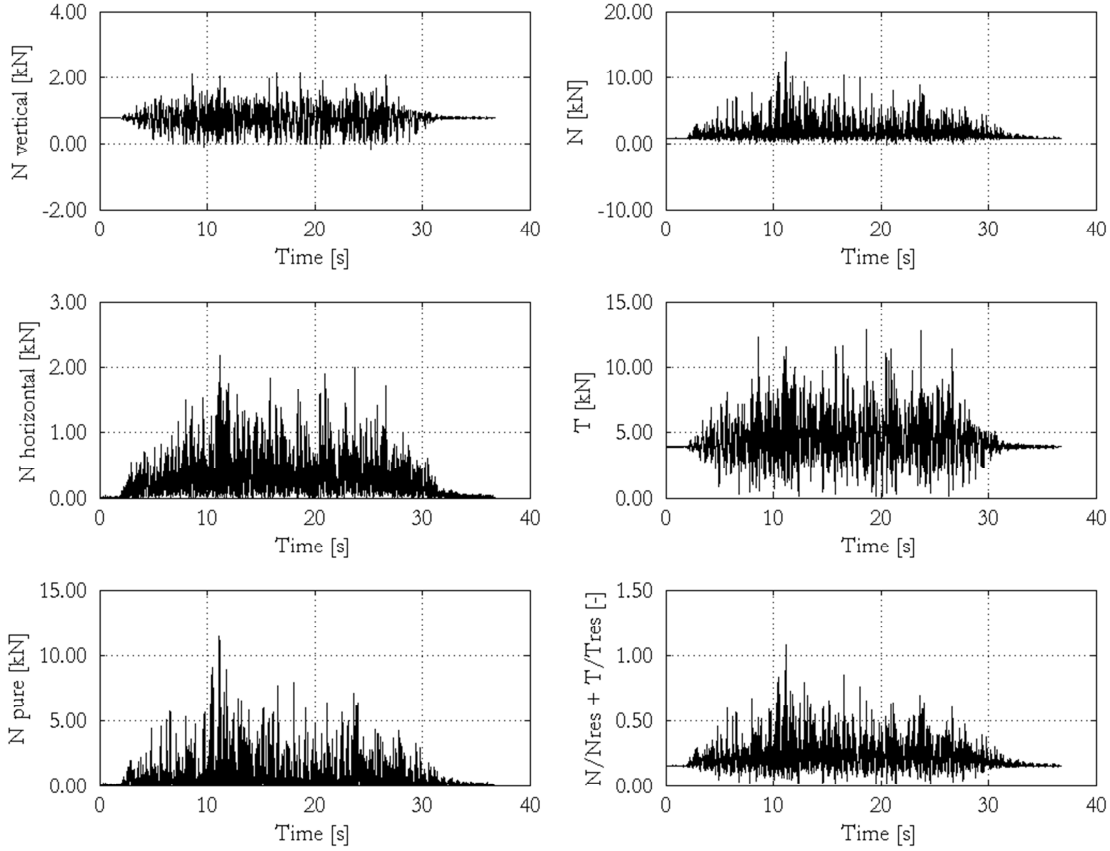

Figure 3.19 Loads acting on MEC6 specimen in test session 3 – 1.10g of ZPA testing step; N = axial load, T = shear load, N/Nres+T/Tres = normalized force for design load combination

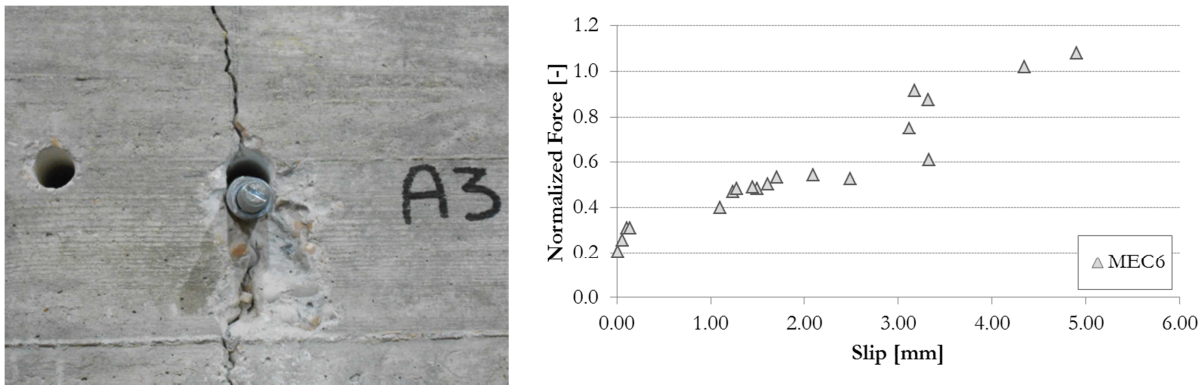

Figure 3.20 View of MEC6 specimen after test session 3. Load vs displacement graph for MEC6

3.4.1.7. Remarks about MEC specimen behaviour

The MEC specimens in both uncracked and cracked conditions showed a substantial agreement among them on the load-slip curves for each different support condition. In the first linear branch all the specimens has a similar trend while a more widespread behavior

was observed in the second part of the curves. The point at which the specimens loss the linear behavior, both in terms of load and slip, is substantially similar while the ultimate values show a wider difference. Furthermore in the first linear part the slip values for the specimen on uncracked support are substantially lower than those of anchors on cracked support for the same acting load. In any case the failure was occurred for this kind of anchor.

Table 3.9 Summarizing table for all the specimens with the maximum sustained actions in tension and shear, the maximum normalized force and the relevant slipping, the maximum slip

	N_{max}	V_{max}	$Fnorm_{max}$	δ_F	δ_{max}
Specimen ref.	kN	kN	-	mm	mm
MEC1	7.781	6.539	0.497	0.277	0.277
MEC2	7.177	8.702	0.647	2.418	2.418
MEC3	9.433	7.759	0.598	0.763	0.763
MEC4	7.989	10.946	0.753	2.347	2.347
MEC5	12.372	10.016	0.780	1.141	1.454
MEC6	13.965	10.182	1.081	4.901	4.901

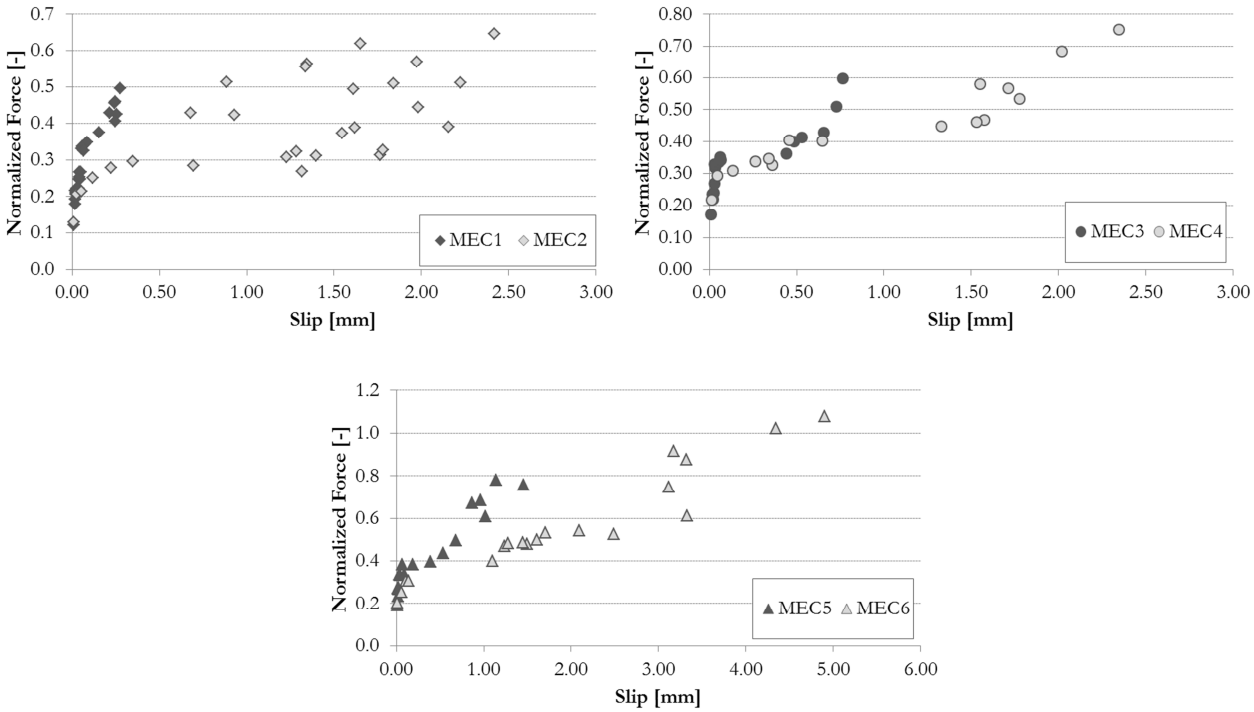

Figure 3.21 MEC specimens: load-displacement graphs for uncracked (dark grey) and cracked (light grey) conditions

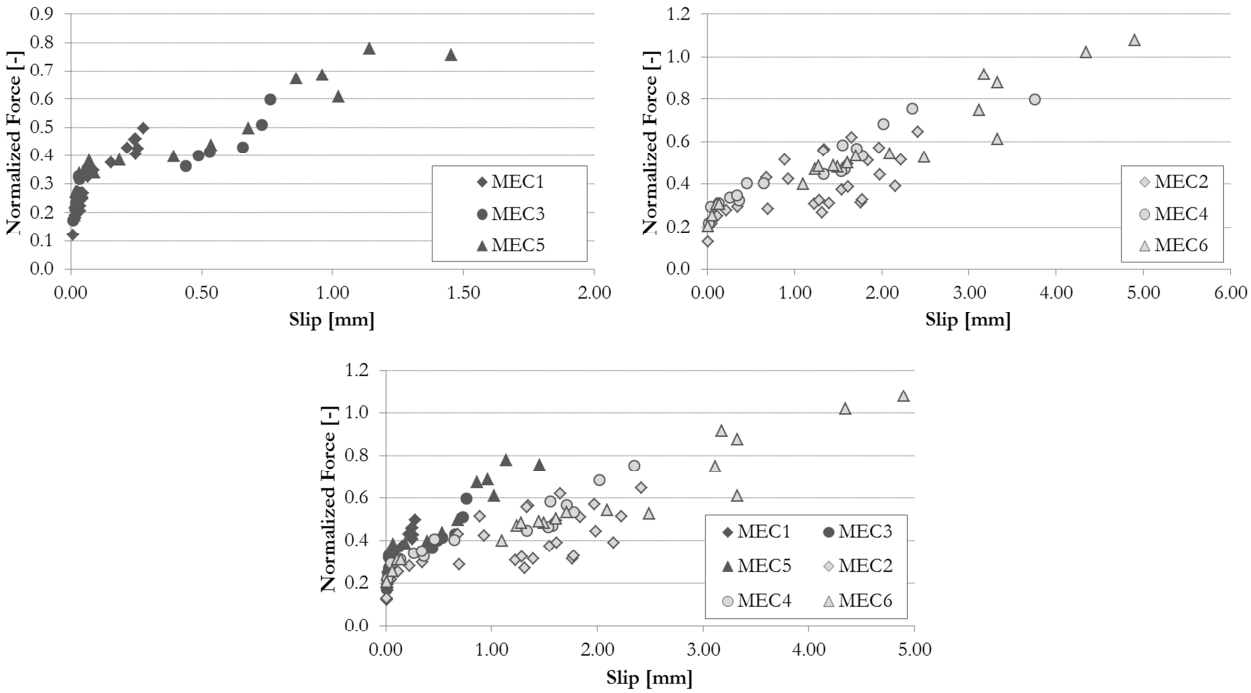

Figure 3.22 Summarizing load-displacement curves for MEC specimens in uncracked (dark grey) and cracked (light grey) conditions

3.4.2. Undercut Anchor (U)

This paragraph includes the results of the metal expansion anchor U M10 in uncracked and cracked concrete. A total of 4 specimens were tested in the first 2 test sessions with the concrete structural unit. Two of them were installed in a 0.80mm wide crack. The component fixed with UC specimens consisted in a 400kg steel plate.

Figure 3.23 View of metal undercut anchor UC M10

Table 3.10 Installation features for metal undercut anchor specimens

Specimen reference	Test session	Component reference	Mass [kg]	Height from table [cm]	Crack	Measured crack width [mm]
UC1	TS1	F1	400	115	No	
UC2	TS1	E1	400	115	Yes	0.805
UC3	TS2	F2	400	155	No	
UC4	TS2	E2	400	155	Yes	0.813

3.4.2.1. UC specimen 1

Specimen 1 of undercut anchor was installed in uncracked support. It did not reach failure after having withstood all of the testing steps in test session 1. The anchor experienced a bending of the stud and a cracking of the external sleeve at the end of the

testing. The progressive slippage of the anchor is mainly caused by axial forces acting on the fixing point instead. The base material has manifested no damages due to the installation in uncracked support. A concrete detachment of 2x1x0.5cm was observed indeed below the anchoring point.

Among all the experimental steps, the maximum dynamic loads -related to the instant of peak normalized force, namely 1.70 - acting on the specimen, consisted of almost 6.5kN in tension and 11.8kN in shear.

The measured slipping of the anchor during the test session 1 increased with an inflected curve, with an initial displacement probably when reaching hole interlock surface, up to 0.7mm. In this case the maximum slip value for the specimen is that related to the experimental step of maximum loading.

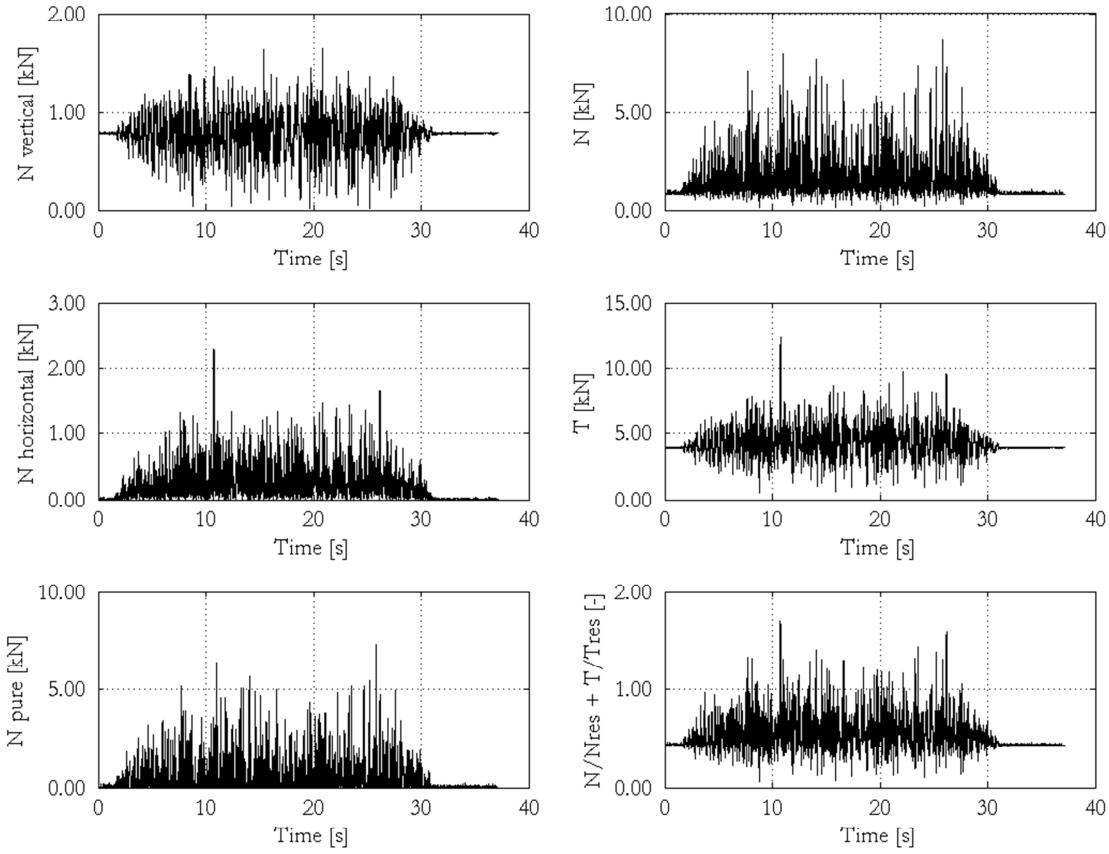

Figure 3.24 Loads acting on UC1 specimen in test session 1 – 1.10g of ZPA testing step; N = axial load, T = shear load, N/Nres+T/Tres = normalized force for design load combination

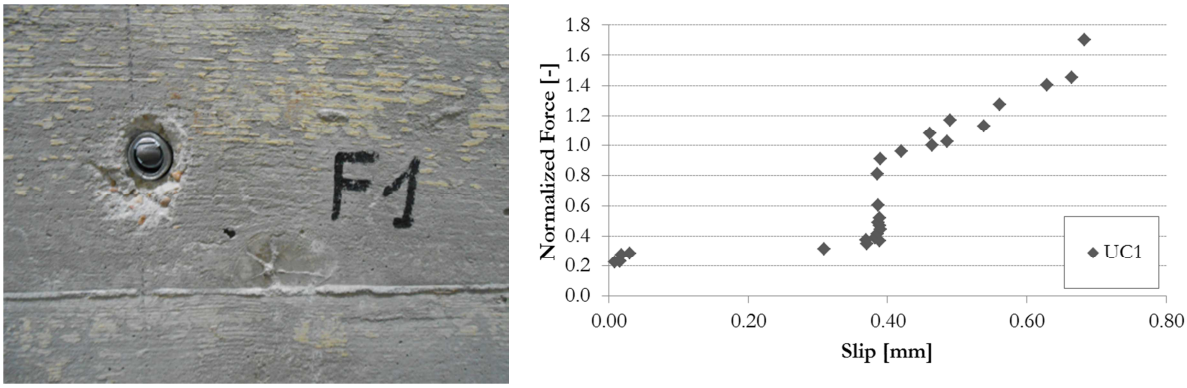

Figure 3.25 View of UC1 specimen after test session 1. Load vs displacement graph for UC1

3.4.2.2. UC specimen 2

Specimen 2 of undercut anchor was installed in the crack. It did not reach failure after having withstood all of the testing steps in test session 1. The anchor experienced a bending of the stud and an opening of the external sleeve. The progressive slippage of the anchor is mainly caused by axial forces acting on the fixing point instead. The base material has manifested an evident damage state due to the installation in cracked support. A concrete detachment of 3x3x1cm was observed indeed around the anchoring point. The hole slightly enlarged because of cyclic displacement of the specimen being affected by dynamic loading.

Among all the experimental steps, the maximum dynamic loads -related to the instant of peak normalized force, namely 1.89 - acting on the specimen, consisted of 8.2kN in tension and 8.0kN in shear.

The measured slipping of the anchor during the test session 1 increased with an inflected curve, with a linear end, up to 2.0mm. In this case the maximum slip value for the specimen is that related to the experimental step of maximum loading.

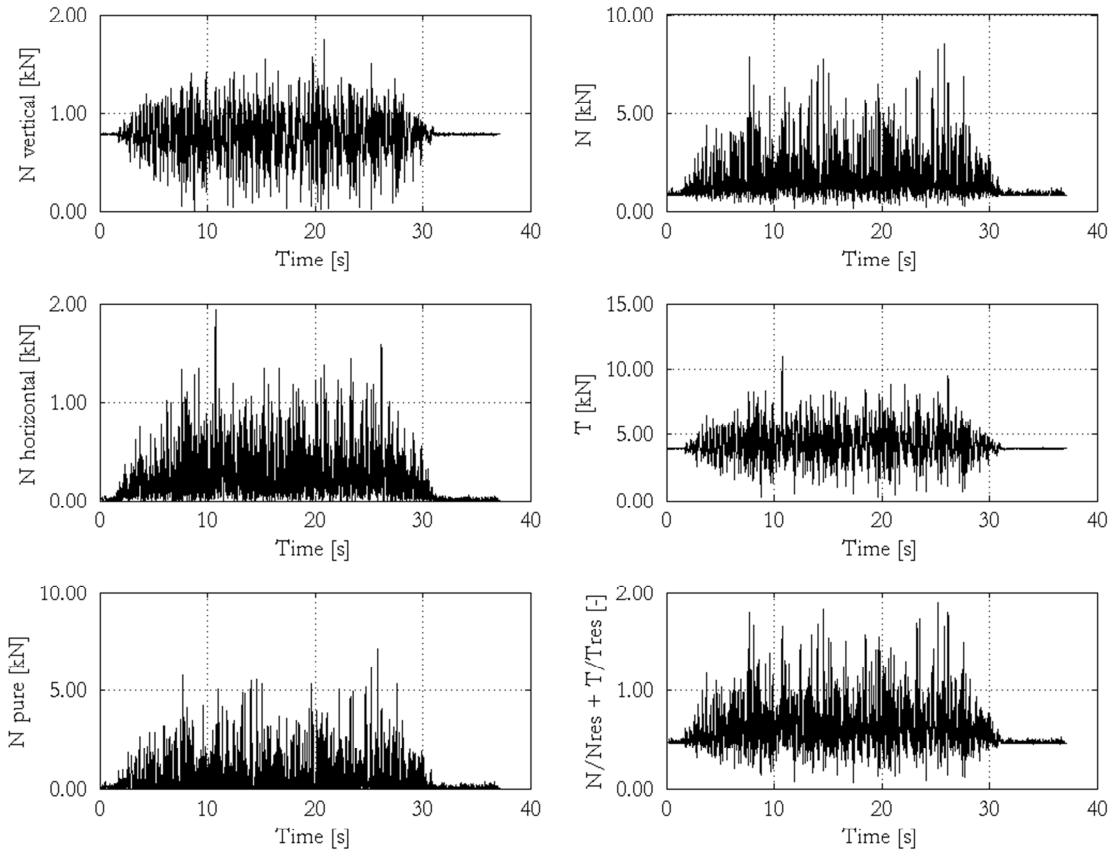

Figure 3.26 Loads acting on UC2 specimen in test session 1 – 1.10g of ZPA testing step; N = axial load, T = shear load, N/Nres+T/Tres = normalized force for design load combination

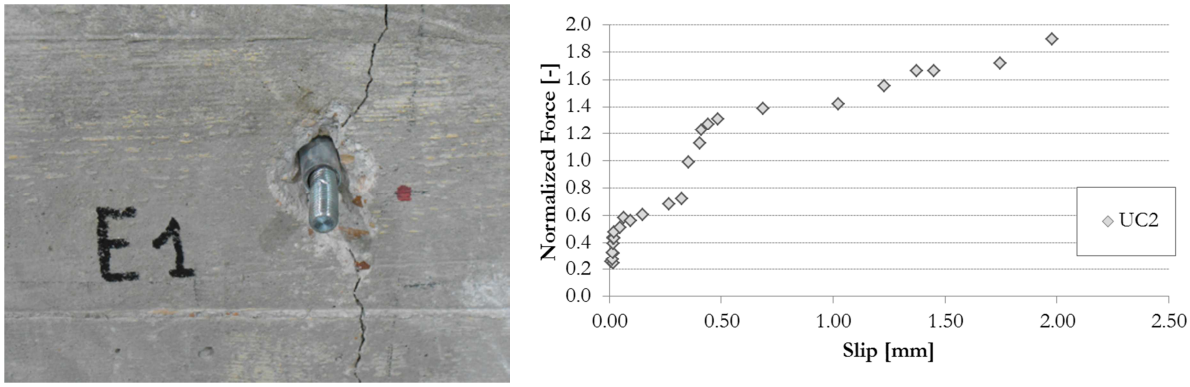

Figure 3.27 View of UC2 specimen after test session 1. Load vs displacement graph for UC2

3.4.2.3. UC specimen 3

Specimen 3 of undercut anchor was installed in uncracked support. It did not reach failure after having withstood all of the testing steps in test session 2. The anchor experienced a bending of the stud and an opening in the down part of the external sleeve at the end of the testing. The progressive slippage of the anchor is mainly caused by axial forces acting on the fixing point instead. The base material has manifested no damages due to the installation in uncracked support. A concrete detachment of 2x1x0.5cm was observed indeed below the anchoring point. The hole enlarged of about 0.5cm because of cyclic displacement of the specimen being affected by dynamic loading.

Among all the experimental steps, the maximum dynamic loads -related to the instant of peak normalized force, namely 1.37 - acting on the specimen, consisted of 7.0kN in tension and 7.4kN in shear.

The measured slipping of the anchor during the test session 2 increased with an almost linear plot up to 0.8mm. In this case the maximum slip value for the specimen is different from that related to the experimental step of maximum loading, which was of 0.6mm.

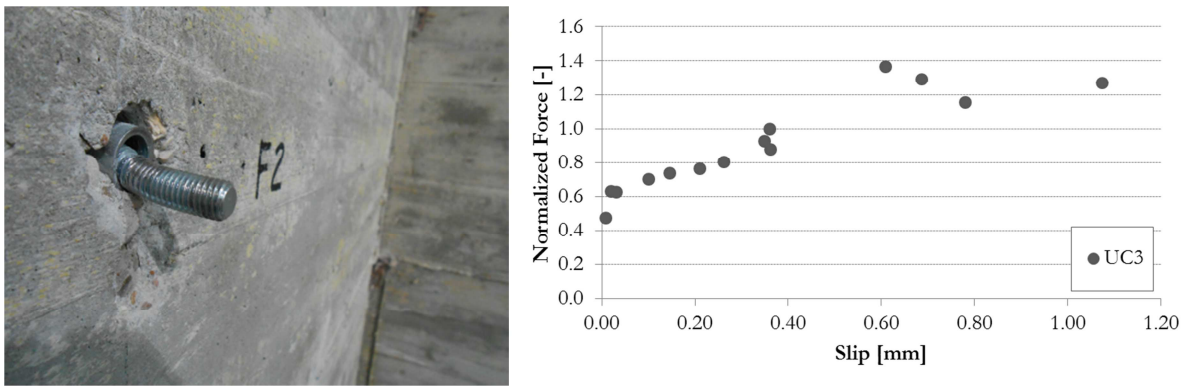

Figure 3.28 View of UC3 specimen after test session 2. Load vs displacement graph for UC3

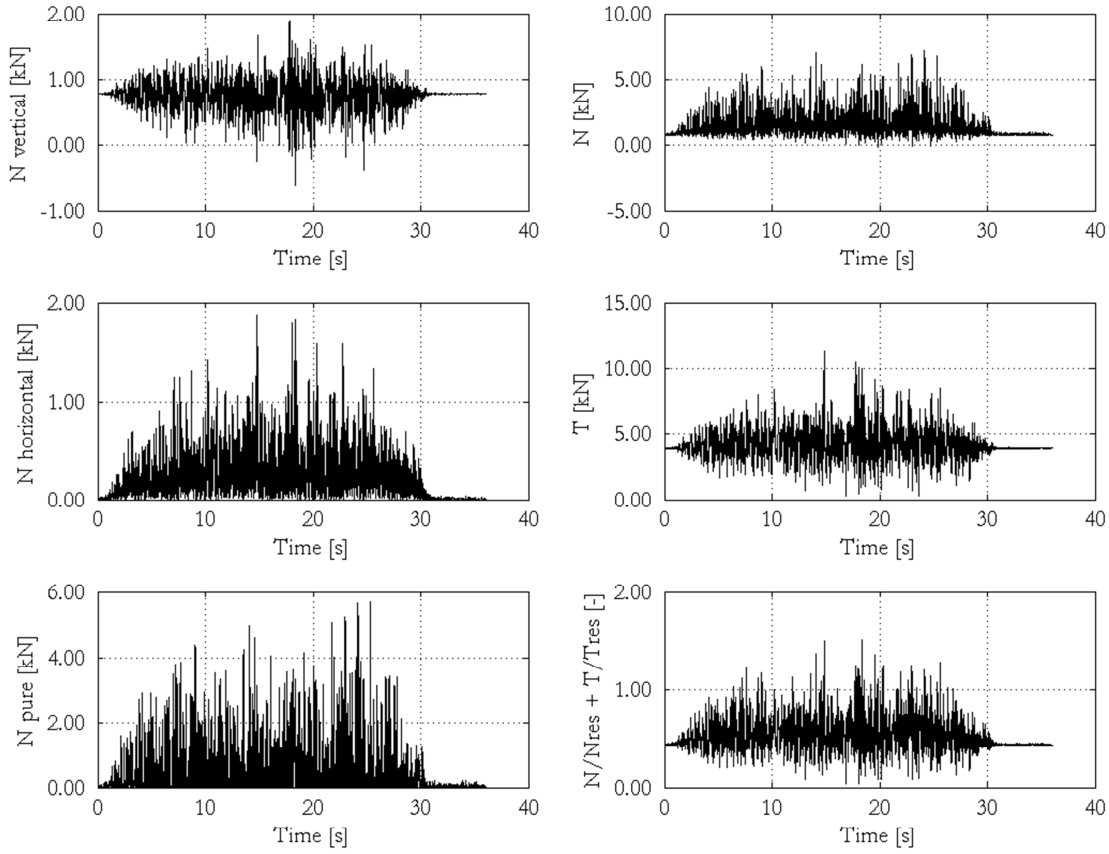

Figure 3.29 Loads acting on UC3 specimen in test session 2 – 1.00g of ZPA testing step; N = axial load, T = shear load, N/Nres+T/Tres = normalized force for design load combination

3.4.2.4. UC specimen 4

Specimen 4 of undercut anchor was installed in the crack. It did not reach failure after having withstood all of the testing steps in test session 2. The anchor experienced a bending of the stud and an opening of the external sleeve. The progressive slippage of the anchor is mainly caused by axial forces acting on the fixing point instead. The base material has manifested an evident damage state due to the installation in cracked support. A concrete detachment of 11x9x1cm was observed indeed around the anchoring point. The hole enlarged of about 1cm because of cyclic displacement of the specimen being affected by dynamic loading.

Among all the experimental steps, the maximum dynamic loads -related to the instant of peak normalized force, namely 1.74 - acting on the specimen, consisted of 7.4kN in tension and 7.6kN in shear.

The measured slipping of the anchor during the test session 2 increased with an inflected curve up to 1.4mm. In this case the maximum slip value for the specimen is that related to the experimental step of maximum loading.

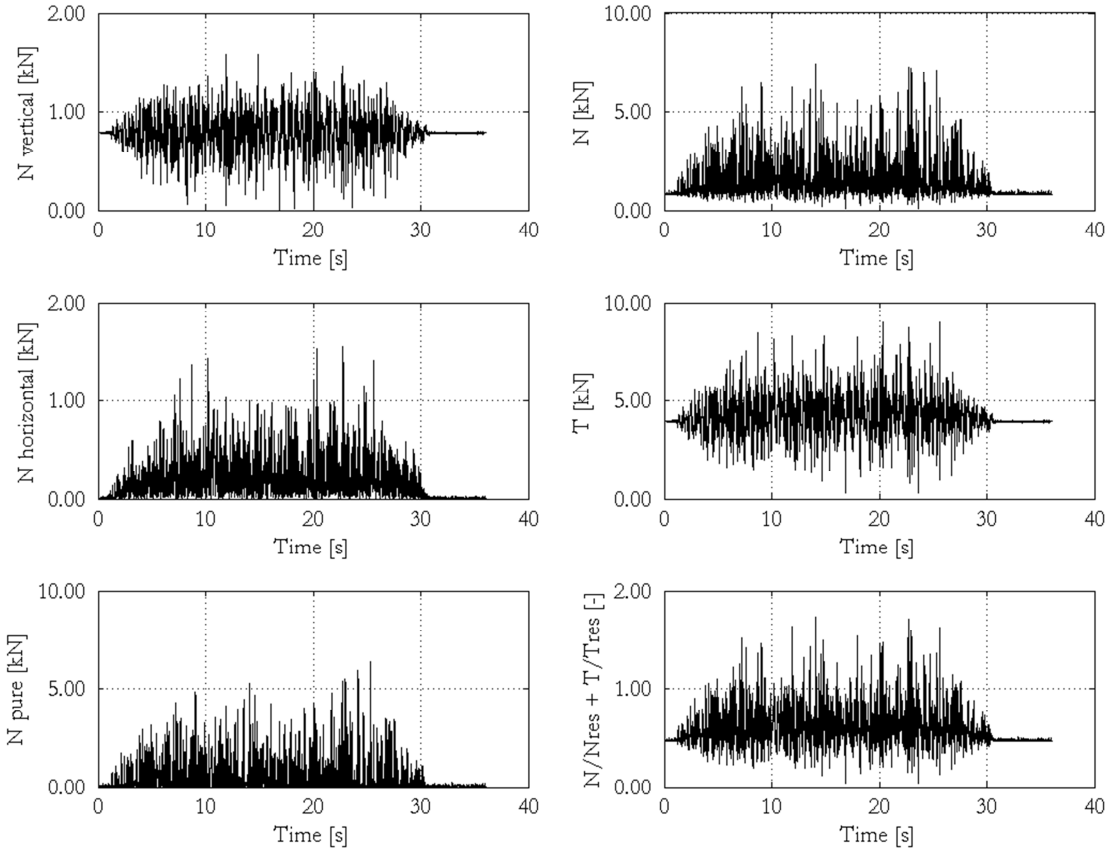

Figure 3.30 Loads acting on UC4 specimen in test session 2 – 1.00g of ZPA testing step; N = axial load, T = shear load, N/Nres+T/Tres = normalized force for design load combination

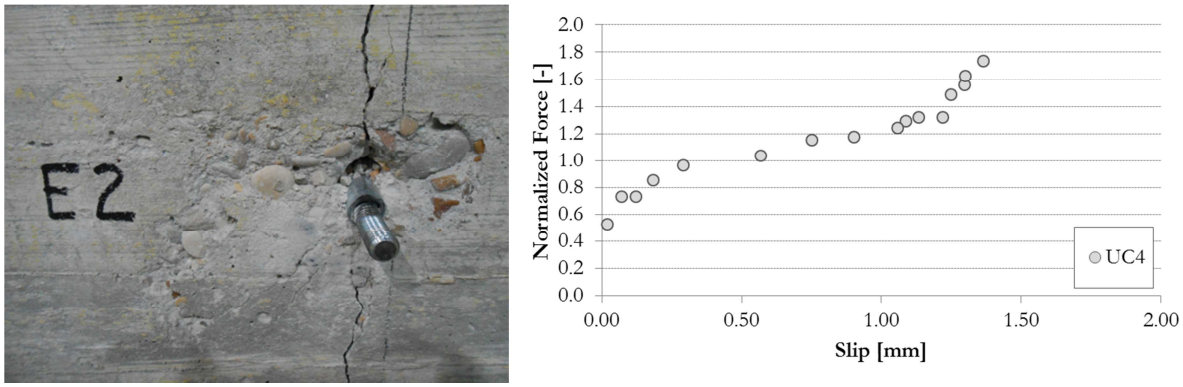

Figure 3.31 View of UC4 specimen after test session 2. Load vs displacement graph for UC4

3.4.2.5. Remarks about UC specimen behaviour

All the UC anchors manifested a similar overall behavior even some local differences should be highlighted. In most cases, independently from the support condition, the first part of the curve shows very limited slip values. Over this first part a linear increasing trend can be identified up to the attainment of the maximum value in terms of both, load and slip. Only in a case (UC1) higher slip values were recorded in the initial part of the curve, even if over this the increasing on the load in relation to a limited slip increase can be observed. In that case the overall behavior seems to be postponed and this could be

ascribed to a not perfect installation of the anchor that completed the undercut expansion during the first steps of the test. In all cases the UC anchors did not fail.

Table 3.11 Summarizing table for all the specimens with the maximum sustained actions in tension and shear, the maximum normalized force and the relevant slipping, the maximum slip

	N_{max}	V_{max}	$F_{norm\ max}$	δ_F	δ_{max}
Specimen ref.	kN	kN	-	mm	mm
UC1	6.409	11.751	1.703	0.683	0.683
UC2	8.243	8.011	1.894	1.979	1.979
UC3	7.003	7.410	1.367	0.609	0.780
UC4	7.395	7.596	1.736	1.365	1.365

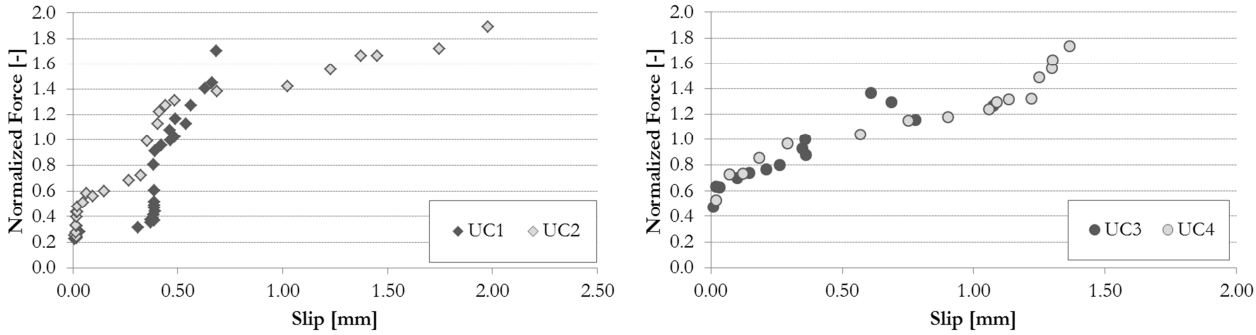

Figure 3.32 UC specimens: load-displacement graphs for uncracked (dark grey) and cracked (light grey) conditions

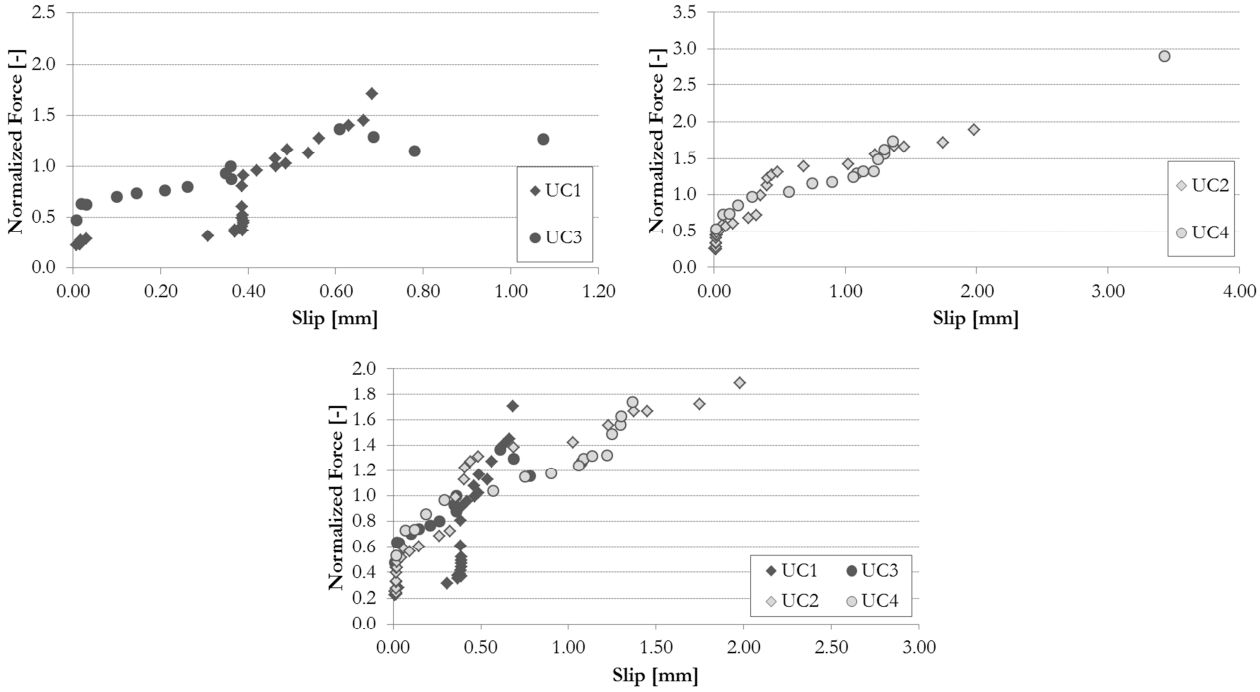

Figure 3.33 Summarizing load-displacement curves for UC specimens in uncracked (dark grey) and cracked (light grey) conditions

3.4.3. Adhesive Anchor (A)

This paragraph includes the results of the chemical anchor A with a M16 stud in uncracked and cracked concrete. A total of 4 specimens were tested in the first 2 test sessions with the concrete structural unit. Two of them were installed in a 0.80mm wide crack. The component fixed with AC specimens consisted in a 400kg steel plate. The four specimens were installed using a standard steel stud.

Figure 3.34 View of chemical anchor with the M16 standard steel stud

Table 3.12 Installation features for chemical anchor specimens

Specimen reference	Test session	Component reference	Mass [kg]	Height from table [cm]	Crack	Measured crack width [mm]
AC1	TS1	C1	400	115	No	
AC2	TS1	D1	400	115	Yes	0.809
AC3	TS2	C2	400	155	No	
AC4	TS2	D2	400	155	Yes	0.806

3.4.3.1. AC specimen 1

Specimen 1 of adhesive anchor was installed in uncracked support. It did not reach failure after having withstood all of the testing steps in test session 1. Both the anchorage system and the concrete surface were not affected by any relevant damage. Almost no slippage occurred to the anchor. The base material has manifested no damages thanks to the installation in uncracked support.

Among all the experimental steps, the maximum dynamic loads -related to the instant of peak normalized force, namely 0.40 - acting on the specimen, consisted of 5.2kN in tension and 8.7kN in shear.

The measured slipping of the anchor during the test session 1 increased with an almost linear plot up to 0.5mm. In this case the maximum slip value for the specimen is that related to the experimental step of maximum loading.

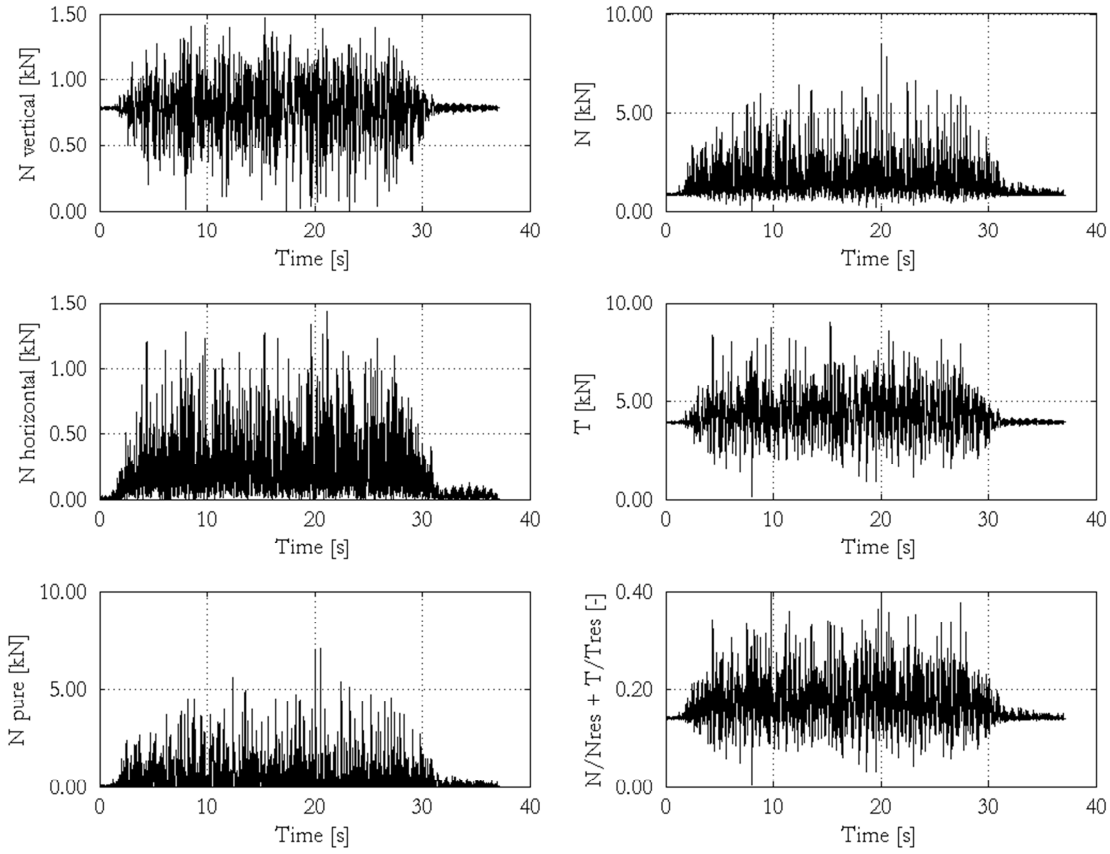

Figure 3.35 Loads acting on AC1 specimen in test session 1 – 1.10g of ZPA testing step; N = axial load, T = shear load, N/Nres+T/Tres = normalized force for design load combination

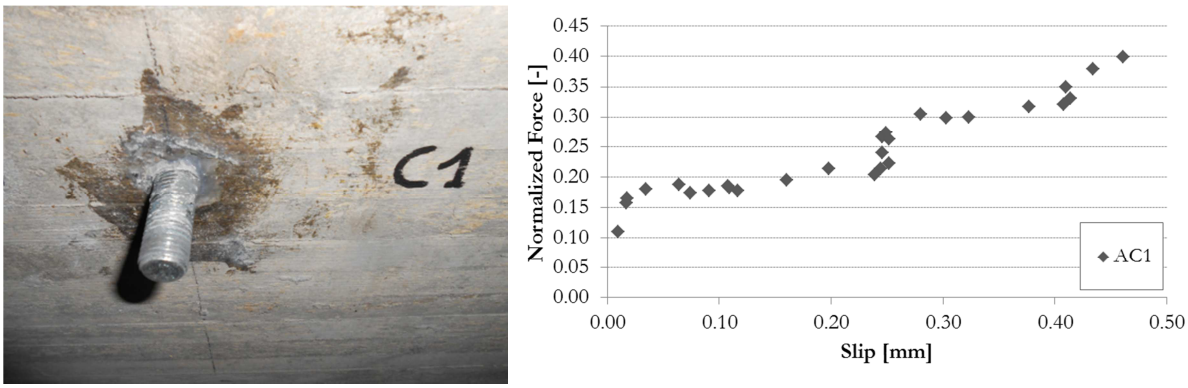

Figure 3.36 View of AC1 specimen after test session 1. Load vs displacement graph for AC1

3.4.3.2. AC specimen 2

Specimen 2 of adhesive anchor was installed in the crack. It reached failure at a nominal level of peak acceleration of 0.55g in the test session 1. The failure mode of anchors installed in the cracked support was related to the pull-out of the entire anchoring system, thus causing the detachment of a concrete cone from the base material. The specimen have shown a bending strain due to shear forces, while the expelled concrete cone had a depth of about 4cm. The base material has manifested an evident damage state with a concrete detachment of 9x11x4cm was observed indeed around the anchoring point. The hole enlarged because of cyclic displacement of the specimen being affected by dynamic loading.

Among all the experimental steps, the maximum dynamic loads -related to the instant of peak normalized force, namely 0.46 - acting on the specimen, consisted of 5.8kN in tension and 8.4kN in shear.

The measured slipping of the anchor during the test session 1 increased with an inflected curve up to 4.4mm. In this case the maximum slip value for the specimen is that related to the experimental step of maximum loading.

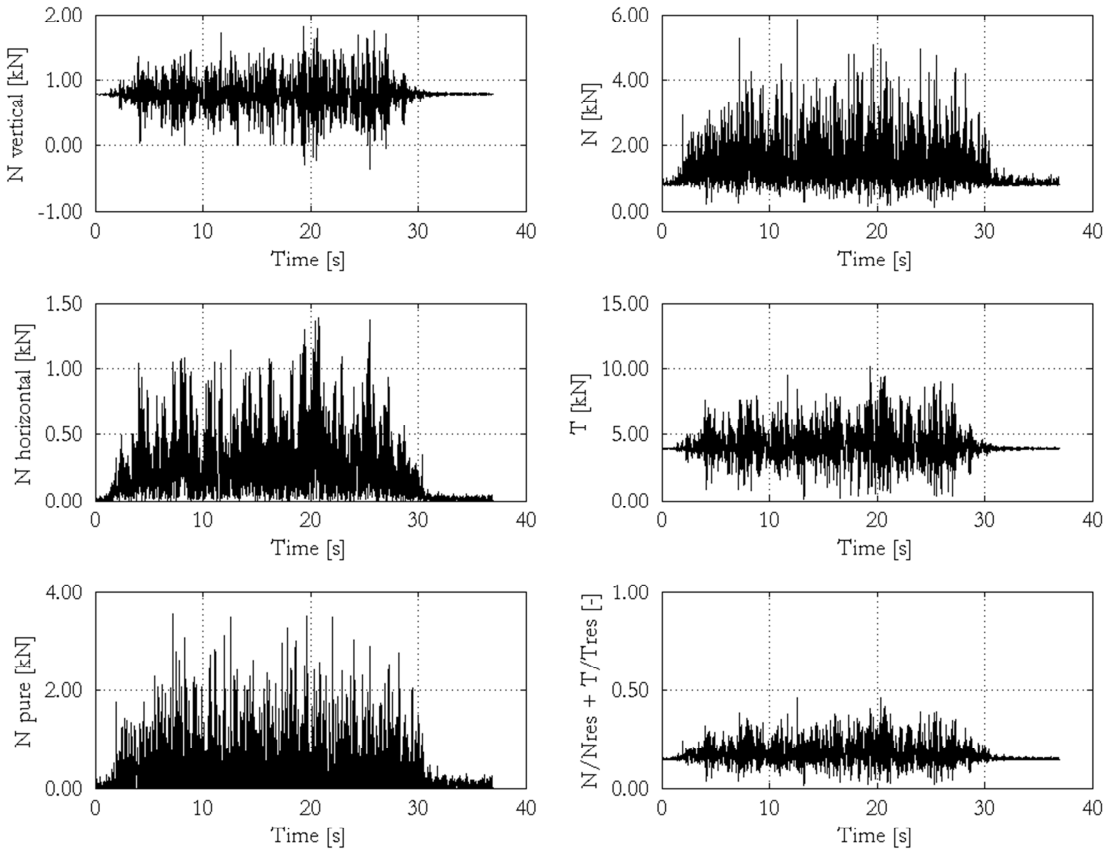

Figure 3.37 Loads acting on AC2 specimen in test session 1 – 0.60g of ZPA testing step; N = axial load, T = shear load, N/Nres+T/Tres = normalized force for design load combination

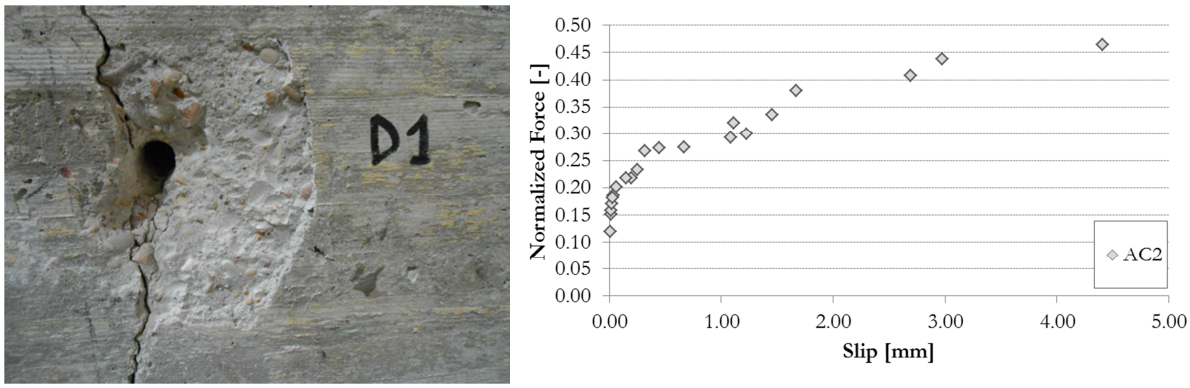

Figure 3.38 Failure mode of AC2 specimen after test session 1. Load vs displacement graph for AC2

3.4.3.3. AC specimen 3

Specimen 3 of adhesive anchor was installed in uncracked support. It didn't reach failure after having withstood all of the testing steps in test session 2. Both the anchorage system and the concrete surface were not affected by any relevant damage. Almost no slippage occurred to the anchor. The base material has manifested no damages thanks to the installation in uncracked support.

Among all the experimental steps, the maximum dynamic loads -related to the instant of peak normalized force, namely 0.45 - acting on the specimen, consisted of 5.7kN in tension and 10.2kN in shear.

The measured slipping of the anchor during the test session 2 increased with an almost linear plot up to 1.6mm. In this case the maximum slip value for the specimen is that related to the experimental step of maximum loading.

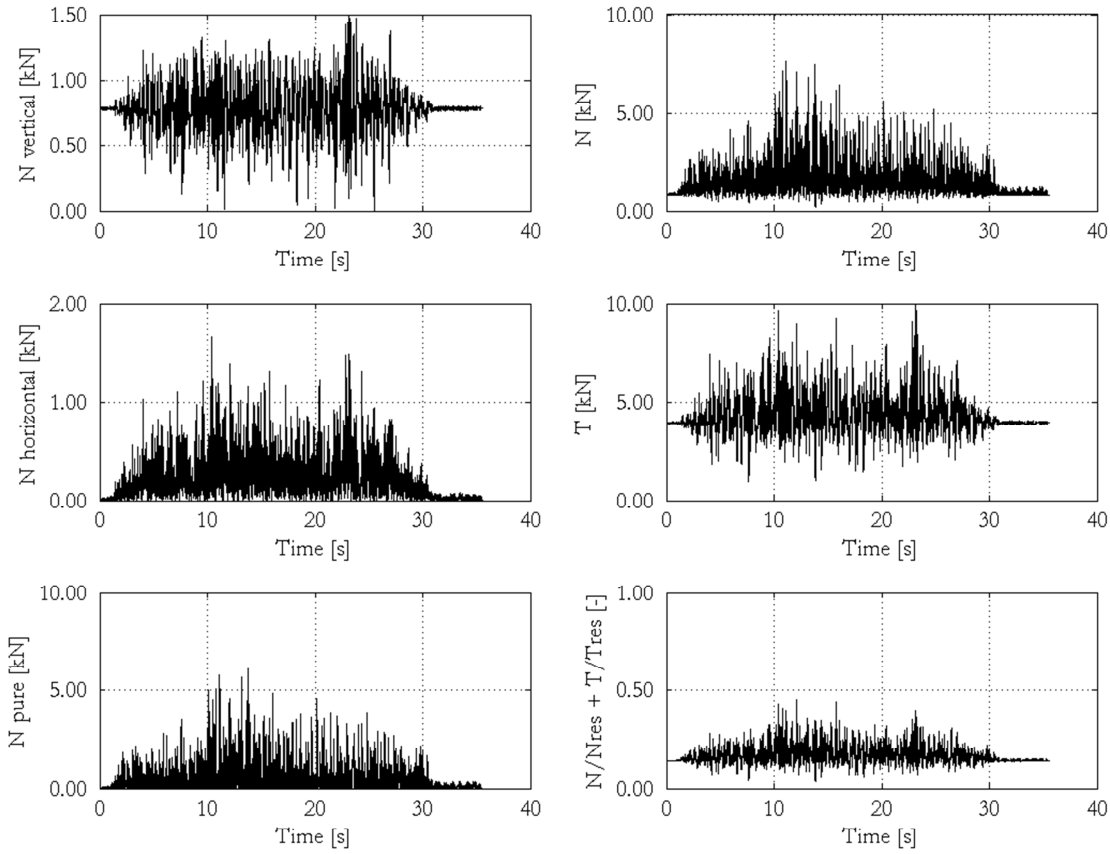

Figure 3.39 Loads acting on AC3 specimen in test session 2 – 0.90g of ZPA testing step; N = axial load, T = shear load, N/Nres+T/Tres = normalized force for design load combination

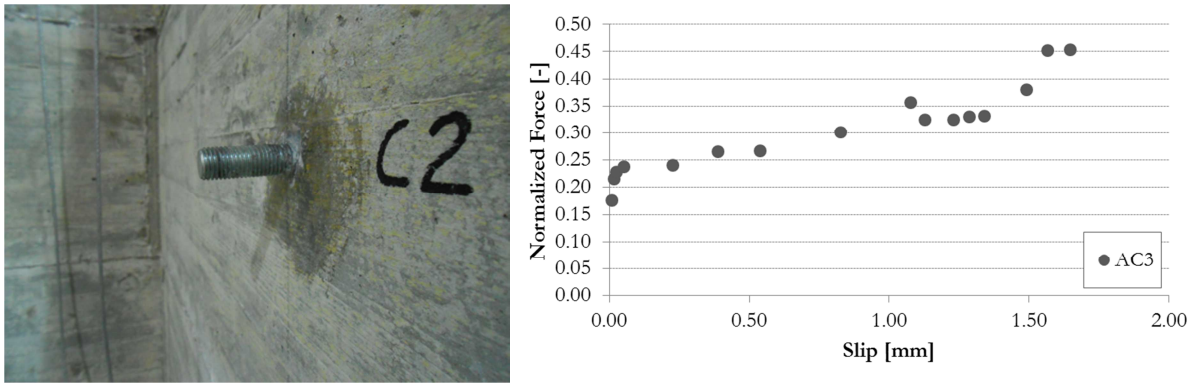

Figure 3.40 View of AC3 specimen after test session 2. Load vs displacement graph for AC3

3.4.3.4. AC specimen 4

Specimen 4 of adhesive anchor was installed in the crack. It reached failure at a nominal level of peak acceleration of 0.60g in the test session 2. The failure mode of anchors installed in the cracked support was related to the pull-out of the entire anchoring system, thus causing the detachment of a concrete cone from the base material. The specimen have shown a bending strain due to shear forces, while the expelled concrete cone had a depth of about 4cm. The base material has manifested an evident damage state with a concrete detachment of 7x9x4cm was observed indeed around the anchoring point, especially in the lower part. The hole enlarged because of cyclic displacement of the specimen being affected by dynamic loading.

Among all the experimental steps, the maximum dynamic loads -related to the instant of peak normalized force, namely 0.41 - acting on the specimen, consisted of 5.2kN in tension and 7.2kN in shear.

The measured slipping of the anchor during the test session 2 increased with an almost linear plot up to 2.2mm. In this case the maximum slip value for the specimen is different from that related to the experimental step of maximum loading, which was of 1.7mm.

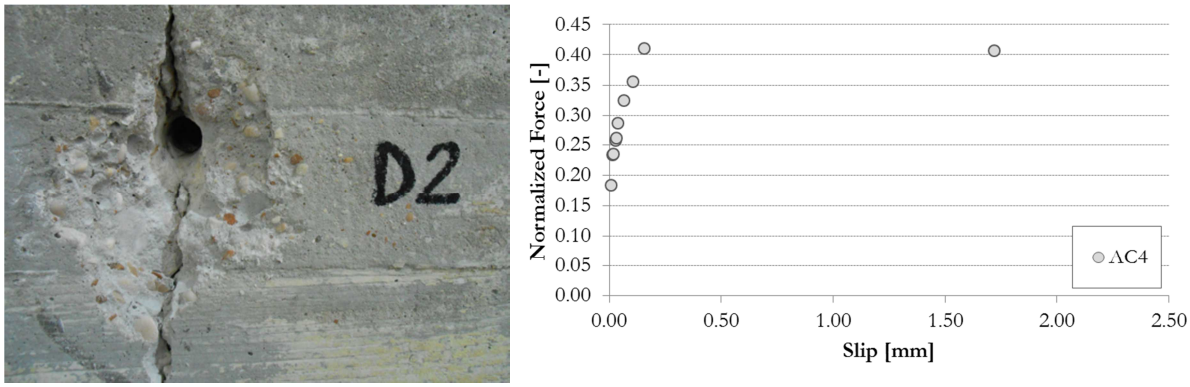

Figure 3.41 Failure mode of AC4 specimen after test session 2. Load vs displacement graph for AC4

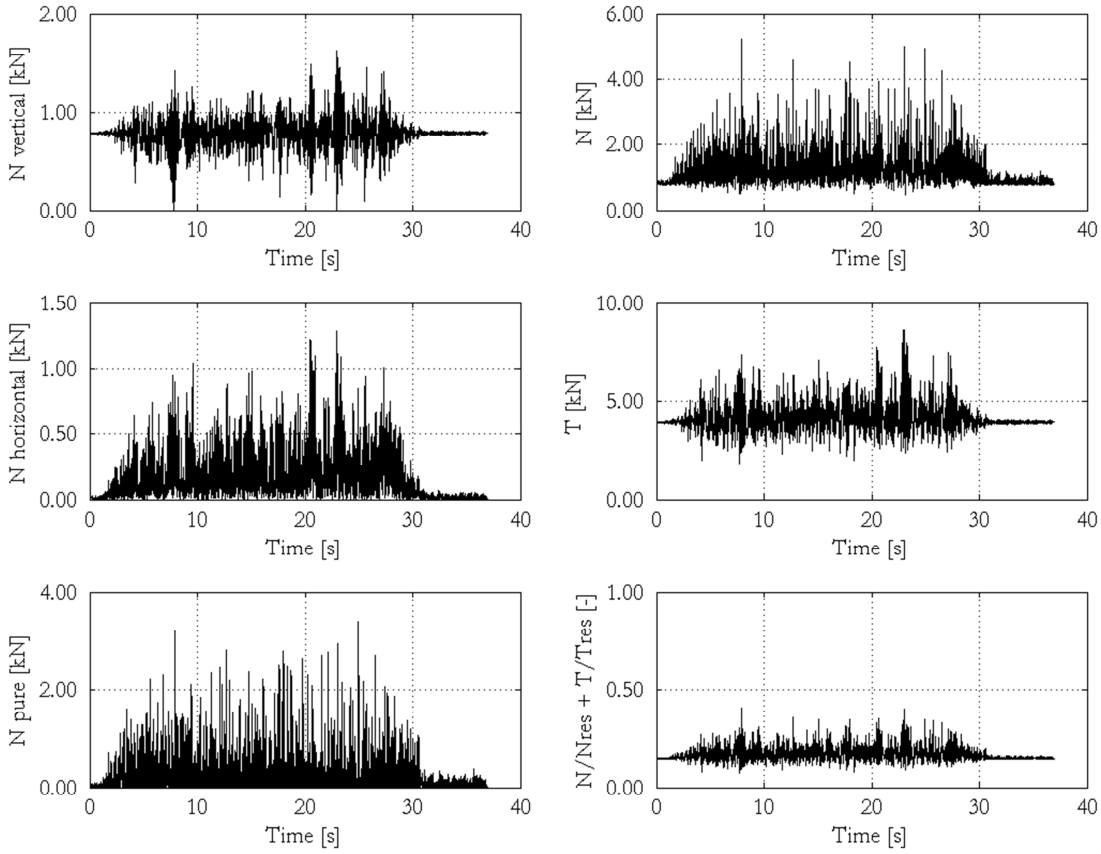

Figure 3.42 Loads acting on AC4 specimen in test session 2 – 0.50g of ZPA testing step; N = axial load, T = shear load, N/Nres+T/Tres = normalized force for design load combination

3.4.3.5. Remarks about AC specimen behaviour

The AC specimens, characterized by the use of a normal steel stud, showed different overall behaviours even if considering the same conditions of the support. About the specimens on uncracked concrete both manifested a certain slippage over a first part with limited slip. Nevertheless the failure values in terms of displacement are substantially different. This can be also observed for the specimens on cracked concrete. However, on the other hand, the failure values in terms of load are in agreement between them, considering the same support condition. The failure load of anchors installed on uncracked concrete are higher than those installed on cracked support. These observations highlight the higher sensitivity of this kind of anchor to the installation procedure.

Table 3.13 Summarizing table for all the specimens with the maximum sustained actions in tension and shear, the maximum normalized force and the relevant slipping, the maximum slip

	N_{max}	V_{max}	$F_{norm\ max}$	δ_F	δ_{max}
Specimen ref.	kN	kN	-	mm	mm
AC1	5.217	8.744	0.399	0.461	0.461
AC2	5.838	8.413	0.464	4.409	4.409
AC3	5.666	10.162	0.454	1.647	1.647
AC4	5.228	7.244	0.407	1.721	2.249

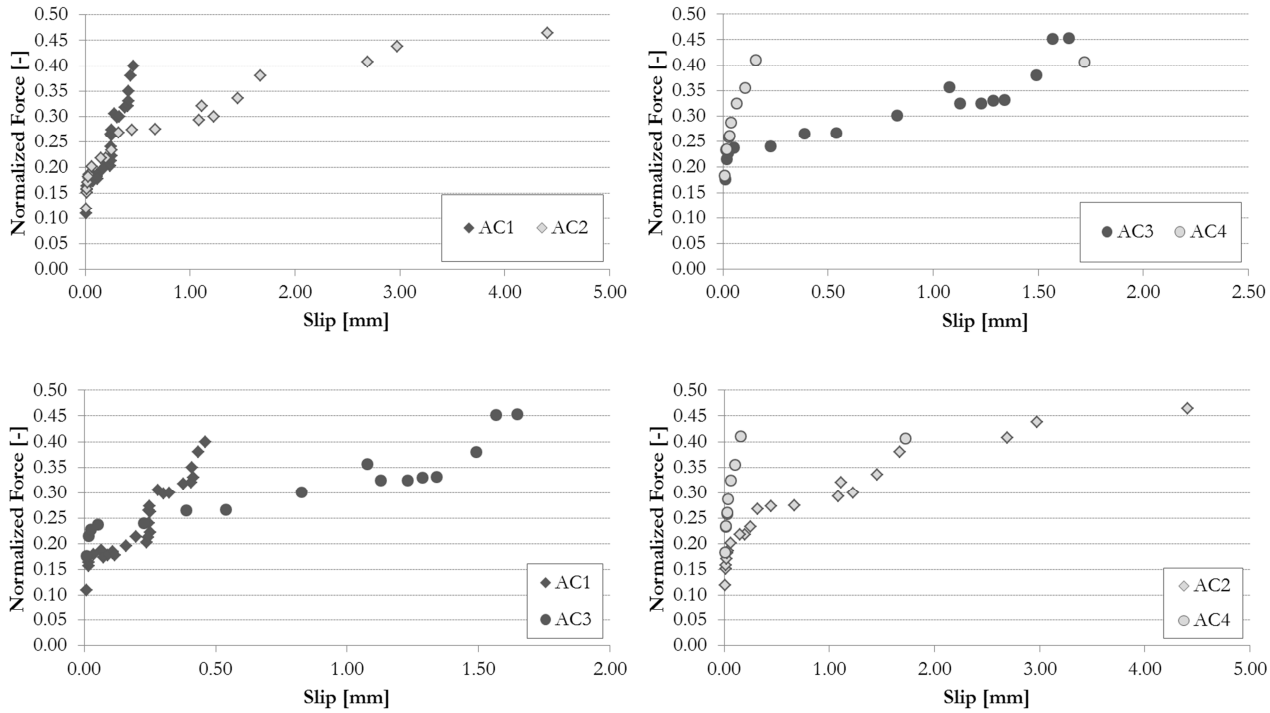

Figure 3.43 AC specimens: load-displacement graphs for uncracked (dark grey) and cracked (light grey) conditions

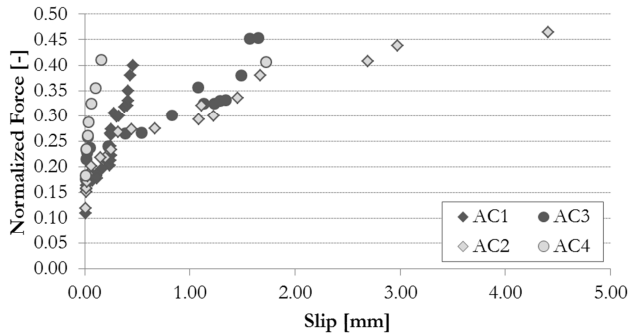

Figure 3.44 Load-displacement curves for AC specimens in uncracked (dark grey) and cracked (light grey) conditions

3.4.4. Plastic Expansion Anchor (PE)

This paragraph includes the results of the plastic expansion anchor PE 10x80 in uncracked and cracked concrete. A total of 6 specimens were tested in the 3 test sessions with the concrete structural unit. Three of them were installed in a 0.35mm wide crack. The component fixed with PEC specimens consisted in a 200kg steel plate for TS1 and TS2 and in a 250kg steel plate for TS3.

Figure 3.45. View of metal expansion anchor PEC 10x80.

Table 3.14. Installation features for plastic expansion anchor specimens.

Specimen reference	Test session	Component reference	Mass [kg]	Height from table [cm]	Crack	Measured crack width [mm]
PEC1	TS1	G1	200	115	No	
PEC2	TS1	H1	200	115	Yes	0.357
PEC3	TS2	G2	200	155	No	
PEC4	TS2	H2	200	155	Yes	0.341
PEC5	TS3	G3	250	195	No	
PEC6	TS3	H3	250	195	Yes	0.359

3.4.4.1. PEC specimen 1

Specimen 1 of plastic expansion anchor was installed in uncracked concrete. It didn't reach failure after having withstood all of the testing steps in test session 1. A light shear deformation occurred to the screw and the external sleeve was slightly flattened at the end of the testing. The progressive slippage of the anchor is mainly caused by axial forces acting on the fixing point. The base material has manifested light damages and a concrete detachment of 3x3x0.5cm was observed indeed below the anchoring point.

Among all the experimental steps, the maximum dynamic loads -related to the instant of peak normalized force, namely 1.03 - acting on the specimen, consisted of 2.5kN in tension and 3.7kN in shear.

The measured slipping of the anchor during the test session 1 increased with an inflected curve up to 0.6mm. In this case the maximum slip value for the specimen is different from that related to the experimental step of maximum loading, which was of 0.58mm.

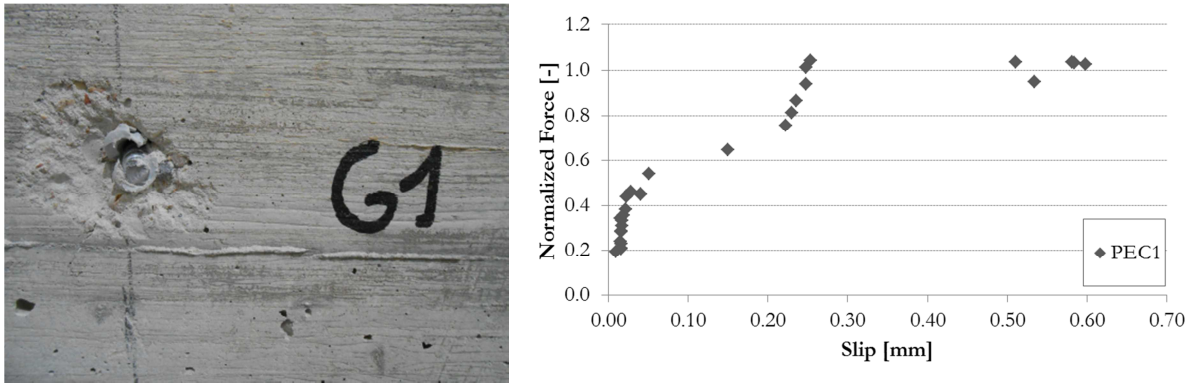

Figure 3.46 View of PEC1 specimen after test session 1. Load vs displacement graph for PEC1

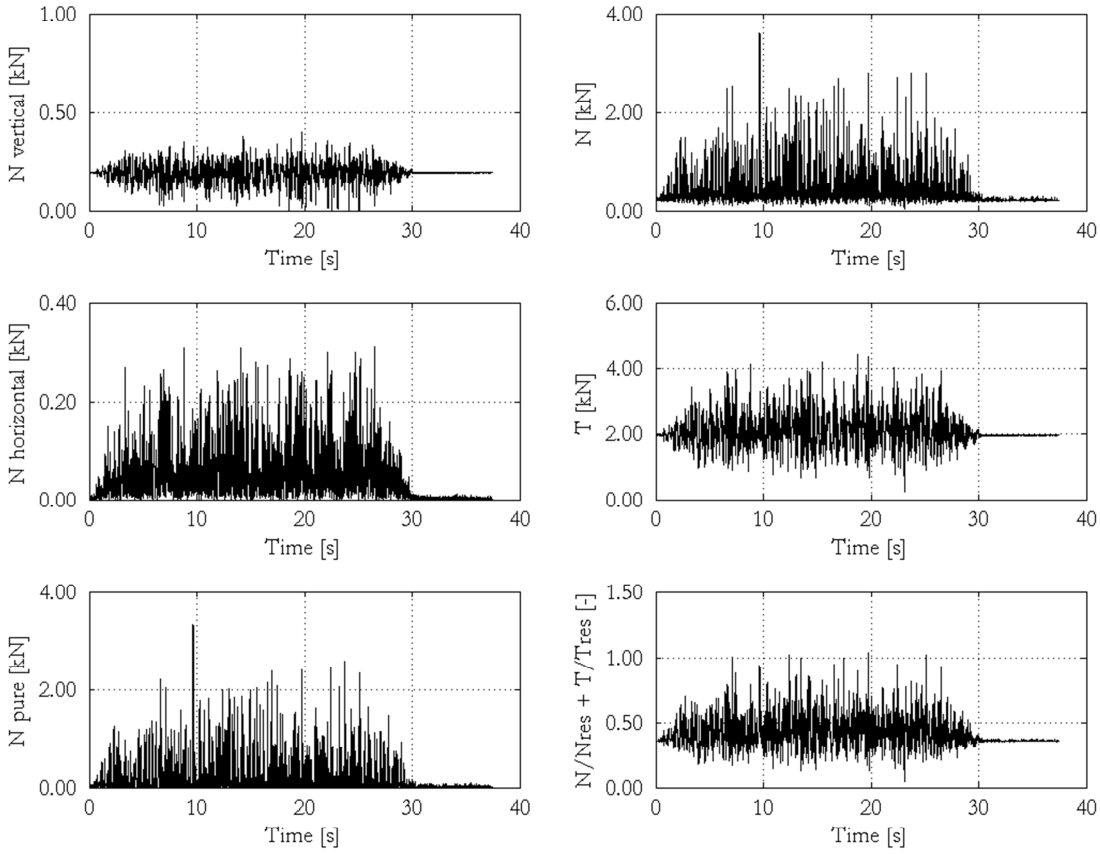

Figure 3.47 Loads acting on PEC1 specimen in test session 1 – 1.00g of ZPA testing step; N = axial load, T = shear load, N/Nres+T/Tres = normalized force for design load combination

3.4.4.2. PEC specimen 2

Specimen 2 of plastic expansion anchor was installed in the crack. It reached failure at a nominal level of peak acceleration of 0.90g in the test session 1. The damage to the fastening system was mainly caused by a high shear deformation, combined with a progressive slippage of the anchor. The observed failure mode of the specimen was related to the slipping of the screw from the base material and the relative slipping between screw and sleeve, with the rupture of the plastic sleeve, which are mechanisms related to axial and shear actions respectively. The base material experienced only limited damages as a concrete detachment of 2x3x1cm was observed below the anchoring point.

Among all the experimental steps, the maximum dynamic loads -related to the instant of peak normalized force, namely 1.52 - acting on the specimen, consisted of 2.2kN in tension and 3.9kN in shear.

The measured slipping of the anchor during the test session 1 increased with an inflected curve up to 3.4mm. In this case the maximum slip value for the specimen is different from that related to the experimental step of maximum loading, which was of 1.5mm.

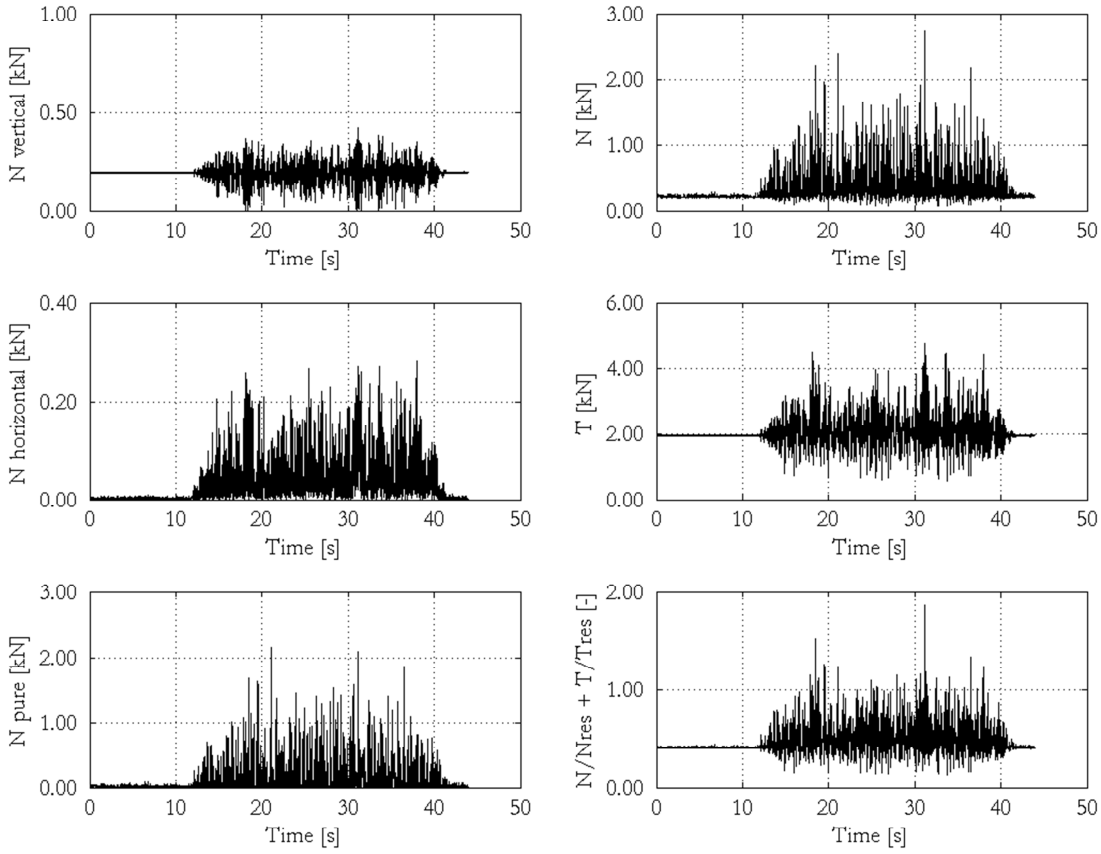

Figure 3.48 Loads acting on PEC2 specimen in test session 1 – 0.75g of ZPA testing step; N = axial load, T = shear load, N/Nres+T/Tres = normalized force for design load combination

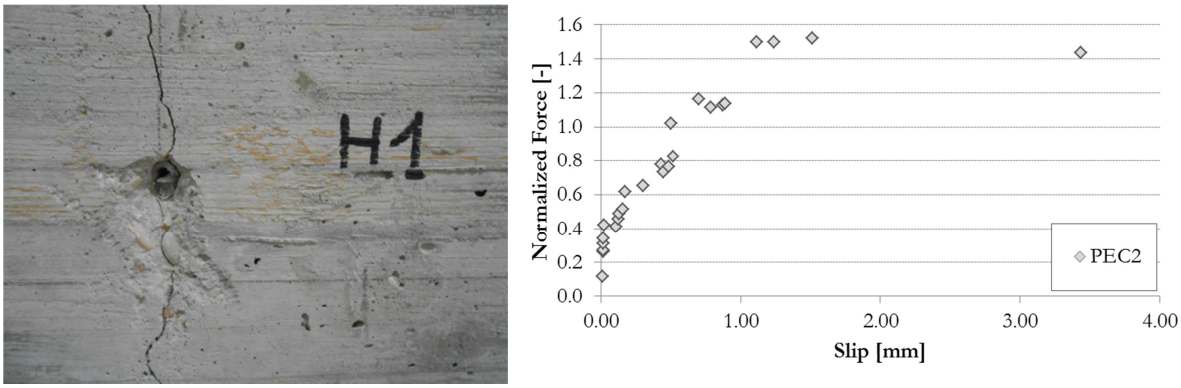

Figure 3.49 Failure mode of PEC2 specimen after test session 1. Load vs displacement graph for PEC2

3.4.4.3. PEC specimen 3

Specimen 3 of plastic expansion anchor was installed in uncracked concrete. It did not reach failure after having withstood all of the testing steps in test session 2. A light shear deformation occurred to the screw and the external sleeve at the end of the testing. The progressive slippage of the anchor is mainly caused by axial forces acting on the fixing point. The base material has manifested light damages and a concrete detachment of 2x2x0.5cm was observed indeed below the anchoring point.

Among all the experimental steps, the maximum dynamic loads -related to the instant of peak normalized force, namely 1.03 - acting on the specimen, consisted of 1.6kN in tension and 4.6kN in shear.

The measured slipping of the anchor during the test session 3 increased with an almost linear plot up to 0.6mm. In this case the maximum slip value for the specimen is different from that related to the experimental step of maximum loading, which was of 0.5mm.

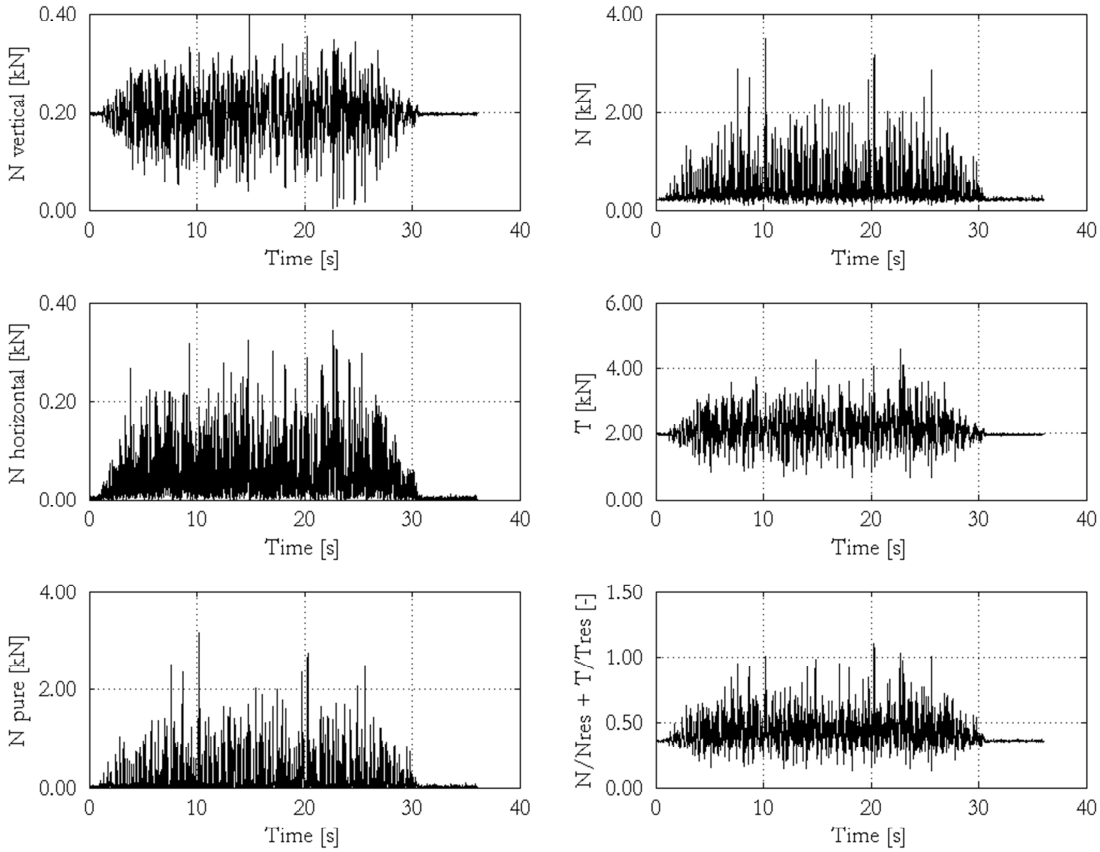

Figure 3.50 Loads acting on PEC3 specimen in test session 2 – 1.00g of ZPA testing step; N = axial load, T = shear load, N/Nres+T/Tres = normalized force for design load combination

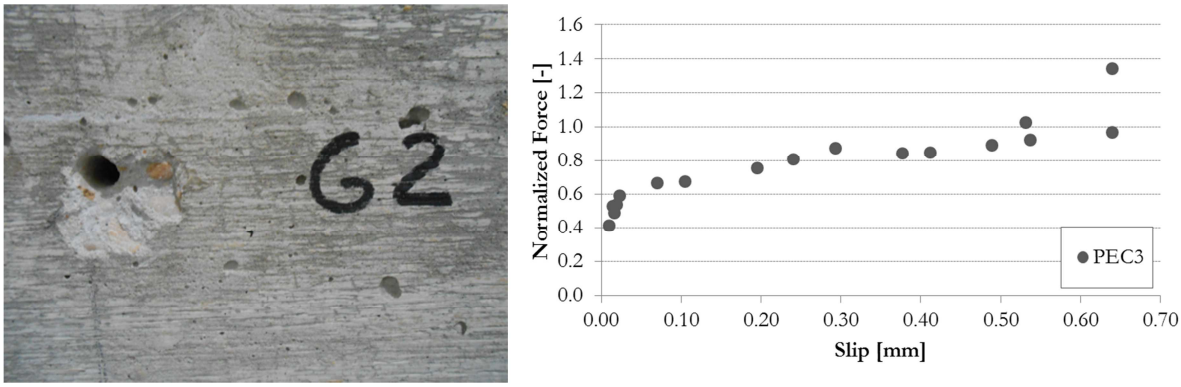

Figure 3.51 Failure mode of PEC3 specimen after test session 2. Load vs displacement graph for PEC3

3.4.4.4. PEC specimen 4

Specimen 4 of plastic expansion anchor was installed in the crack. It reached failure at a nominal level of peak acceleration of 1.00g in the test session 2. The damage to the fastening system was mainly caused by a high shear deformation, combined with a progressive slippage of the anchor. The observed failure mode of the specimen occurred for the steel failure of the screw with subsequent rupture of the plastic sleeve, which is a mechanism related to shear actions. The base material experienced only limited damages as a concrete detachment of 2x1x0.5cm was observed below the anchoring point.

Among all the experimental steps, the maximum dynamic loads -related to the instant of peak normalized force, namely 1.88 - acting on the specimen, consisted of 3.0kN in tension and 4.0kN in shear.

The measured slipping of the anchor during the test session 2 increased, with a two-angle linear plot, up to 2.7mm. In this case the maximum slip value for the specimen is that related to the experimental step of maximum loading.

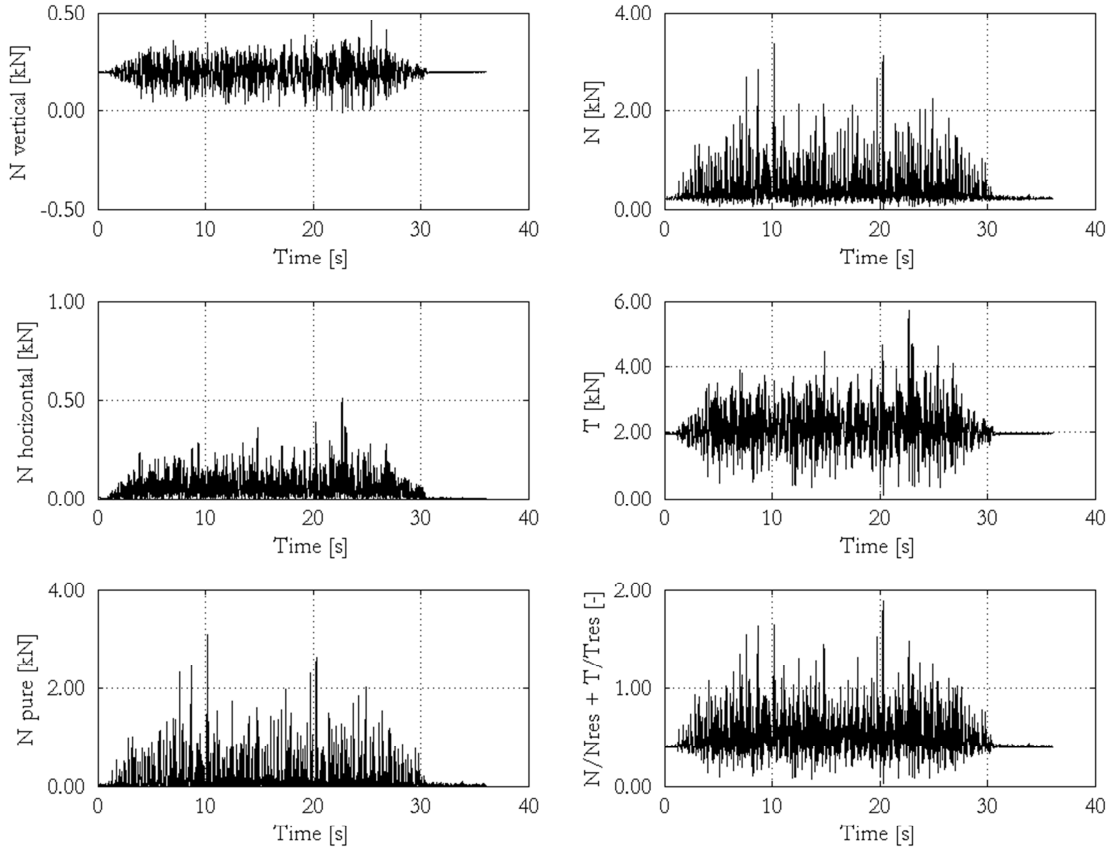

Figure 3.52 Loads acting on PEC4 specimen in test session 2 – 1.00g of ZPA testing step; N = axial load, T = shear load, N/Nres+T/Tres = normalized force for design load combination

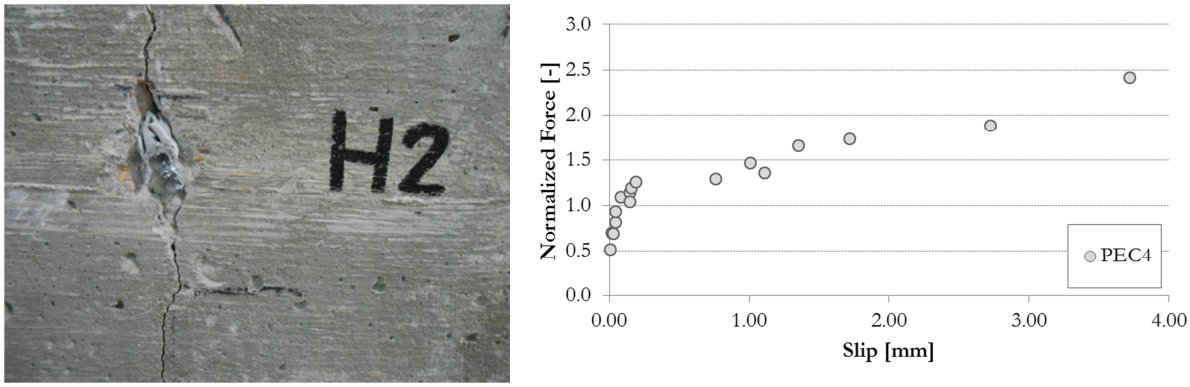

Figure 3.53 Failure mode of PEC4 specimen after test session 2. Load vs displacement graph for PEC4

3.4.4.5. PEC specimen 5

Specimen 5 of plastic expansion anchor was installed in uncracked concrete. It reached failure at a nominal level of peak acceleration of 1.00g in the test session 3. The damage to the fastening system was mainly caused by a high shear deformation, combined with a progressive slippage of the anchor. The observed failure mode of the specimen occurred for the steel failure of the screw with subsequent rupture of the plastic sleeve, which is a mechanism related to shear actions. The base material has manifested almost no damages and a concrete detachment of 1x1x0.5cm was observed indeed below the anchoring point.

Among all the experimental steps, the maximum dynamic loads -related to the instant of peak normalized force, namely 1.14 - acting on the specimen, consisted of 2.8kN in tension and 4.0kN in shear.

The measured slipping of the anchor during the test session 3 increased with an inflected curve up to 1.4mm. In this case the maximum slip value for the specimen is different from that related to the experimental step of maximum loading, which was of 1.1mm.

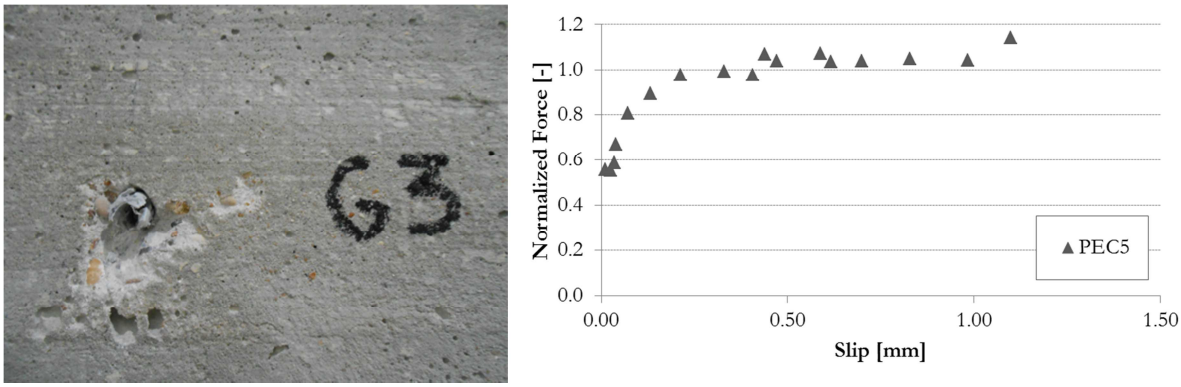

Figure 3.54 Failure mode of PEC5 specimen after test session 3. Load vs displacement graph for PEC5

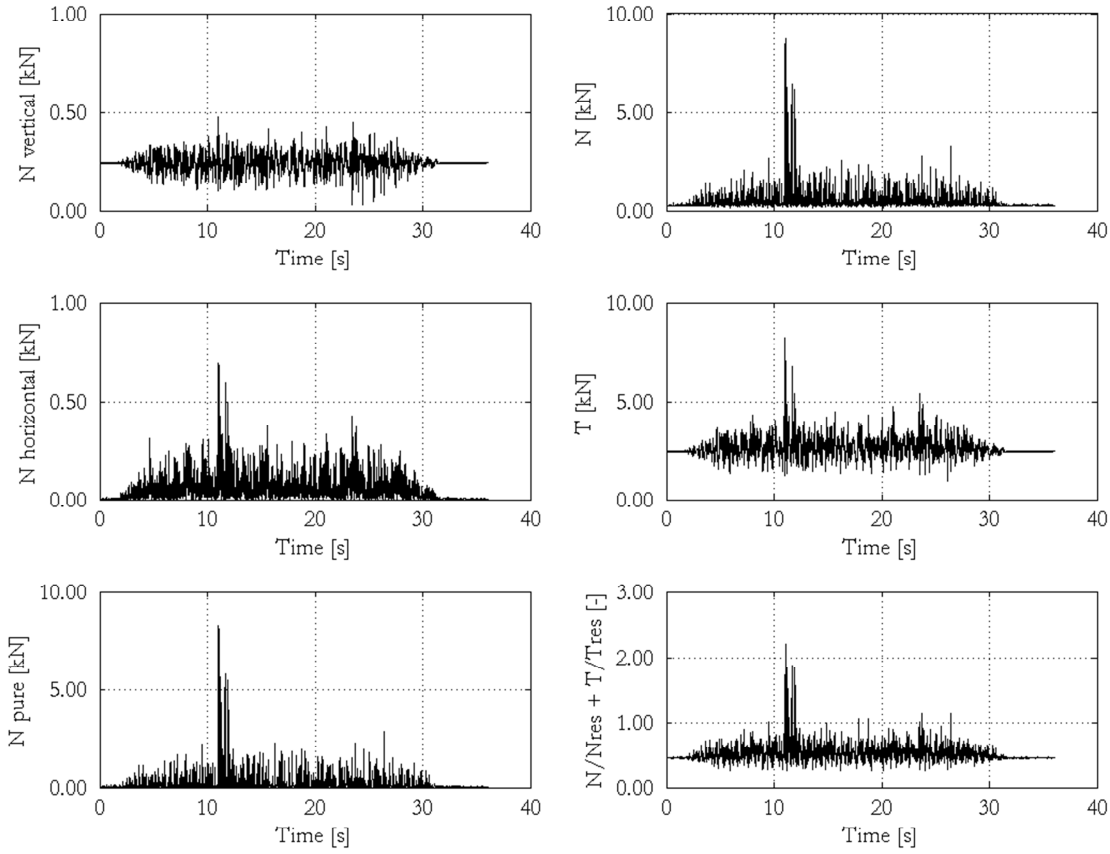

Figure 3.55 Loads acting on PEC5 specimen in test session 3 – 0.80g of ZPA testing step; N = axial load, T = shear load, N/Nres+T/Tres = normalized force for design load combination

3.4.4.6. PEC specimen 6

Specimen 6 of plastic expansion anchor was installed in the crack. It reached failure at a nominal level of peak acceleration of 0.90g in the test session 3. The damage to the fastening system was mainly caused by a high shear deformation, combined with a progressive slippage of the anchor. The observed failure mode of the specimen was related to the slipping of the screw from the base material and the relative slipping between screw and sleeve, with the rupture of the plastic sleeve, which are mechanisms related to axial and shear actions respectively. The base material experienced only limited damages as a concrete detachment of 2x2x1cm was observed below the anchoring point.

Among all the experimental steps, the maximum dynamic loads -related to the instant of peak normalized force, namely 2.05 - acting on the specimen, consisted of 3.3kN in tension and 4.4kN in shear.

The measured slipping of the anchor during the test session 3 increased with an almost linear plot up to 2.6mm. In this case the maximum slip value for the specimen is different from that related to the experimental step of maximum loading, which was of 1.7mm.

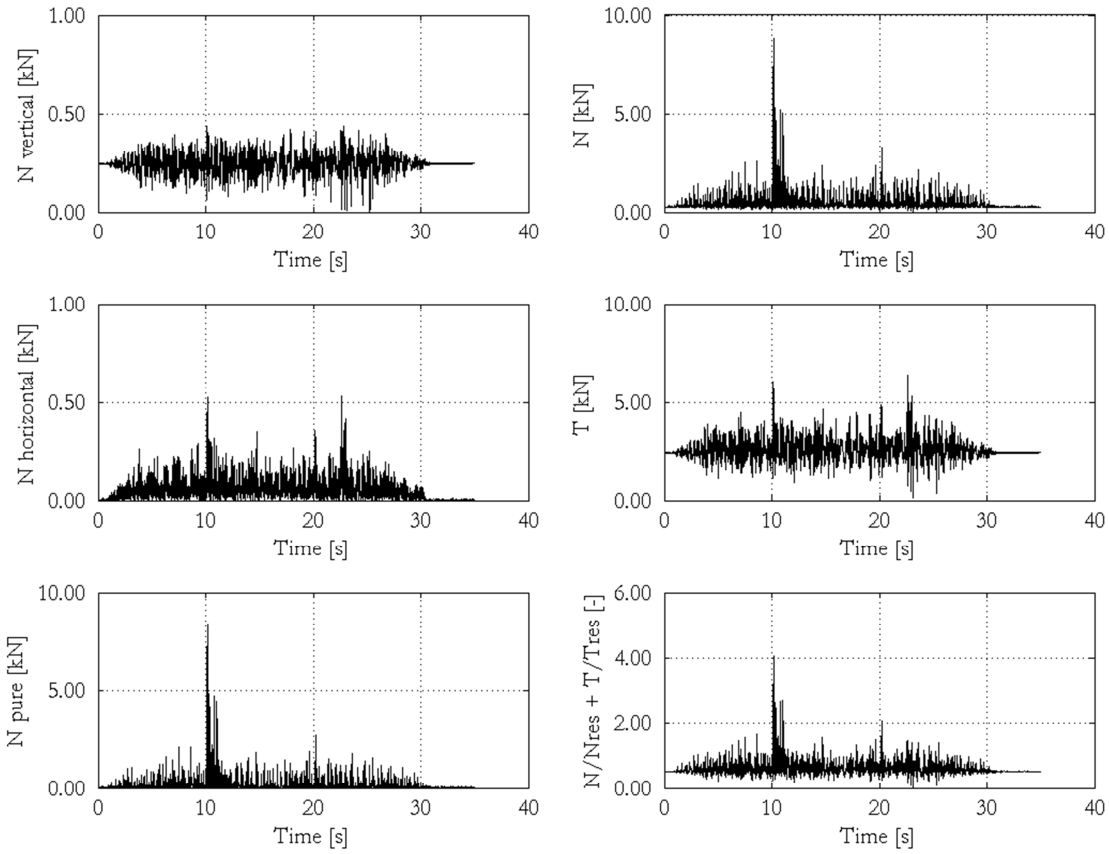

Figure 3.56 Loads acting on PEC6 specimen in test session 3 – 0.80g of ZPA testing step; N = axial load, T = shear load, N/Nres+T/Tres = normalized force for design load combination

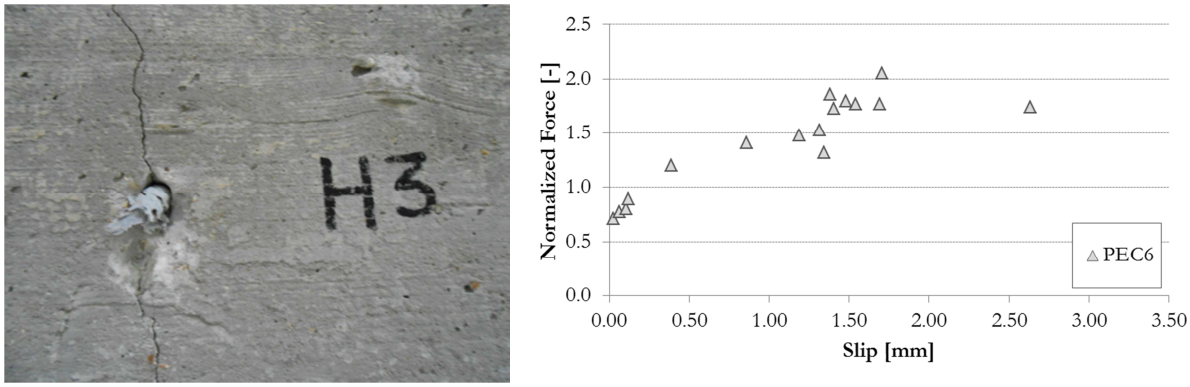

Figure 3.57 Failure mode of PEC6 specimen after test session 3. Load vs displacement graph for PEC6

3.4.4.7. Remarks about PEC specimen behaviour

The specimens on uniform support conditions show a substantial agreement among them, even if with limited local differences. The specimens on uncracked concrete are characterized by a first linear branch with limited values of slip. Over the value of normalized force of 0.6 the behavior appear to be more widespread. The failure occurred for different values of slip but the ultimate loads are almost equals. A similar behavior dividing the load-slip curves in two subsequent parts can be also observed for the specimens installed on cracked concrete. Nevertheless the specimen PEC6 slightly differ from the remaining ones since the slip is greater also for limited values of load. The failure loads are also in this case in accordance.

Table 3.15 Summarizing table for all the specimens with the maximum sustained actions in tension and shear, the maximum normalized force and the relevant slipping, the maximum slip

Specimen ref.	N_{max} kN	V_{max} kN	$F_{norm\ max}$ -	δ_F mm	δ_{max} mm
PEC1	2.480	3.665	1.034	0.581	0.598
PEC2	2.213	3.874	1.520	1.516	3.437
PEC3	1.599	4.557	1.026	0.532	0.640
PEC4	3.043	4.041	1.880	2.723	2.723
PEC5	2.801	3.975	1.140	1.098	1.365
PEC6	3.308	4.438	2.051	1.708	2.635

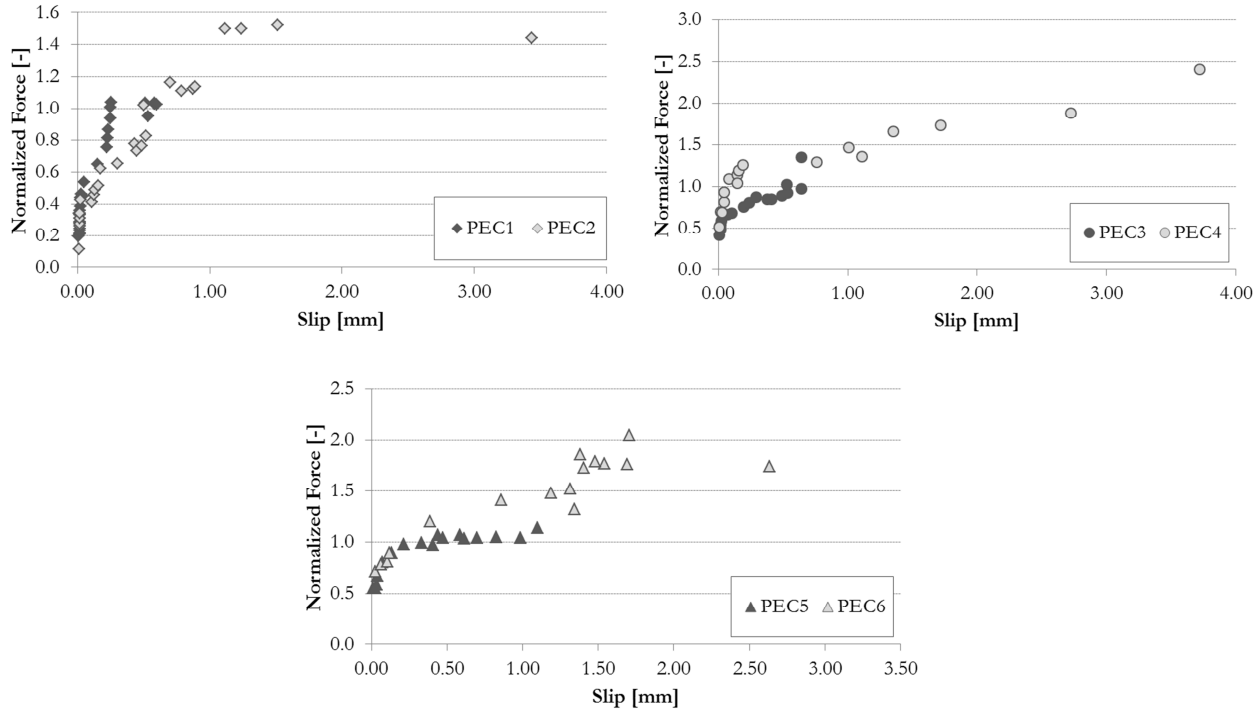

Figure 3.58 PEC specimens: load-displacement graphs for uncracked (dark grey) and cracked (light grey) conditions

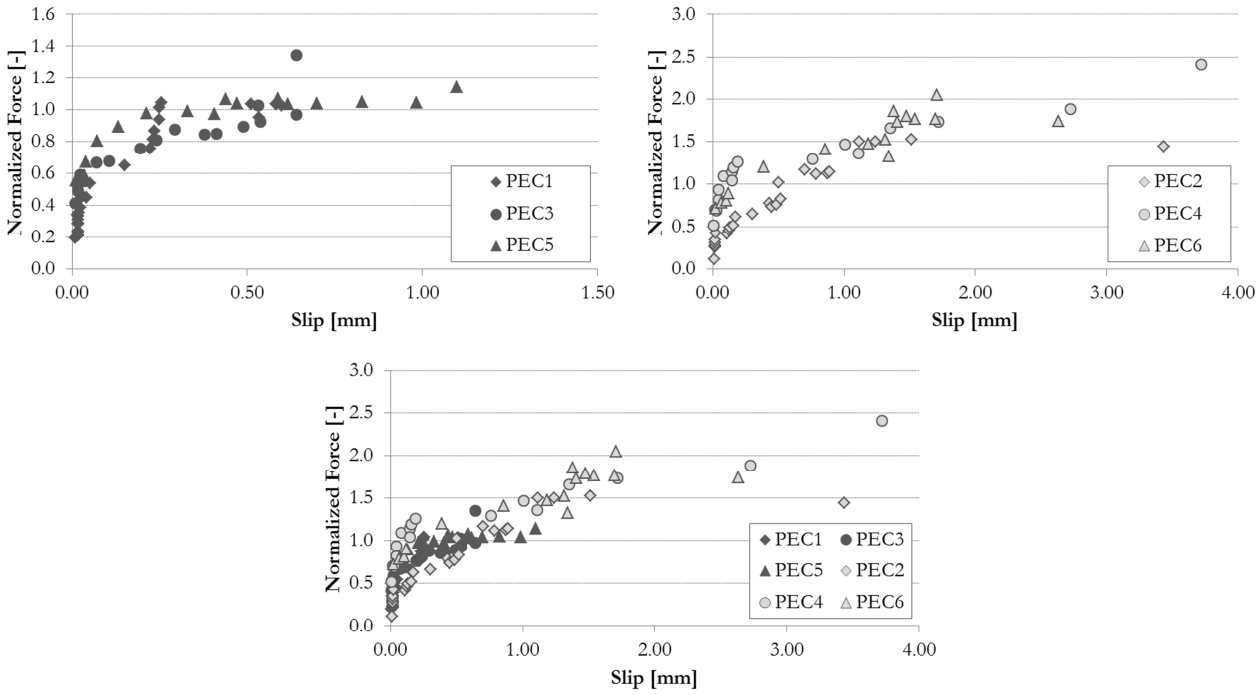

Figure 3.59 Summarizing load-displacement curves for PEC specimens in uncracked (dark grey) and cracked (light grey) conditions

3.4.5. Plastic Fibre Expansion Anchor (PFE)

This paragraph includes the results of the plastic-fibre expansion anchor PFE 8x50 in uncracked and cracked concrete. A total of 3 specimens were tested in the third test session with the concrete structural unit. One of them were installed in a 0.35mm wide crack. The component fixed with PFEC specimens consisted in a 85kg steel plate.

Figure 3.60 View of plastic-fibre expansion anchor PFEC 8x50

Table 3.16 Installation features for plastic-fibre expansion anchor specimens

Specimen reference	Test session	Component reference	Mass [kg]	Height from table [cm]	Crack	Measured crack width [mm]
PFEC1	TS3	F3	85	60	No	-
PFEC2	TS3	I3	85	60	No	-
PFEC3	TS3	E3	85	60	Yes	0.359

3.4.5.1. PFEC specimen 1

Specimen 1 of plastic expansion anchor was installed in uncracked concrete. It reached failure at a nominal level of peak acceleration of 1.10g in the test session 3. The failure mode experienced by the anchor specimen was related to the steel failure of the screw because of the shear forces acting on the fixing point. Moreover a further secondary damage related to the axial slippage of the plastic sleeve from the base

material could be observed. A progressive relevant slippage of the anchor (1cm) was observed after the test session. The base material experienced limited damages as a concrete detachment of 3x3x0.5cm was observed below the anchoring point.

Among all the experimental steps, the maximum dynamic loads -related to the instant of peak normalized force, namely 1.49 - acting on the specimen, consisted of 1.0kN in tension and 1.5kN in shear.

The measured slipping of the anchor during the test session 3 increased, with a two-angle linear plot, up to 2.2mm. In this case the maximum slip value for the specimen is that related to the experimental step of maximum loading.

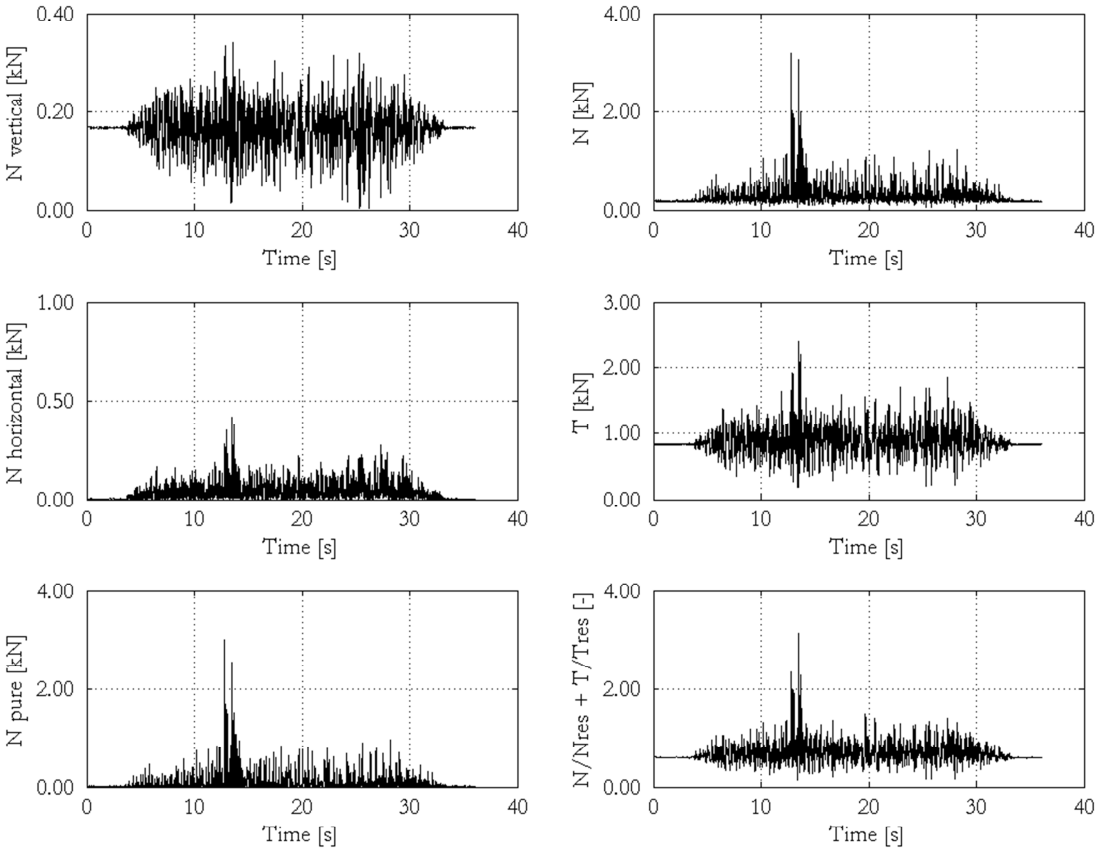

Figure 3.61 Loads acting on PFEC1 specimen in test session 3 – 1.00g of ZPA testing step; N = axial load, T = shear load, N/Nres+T/Tres = normalized force for design load combination

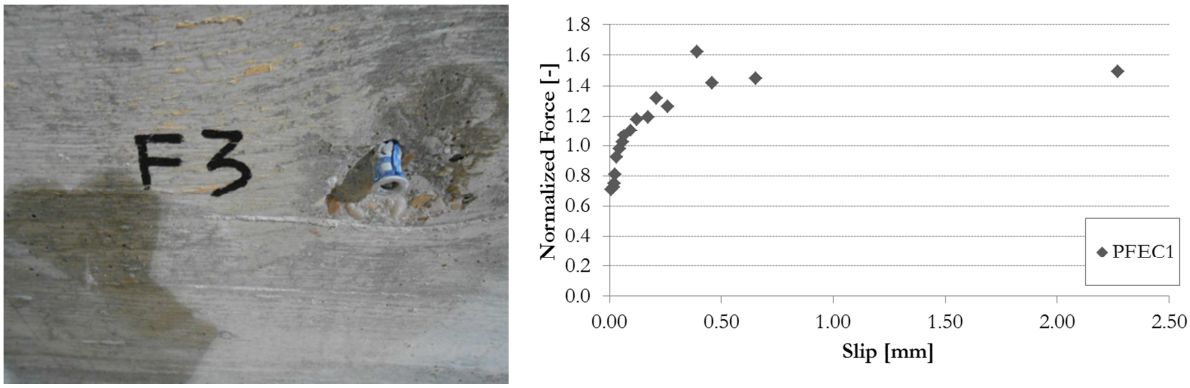

Figure 3.62 Failure mode of PFEC1 specimen after test session 3. Load vs displacement graph for PFEC1

3.4.5.2. PFEC specimen 2

Specimen 2 of plastic expansion anchor was installed in uncracked concrete. It did not reach failure after having withstood all of the testing steps in test session 3. A weakening of the steel occurred to the transversal section of the screw due to the shear forces acting on the fixing point. A very light slippage of the anchor (0.2cm) is observed, which was mainly caused by axial forces acting on the fixing point. The base material has manifested no damages and no concrete detachment around the anchoring point.

Among all the experimental steps, the maximum dynamic loads -related to the instant of peak normalized force, namely 1.63 - acting on the specimen, consisted of 1.4kN in tension and 1.4kN in shear.

The measured slipping of the anchor during the test session 3 increased with an almost linear plot up to 2.2mm. In this case the maximum slip value for the specimen is different from that related to the experimental step of maximum loading, which was of 1.6mm.

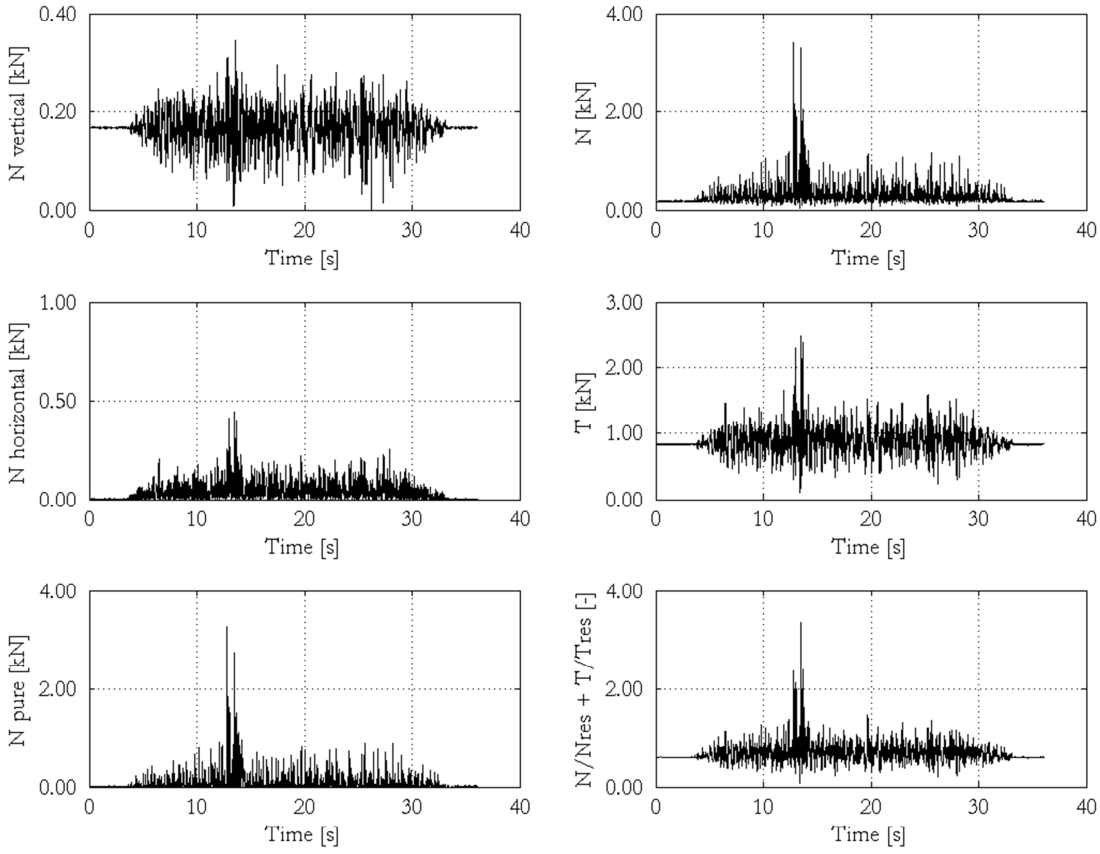

Figure 3.63 Loads acting on PFEC2 specimen in test session 3 – 1.00g of ZPA testing step; N = axial load, T = shear load, N/Nres+T/Tres = normalized force for design load combination

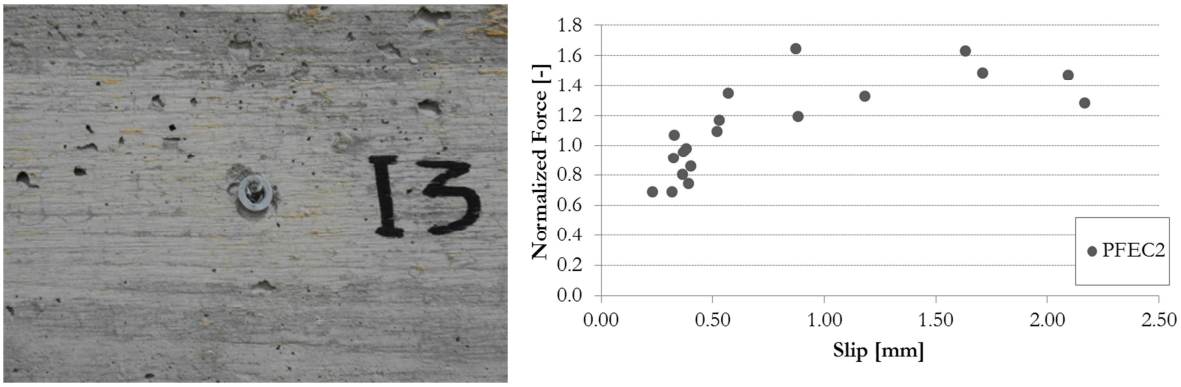

Figure 3.64 View of PFEC2 specimen after test session 3. Load vs displacement graph for PFEC2

3.4.5.3. PFEC specimen 3

Specimen 3 of plastic-fibre expansion anchor was installed in the crack. It reached failure at a nominal level of peak acceleration of 0.75g in the test session 3. The failure mode experienced by the anchor specimen was related to the steel failure of the screw because of the shear forces acting on the fixing point. Moreover a further secondary damage related to the axial slippage of the plastic sleeve from the base material could be observed. A progressive relevant slippage of the anchor (2.5cm) was observed after the test session. The base material experienced limited damages as a concrete detachment of 5x3x0.5cm was observed below the anchoring point.

Among all the experimental steps, the maximum dynamic loads -related to the instant of peak normalized force, namely 1.48 - acting on the specimen, consisted of 1.9kN in tension and 0.6kN in shear.

The measured slipping of the anchor during the test session 3 increased, with a two-angle linear plot, up to 3.7mm. In this case the maximum slip value for the specimen is that related to the experimental step of maximum loading.

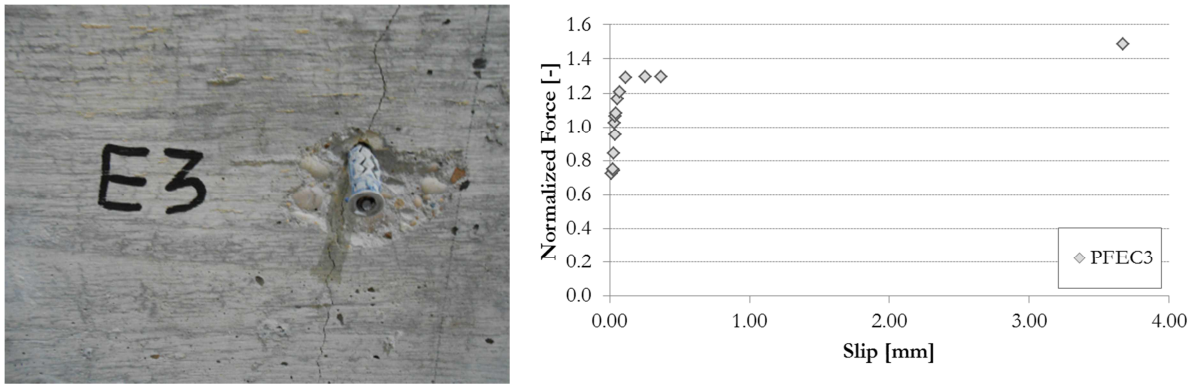

Figure 3.65 Failure mode of PFEC3 specimen after test session 3. Load vs displacement graph for PFEC3

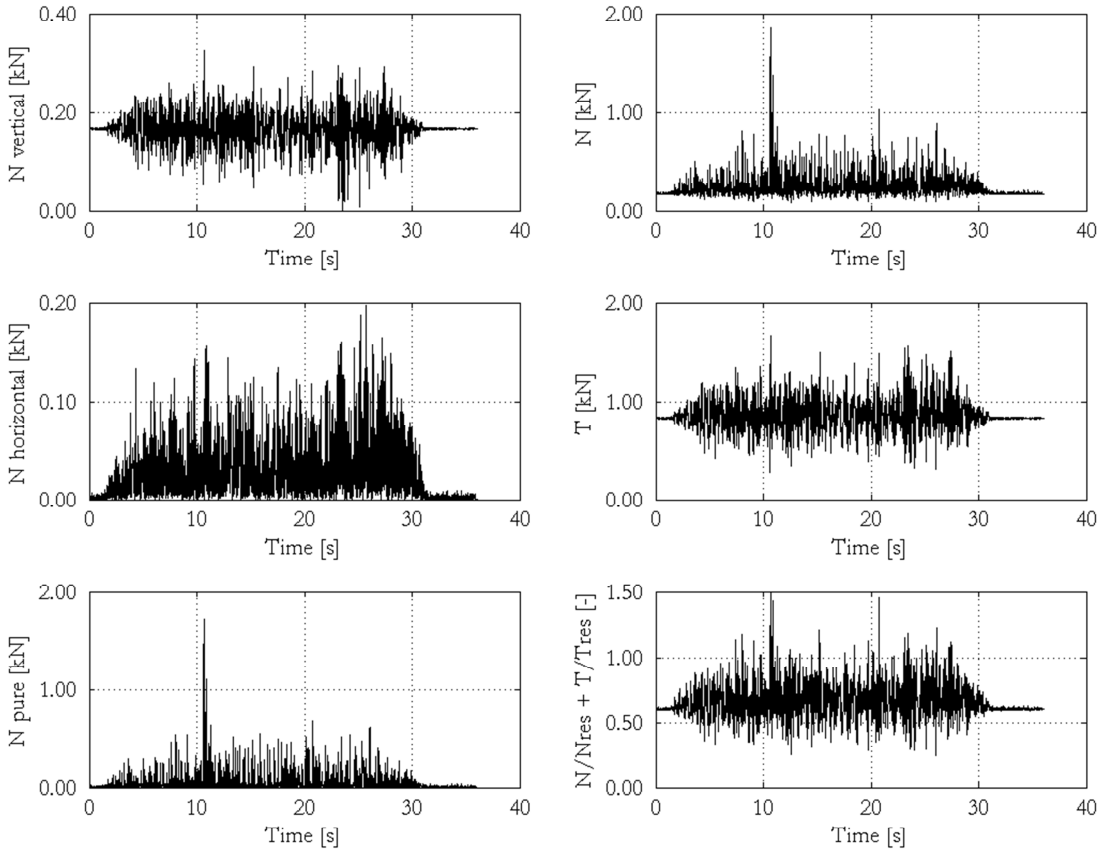

Figure 3.66 Loads acting on PFEC3 specimen in test session 3 – 0.70g of ZPA testing step; N = axial load, T = shear load, N/Nres+T/Tres = normalized force for design load combination

3.4.5.4. Remarks about PFEC specimen behaviour

The PFEC specimens showed the same failure mode, mainly related to the shear action. The load-slip curves are almost similar. Up to a value of normalized force equal to 1.0 the slippage is limited while over this the displacement of the mass gradually increases.

Table 3.17 Summarizing table for all the specimens with the maximum sustained actions in tension and shear, the maximum normalized force and the relevant slipping, the maximum slip

	N_{max}	V_{max}	$F_{norm\ max}$	δ_F	δ_{max}
Specimen ref.	kN	kN	-	mm	mm
PFEC1	0.951	1.542	1.493	2.272	2.272
PFEC2	1.362	1.363	1.632	1.631	2.166
PFEC3	1.857	0.622	1.484	3.674	3.674

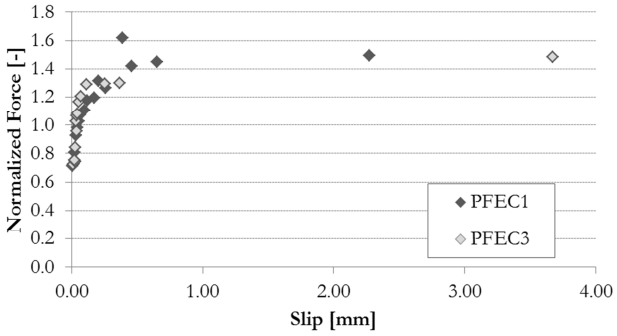

Figure 3.67 Summarizing load-displacement curves for PFEC specimens in uncracked (dark grey) and cracked (light grey) conditions

3.4.6. Real Application

The above presented fixtures, related to the specimens, consisted in steel plates with a mass selected in order to obtain characterizing data. Besides that during test session 3 some anchor types were used to evaluate the fixing of real non-structural components such as a water-heater and a monitor. This kind of fixing applications underwent to the experimental steps of TS3 without the occurrence of anchoring failure by withstanding the seismic actions induced by the table and filtered through the structure.

3.4.6.1. Water heater

In test session 3 a water heater was fixed to the concrete wall, in non-cracked condition, at a height of about 2m, in order to simulate a real case application and evaluate the anchor behaviour. The fixing was realized with two anchoring points using AC anchor type and a M10 standard stud. The component withstood to all the experimental steps up to 1.10g of nominal ZPA induced to the table.

Among the experimental steps, the maximum peak acceleration measured on the wall was greater than 2.0g in X direction and greater than 2.5g in Y direction.

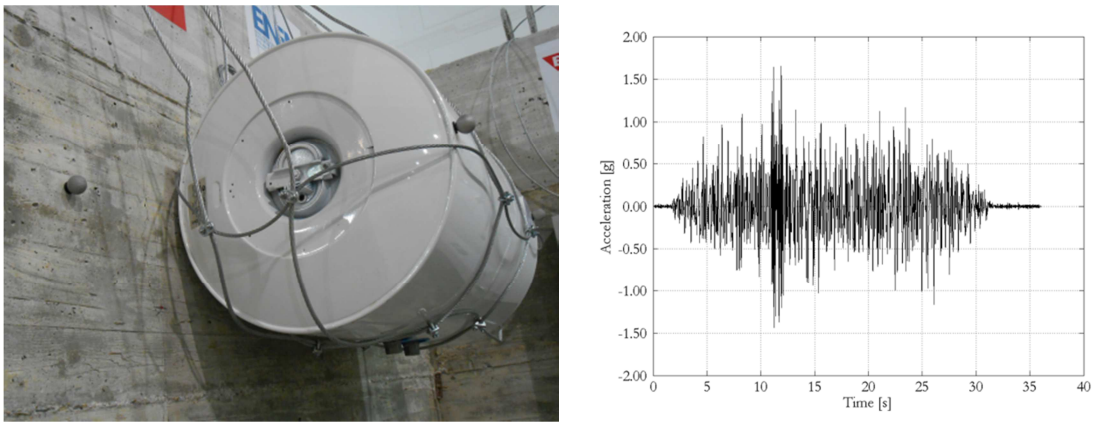

Figure 3.68 Anchorage of a water heater to concrete wall by means of two fixing points with A anchors and M10 steel stud

3.4.6.2. Monitor

In test session 3 a monitor was fixed to the concrete wall, in non-cracked condition, at a height of about 1.2m from the table, in order to simulate a real case application and evaluate the anchor behaviour. The fixing was realized with six anchoring points using PFE anchor type. The component withstood to all the experimental steps up to 0.80g of nominal ZPA induced to the table. Among the experimental steps, the maximum peak acceleration measured on the wall was about 1.5g in both X and Y directions.

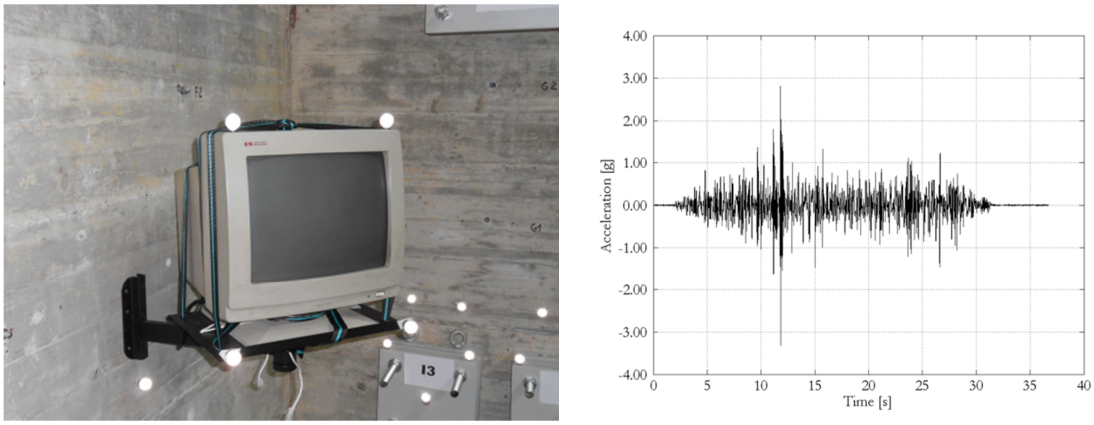

Figure 3.69 Anchorage of a monitor to concrete wall by means of six fixing points with PFE anchors

4. SHAKING TABLE TESTS IN MASONRY

In this chapter the shaking table tests results of post-installed anchors installed in hollow brick masonry infill walls are presented. First facts about the test setup for the masonry structural unit are reported. Subsequently, the testing sessions realization and the data processing analyses are described. Finally the test results divided by specimens are listed in the last part of the section.

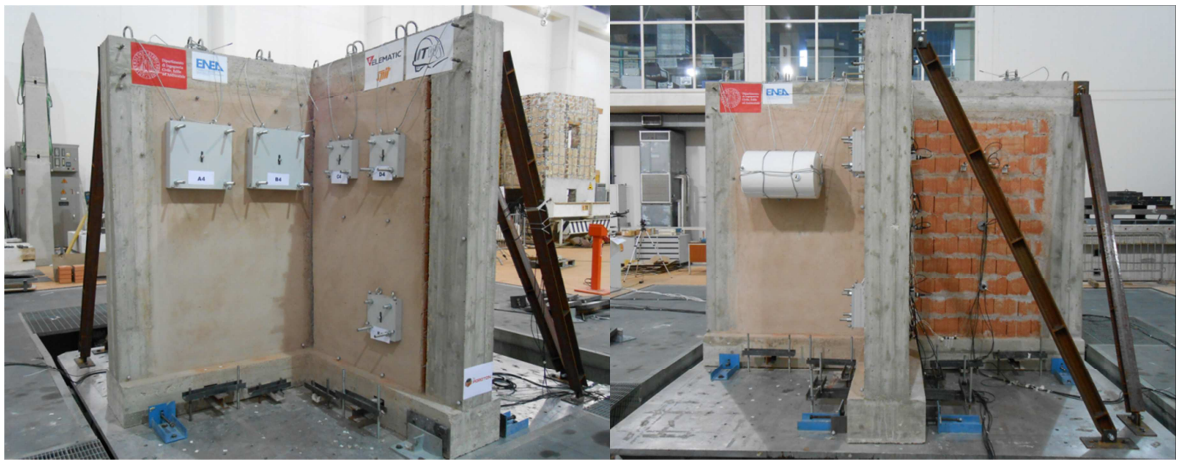

Figure 4.1 Views of the masonry infill wall structural unit under testing

4.1. TEST SETUP

The instrumentation patterns for the two test sessions and the testing plan, namely a list of all the input signals given to the table in the test sessions for the masonry infill walls structural unit are presented within this paragraph.

4.1.1. Instrumentation

In the masonry test sessions the infill walls, the reinforced concrete frame and the anchor specimens were instrumented through the data acquisition systems presented in §2.2.6. Accelerations and displacements were monitored in order to register the dynamic behaviour of the attached components as well as the structural parts and the anchoring systems under testing. The seismic loading, namely a combination of shear and tension forces, referred to the relative slipping of the specimens would allowed an evaluation of their behaviour in critical conditions.

In test session 4 as shown in Figure 4.2 and Table 4.1, a total of twentyfour unidirectional accelerometers was mounted, among which four were placed at the base of the structure and the remaining were installed on the walls. Moreover two potentiometers were used to measure displacements of specimens.

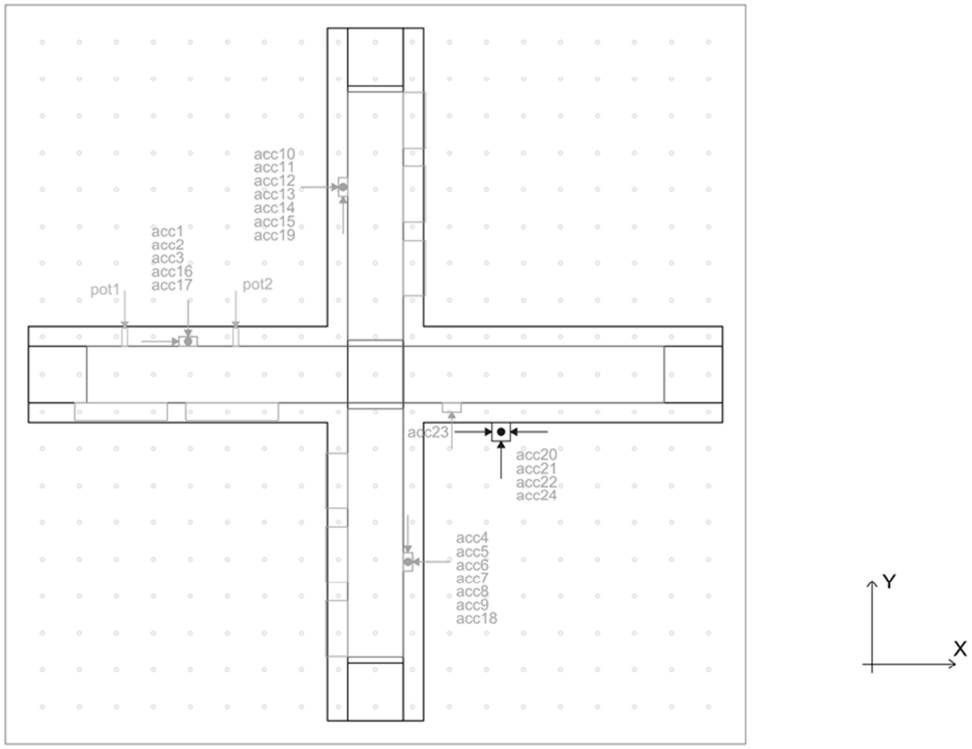

Figure 4.2 Setup instrumentation for TS4; system 1

Table 4.1 Instrumentation adopted in test session 4

No.	Name	Captured quantity	Units	Specimen	Wall	Measurement range	Manufacturer
1	acc1	-Z_Acceleration	g	AM	8	0.50g	PCB Piezotronics
2	acc2	+X_Acceleration	g	AM	8	0.50g	PCB Piezotronics
3	acc3	-Y_Acceleration	g	AM	8	0.50g	PCB Piezotronics
4	acc4	-Z_Acceleration	g	PFEM	3	0.50g	PCB Piezotronics
5	acc5	-Y_Acceleration	g	PFEM	3	0.50g	PCB Piezotronics
6	acc6	-X_Acceleration	g	PFEM	3	0.50g	PCB Piezotronics
7	acc7	-Z_Acceleration	g	PFEM	3	0.50g	PCB Piezotronics
8	acc8	-Y_Acceleration	g	PFEM	3	0.50g	PCB Piezotronics
9	acc9	-X_Acceleration	g	PFEM	3	0.50g	PCB Piezotronics
10	acc10	-Z_Acceleration	g	PEM	7	0.50g	PCB Piezotronics
11	acc11	+Y_Acceleration	g	PEM	7	0.50g	PCB Piezotronics
12	acc12	+X_Acceleration	g	PEM	7	0.50g	PCB Piezotronics
13	acc13	-Z_Acceleration	g	PEM	7	0.50g	PCB Piezotronics
14	acc14	+Y_Acceleration	g	PEM	7	0.50g	PCB Piezotronics
15	acc15	+X_Acceleration	g	PEM	7	0.50g	PCB Piezotronics
16	acc16	-Y_Acceleration	g	wall	8	0.50g	PCB Piezotronics
17	acc17	-Y_Acceleration	g	wall	8	0.50g	PCB Piezotronics
18	acc18	-X_Acceleration	g	wall	3	0.50g	PCB Piezotronics
19	acc19	+X_Acceleration	g	wall	7	0.50g	PCB Piezotronics
20	acc20	-X_Acceleration	g	-	base	2.50g	PCB Piezotronics
21	acc21	+Y_Acceleration	g	-	base	2.50g	PCB Piezotronics
22	acc22	-Z_Acceleration	g	-	base	2.50g	PCB Piezotronics
23	acc23	+Y_Acceleration	g	wall	4	2.50g	PCB Piezotronics
24	acc24	+X_Acceleration	g	-	base	2.50g	PCB Piezotronics
26	pot1	-Y_Displacement	mm	AM1	8	50mm	**novo**technik
27	pot2	-Y_Displacement	mm	AM2	8	50mm	**novo**technik

In test session 5, as shown in Figure 4.3 and Table 4.2, the instrumentation layout was similar to the previous session, only the two potentiometers were missing as the displacements were already recorded by the spatial positioning system.

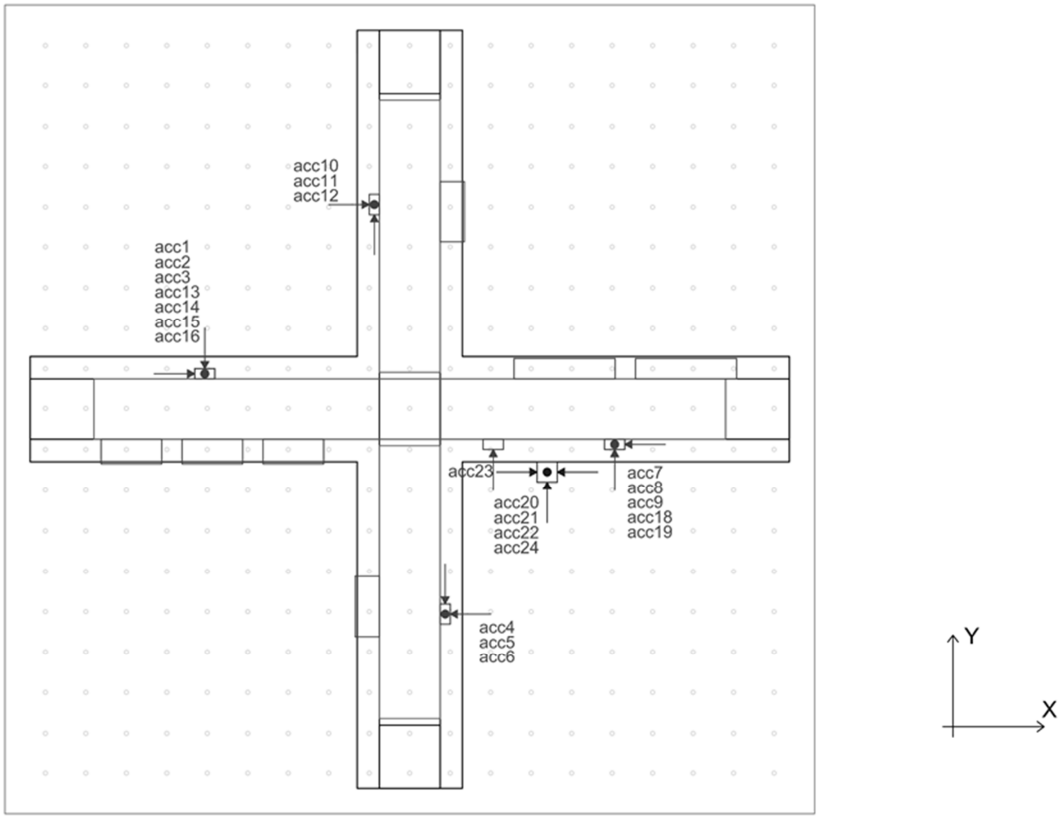

Figure 4.3 Setup instrumentation for TS5; system 1

Table 4.2 Instrumentation adopted in test session 5

No.	Name	Captured quantity	Units	Specimen	Wall	Measurement range	Manufacturer
1	acc1	-Z_Acceleration	g	PEM	8	0.50g	PCB Piezotronics
2	acc2	+X_Acceleration	g	PEM	8	0.50g	PCB Piezotronics
3	acc3	-Y_Acceleration	g	PEM	8	0.50g	PCB Piezotronics
4	acc4	-Z_Acceleration	g	PFEM	3	0.50g	PCB Piezotronics
5	acc5	-Y_Acceleration	g	PFEM	3	0.50g	PCB Piezotronics
6	acc6	-X_Acceleration	g	PFEM	3	0.50g	PCB Piezotronics
7	acc7	-Z_Acceleration	g	AM	4	0.50g	PCB Piezotronics
8	acc8	-X_Acceleration	g	AM	4	0.50g	PCB Piezotronics
9	acc9	+Y_Acceleration	g	AM	4	0.50g	PCB Piezotronics
10	acc10	-Z_Acceleration	g	PFEM	7	0.50g	PCB Piezotronics
11	acc11	+Y_Acceleration	g	PFEM	7	0.50g	PCB Piezotronics
12	acc12	+X_Acceleration	g	PFEM	7	0.50g	PCB Piezotronics
13	acc13	-Z_Acceleration	g	PEM	8	0.50g	PCB Piezotronics
14	acc14	+X_Acceleration	g	PEM	8	0.50g	PCB Piezotronics
15	acc15	-Y_Acceleration	g	PEM	8	0.50g	PCB Piezotronics
16	acc16	-Y_Acceleration	g	wall	8	0.50g	PCB Piezotronics
17	acc18	+Y_Acceleration	g	wall	4	0.50g	PCB Piezotronics
18	acc19	+Y_Acceleration	g	wall	4	0.50g	PCB Piezotronics
19	acc20	-X_Acceleration	g	-	base	2.50g	PCB Piezotronics
20	acc21	+Y_Acceleration	g	-	base	2.50g	PCB Piezotronics
21	acc22	+Z_Acceleration	g	-	base	2.50g	PCB Piezotronics
22	acc23	+Y_Acceleration	g	wall	4	2.50g	PCB Piezotronics
23	acc24	+X_Acceleration	g	-	base	2.50g	PCB Piezotronics

4.1.2. Testing Plan

The experimental campaign has been developed in five subsequent sessions, each one corresponding to an independent load history related to specimens and structural units behaviour. Every test session has consisted of successive steps with a nominal increased peak of 0.05g. The first three test sessions have been performed on the concrete structure while the remaining two on the RC frame with masonry infill walls. A full list of the performed steps for each session is reported in Table 4.4. The maximum attained nominal acceleration is listed in Table 4.3.

Table 4.3 Test sessions features

Session	Base material	ZPA[2] max
TEST SESSION 4	HBM[1]	1.20g
TEST SESSION 5	HBM[1]	1.10g

[1]HBM = Hollow brick masonry;
[2]ZPA = Zero Period Acceleration (AC156, 2010).

The ZPA could be considered as the acceleration to which the non-structural component was subjected being filtered by the structure, according to its dynamic properties. Moreover this acceleration depends on the location of the fixed component inside the building, especially in terms of ratio between height of installation point and total height.

Table 4.4 List of performed steps for each test session

No.	Test 4	Test 5
1	0.05g	0.70g
2	0.10g	0.90g
3	0.15g	1.00g
4	0.20g	1.10g
5	0.25g	1.20g
6	0.30g	-
7	0.35g	-
8	0.40g	-
9	0.45g	-
10	0.50g	-
11	0.55g	-
12	0.60g	-
13	0.65g	-
14	0.70g	
15	0.75g	-
16	0.80g	-
17	0.85g	-
18	0.90g	-
19	1.00g	-

4.2. EXPERIMENTAL OBSERVATIONS

The description of the realization of the testing in masonry can be useful to understand the immediate facts on the seismic behaviour of the anchor specimens. The two testing sessions were carried out with a different methodology compared to the three sessions made with concrete structural unit. The variable was no longer the support condition but the loading procedure. For the test session 4 indeed the test plan was similar to the previous sessions, with subsequent input signals scaled at increasing ZPA values (Table 4.5). In test session 5 the acceleration time history given to the table was directly scaled by limited reference ZPA values, namely those related to the failure observed during TS4. Hence the ZPA values 0.70g, 0.80g and 1.00g were taken as a reference respectively for the plastic anchor type A, for the chemical anchor and for the plastic anchor type B. A procedure was defined indeed which provided an evaluation on a single shaking signal. That procedure was chosen also to evaluate the influence of the test plan with several time histories given to the specimens and the structural unit through the table. That allowed a comparison between the two different methodologies to be done, highlighting possible differences in the results.

In general it was observed that the slipping of the specimens before to reach failure showed low values for all anchor types. The observed failure modes during TS4 and TS5 demonstrated to be related to the geometrical and mechanical properties of the base material. Such aspects contributed to the definition of the failure modes for the different anchor types under testing.

The failure of the chemical anchor affected an extended surface of the brick where it was installed in. In particular a failure involving the whole external shell was observed and in some cases parts of the internal web. For one case also a partial separation between the resin and the steel stud was noticed. One chemical anchor specimen did not experience any failure at the end of TS5.

The plastic expansion anchor type A showed a pull-out failure after a damage of the hole on the external shell of the brick and a detachment of a plaster area around the specimen installation point. For the various specimens of the two test sessions the failure modes occurred with very similar characteristics.

The plastic expansion anchor type B showed in all cases a slipping of the plastic sleeve, as a secondary failure mode, and final collapse of the system caused by shear steel failure of the screw. The slipping of the anchoring system specimens under testing varied within values lower than 10mm.

Due to the different mass attached to the different anchor typologies a direct comparison was not possible. Nevertheless, for all the anchor types, it can be observed that the resistance registered in TS5 was slightly higher, in a range from 0 to 20%, than the values registered with TS4 test plan.

Table 4.5 Nominal peak accelerations related to specimens failure (*no failure occurred)

Non-Str. Comp.	Anchor type	Nominal failure ZPA
A4	adhesive	0.85g
A5	plastic expansion (A)	0.90g
B4	adhesive	0.90g
B5	plastic expansion (A)	0.90g
C4	plastic expansion (B)	1.00g
C5	plastic expansion (A)	1.20g*
D4	plastic expansion (B)	1.00g
D5	plastic expansion (B)	0.90g
E4	plastic expansion (B)	1.00g*
E5	adhesive	1.10g*
F4	plastic expansion (A)	0.65g
F5	adhesive	1.10g
G4	plastic expansion (A)	0.70g
G5	plastic expansion (B)	1.10g*
H4	plastic expansion (A)	1.00g*

4.3. DATA PROCESSING

A first evaluation considers the comparison between accelerations captured directly by the accelerometers and those computed from the displacements recorded through the spatial positioning system. The values of the acceleration measures at the ground level allow a verification of the input signal while those from sensors fixed at a certain height provide information on the structural units response. The values recorded on the masses give an indication on the dynamic behaviour of different fixtures. These values mainly depend on the connection condition which developed during the testing. Therefore indirectly it is possible to observe the behaviour of post-installed anchor specimens in addition to the immediate experimental observations, i.e. specimens failure modes and maximum peak acceleration suffered.

The considered tri-axial accelerations refer: (1) to the sensors for the control of the testing system, (2) to accelerometers attached to the shaking table and (3) to the accelerometers fixed to the walls at the fixtures height, in addition to (4) to the acceleration values obtained from the displacement of markers. The most relevant ones are those installed at the base beam of the structures and those on the steel masses.

The aim of this first processing phase was to go backward to the design stage of the experimental campaign evaluating and discussing the setup decisions and validating the assumptions considered previous to the testing.

4.3.1. Analysis of Accelerations

The analysis of the structural units response subjected to the input signal is a preliminary fundamental consideration to be developed for a complete understanding of the connection trend behaviour. The purpose is to verify the amplification which the

anchored elements were subjected to during the shaking as well as to verify the results about the amplification ratio between base and anchoring height obtained from the design of the experimental campaign.

4.3.1.1. Comparison of Measures

Two FE Models were created in order to predict the stiffness of both structures and thus the foresee accelerations acting at the wall fixing height (Mazzon et al. 2013b). It is therefore needed to validate the designed testing layout according to the expected accelerations at different heights. The amplification acceleration ratio allows the influence of the structure and its filtering action to be evaluated.

Figure 4.4 shows the trend of the measured accelerations with reference to the nominal step for the case of a test session in the masonry structural unit. The charts underline as the input ("achieved" signal) and the values recorded on the shaking table ("Table" signal) substantially agree along the whole test except for the last steps on some sessions.

A more noticeable difference can be noticed if the input/table signal and the valued recorded on the support at the fixing points ("wall" signal) are compared. In that case the influence of the structure can be clearly identified and in general this induces an amplification of accelerations and a modification of frequencies. This modification along the test is especially evident for the case of the masonry infill wall unit. This is probably due to the continuous increasing damage induced on the infill walls that cracked and split out parts of the top row of all the masonry panels.

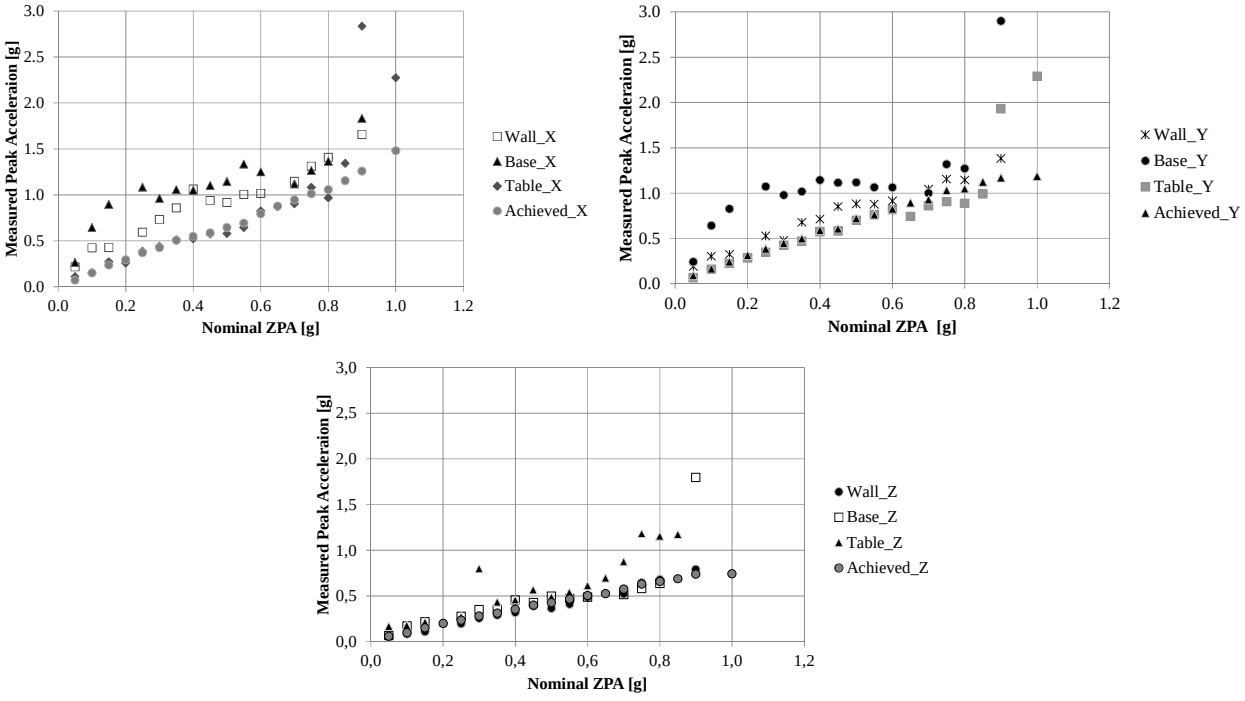

Figure 4.4 Example of measured peak accelerations for the masonry infill walls unit (test session 4)

In this section a study on the relation between accelerations measured on the structural unit walls, at fixing height, and on the fixtures is presented. This kind of investigation allows the presence of variation of trend behaviour of specimens to be recognized, i.e. whether after a certain number of testing steps the specimen behaviour modified depending on the decreasing of stiffness, that is related to the progressive damage of the

fastening system. Such finding leads to get information on where a discontinuity point, related to specimen slipping from the base material surface, can be found.

As regards the testing in masonry it can be observed more differences in the relation trend through the time history steps than what noticed in the concrete structural unit.

Each anchor type showed a different behaviour especially for test session 5 when the value of fixture acceleration is always less than the acceleration measured on the wall, at the same height. In those cases also the type of wall restraint has to be taken into account. A further study can be carried out in the future in order to relate the behaviour of specimens to the behaviour of the masonry infill wall they are installed in.

Concerning the chemical anchor (Figure 4.5a) after the first steps with low ZPA when the relation is linear, the amplification of acceleration measured on the fixture starts decreasing. Plastic expansion anchor type A (Figure 4.5b) shows a behaviour similar to the previous anchor type in test session 4, i.e. a linear trend of relation, but a more significant decrease of fixture acceleration in test session 5, when the wall behaviour has also to take into account. Finally, plastic expansion anchor (Figure 4.5c) distinguishes among other types as the acceleration ratio from the beginning is greater than 1 and it stays over the bisecting line excepted few points of test session 5, where also the wall behaviour may affect the data. This finding means that the fixture in case (c) was more free to move due to connection behaviour of that particular anchor type.

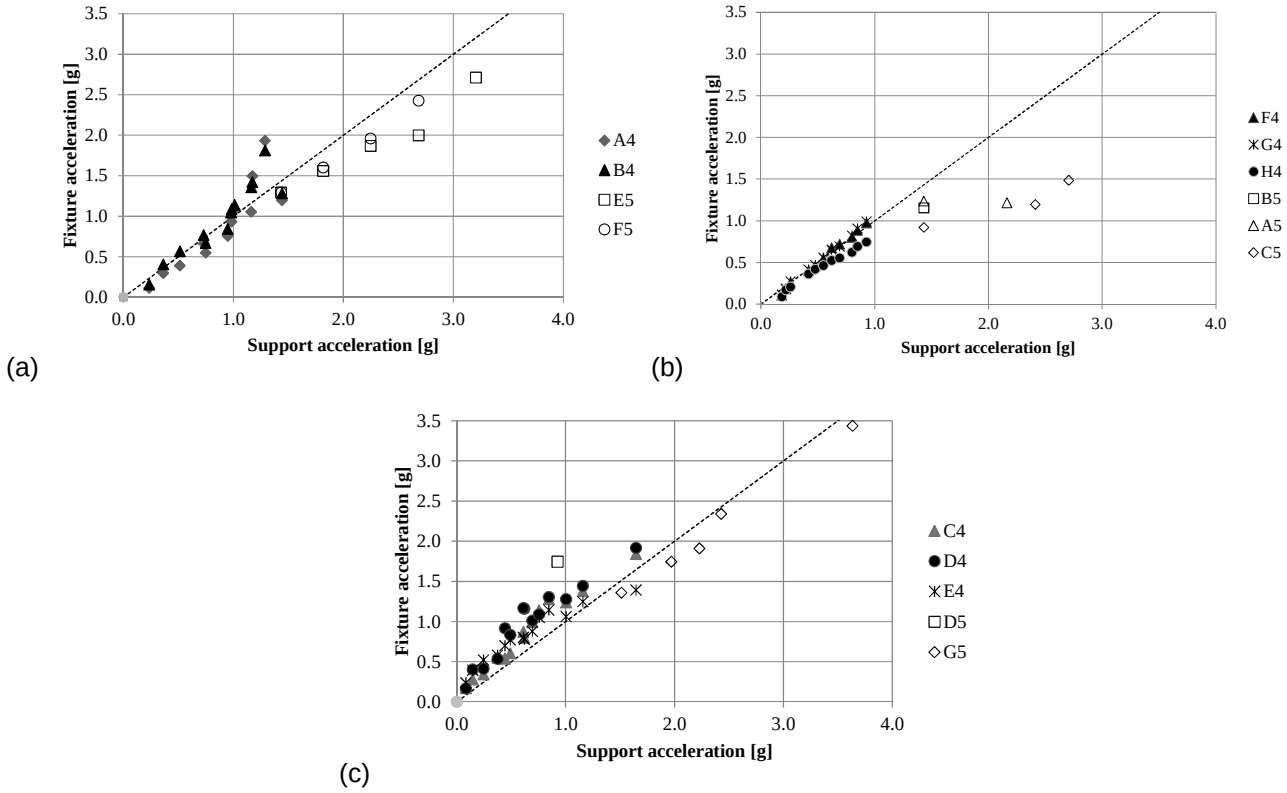

Figure 4.5 Maximum recorded acceleration on the fixture versus maximum recorded acceleration on the support at each testing step for masonry application of chemical anchor (a), plastic expansion anchor type A (b) and plastic expansion anchor type B (c)

4.3.1.2. Conclusive Remarks

The preliminary analyses of accelerations after the shake-table testing of post-installed anchors reveal the progressive damage of the structural units. This overall behaviour is more evident for the RC structure with masonry infill walls.

The linear trend observed on the acceleration ratio between mass and support underlines as the anchor specimens were able to transfer the whole acceleration from the structure to the fixture. This was analysed in terms of peak measured acceleration, up to almost the last testing steps. Concerning the masonry infill wall structural unit there is a difference in the outcomes of a particular anchor type (plastic expansion type B) which provided the fixture with an amplification of peak acceleration, as the mean of the data points lays above the bisecting line.

The presented analyses also allow a difference in the behaviour of different anchor typologies to be studied. The plastic expansion anchors showed a variation on their overall behaviour. This was more evident for the installation in the masonry support, rather than that in concrete.

The above presented analyses of acceleration are a fundamental step for the computation of loads acting on the different anchor typologies. In the case of fastenings that manifested an overall linear trend the possible relative acceleration will not have a relevant influence on the computation of the acting load. Differently the relative acceleration should be taken into account when the ratio deviates from the linear trend.

4.3.1.3. Calculation of Actions on Anchors

The approach considered to compute the forces acting on the tested anchors in masonry infill walls structural unit is the same of what arranged for the concrete structural unit. Therefore concerning this issue the content included in section §3.3.1.3 of the present document are valid and should be consulted.

4.4. TEST RESULTS

In the following section the experimental outcomes of the testing, the results of data analyses and a general comment on the seismic behaviour of various anchor types are reported with a recurrent order. Paragraphs distinguish for anchor type and include test results and observations for each specimen. The relevant aspects taken into account for the different specimens are the load history related to the maximum action withstood by the specimen in the test session, the failure mode and the slipping vs load plot. Moreover after all the specimens are presented separately, at the end of every paragraph, a summarizing part with a comparison among the specimens. In particular the maximum forces for every anchor specimen are reported in a table together with the slipping related to maximum load and the maximum slipping. Such general information is also provided graphically with the melting of all the specimen seismic behaviour curves, showing the slipping towards the peak combined load sustained in a testing step. Hence it is of importance to find out the dynamic resistance level for the anchor with respect to the static one.

Table 4.6 Anchor types under dynamic testing in masonry

Anchor type	Tested specimens	Type reference
Chemical bond	4	AM
Plastic expansion	6	PEM
Plastic Fibre expansion	5	PFEM

The load-slip curves for each specimen consider the maximum values for both quantities for each step. Nevertheless in some cases the loads acting on the anchored masses showed spike values. This behaviour was observed to be in correspondence to the failure of some anchor specimens. The observed peak values could be then the consequence of the impact with the support. In this case those spikes were neglected for the computation of the acting loads.

4.4.1. Adhesive Anchor (A)

This paragraph includes the results of the chemical anchor A M10 stud in hollow masonry infill walls. A total of 4 specimens were tested in the 2 test sessions with the masonry structural unit. The component fixed with AM specimens consisted in a 200kg steel plate.

Figure 4.6 View of chemical anchor AM M10 and accessory for hollow material

Table 4.7 Installation features for chemical anchor specimens

Specimen reference	Test session	Component reference	Mass [kg]	Height from table [cm]
AM1	TS4	A4	200	171
AM2	TS4	B4	200	171
AM3	TS5	E5	200	112
AM4	TS5	F5	200	112

4.4.1.1. AM specimen 1

Specimen 1 of adhesive anchor was installed in hollow bricks. It reached failure at a nominal level of peak acceleration of 0.85g in the test session 4. The specimen experienced a failure which involved the external brick shell and part of the internal brick web. In particular the collapse occurred to the entire face shell and part of second and third webs. In addition the detachment of a relevant portion of plaster (50x35cm) in the wall surface around the fixing point should be also mentioned. The tested specimen showed an absence of any slippage before failure.

Among all the experimental steps, the maximum dynamic loads -related to the instant of peak normalized force, namely 5.67 - acting on the specimen, consisted of 4.1kN in tension and 3.0kN in shear.

The measured slipping of the anchor during the test session 4 increased with an almost linear plot up to 1.7mm. In this case the maximum slip value for the specimen is different from that related to the experimental step of maximum loading, which was of 0.5mm.

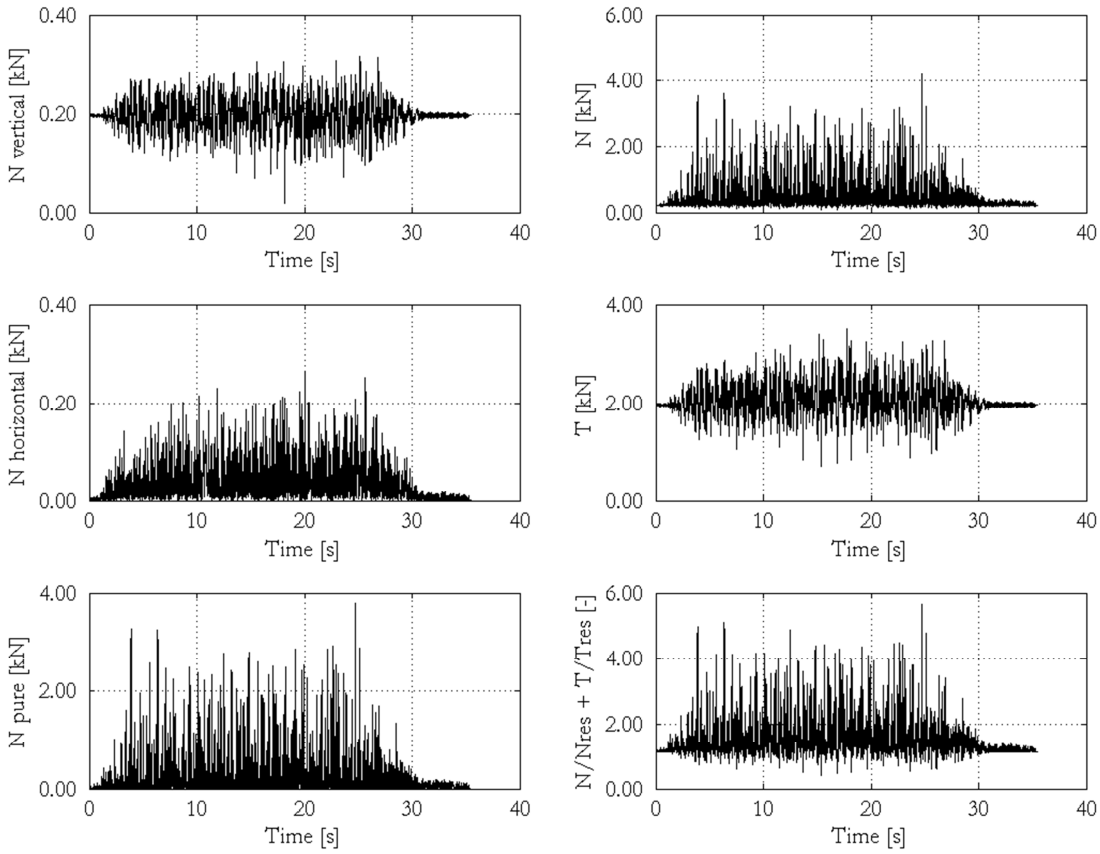

Figure 4.7 Loads acting on AM1 specimen in test session 4 – 0.80g of ZPA testing step; N = axial load, T = shear load, N/Nres+T/Tres = normalized force for design load combination

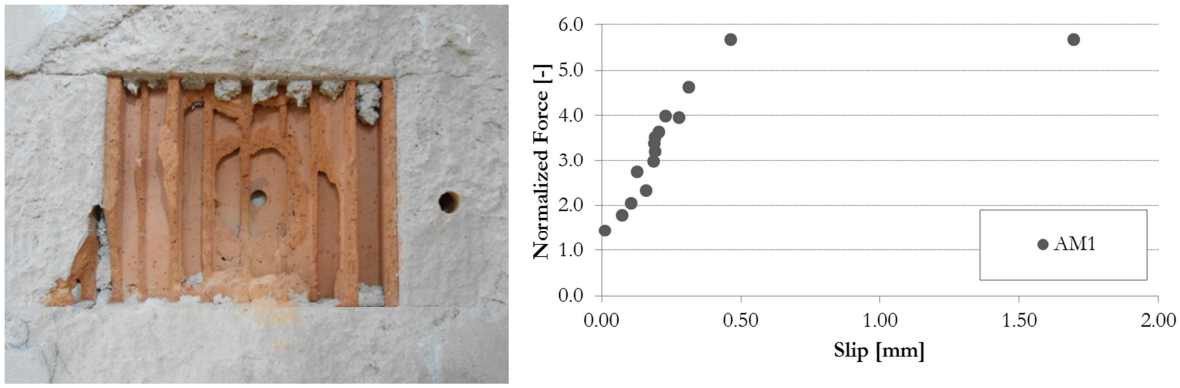

Figure 4.8 Failure mode of AM1 specimen after test session 4. Load vs displacement graph for AM1

4.4.1.2. AM specimen 2

Specimen 2 of adhesive anchor was installed in hollow bricks. It reached failure at a nominal level of peak acceleration of 0.90g in the test session 4. The specimen experienced a failure which involved the external brick shell and part of the internal brick web. In particular the collapse occurred to a limited part of the face shell and part of the web. Besides a failure between the resin and the stud was observed. In addition the detachment of a relevant portion of plaster (15x17cm) in the wall surface around the fixing

point should be also mentioned. The tested specimen showed an absence of any slippage before failure.

Among all the experimental steps, the maximum dynamic loads -related to the instant of peak normalized force, namely 5.37 - acting on the specimen, consisted of 3.9kN in tension and 2.7kN in shear.

The measured slipping of the anchor during the test session 4 increased, with an slightly inflected curve, up to 1.8mm. In this case the maximum slip value for the specimen is different from that related to the experimental step of maximum loading, which was of 1.4mm.

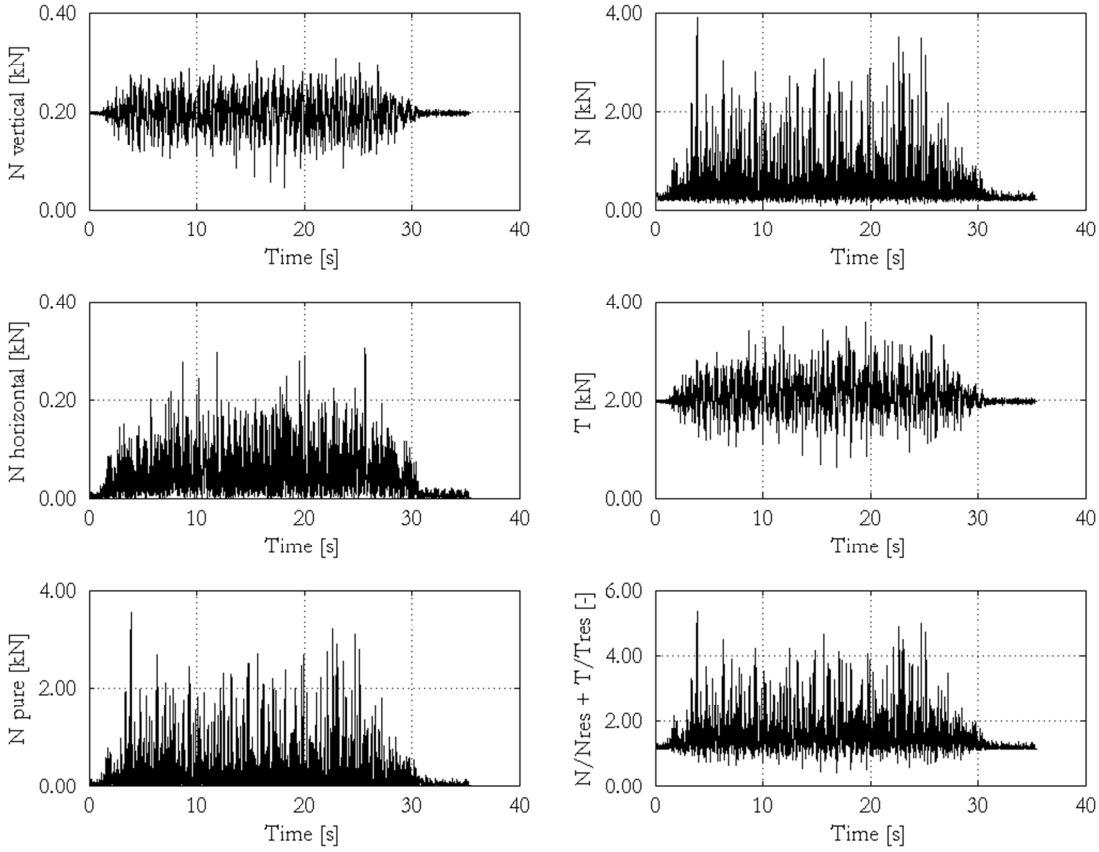

Figure 4.9 Loads acting on AM2 specimen in test session 4 – 0.80g of ZPA testing step; N = axial load, T = shear load, N/Nres+T/Tres = normalized force for design load combination

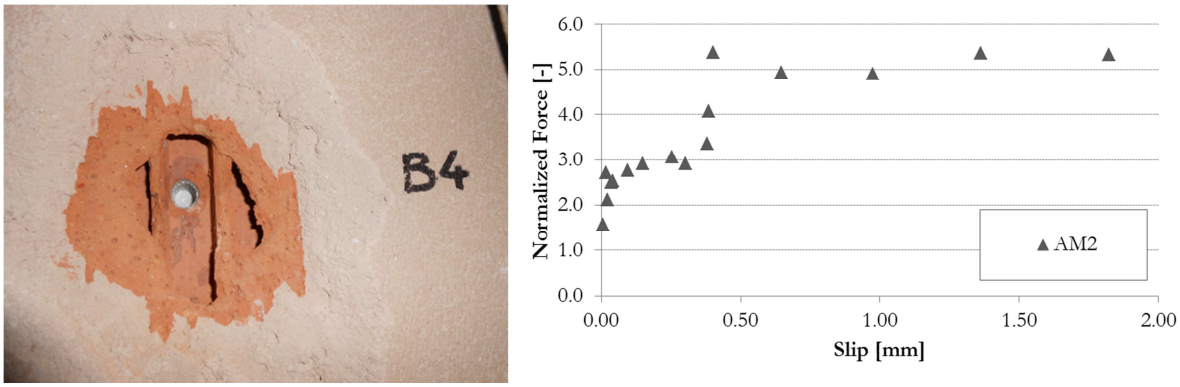

Figure 4.10 Failure mode of AM2 specimen after test session 4. Load vs displacement graph for AM2

4.4.1.3. AM specimen 3

Specimen 3 of adhesive anchor was installed in hollow bricks. It didn't reach failure after having withstood all of the testing steps in test session 5. The specimen experienced no damage during the testing. The base material showed light damages. Indeed a limited detachment of plaster (2x2x0.5cm) in the wall surface below the fixing point should be also mentioned. The tested specimen showed an absence of any slippage.

Among all the experimental steps, the maximum dynamic loads -related to the instant of peak normalized force, namely 6.21 - acting on the specimen, consisted of 5.1kN in tension and 1.9kN in shear.

The measured slipping of the anchor during the test session 5 increased, with an almost linear plot, up to 4.3mm. In this case the maximum slip value for the specimen is that related to the experimental step of maximum loading.

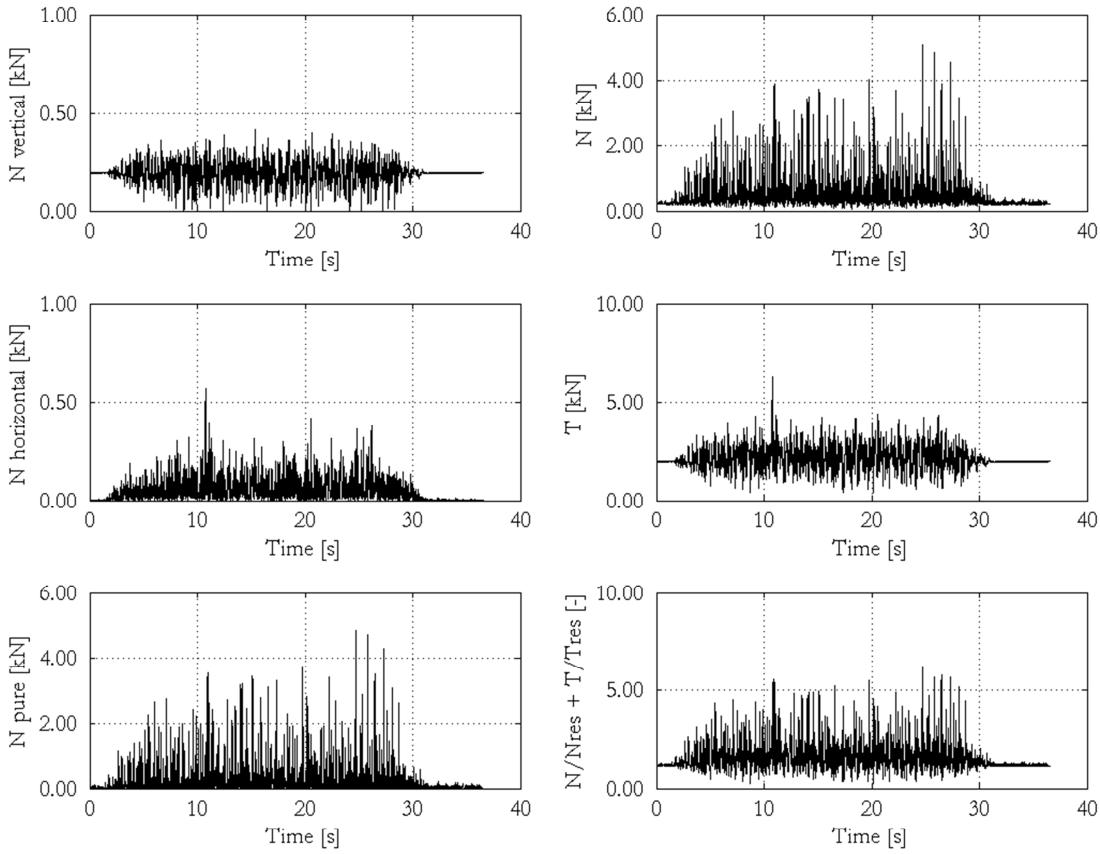

Figure 4.11 Loads acting on AM3 specimen in test session 5 – 1.20g of ZPA testing step; N = axial load, T = shear load, N/Nres+T/Tres = normalized force for design load combination

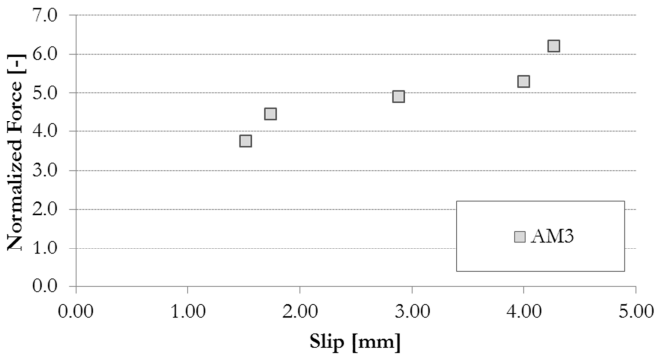

Figure 4.12 View of AM3 specimen after test session 5. Load vs displacement graph for AM3

4.4.1.4. AM specimen 4

Specimen 4 of adhesive anchor was installed in hollow bricks. It reached failure at a nominal level of peak acceleration of 1.10g in the test session 5. The specimen experienced a failure which involved the external brick shell and part of the internal brick web. In particular the collapse occurred to the entire face shell and part of second web. In addition the detachment of a relevant portion of plaster (35x40cm) in the wall surface around the fixing point should be also mentioned. The tested specimen showed an absence of any slippage before failure.

Among all the experimental steps, the maximum dynamic loads -related to the instant of peak normalized force, namely 4.95 - acting on the specimen, consisted of 4.0kN in tension and 1.6kN in shear.

The measured slipping of the anchor during the test session 5 increased, with an almost linear plot, up to 1.5mm. In this case the maximum slip value for the specimen is that related to the experimental step of maximum loading.

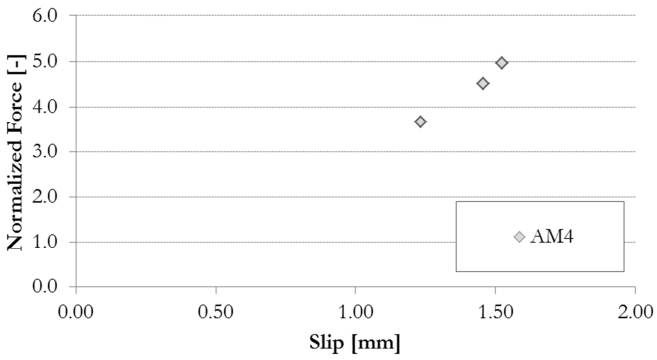

Figure 4.13 Failure mode of AM4 specimen after test session 5. Load vs displacement graph for AM4

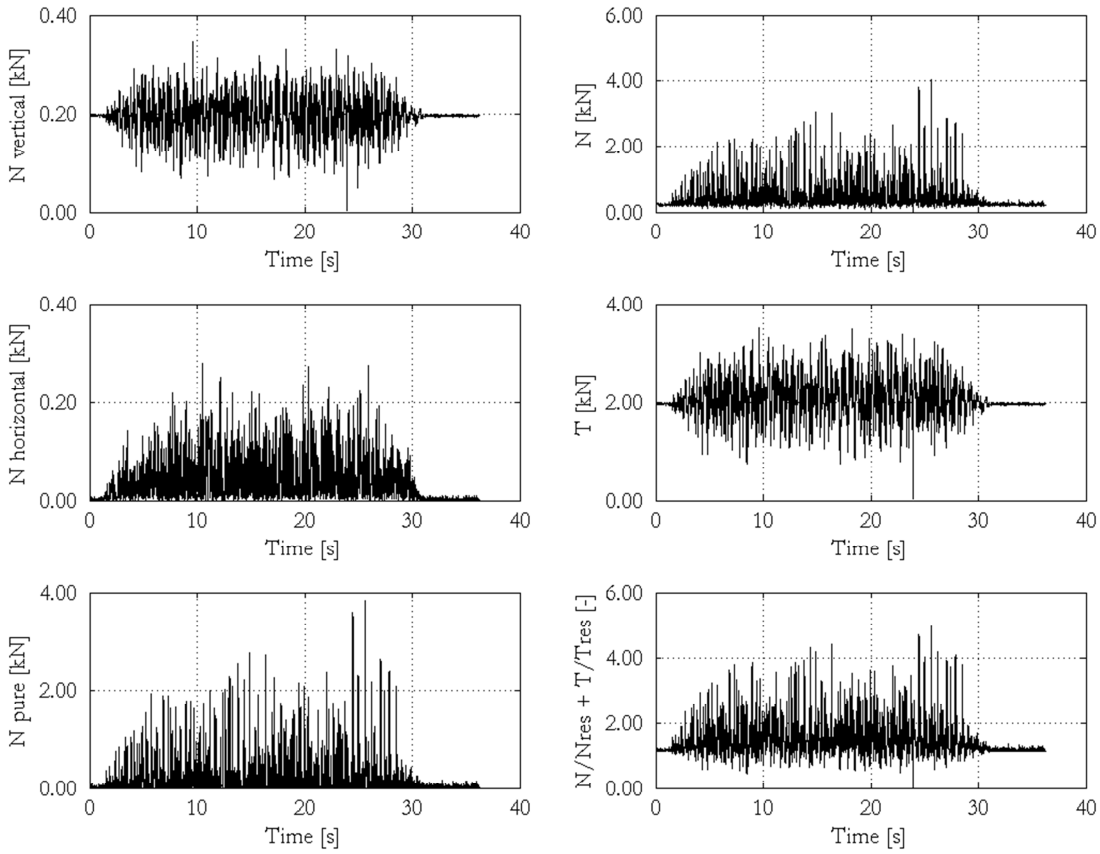

Figure 4.14 Loads acting on AM4 specimen in test session 5 – 1.00g of ZPA testing step; N = axial load, T = shear load, N/Nres+T/Tres = normalized force for design load combination

4.4.1.5. Remarks about AM specimen behaviour

The adhesive anchors installed on masonry support showed a linear behaviour up to about 0.50mm of slip. Over this value the sustained load is almost constant. A substantial agreement can be observed among the specimens of the TS4. Different ultimate value can be observed in terms of displacement while the variation of the failure load is limited. In TS5 the failure load reflect the value found in TS4, even if the slip is higher. In most cases the rupture was due to the failure of the external shell of bricks.

Table 4.8 Summarizing table for all the specimens with the maximum sustained actions in tension and shear, the maximum normalized force and the relevant slipping, the maximum slipping

	N_{max}	V_{max}	$F_{norm\ max}$	δ_F	δ_{max}
Specimen ref.	kN	kN	-	mm	mm
AM1	4.066	2.992	5.674	0.464	1.695
AM2	3.901	2.706	5.365	1.361	1.823
AM3	5.064	1.945	6.210	4.268	4.268
AM4	4.014	1.606	4.953	1.523	1.523

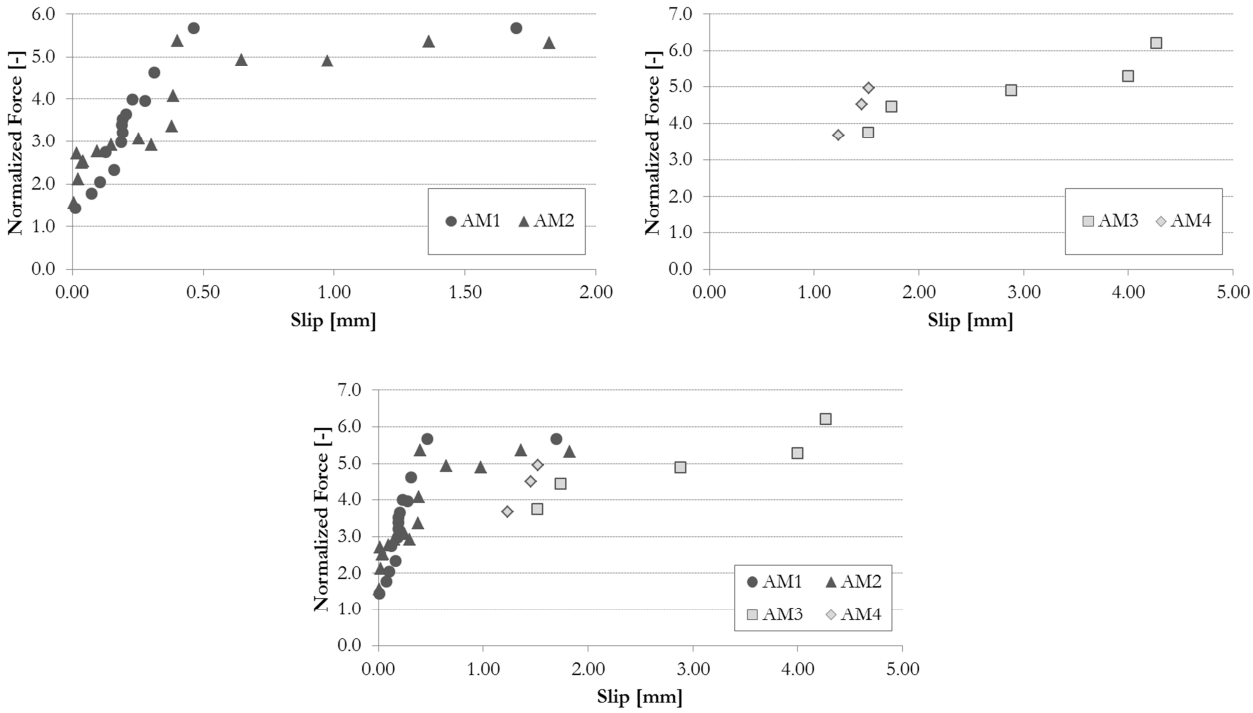

Figure 4.15 Summarizing load-displacement curves for AM specimens (test 4, dark grey; test 5 light grey)

4.4.2. Plastic Expansion Anchor (PE)

This paragraph includes the results of the plastic expansion anchor PE 10x80 in hollow masonry infill walls. A total of 6 specimens were tested in the 2 test sessions with the masonry structural unit. The component fixed with PEM specimens consisted in a 85kg steel plate.

Figure 4.16 View of plastic expansion anchor PE 10x80

Table 4.9 Installation features for plastic expansion anchor specimens

Specimen reference	Test session	Component reference	Mass [kg]	Height from table [cm]
PEM1	TS4	F4	85	171
PEM2	TS4	G4	85	171
PEM3	TS4	H4	85	51
PEM4	TS5	A5	85	112
PEM5	TS5	B5	85	112
PEM6	TS5	C5	85	51

4.4.2.1. PEM specimen 1

Specimen 1 of plastic expansion anchor was installed in hollow bricks. It reached failure at a nominal level of peak acceleration of 0.65g in the test session 4. The specimen highlighted a failure due to the extraction from the support (pull-out) also caused by an

enlargement of the installation hole in the brick shell and by the detachment of a relevant plaster zone around the fixing point. This failure mode is related to the axial forces acting on the fixing points. The base material experienced relevant damages as a plaster detachment of 8x13cm was observed around the anchoring point.

Among all the experimental steps, the maximum dynamic loads -related to the instant of peak normalized force, namely 2.94 - acting on the specimen, consisted of 1.0kN in tension and 1.0kN in shear.

The measured slipping of the anchor during the test session 4 increased, with an slightly inflected curve, up to 1.3mm. In this case the maximum slip value for the specimen is different from that related to the experimental step of maximum loading, which was of 0.8mm.

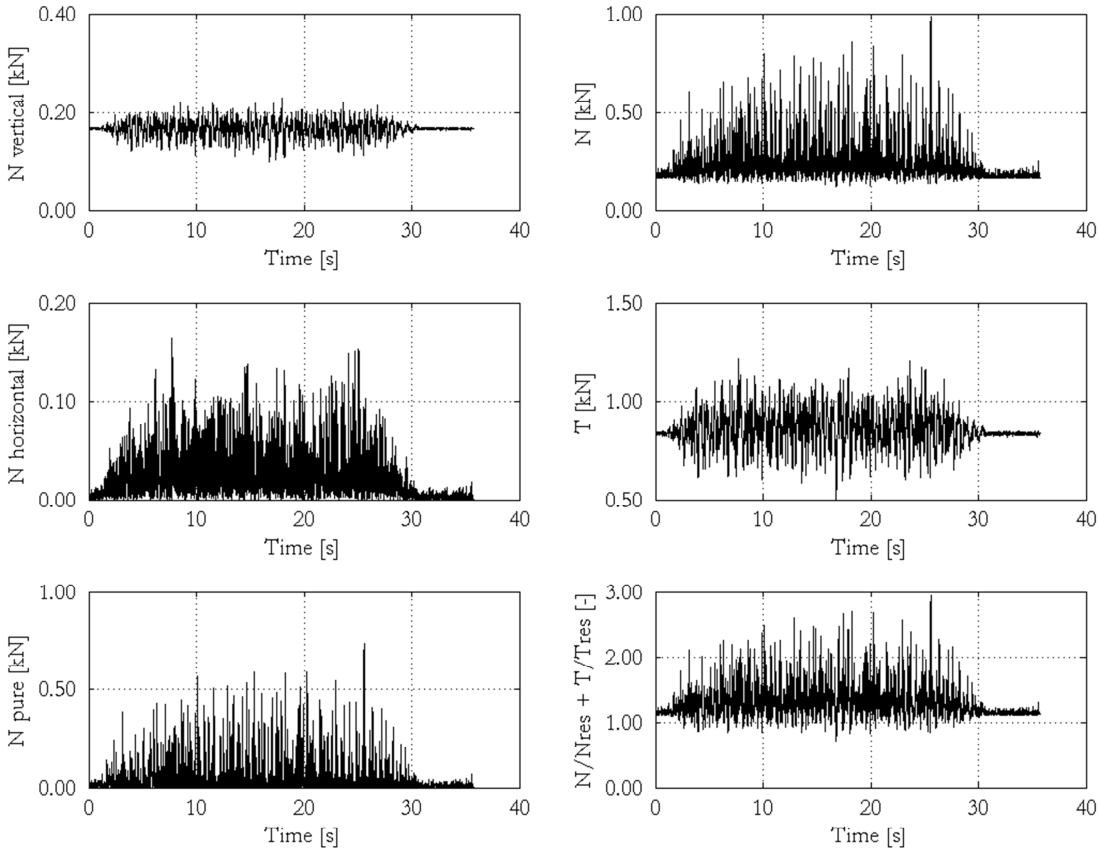

Figure 4.17 Loads acting on PEM1 specimen in test session 4 – 0.55g of ZPA testing step; N = axial load, T = shear load, N/Nres+T/Tres = normalized force for design load combination

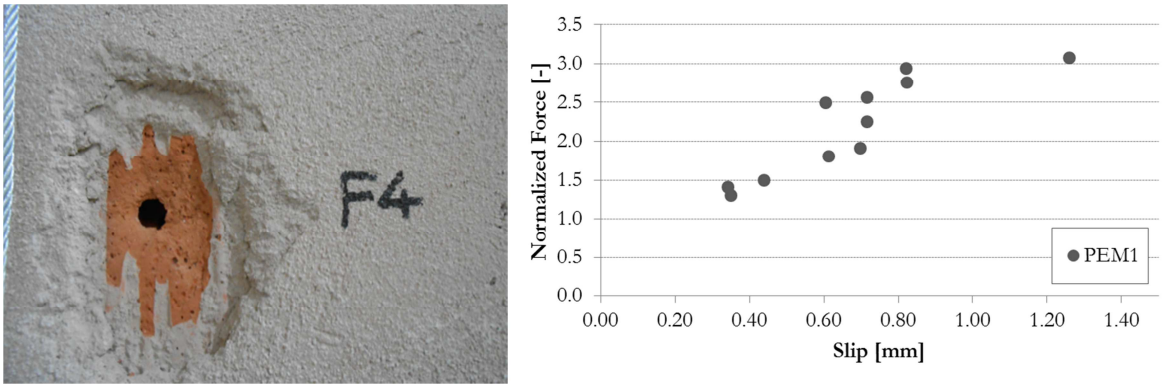

Figure 4.18 Failure mode of PEM1 specimen after test session 4. Load vs displacement graph for PEM1

4.4.2.2. PEM specimen 2

Specimen 2 of plastic expansion anchor was installed in hollow bricks. It reached failure at a nominal level of peak acceleration of 0.70g in the test session 4. The specimen highlighted a failure due to the extraction from the support (pull-out) also caused by an enlargement of the installation hole in the brick shell and by the detachment of a relevant plaster zone around the fixing point. This failure mode is related to the axial forces acting on the fixing points. The base material experienced relevant damages as a plaster detachment of 5x6cm was observed around the anchoring point.

Among all the experimental steps, the maximum dynamic loads -related to the instant of peak normalized force, namely 3.12 - acting on the specimen, consisted of 1.0kN in tension and 1.1kN in shear.

The measured slipping of the anchor during the test session 4 increased, with an almost linear plot, up to 1.4mm. In this case the maximum slip value for the specimen is different from that related to the experimental step of maximum loading, which was of 1.0mm.

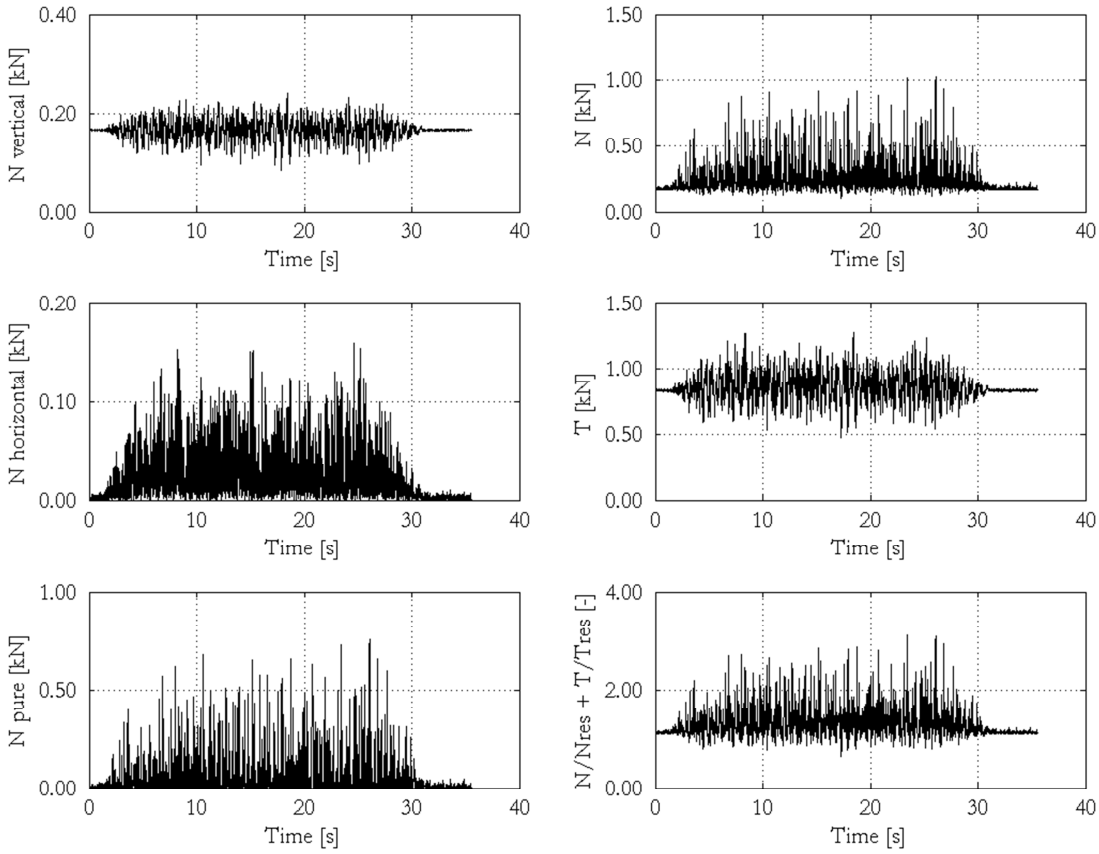

Figure 4.19 Loads acting on PEM2 specimen in test session 4 – 0.60g of ZPA testing step; N = axial load, T = shear load, N/Nres+T/Tres = normalized force for design load combination

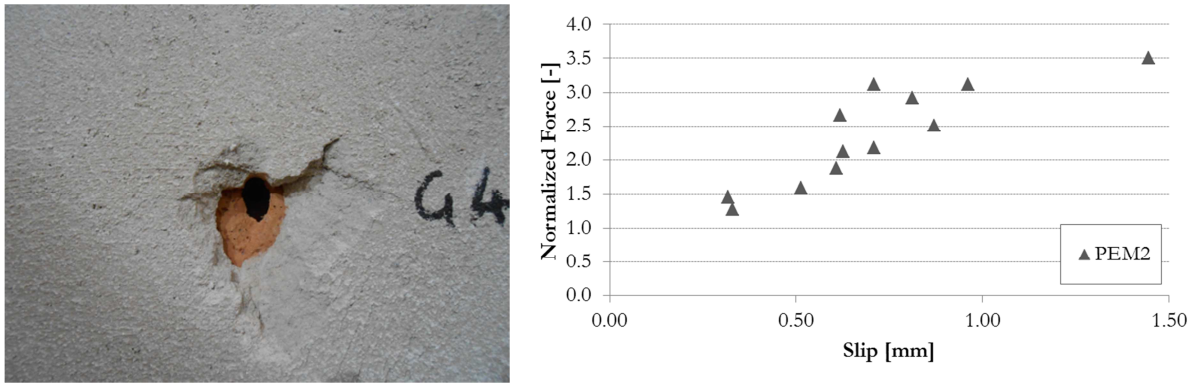

Figure 4.20 Failure mode of PEM2 specimen after test session 4. Load vs displacement graph for PEM2

4.4.2.3. PEM specimen 3

Specimen 3 of plastic expansion anchor was installed in hollow bricks. It did not reach failure after having withstood all of the testing steps in test session 4. The base material experienced very light damages as a plaster detachment of 2x3x1cm was observed around the anchoring point.

Among all the experimental steps, the maximum dynamic loads -related to the instant of peak normalized force, namely 4.25 - acting on the specimen, consisted of 1.6kN in tension and 1.1kN in shear.

The measured slipping of the anchor during the test session 4 increased, with an slightly inflected curve, up to 6.7mm. In this case the maximum slip value for the specimen is different from that related to the experimental step of maximum loading, which was of 6.0mm.

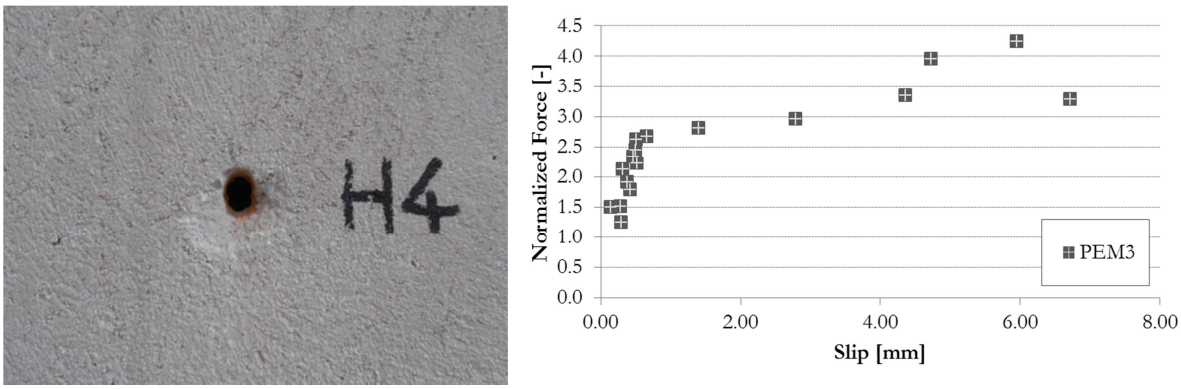

Figure 4.21 Failure mode of PEM3 specimen after test session 4. Load vs displacement graph for PEM3

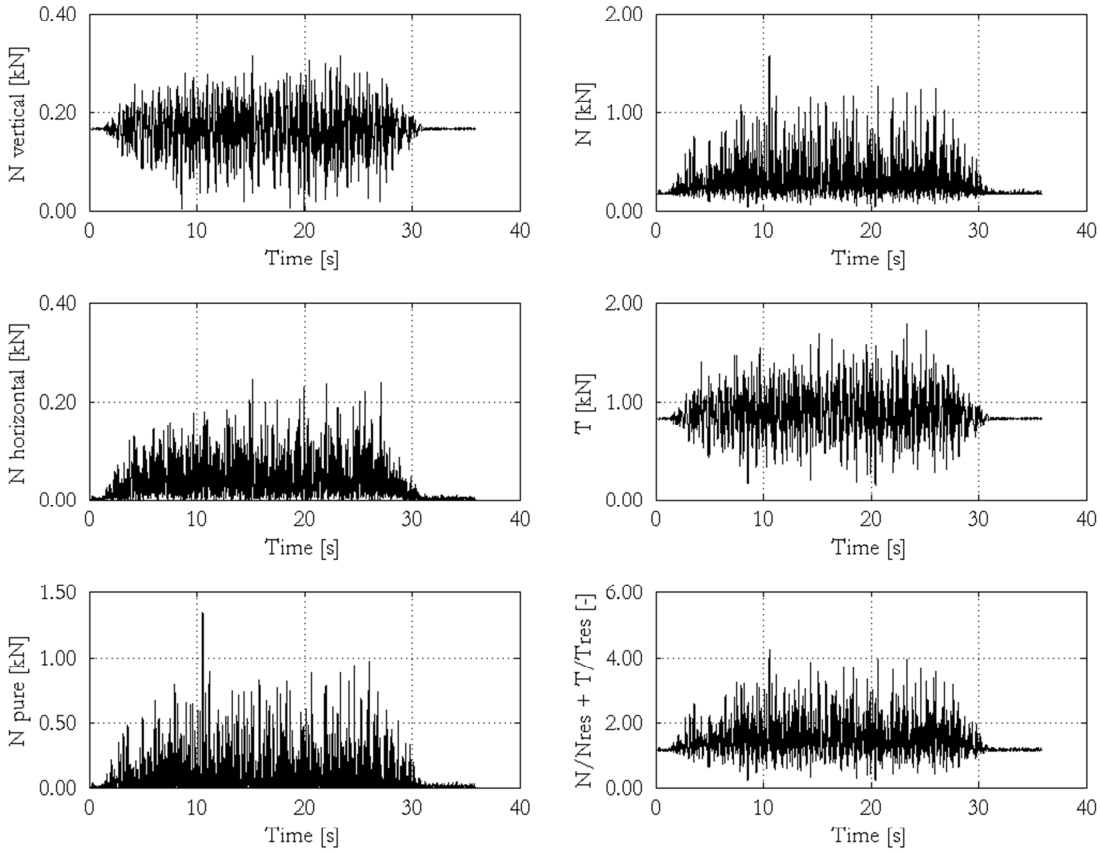

Figure 4.22 Loads acting on PEM3 specimen in test session 4 – 0.90g of ZPA testing step; N = axial load, T = shear load, N/Nres+T/Tres = normalized force for design load combination

4.4.2.4. PEM specimen 4

Specimen 4 of plastic expansion anchor was installed in hollow bricks. It reached failure at a nominal level of peak acceleration of 0.90g in the test session 5. The specimen highlighted a failure due to the extraction from the support (pull-out) also caused by an enlargement of the installation hole in the brick shell and by the detachment of a relevant plaster zone around the fixing point. This failure mode is related to the axial forces acting on the fixing points. The base material experienced relevant damages as a plaster detachment of 15x12cm was observed around the anchoring point.

Among all the experimental steps, the maximum dynamic loads -related to the instant of peak normalized force, namely 3.35 - acting on the specimen, consisted of 1.1kN in tension and 1.1kN in shear.

The maximum measured slipping of the anchor during test session 5 was 1.5mm in the first experimental step. After that the specimen reached failure.

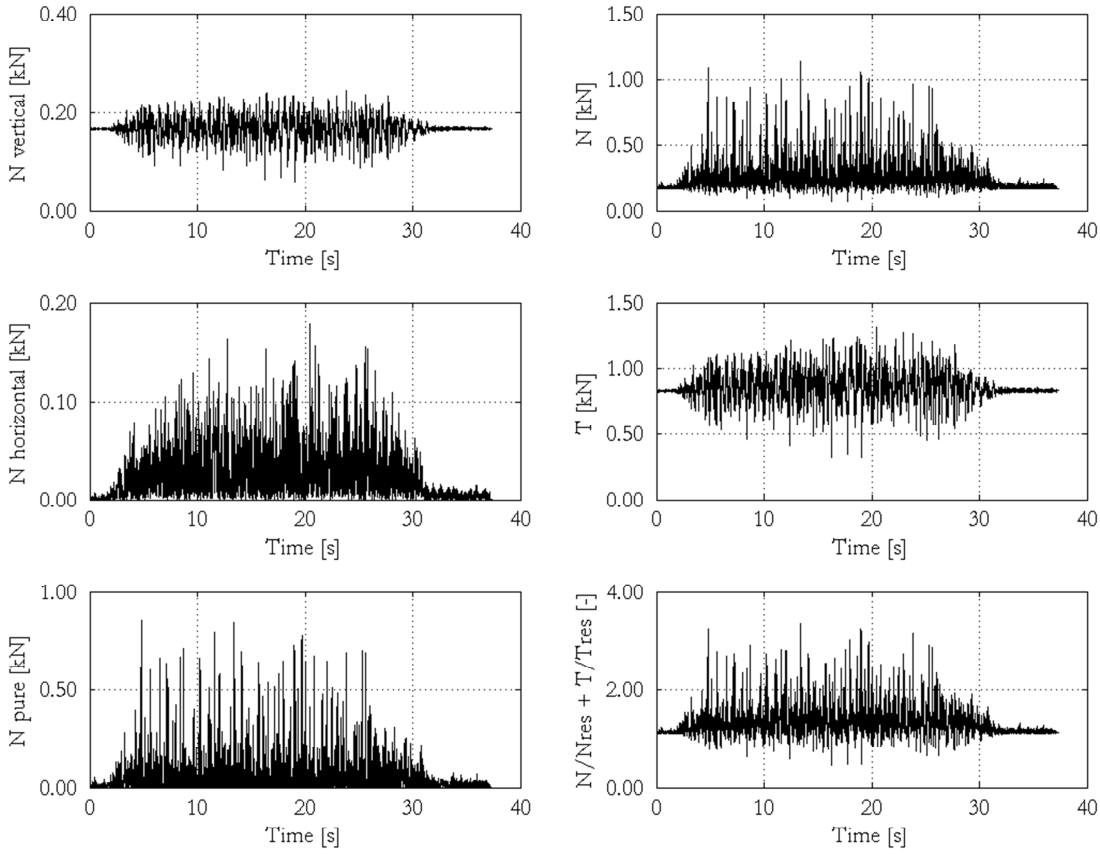

Figure 4.23 Loads acting on PEM4 specimen in test session 5 – 0.70g of ZPA testing step; N = axial load, T = shear load, N/Nres+T/Tres = normalized force for design load combination

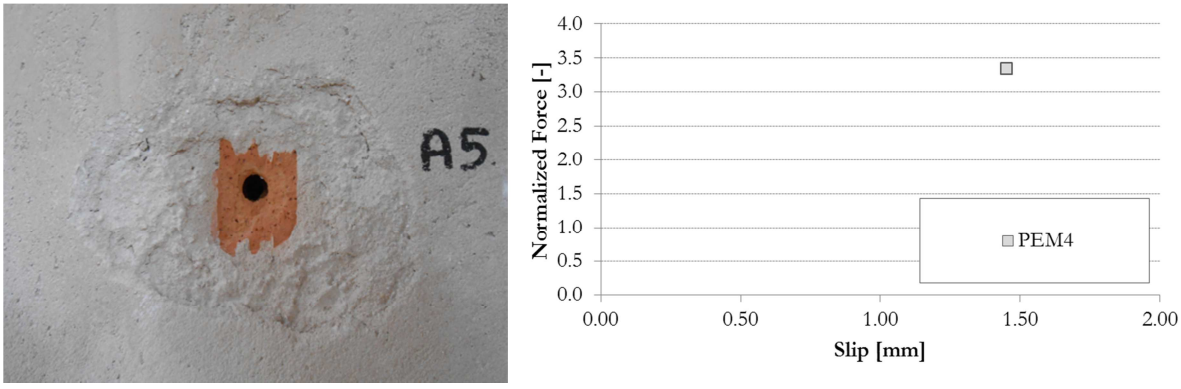

Figure 4.24 Failure mode of PEM4 specimen after test session 5. Load vs displacement graph for PEM4

4.4.2.5. PEM specimen 5

Specimen 5 of plastic expansion anchor was installed in hollow bricks. It reached failure at a nominal level of peak acceleration of 0.90g in the test session 5. The specimen highlighted a failure due to the extraction from the support (pull-out) also caused by an enlargement of the installation hole in the brick shell and by the detachment of a relevant plaster zone around the fixing point. This failure mode is related to the axial forces acting on the fixing points. The base material experienced relevant damages as a plaster detachment of 18x13cm was observed around the anchoring point.

Among all the experimental steps, the maximum dynamic loads -related to the instant of peak normalized force, namely 3.41 - acting on the specimen, consisted of 1.0kN in tension and 1.4kN in shear.

The maximum measured slipping of the anchor during test session 5 was 1.9mm in the first experimental step. After that the specimen reached failure.

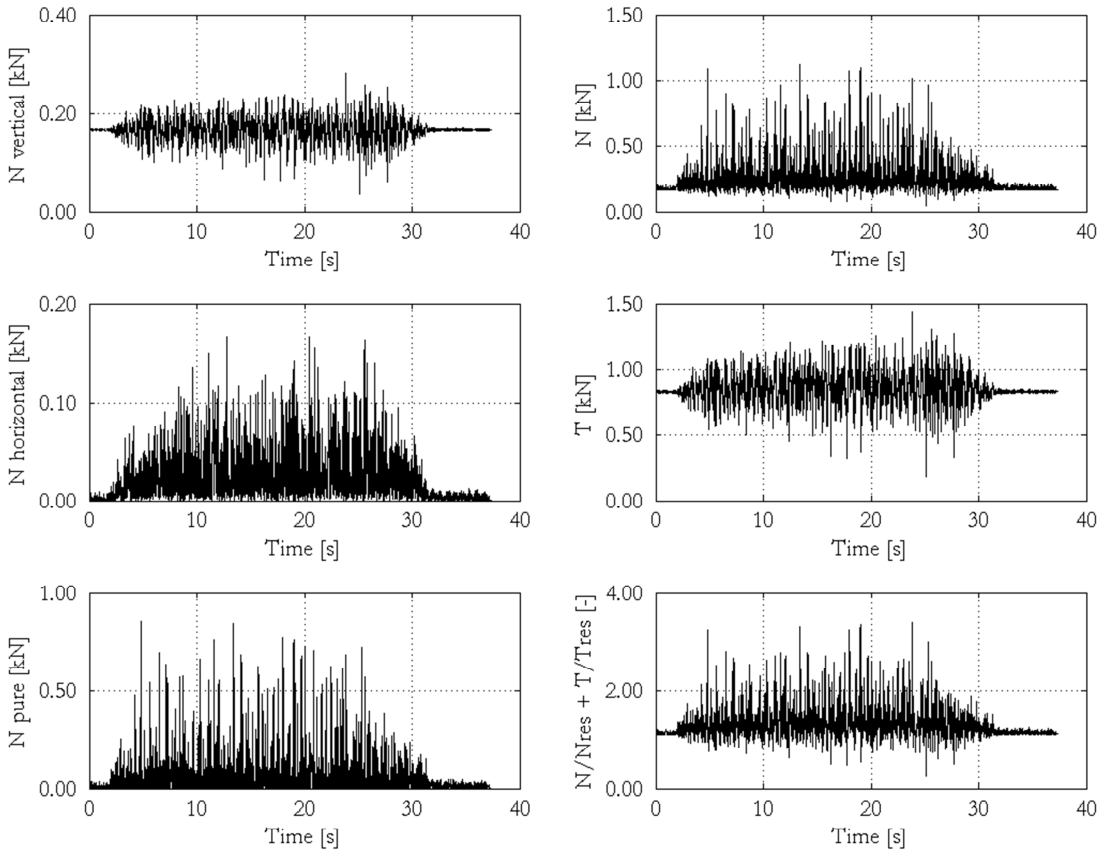

Figure 4.25 Loads acting on PEM5 specimen in test session 5 – 0.70g of ZPA testing step; N = axial load, T = shear load, N/Nres+T/Tres = normalized force for design load combination

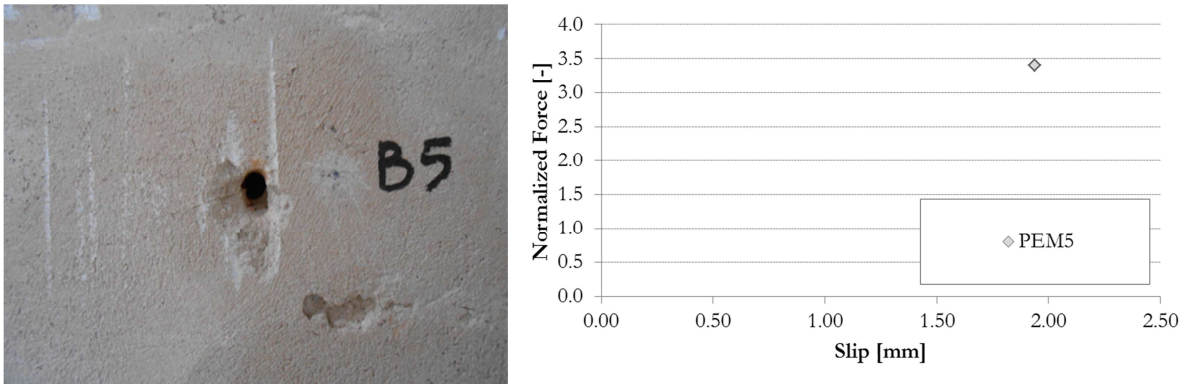

Figure 4.26 Failure mode of PEM5 specimen after test session 5. Load vs displacement graph for PEM5

4.4.2.6. PEM specimen 6

Specimen 6 of plastic expansion anchor was installed in hollow bricks. It did not reach failure after having withstood all of the testing steps in test session 5. The base material experienced very light damages as a plaster detachment of 2x2x0.5cm was observed around the anchoring point.

Among all the experimental steps, the maximum dynamic loads -related to the instant of peak normalized force, namely 3.88 - acting on the specimen, consisted of 1.2kN in tension and 1.5kN in shear.

The measured slipping of the anchor during the test session 5 increased, with an almost linear plot, up to 3.5mm. In this case the maximum slip value for the specimen is that related to the experimental step of maximum loading.

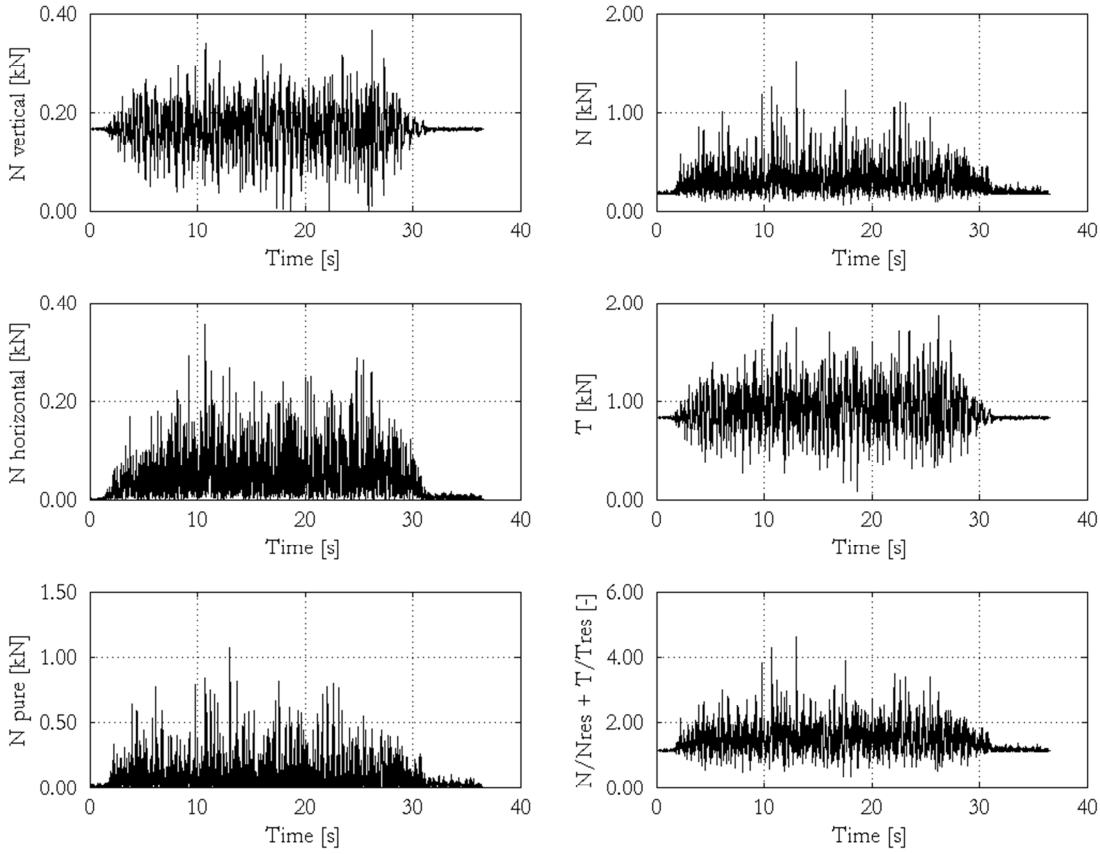

Figure 4.27 Loads acting on PEM6 specimen in test session 5 – 1.20g of ZPA testing step; N = axial load, T = shear load, N/Nres+T/Tres = normalized force for design load combination

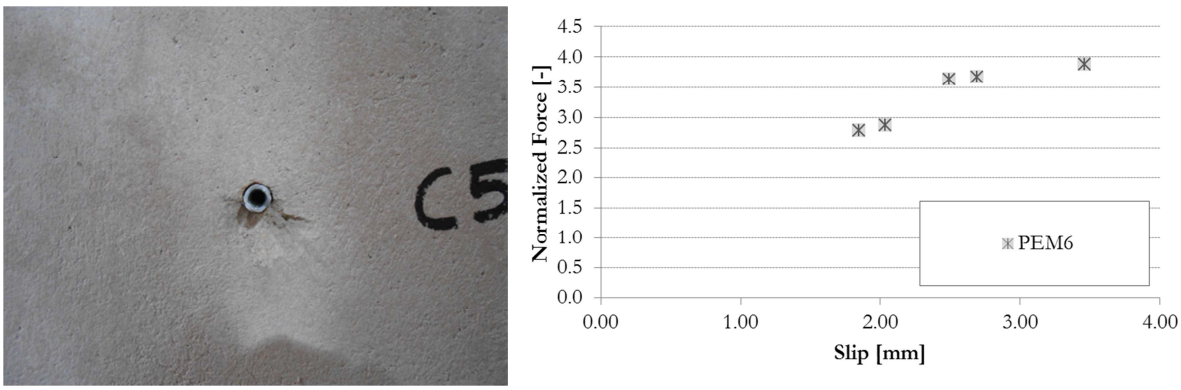

Figure 4.28 View of PEM6 specimen after test session 5. Load vs displacement graph for PEM6

4.4.2.7. Remarks about PEM specimen behaviour

The results of the PEM specimens are fully in agreement among them. This is especially evident in the first linear branch of the curve, up to about 1mm of slip. Over this value the slippage suddenly increase the load being substantially constant. The TS5 confirms the previous observations in terms of failure load while the slip results to be higher but this could be a consequence of the different testing methodology adopted.

Table 4.10 Summarizing table for all the specimens with the maximum sustained actions in tension and shear, the maximum normalized force and the relevant slipping, the maximum slip

	N_{max}	V_{max}	$Fnorm_{max}$	δ_F	δ_{max}
Specimen ref.	kN	kN	-	mm	mm
PEM1	0.985	0.975	2.941	0.821	1.260
PEM2	1.015	1.098	3.117	0.961	1.446
PEM3	1.564	1.095	4.249	5.959	6.721
PEM4	1.133	1.087	3.351	1.452	1.452
PEM5	1.017	1.406	3.408	1.939	1.939
PEM6	1.226	1.451	3.881	3.460	3.460

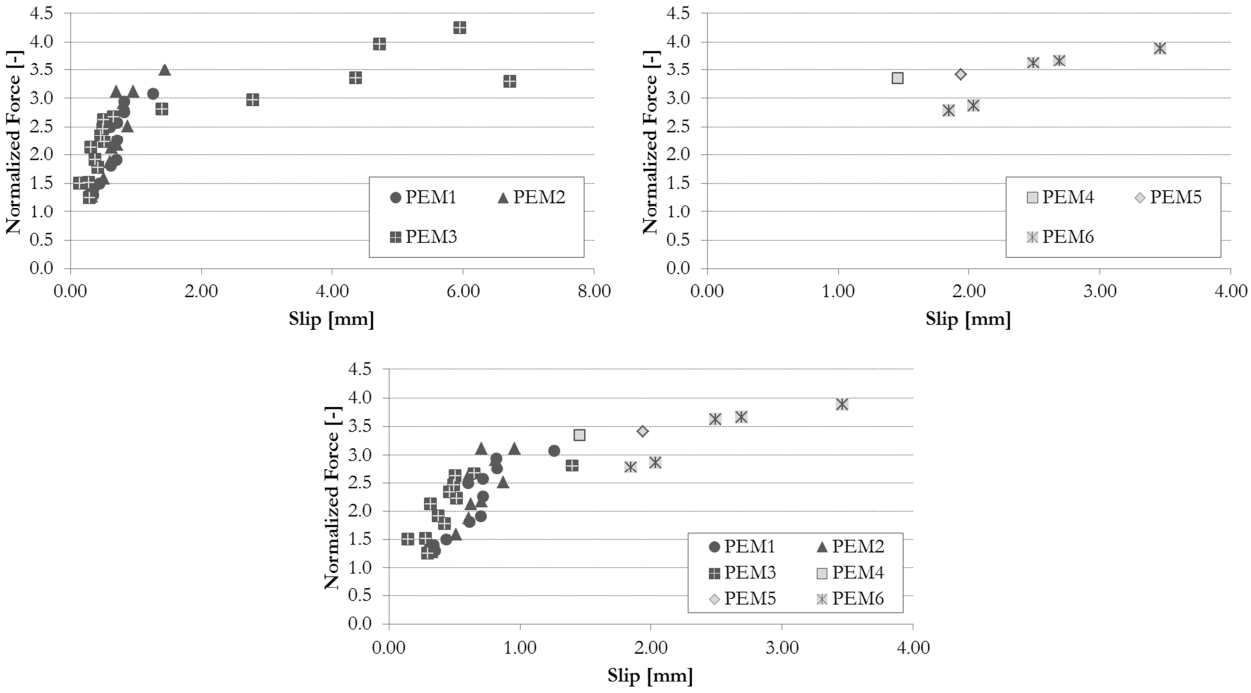

Figure 4.29 Summarizing load-displacement curves for AM specimens (test 4, dark grey; test 5 light grey)

4.4.3. Plastic Fibre Expansion Anchor (PFE)

This paragraph includes the results of the plastic-fibre anchor PFE 8x50 in hollow masonry infill walls. A total of 5 specimens were tested in the 2 test sessions with the

masonry structural unit. The component fixed with PFEM specimens consisted in a 50kg steel plate.

Figure 4.30 View of plastic-fibre expansion anchor PFE 8x50.

Table 4.11 Installation features for plastic-fibre expansion anchor specimens

Specimen reference	Test session	Component reference	Mass [kg]	Height from table [cm]
PFEM1	TS4	C4	50	171
PFEM2	TS4	D4	50	171
PFEM3	TS4	E4	50	51
PFEM4	TS5	D5	50	112
PFEM5	TS5	G5	50	112

4.4.3.1. PFEM specimen 1

Specimen 1 of plastic expansion anchor was installed in hollow masonry. It reached failure at a nominal level of peak acceleration of 1.00g in the test session 4. The failure mode experienced by the anchor specimen was related to the steel failure of the screw because of the shear forces acting on the fixing point. Moreover a further secondary damage related to the axial slippage of the plastic sleeve from the base material could be observed. A progressive small slippage of the anchor (0.2cm) was observed after the test session. The base material experienced limited damages as a plaster detachment of 2x3x0.5cm was observed around the anchoring point.

Among all the experimental steps, the maximum dynamic loads -related to the instant of peak normalized force, namely 2.68 - acting on the specimen, consisted of 1.0kN in tension and 0.5kN in shear.

The measured slip of the anchor during the test session 4 increased, with an inflected plot, up to 12.1mm. In this case the maximum slip value for the specimen is that related to the experimental step of maximum loading.

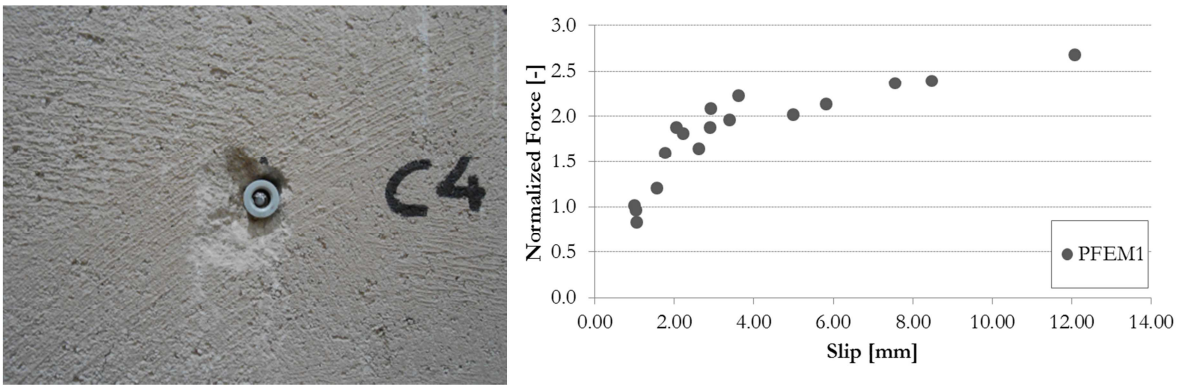

Figure 4.31 Failure mode of PFEM1 specimen after test session 4. Load vs displacement graph for PFEM1

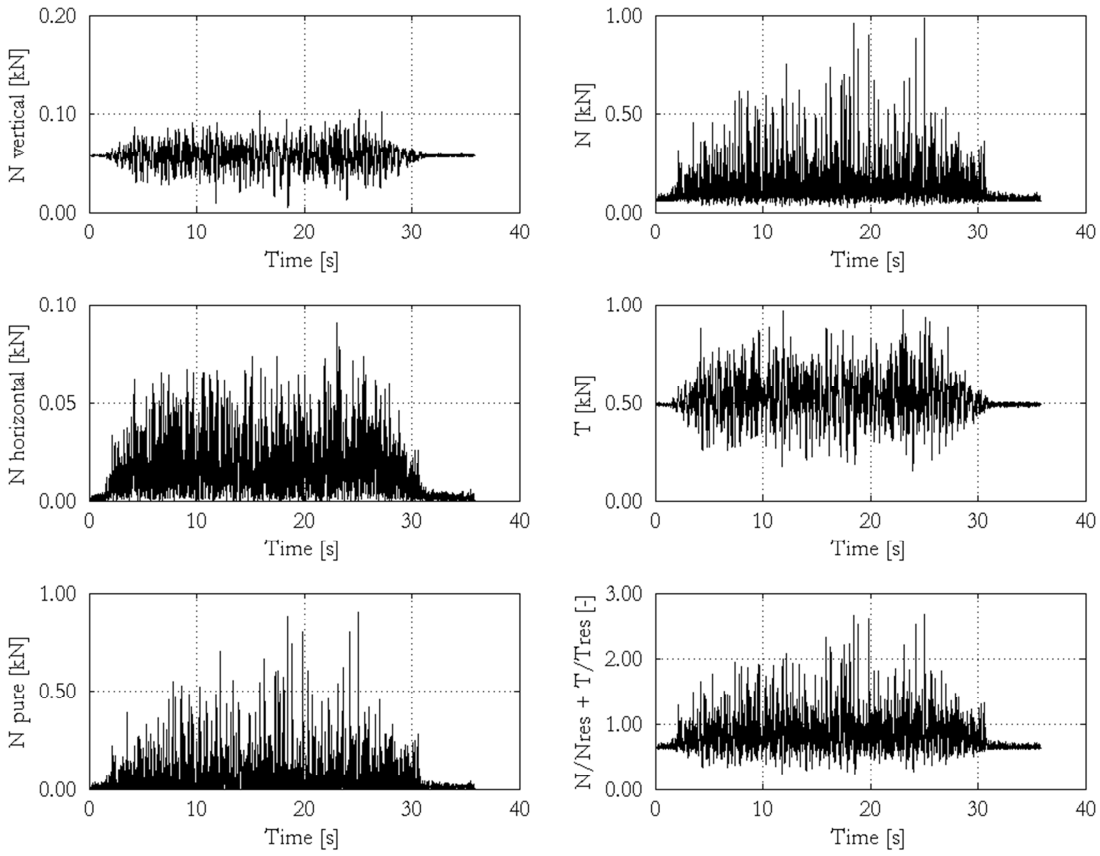

Figure 4.32 Loads acting on PFEM1 specimen in test session 4 – 0.90g of ZPA testing step; N = axial load, T = shear load, N/Nres+T/Tres = normalized force for design load combination

4.4.3.2. PFEM specimen 2

Specimen 2 of plastic expansion anchor was installed in hollow masonry. It reached failure at a nominal level of peak acceleration of 1.00g in the test session 4. The failure mode experienced by the anchor specimen was related to the steel failure of the screw because of the shear forces acting on the fixing point. Moreover a further secondary damage related to the axial slip of the plastic sleeve from the base material could be observed. A progressive slip of the anchor (10cm) was observed after the test session. The base material experienced limited damages as a plaster detachment of 4x3x1cm was observed around the anchoring point.

Among all the experimental steps, the maximum dynamic loads -related to the instant of peak normalized force, namely 2.71 - acting on the specimen, consisted of 1.0kN in tension and 0.5kN in shear.

The measured slip of the anchor during the test session 4 increased, with an almost linear plot, up to 3.8mm. In this case the maximum slip value for the specimen is that related to the experimental step of maximum loading.

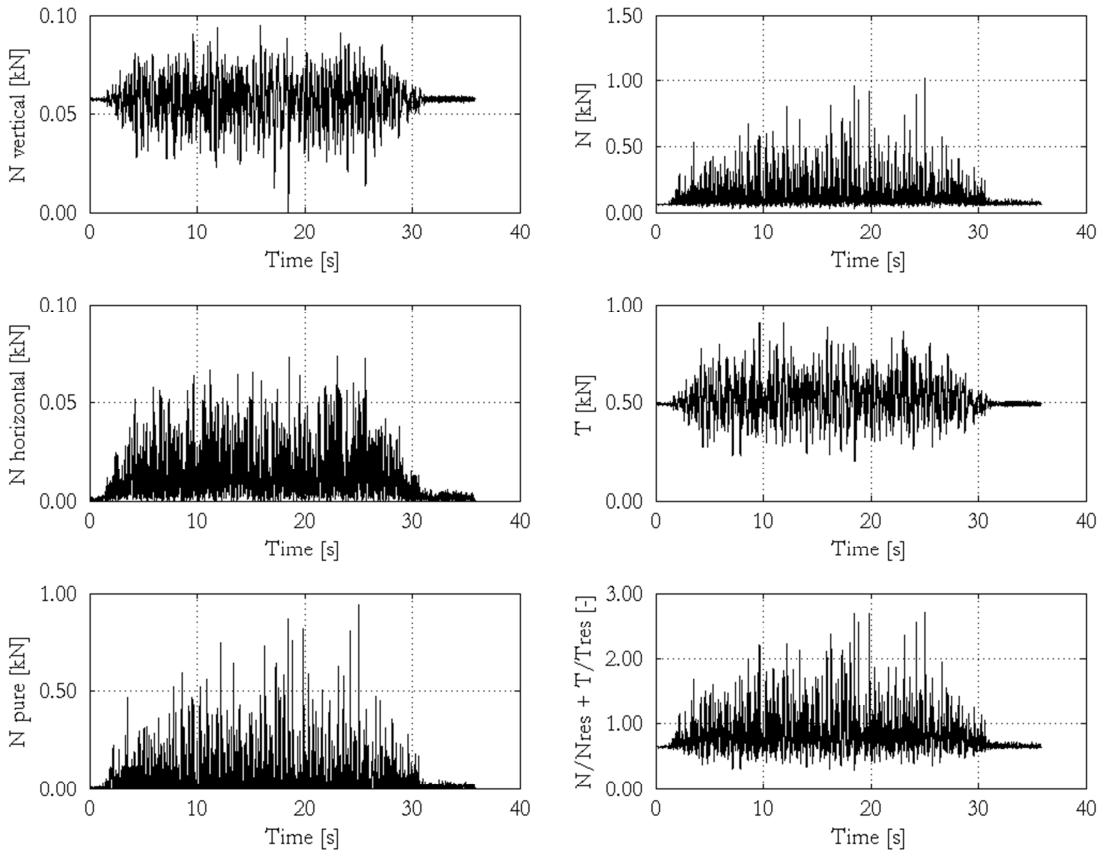

Figure 4.33 Loads acting on PFEM2 specimen in test session 4 – 0.90g of ZPA testing step; N = axial load, T = shear load, N/Nres+T/Tres = normalized force for design load combination

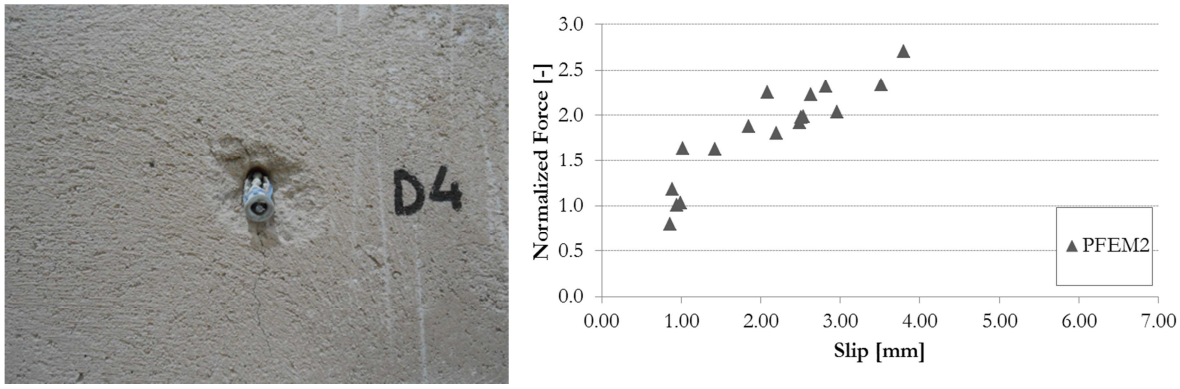

Figure 4.34 Failure mode of PFEM2 specimen after test session 4. Load vs displacement graph for PFEM2

4.4.3.3. PFEM specimen 3

Specimen 3 of plastic expansion anchor was installed in hollow masonry. It did not reach failure after having withstood all of the testing steps in test session 4. The base material experienced no damages and no plaster detachment was observed around the anchoring point.

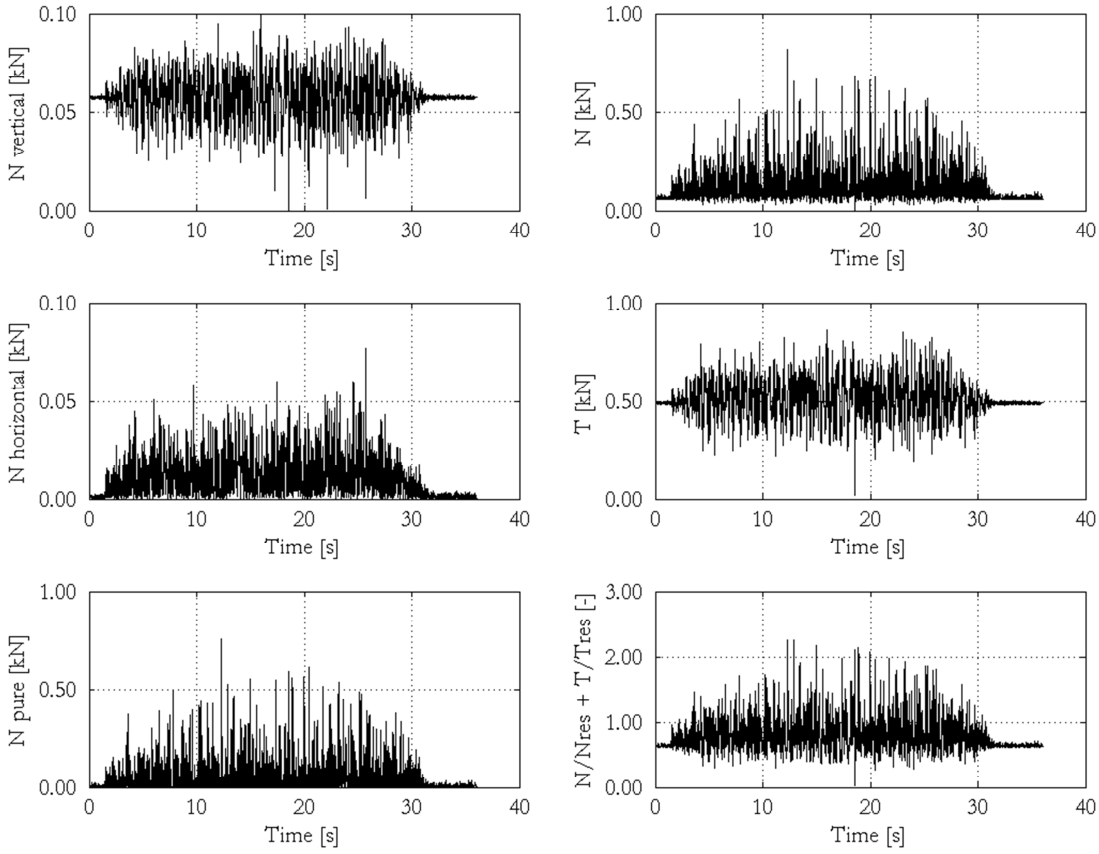

Figure 4.35 Loads acting on PFEM3 specimen in test session 4 – 1.00g of ZPA testing step; N = axial load, T = shear load, N/Nres+T/Tres = normalized force for design load combination

Among all the experimental steps, the maximum dynamic loads -related to the instant of peak normalized force, namely 2.26 - acting on the specimen, consisted of 0.8kN in tension and 0.5kN in shear.

The measured slipping of the anchor during the test session 4 increased, with an almost linear plot, up to 5.4mm. In this case the maximum slip value for the specimen is that related to the experimental step of maximum loading.

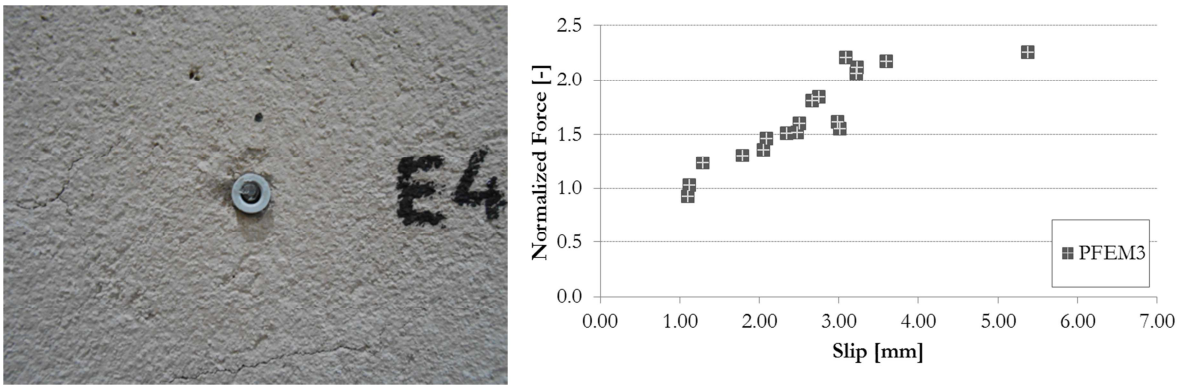

Figure 4.36 View of PFEM3 specimen after test session 4. Load vs displacement graph for PFEM3

4.4.3.4. PFEM specimen 4

Specimen 4 of plastic expansion anchor was installed in hollow masonry. It reached failure at a nominal level of peak acceleration of 0.90g in the test session 5. The failure mode experienced by the anchor specimen was related to the steel failure of the screw

because of the shear forces acting on the fixing point. Moreover a further secondary damage related to the axial slippage of the plastic sleeve from the base material could be observed. A progressive slippage of the anchor (0.5cm) was observed after the test session. The base material experienced limited damages as a plaster detachment of 4x5x1cm was observed around the anchoring point.

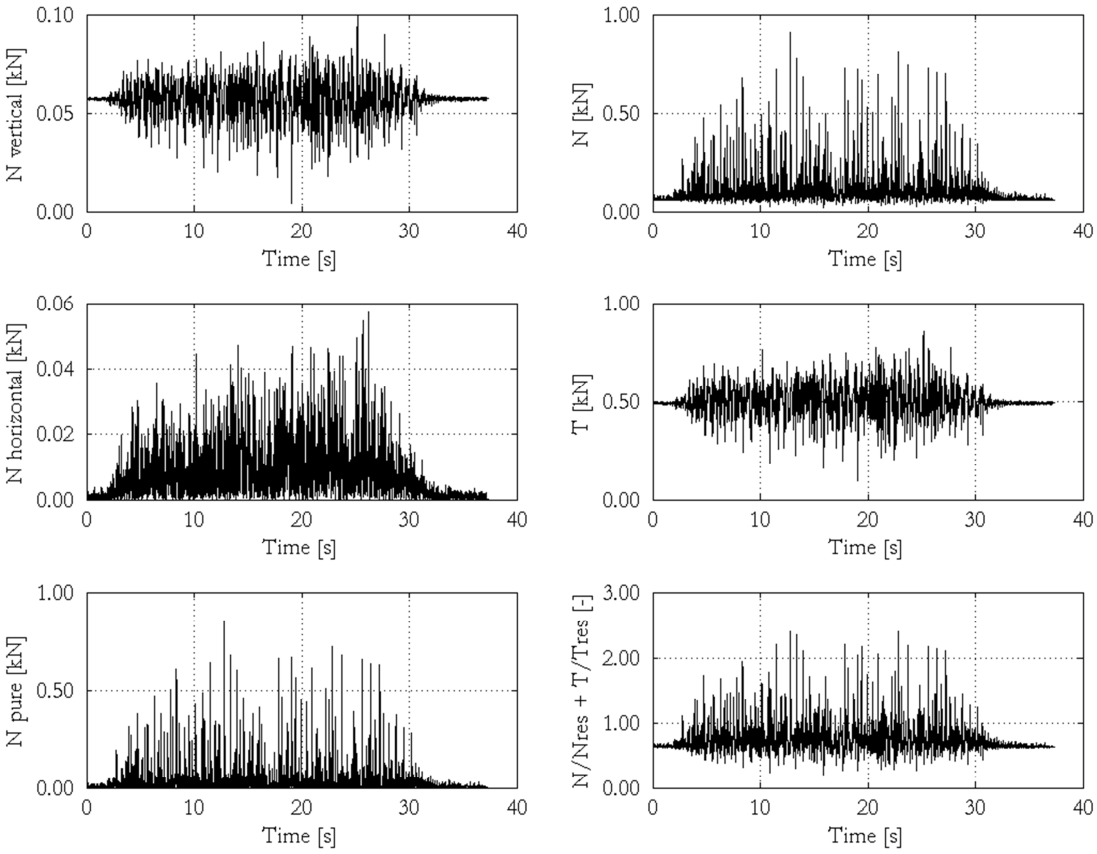

Figure 4.37 Loads acting on PFEM4 specimen in test session 5 – 0.70g of ZPA testing step; N = axial load, T = shear load, N/Nres+T/Tres = normalized force for design load combination

Among all the experimental steps, the maximum dynamic loads -related to the instant of peak normalized force, namely 2.41 - acting on the specimen, consisted of 0.8kN in tension and 0.6kN in shear.

The maximum measured slipping of the anchor during test session 5 was 6.4mm in the first experimental step. After that the specimen reached failure.

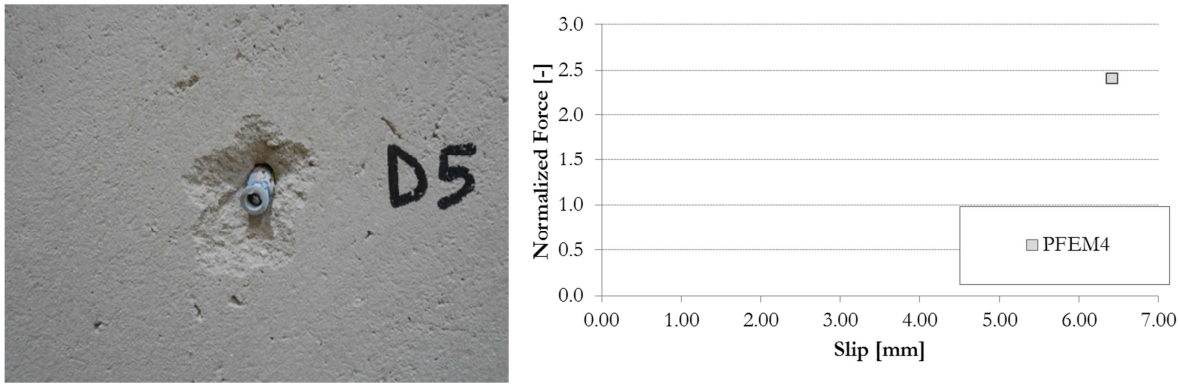

Figure 4.38 Failure mode of PFEM4 specimen after test session 5. Load vs displacement graph for PFEM4

4.4.3.5. PFEM specimen 5

Specimen 5 of plastic expansion anchor was installed in hollow masonry. It did not reach failure after having withstood all of the testing steps in test session 5. A progressive small slippage of the anchor (0.1cm) was observed after the test session. The base material experienced no damages and no plaster detachment was observed around the anchoring point.

Among all the experimental steps, the maximum dynamic loads -related to the instant of peak normalized force, namely 2.75 - acting on the specimen, consisted of 0.9kN in tension and 0.7kN in shear.

The measured slipping of the anchor during the test session 5 increased, with an almost linear plot, up to 12.6mm. In this case the maximum slip value for the specimen is that related to the experimental step of maximum loading.

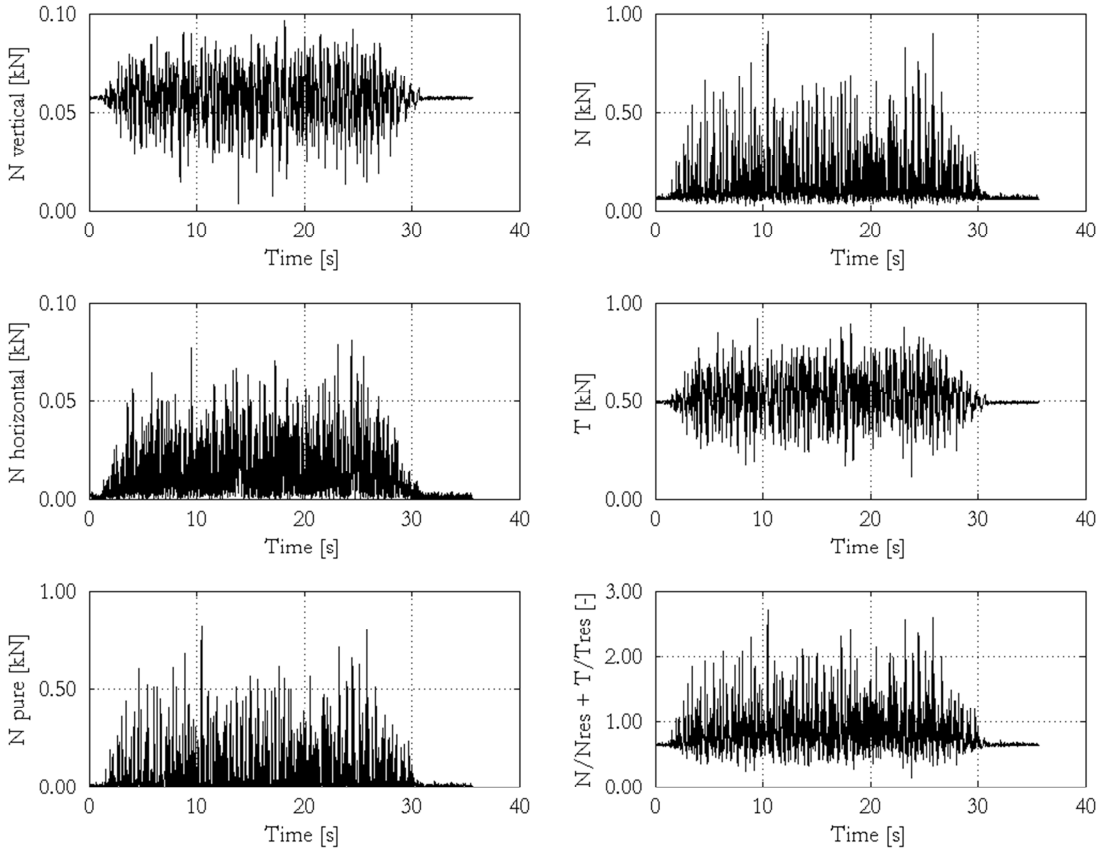

Figure 4.39 Loads acting on PFEM5 specimen in test session 5 – 1.10g of ZPA testing step; N = axial load, T = shear load, N/Nres+T/Tres = normalized force for design load combination

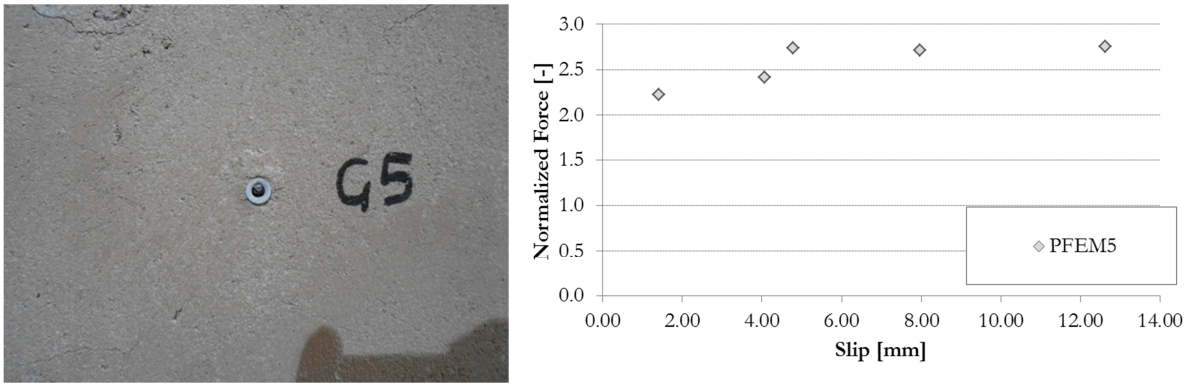

Figure 4.40 View of PFEM5 specimen after test session 5. Load vs displacement graph for PFEM5

4.4.3.6. Remarks about PFEM specimen behaviour

The PFEM specimens show a wide slip. The first linear behavior can be observed up to about 3mm for a value of normalized force equal to 2.0. Over this level the slippage widely increases with a limited increase of the load. This can be observed in all the specimens in TS4 and those in TS5 confirm the failure load that can be sustained. The failure is mainly related to the shear behavior of the anchors.

Table 4.12 Summarizing table for all the specimens with the maximum sustained actions in tension and shear, the maximum normalized force and the relevant slipping, the maximum slip

Specimen ref.	N_{max} kN	V_{max} kN	$F_{norm\ max}$ -	δ_F mm	δ_{max} mm
PFEM1	0.988	0.518	2.681	12.064	12.064
PFEM2	1.015	0.489	2.709	3.797	3.797
PFEM3	0.817	0.468	2.257	5.376	5.376
PFEM4	0.813	0.621	2.407	6.411	6.411
PFEM5	0.932	0.705	2.752	12.627	12.627

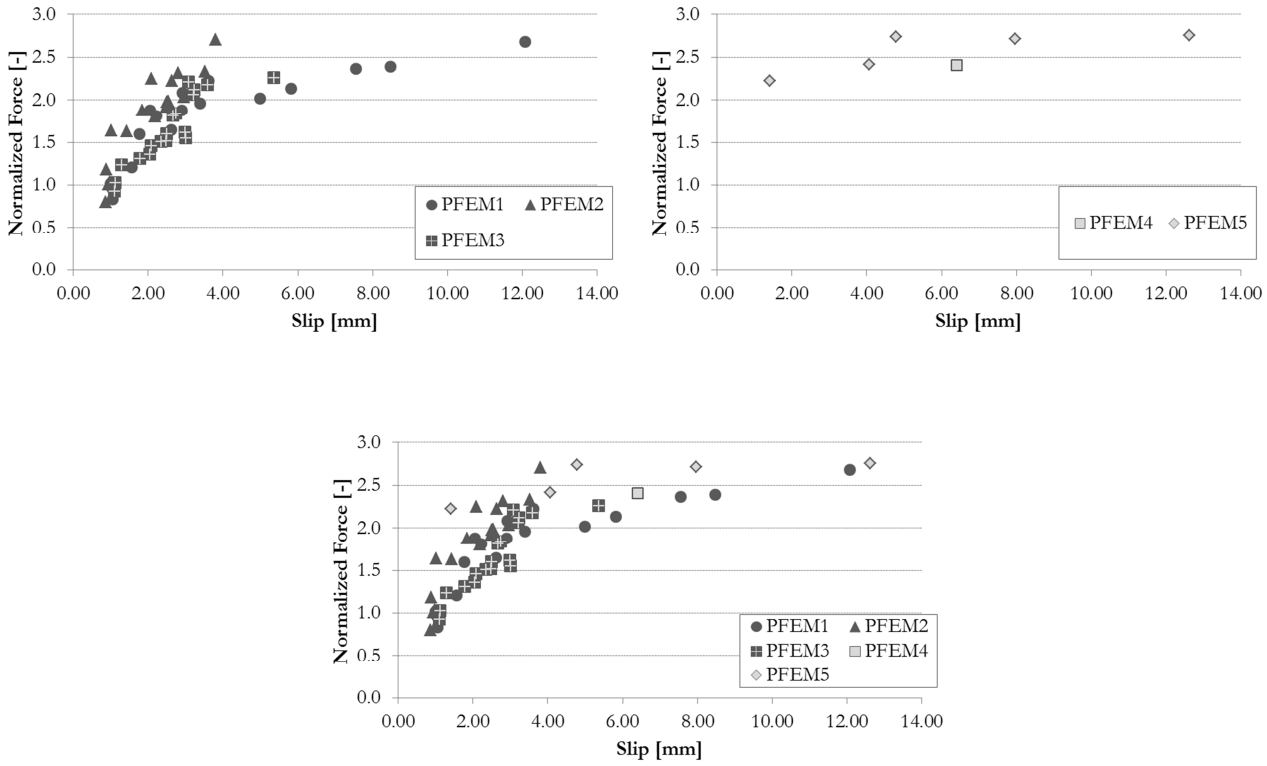

Figure 4.41 Summarizing load-displacement curves for AM specimens (test 4, dark grey; test 5 light grey)

4.4.4. Real Application

The above presented fixtures, related to the specimens, consisted in steel plates with a mass selected in order to obtain characterizing data. Besides that during test session 4 some anchor types were used to evaluate the fixing of real non-structural component such

as a water-heater. This kind of fixing application underwent to the experimental steps of TS4 without the occurrence of anchoring failure by withstanding the seismic actions induced by the table and filtered through the structure.

4.4.4.1. Water heater

In test session 4 a water heater was fixed to the concrete wall, in non-cracked condition, at a height of about 2m, in order to simulate a real case application and evaluate the anchor behaviour. The fixing was realized with two anchoring points using AM anchor type with a M10 standard stud. The component withstood to all the experimental steps up to 0.70g of nominal ZPA induced to the table.

Among the experimental steps, the maximum peak acceleration measured on the wall was greater than 1.5g in X direction and almost 1.5g in Y direction.

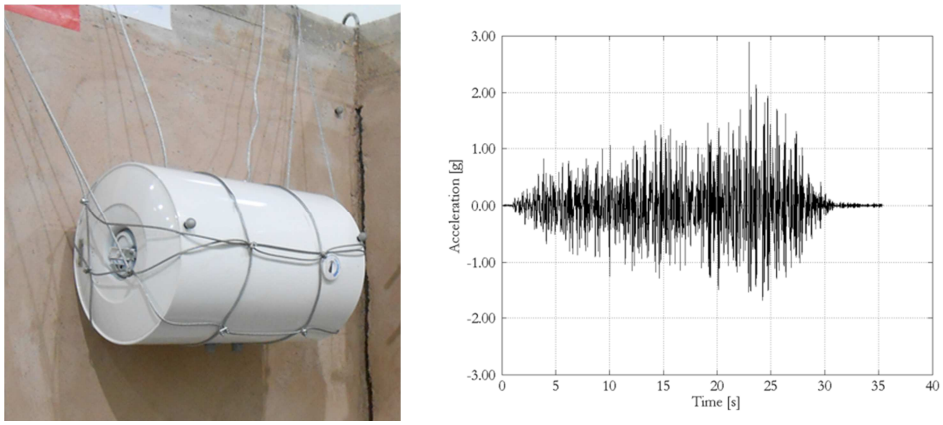

Figure 4.42 Anchorage of a water heater to masonry infill wall by means of two fixing points with AM and M10 steel stud.

5. NON-STRUCTURAL ELEMENTS FASTENING

As indicated by standards and best practice guidelines (ASCE 7-10, FEMA E-74), post-installed anchors represent a primary tool that can by their use and reliability under dynamic loading, modify the seismic response of non-structural elements. A properly designed anchoring system can prevent or limit the damage pattern occurring widely to non-structural components during an earthquake. In order to guarantee such result two main applicative goals should be recognized, namely first when anchors are used as ordinary attachments of a component, second when used as an additional specific technical solution set up to improve the dynamic response of an object. Hence the first issue is about demonstrating the efficaciousness of usual fastening systems, and the latter is about designing a system able to avoid the free rocking or swaying of components, i.e. to ensure a rigid behaviour of the components. To answer to both demands a study on the seismic behaviour of the different existing anchor types was necessary. The in-depth experimental campaign consisting of shaking table tests presented within sections §2, §3 and §4 of this document can be considered as a starting point from which several considerations and applicative case studies should be generated.

5.1. OUTCOMES FROM THE EXPERIMENTAL CAMPAIGN

The report presents the results of the shaking table tests on the considered anchors, as summarized in chapter 1. The analyses were mainly focused to obtain the capacity curves for each anchor typology in terms of load-slip behaviour. The trend of each specimen was analysed and compared with the other ones of the same typology. These analyses allowed the failure load and both ultimate and maximum slip values to be identified. The damages and failure mechanisms were also identified for each anchor.

Further analyses can be developed to deepen the knowledge of the dynamic and mechanical performance of the tested anchors. The hysteretic behaviour could be investigated relating the slip and load values in each instant, thus allowing to study the dissipation capacity of the fasteners.

The investigation could be also completed comparing the obtained results in terms of both failure modes and load-slip curves with the static and quasi-static qualification (according to EOTA procedures) of each anchor in order to compare the different loading conditions. Among all a reliable reducing factor to compute the dynamic strength of each anchor starting from the static mechanical characterization can be evaluated.

The development of expressly designed FE models would allow to widely increase the knowledge of the mechanical behaviour of fasteners. The obtained results would permit to define a modification of product with the aim to improve the overall performances, especially in terms of maximum slip and failure load.

A deeper analysis of data collected from real applications tested under this experimental campaign would permit to obtain an in-depth study that could be used for the design of the connection on real cases.

All the obtained results and the additional analyses should lead to draft technical documents, guidelines and support tools for each tested anchor. These will allow an in-depth knowledge of the seismic behaviour of the product and thus to support professionals on the design of applications in seismic regions. These tools will allow to provide fundamental information and data in the fields not covered by the normative, such as the use of plastic anchors or the application in masonry supports.

5.1.1. Anchors Behaviour

The report presents the results of the shaking table tests on the considered anchors, as summarized in chapter 1. The analyses were mainly focused to obtain the capacity curves for each anchor typology in terms of load-slip behaviour. The trend of each specimen was analysed and compared with the other ones of the same typology. These analyses allowed the failure load and both ultimate and maximum slip values to be identified. The damages and failure mechanisms were also identified for each anchor.

Since metal anchors in concrete did not achieve failure their behaviour can be evaluated mainly through the obtained load-slip graphs. Since this application is included in the European assessment procedure a first comparison can be made and it is presented in §5.1.2.

Metal expansion anchor installed in concrete (MEC) did not show failure in any among the specimens in both non-cracked and cracked support. Nevertheless a different behaviour can be recognized between cracked and non-cracked concrete from the trend of the normalized force vs slip plot shown in Figure 5.1. Specimens in crack concrete (light grey) show larger displacements for the same loading rate.

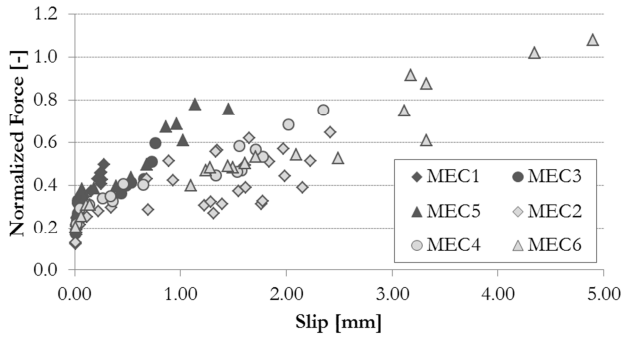

Figure 5.1 Summarizing normalized force vs. slip graph for MEC specimens

Similarly to the previous anchor type the undercut anchor installed in concrete (UC) did not show failure in any among the specimens in both non-cracked and cracked support. Moreover from the trend of the normalized force vs slip plot shown in Figure 5.2 also comparable behaviours were registered for specimens installed in non-cracked or cracked concrete. In fact a substantial difference in the slip of cracked support specimens (light grey) is not observed up to a normalize force equal to 1.0.

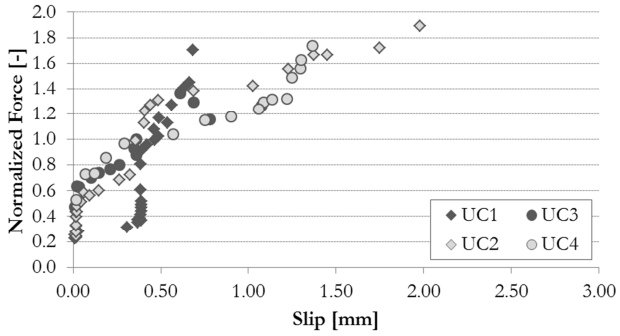

Figure 5.2 Summarizing normalized force vs. slip graph for UC specimens

Chemical anchor in concrete (AC) showed failure for the specimens installed in concrete. In Figure 5.3 the behaviour of the specimens installed in cracked and non-cracked concrete is reported. However in the cracked condition (light grey) a difference in the trend of the plot of normalized force vs load cannot be identified before the failure occurrence. It indicates a more brittle failure mode compared to that arising from the specimens of mechanical expansion anchor.

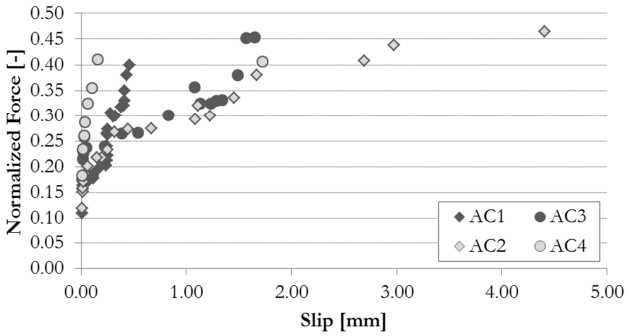

Figure 5.3 Summarizing normalized force vs. slip graph for AC specimens

For the type named plastic expansion anchor (PE) the behaviour evidence in both the two tested base materials is available. For concrete testing (PEC) the load-displacement trend is shown by Figure 5.4 describing both installations in non-cracked and cracked support. Although the occurrence of failure at a previous ZPA nominal level the specimens installed in cracked concrete developed higher forces than the non-cracked concrete (dark grey) due to the varied stiffness of the connection. Also larger displacements for cracked concrete specimens (light grey) were measured during the testing.

For specimens installed in hollow brick masonry (PEM) the load-displacement behaviour is also presented in Figure 5.4. The trend is almost linear and consistent for the various specimens.

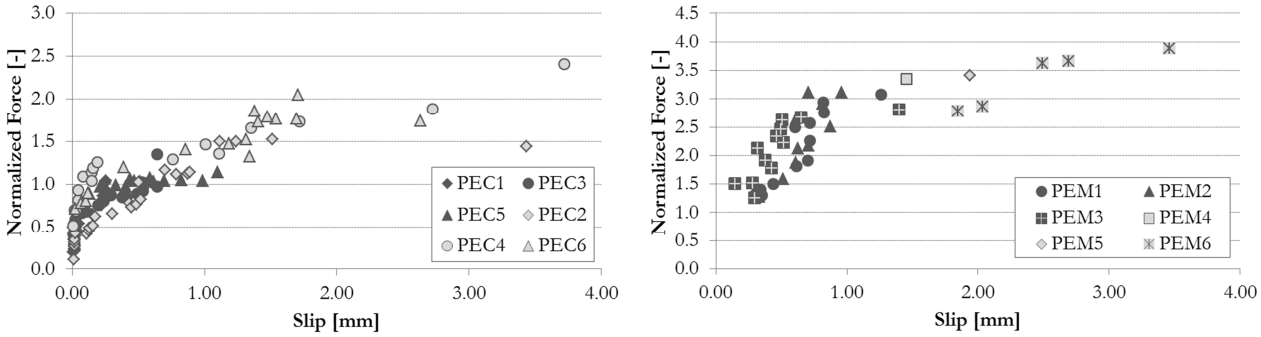

Figure 5.4 Summarizing normalized force vs. slip graph for PEC (left) and PEM (right) specimens

Some additional remarks can be made in observing the resistance values of static and dynamic conditions, whether with tension or shear actions, for PEC specimens installed in non-cracked and cracked concrete, as shown in Table 5.1 and Figure 5.5, Figure 5.6.

When considering the dynamic reduction factor, the several seismic loading steps (described in §3.1.2 of this document) the specimen underwent, should be taken into account. This difference in the testing method does not allow to make directly comparable the terms.

Table 5.1 Indicative resistance values for static and dynamic action, whether tension or shear, in non-cracked and cracked concrete, for PEC specimens

Resistance	N_{max}	V_{max}	N_{max}	V_{max}
	kN	kN	-	-
DYNncc	2.29	4.07	0.24	0.45
DYNcc	2.85	4.12	0.29	0.46
STATncc	9.70	9.00	1.00	1.00
STATcc	5.50	9.00	0.57	1.00

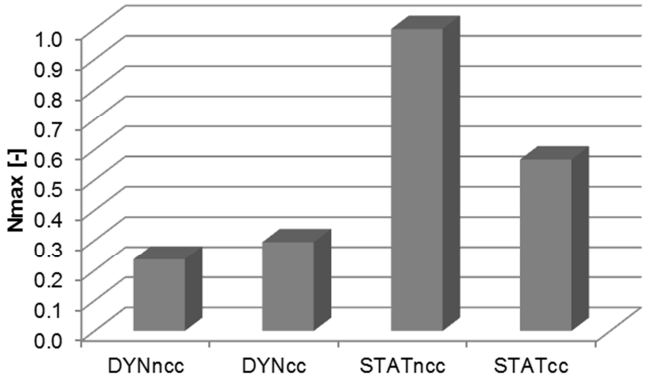

Figure 5.5 Comparison of static and dynamic tensile resistance, in non-cracked and cracked concrete for PEC specimens

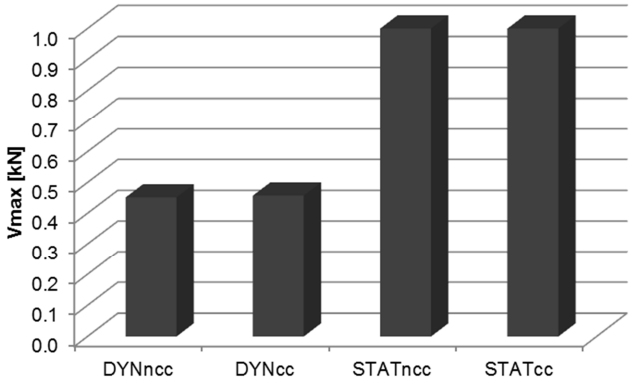

Figure 5.6 Comparison of static and dynamic shear resistance, in non-cracked and cracked concrete for PEC specimens

Also for the plastic-fibre expansion anchor (PFE) the behaviour evidence in both the two tested base materials is available. For concrete testing (PFEC) the load-displacement trend is shown by Figure 5.7 describing both installations in non-cracked and cracked support. Although the observation of a larger ultimate slip in the case of cracked concrete (light grey), the displacements up to a normalized force of 1.3 are comparable.

For specimens installed in hollow brick masonry (PFEM) the load-displacement behaviour is also presented in Figure 5.7. The trend is almost linear and consistent for the various specimens.

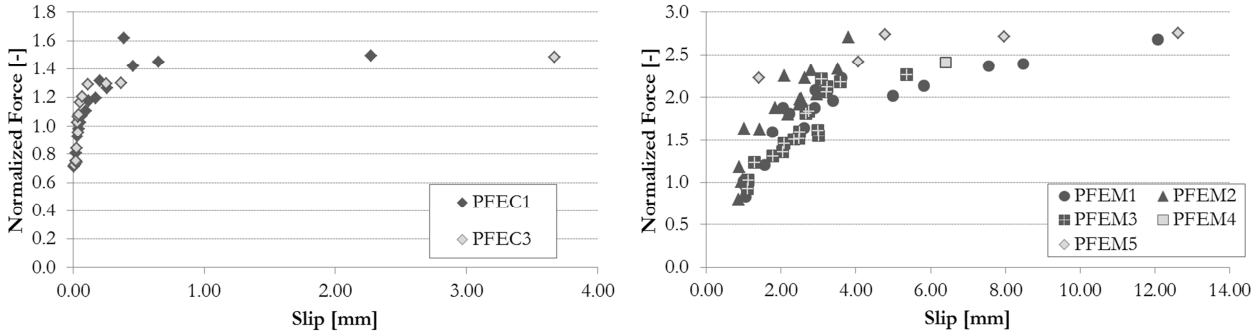

Figure 5.7 Summarizing normalized force vs. slip graph for PFEC (left) and PFEM (right) specimens

Chemical anchor installed in hollow brick masonry (AM) showed larger displacements in TS5 (light grey) rather than TS4 (dark grey), because of the different methodology in the loading procedure. Anyway it is to noted that in such a brittle material the measured displacements were limited, i.e. 2 to 4mm, at severe dynamic loading compared to the design resistance (Figure 5.8). As a consequence it was immediately identified the brick resistance as the factor which drove the fastening system failure.

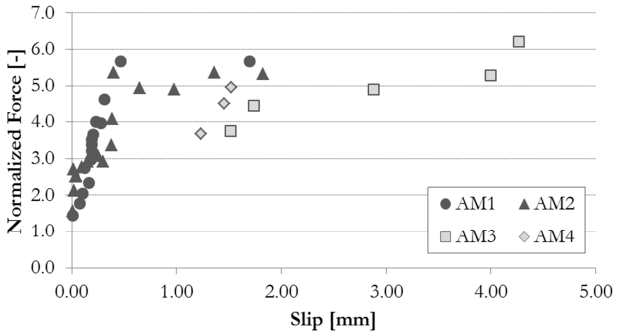

Figure 5.8 Summarizing normalized force vs. slip graph for AM specimens

5.1.2. Comparison to Standardized Assessment Procedure

For mechanical expansion anchor also a comparison with the existing European seismic assessment procedure (ETAG 001 Annex E) is possible. Since the testing procedure included in the qualification standard is articulate in different tests, the main aspect to observe is the admissible displacement showed by the specimens during the testing. Nevertheless a direct comparison cannot be made because of the different loading methodology. Shake-table testing indeed induces simultaneously on the anchor both tension and shear forces, whereas the assessment procedure establishes to test whether only tension or only shear cycle histories (see §1.1.3 of this document).

The limit slip value proposed by the standard is 7mm which has to be measured after 50 load cycles for test C2.3 and at the end of cycling at $\Delta w = 0.5$mm in test C2.5. In the following some sample test results for C2.3 (Table 5.3) and C2.5 (Table 5.4) are presented.

In Table 5.2 the results of the MEC specimens installed in cracked concrete of shake-table testing are reported. It can be noted that up to the achieved loading rate the maximum displacements stay below such limit.

Table 5.2 Shake-table test outcomes for MEC specimens installed in cracked concrete

	N_{max}	V_{max}	$Fnorm_{max}$	δ_F	δ_{max}
Specimen ref.	kN	kN	-	Mm	mm
MEC2	7.177	8.702	0.647	2.418	2.418
MEC4	7.989	10.946	0.753	2.347	2.347
MEC6	13.965	10.182	1.081	4.901	4.901

Table 5.3 Results of the assessment procedure for five samples of the same anchor type of MEC according to C2.3 test (ETAG 001 Annex E)

	N_{max}	$\delta_{(0.5N/Nmax)}$	$\delta_{(N/Nmax)}$
Specimen ref.	kN	mm	mm
1	25.2	1.17	4.93
2	25.2	0.75	4.33
3	25.2	3.51	23.9
4	15.1	1.88	11.39
5	15.1	0.07	1.95

Table 5.4 Results of the assessment procedure for five samples of the same anchor type of MEC according to C2.5 test (ETAG 001 Annex E)

	N_{w1}	N_{w2}	$N_{Ru,i}$	δ_{50}	δ_{90}
Specimen ref.	kN	kN	kN	mm	mm
1	8.3	10.3	18.4	9.83	27.56
2	8.3	10.3	20.7	7.08	27.63
3	7.5	9.3	15.1	12.30	34.00
4	6.0	7.5	36.2	2.46	18.64
5	6.0	7.5	21.3	2.48	24.38

5.2. SEISMIC RISK REDUCTION FOR MUSEUMS CONTENTS

Earthquakes cause serious effects to cultural heritage and therefore can jeopardize the cultural identity of a County. Regions where both an high seismic hazard and an intense historical and cultural asset are concentrated, such as Mediterranean area, South America and Middle East, started to study new methods of preventing or at least monitoring and reducing these effects.

In the following some of the fundamental principles for a seismic risk mitigation involving art objects are presented concisely, according to what included in the relevant state-of-art (see §1.2.1.2).

- A primary action is to lower the centre of gravity of art objects by modifying the geometrical configuration or the weight distribution of the display system. An example of this practice is the use of additional sand to fill in the display cases base.
- The anchoring of art objects to support and connection systems which can attach rigidly the display system to the building structure. Such a solution, which is usually a good practice, fully transfer the seismic action to anchored object, which may undergo to excessive stress.
- Furthermore, the seismic isolation devices can be recognized as one of the best solution since this system allows the displacement of components and of the building to be decoupled. On the other end this solution is quite expensive and technically sophisticated, hence it is unlikely to be applied pervasively.

According to what already said for non-structural elements in general (§5), the use of anchoring systems in the field of art objects or single monuments can be substantially subdivided into two functions. A first use can be recognized as ordinary and regards the connection of elements which necessarily, for displaying technology, have to be attached to the structure or to other non-structural elements, e.g. infill walls. An example of this application is represented by paintings or stone plates displaying systems which are directly attached to walls (Figure 5.9). Whereas the second case deals with the realization of additional restraints for the displayed object so that to reduce the risk of damages with the earthquake occurrence.

In the first case attention should be paid to the use of adequate fastening systems according to the base material of the supporting element. Anchors or anchor groups should be designed according to the relevant standards and guidelines, namely the documents presented in §1.1.3. In such provisions, which are divided by anchor type and base material, the assessment procedures, the design methods and the setting instructions are included. In particular the guideline ETAG 001, dealing with metal anchors installed in concrete, is the only one to provide a seismic assessment procedure. Moreover the technical report TR 045 provides additional specific requirements for the design of metal anchors in concrete under seismic actions. The remaining applicative uses of fastenings are not covered by any design or assessment document, since ETAG 020 and ETAG 029, dealing respectively with plastic anchors in various base materials and chemical anchors in masonry, are valid only in a static loading field.

The second case collects all those actions which can be considered good practices to reduce diffusely the risk of damages due to overturning, excessive sliding and impact the displayed art objects. The anchoring of museum display cases to the floor is one of the solutions to adopt in order to avoid the overturning of the entire system. Also local solutions to contrast inertial forces generated by the objects belong to that case. Further risk mitigation actions can be represented by additional fastening elements (Figure 5.10) than the ordinary support which can prevent the free rocking of the object. In this latter instance the eventuality of excessive tensional stress of the art object has to be verified.

Figure 5.9 Examples of ordinary use of anchoring systems in the attachment of art objects to structural elements

Figure 5.10 Examples of seismic risk mitigation for art object by means of anchoring systems

Figure 5.9 and Figure 5.10 refer to an on-site survey campaign which University of Padua carried out within the national project ARCUS driven by MIBAC[6]. For the above mentioned project a vulnerability analysis of the displaying types was realized starting from collecting data. A survey sheet was prepared previously on the basis of the state-of-art included in §1.2.1.2. In addition to that also the presence of fastening was evaluated for the art object as for the displaying support. In order to evaluate the vulnerability of the whole system indeed it is of importance to know whether to consider the art object fixed to its support and to the building.

The survey sheet (see Annex D) made to evaluate the displayed art objects was thought in order to offer a method of seismic vulnerability assessment pervasively but in-depth. Indeed with the compiling of the sheet two different levels of evaluation are possible.

The first level is the one related to a classification of the object and its support and provides a fast judgement on the seismic risk of the museum assets, i.e. summary information on the expectable dynamic responses and damage mechanisms for the objects. As a consequence of such procedure some punctual mitigation actions can be planned and a global view on the priorities can be achieved.

The second level, provides a more detailed analysis and takes into account simultaneously the structural response of the building and the location of the object within

[6] Italian Ministry of Cultural Heritage and Activities

it. Such evaluation method can be applied for specific cases when in-depth studies are required.

In Figure 5.11 the total number of the evaluated objects is reported distinguishing the objects displayed in the public areas from those stored into depositories or offices.

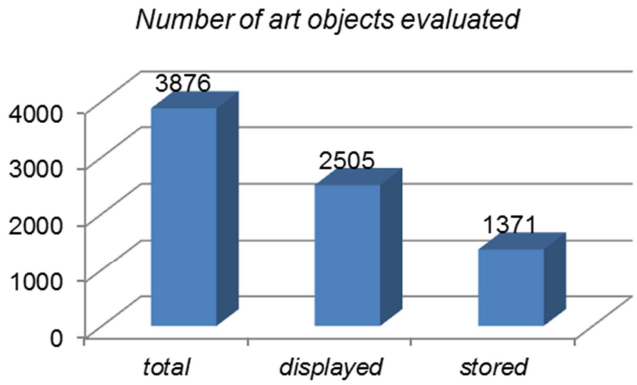

Figure 5.11 Number of art objects evaluated in ARCUS project

In order to group the art objects according to recognized damage mechanisms and dynamic responses, the first classification to made is according to the object type (Table 5.5). Such categorization (Figure 5.12) considers the shape of the object and its dimensions. Figure 5.13 shows the type distribution along the various storeys of the considered museum buildings.

Table 5.5 Classification of art objects typologies according to (Augusti and Ciampoli 1996, Liberatore 2000)

Category	*Object description*	*Reference*	*Examples*
T1	Small flat-bottomed objects	VASE	Small vases, ceramic ware, glasses
T2	Small not flat-bottomed objects	BUST	Busts, jewels, grave goods
T3	Large objects	STAT	Statues and sculptures, large vases, stone plates, columns and capitals, wood furniture
T4	Paintings and panels in general	QUAD	Paintings on canvas or wood
T5	Objects attached to the ceiling	LAMP	Chandeliers and suspended objects
T6	Others	MISC	All what is not included in T1-T5

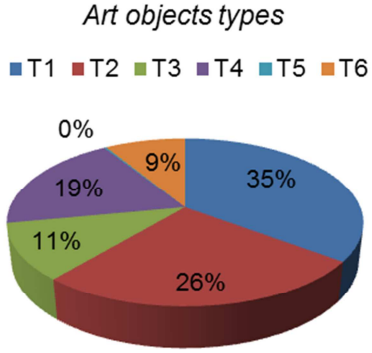

Figure 5.12 Art objects divided by type

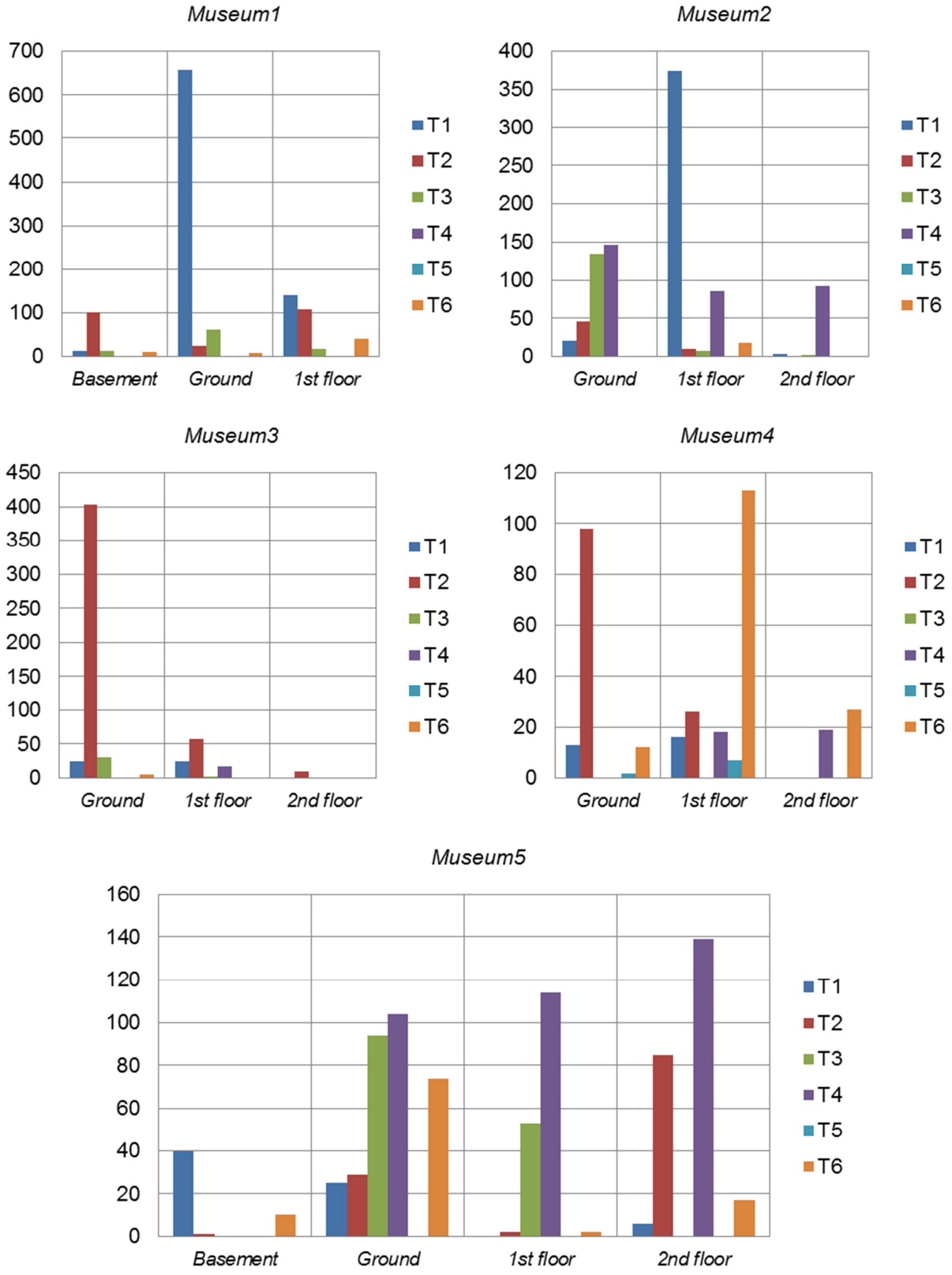

Figure 5.13 Art objects types divided by storey in the evaluated museum buildings

A further classification of the objects was made by the support type, i.e. the geometrical features of the system, according to Table 5.6. These data (Figure 5.14) help in the identification of the dynamic response of the art object and the related displaying system.

For identifying the seismic response the presence of anchorage between art object and support and then between support and building was reported. In that way four constraint

degree cases were recognized, namely no fastening, fastening only between object and support, only between support and building, fastening between object and building. In the case of pictures or generic objects attached to walls or ceiling, a judgement of complete fastening was assigned when efficacious restraint hooks able to avoid the rocking were found.

In Figure 5.14 the data collected on the evaluated specimen are shown. A large quantity of the specimen (42%) are not fastened at all in both the interfaces. Those art objects can freely slide and rock during an earthquake.

Table 5.6 Classification of art objects support systems according to (Augusti and Ciampoli 1996, Liberatore 2000)

Group	*Category*	*Description*	*Possible related types*
Objects supported on a flat plane	A1	On the floor	T1, T2, T3,T6
	A2	On a pedestal	T1, T2, T3,T6
	A3	In display cases	T1, T2, T6
	A4	On cantilever or in wall cases	T1, T2, T6
Objects fixed on a flat plane or a pedestal	B	Objects fixed on a flat plane or a pedestal	T1, T2, T3,T6
Suspended/ hanging objects	C1	Suspended on a wall	T4, T6
	C2	Hanging from the ceiling	T5, T6

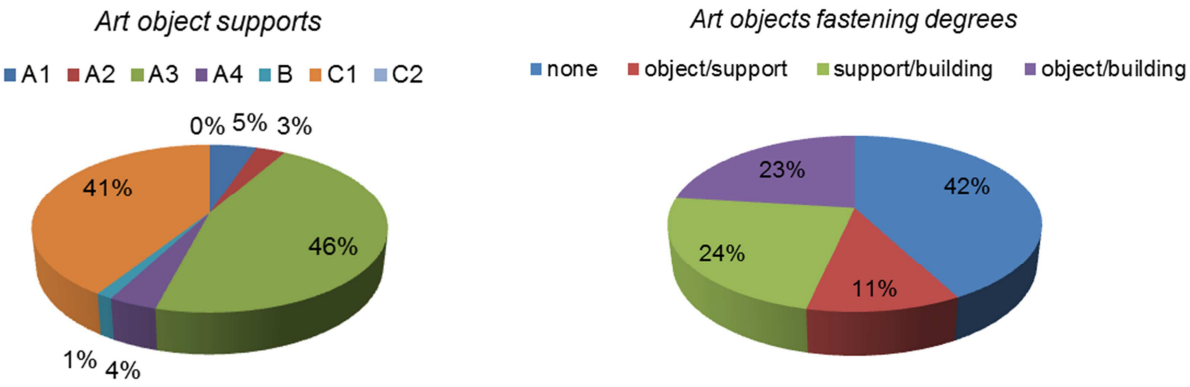

Figure 5.14 Art objects subdivided by displaying support (left). Fastening degrees between art objects, supports and building (right)

5.2.1. Art Objects

After having collected and analysed the data on art objects presented in the previous paragraphs some further studies can be realized. For instance applicative case studies regarding the fastening of art objects are shown in the following. Also in such application studies, the distinction between ordinary fastening and additional fastening, already illustrated in §5.2, is maintained.

In particular Figure 5.15 Ordinary fastening of art objects by means of plastic expansion anchor (left) and chemical anchor (right)Figure 5.15 shows some examples of common fastening of art objects observed during Arcus survey campaign.

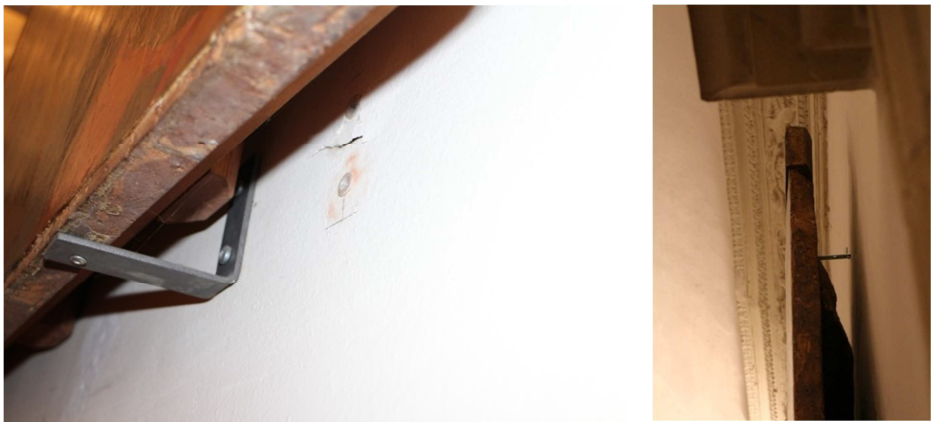

Figure 5.15 Ordinary fastening of art objects by means of plastic expansion anchor (left) and chemical anchor (right)

5.2.2. Museum Display Cases

After having collected and analysed the data on art objects presented in the previous paragraphs some further studies can be realized. Applicative case studies regarding the fastening of display cases, or museum displaying systems in general, are shown in the following. Some examples of art object displaying system which are commonly fastened to the building is reported in Figure 5.16.

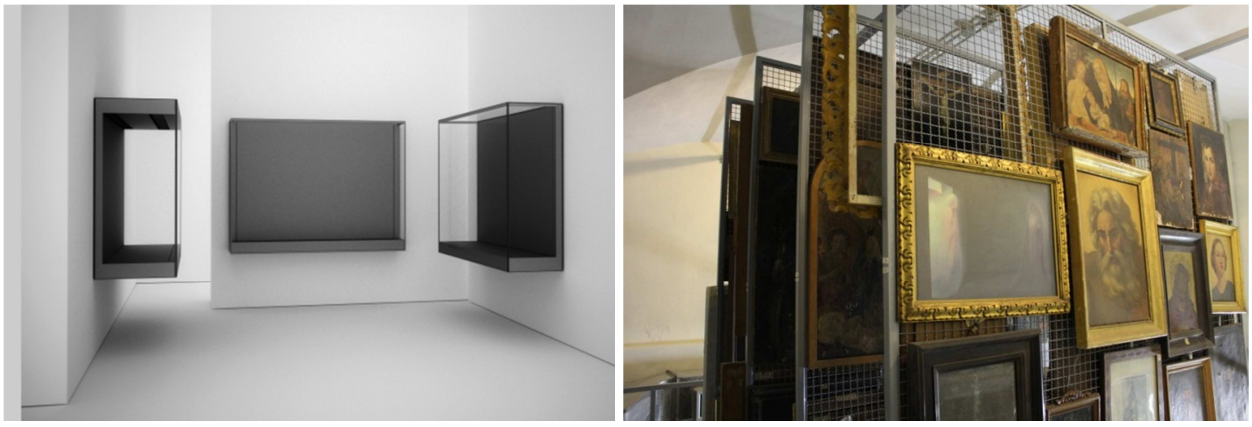

Figure 5.16 Examples of art object displaying system which are typically fastened to the building

5.3. SEISMIC PROTECTION OF STRATEGIC BUILDING EQUIPMENT

As stated in various sections within this document (§1.2, §5, and §6.3) an important issue to cover in the field of earthquake engineering is to seek solutions able to minimize the seismic damage of non-structural components, especially when they are installed in critical facilities and they serve as fundamental building utility system. One of the most urgent target is to give an answer to the demand of continuity in the functionality of these particular components also when cities are stricken by earthquake phenomena and immediately after that.

A methodology to meet this target is represented by studying the response to seismic events of specific fundamental components, that is undergoing components to

assessment procedures and designing such systems according to the latest available provisions worldwide.

In this paragraph the study activities related to the seismic design of the anchorage in fire suppression systems are summarized.

5.3.1. Protection of Fire Suppression Systems

For the design of the connection components of fire suppression systems, which are usually realized by means of post-installed concrete anchors, various guidelines should be considered. In fact the anchorage requirements included in standards concerning both post-installed anchors (TR 045 2013) and fire suppression systems (NFPA 13 2013, FM 2-8 2010) should be taken into account.

The design of metal anchors used in concrete and in high risk seismic regions has to be referred to TR 045 (2013). The document provides an immediate distinction of the design according to the application, whether structural (connection type A) or non-structural (connection type B), and four importance levels related to the building where the design is located in. The two output categories are consistent to assessment procedure classes presented in ETAG001 Annex E, namely C1 and C2 respectively for lower and higher required performances. Therefore considering the table taken from the mentioned relevant TR (Table 5.7), for non-structural components operating in critical facility of a region with seismicity level larger than low ($a_g \cdot S > 0.10\ g$) the required anchor category is C2, the most severe.

Table 5.7 Recommended seismic performance categories for anchors (TR 045 2013)

Seismicity level[a]		**Importance Class acc. to EN 1998-1:2004, 4.2.5**			
Class	$a_g \cdot S$ [c]	I	II	III	IV
Very low[b]	$a_g \cdot S \le 0{,}05\ g$	No additional requirement			
Low[b]	$0{,}05\ g < a_g \cdot S \le 0{,}10\ g$	C1	C1 [d] or C2 [e]		C2
> low	$a_g \cdot S > 0{,}10\ g$	C1	C2		

[a] The values defining the seismicity levels are may be found in the National Annex of EN 1988-1.
[b] Definition according to EN 1998-1:2004, 3.2.1.
[c] a_g = design ground acceleration on Type A ground (EN 1998-1:2004, 3.2.1), S = soil factor (see e.g. EN 1998-1:2004, 3.2.2).
[d] C1 for Type 'B' connections (see 5.1)
[e] C2 for Type 'A' connections (see 5.1)

Thus the anchors to use in such design should be assessed for cracked concrete (ETAG 001 option 1) and use under seismic actions (ETAG001 Annex E) with C2 assessment category. The design approaches can be three and are reported in the following (TR 045 2013).

a) Without considering the anchor ductility.
a1) Capacity design: yielding in the fixture (baseplate) or in the attached element
a2) Elastic design: an elastic behaviour for both the structure and the anchorage is assumed to occur; for connections B (of non-structural elements) the seismic actions can be calculated according to the simplified method shown in §5.5.4. of TR 045.

b) Considering the anchor ductility.
The anchor bolt is assumed as energy dissipator in the tensile cyclic loading. The steel resistance should be designed to be less than the base material allowing an elongation of the anchor of 8d.

The calculation of the seismic action for non-structural elements is usually realized through a2) approach, thus §5.5.4. of TR 045 is observed. This section refers to the provisions already existing in Eurocode 8, §4.3.5. and described in section §1.1.3 of this thesis. Some significant points in the action calculations should be noted. The importance factor of Eq. 1.10 reported in §1.2.2 should be larger than 1.5 for anchorage elements of machinery and equipment required for life safety systems, which fire suppression is included in.

For the horizontal action the seismic amplification factor and the q structural factor are given by Table 5.8 if not calculated through the relations proposed. Hence in this case the q factor is equal to 2.0 and the seismic amplification factor is equal to 3.0 and the final equivalent horizontal force relation is reported here below (Eq. 5.1). Similarly the calculation of vertical action, since it is required for the specific component configuration (according to Figure 5.17), has the form shown in Eq. 5.3 and Eq. 5.4. As a consequence Eq. 5.2 reports the final equivalent vertical force in the case of fire suppression systems.

$$F_a = 4.13\ \alpha S \cdot W_a \qquad \text{Eq. 5.1}$$

$$F_{Va} = 2.25\ \alpha_V \cdot W_a \qquad \text{Eq. 5.2}$$

Table 5.8 Values of q_a structural factor and A_a seismic amplification factor (TR 045 2013)

Type of non-structural element	q_a	A_a
Cantilevering parapets or ornamentations	1,0	3,0
Signs and billboards		3,0
Chimneys, masts and tanks on legs acting as unbraced cantilevers along more than one half of their total height		3,0
Hazardous material storage, hazardous fluid piping		3,0
Exterior and interior walls	2,0	1,5
Partitions and facades		1,5
Chimneys, masts and tanks on legs acting as unbraced cantilevers along less than one half of their total height, or braced or guyed to the structure at or above their centre of mass		1,5
Elevators		1,5
Computer access floors, electrical and communication equipment		3,0
Conveyors		3,0
Anchorage elements for permanent cabinets and book stacks supported by the floor		1,5
Anchorage elements for false (suspended) ceilings and light fixtures		1,5
High pressure piping, fire suppression piping		3,0
Fluid piping for non-hazardous materials		3,0
Computer, communication and storage racks		3,0

$$F_{Va} = \frac{S_{Va}\ W_a \gamma_a}{q_a} \qquad \text{Eq. 5.3}$$

$$S_{Va} = \alpha_V \cdot A_a \qquad \text{Eq. 5.4}$$

Where:

W_a weight of the element,
S_{Va} seismic coefficient which includes acceleration,
γ_a importance factor of the element (1 or 1.5),
q_a behaviour factor of the element (1 or 2).
A_a seismic amplification factor of the element.

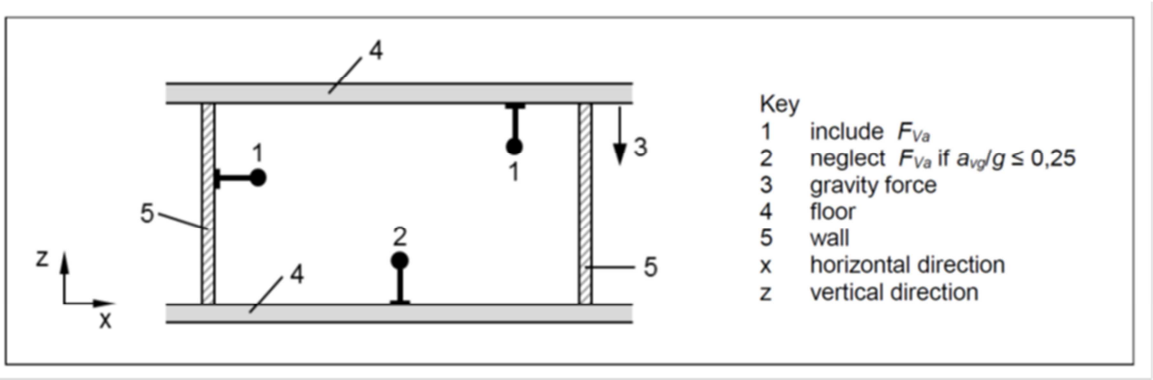

Figure 5.17 Vertical effects of the seismic actions (TR 045 2013)

The United States standard NFPA 13 (2013) provides detailed recommendations for the seismic restraints and supports of fire suppression sprinkler systems. In addition to those also some provisions concerning the sustaining anchorage in multiple base material, namely concrete, timber and steel, are included.

In particular for post-installed anchors in concrete the following main notes are required.

- The fastening installation should be realized above the longitudinal axis height of the beams or on the ceiling.
- A minimum size of anchor bolt in relation to the pipes diameter.
- The anchorage in elements for which is expected a differential motion to occur, should not be realized.
- A seismic qualification according to ACI355.2 (2007) is required.
- The installation of anchors should attain what recommended by the manufacturer.
- Also for gravity load hangers, and not only for seismic bracings, qualified anchors should be used.
- Some admissible load tables for anchors, collecting data from several manufacturers, are presented for a simplified sizing (concrete of various strengths are considered).

Another International standard issued by Factory Mutual insurance company, namely FM 2-8 (2010), proposes seismic bracing as a convenient and efficacious way to design an earthquake resistant fire suppression system. The recommendations included in such document referring to post-installed anchors in concrete are summarized in the following so that also a comparison between the two proposed standards can be possible.

- The use of direct fastening should be avoided.
- If the concrete strength is unknown, the minimum strength level should be considered (17.2 MPa).
- Expansion anchors seismically qualified according to the local assessment standards in force.
- Edge distance should be equal to 12d and the minimum embedment depth should be equal to 6d.
- The capacity of structural element where the installation is realized should be verified.
- The anchor capacity should be established according to ACI318 Appendix D or equivalent local standard.

- Three configurations for the pipe seismic bracing are possible (from 30° to 90°).
- Whether an interaction between various non-structural components is possible also the other component should be braced, e.g. the suspended ceiling system when close to the piping.
- All the mechanical equipment which can affect the functioning of a sprinkler system during an earthquake should be braced, e.g. HVAC, water heaters.
- The water tanks and the fire pump should be protected from seismic actions.
- Chemical anchorage should not be used for gravitational fastenings on the ceiling.

Subsequently to the explanation of the relevant standards, a practical example of the calculation of the seismic forces acting on an anchorage point for a bracing configuration with θ = 45° is presented below. In particular the following relations (Eq. 5.5, Eq. 5.6) consider the axial load and shear load applied on the anchorage, as also shown in Figure 5.18.

$$N_a = \frac{F_a}{\tan 45°} = F_a \qquad \text{Eq. 5.5}$$

$$V_a = F_a \qquad \text{Eq. 5.6}$$

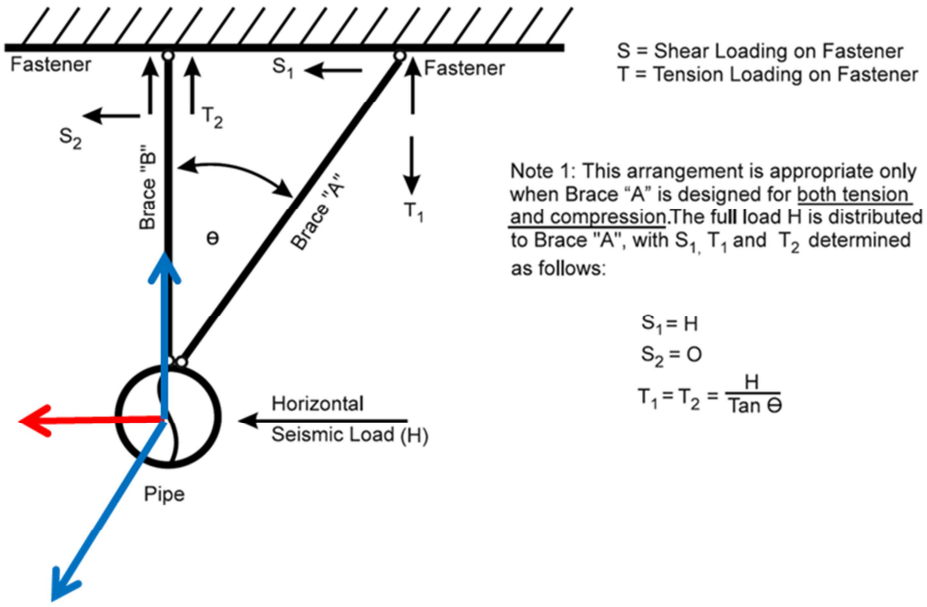

Figure 5.18 One common seismic bracing configuration (θ = 45°) for fire suppression piping (FM 2-8 2010)

6. CONCLUSIONS

In this final chapter some conclusive remarks and general observations originating from the experimental work and the subsequent analyses and case-studies are presented.

The purpose of the research work is deepening the knowledge on the seismic response of different types of post-installed anchors in various base materials, namely non-cracked and cracked concrete and hollow masonry bricks. An experimental campaign on shaking table was carried out in order to defining the primary aspects that drive the anchorage behaviour when subjected to severe dynamic loading. Therefore a summary of the experimental study is reported in the following paragraph. In addition to the testing outcomes, also some considerations on the set up decisions of such a specific laboratory procedure can be identified. In §6.3 the conclusions of the case-studies non the fastening of non-structural elements are presented.

Since the largest part of the research period has been dedicated to the experimental sessions and a fine presentation of the achieved data and results, many future developments are on the way of this topic. Further scientific studies can be made to extend the experimental outcomes to more applicative cases.

Last paragraph (§6.4.2) recalls the context of the research which was firstly presented in the section of this document named *Foreword: Project Explanation* and aims at providing new developments in the industrial project which included this first complete study.

6.1. SEISMIC EVALUATION OF ANCHORS BY SHAKE-TABLE TESTING

An in-depth knowledge on the seismic behaviour of post-installed anchors used in various base materials was achieved by means of several shaking table test sessions. The experimental investigation demonstrated some important aspects in the seismic behaviour evaluation of post-installed anchors.

For metal expansion anchors in concrete important information on the trend of the slipping, in relation to the dynamic loading, is presented. Moreover a concise comparison with results obtained through the seismic assessment according to the relevant European standard was achieved (§5.1.2).

Almost the same was accomplished for metal undercut anchors. Plotting the load-slip curves allowed the seismic behaviour of this traditional post-installed anchor to be studied. The shown slips were little and failure was never reached by the specimens under testing.

For chemical anchors in concrete it was important to define and quantify the difference between the seismic behaviour of non-cracked concrete installations and cracked concrete installations.

The analyses of data for plastic anchors permitted a whole overview on the ability of this type of anchor to withstand seismic loading. As almost all the specimens reached failure indeed, a comparison with the static resistance values was possible. In such a way it could be proposed a seismic reduction factor to use when designing this particular anchoring systems.

The same procedure presented above was followed for non-cracked and cracked concrete installations, but also for hollow brick masonry installations. All what reported concerning plastic expansion anchors should be considered significant since this anchor type is not currently included in any standard provisions.

Finally also chemical anchor installed in hollow brick masonry are out of focus of any standard provisions and thus a particular attention should be given to the results presented deeply in §4.4.1.5. This specific anchoring system was observed to allow high loads bearing. The system resistance depended on the base material properties, thus the choice of the embedment depth should me made carefully in order to induce reinforcement effect into the support element.

6.2. TESTING PROCEDURE

From the experimental campaign realized for deepening the knowledge on the seismic response of post-installed anchoring systems, also some indications on the testing procedure for non-structural elements can be figured out.

In chapter §2 the primary setup features for a shaking table test focalized in evaluating the behaviour of attached non-structural elements are reported. In particular a description of the structural units design, the attached components design and the data capturing systems is included into part §2.2. Besides various considerations on the choice of acceleration time histories to induce to the table are presented in 2.3.

The testing procedure of such a complex investigating campaign can be useful for further researches with a similar focus.

6.3. APPLICATIVE STUDIES ON NON-STRUCTURAL ELEMENTS

A complete state-of-art on the subject of art objects seismic response and in general on the seismic behaviour of non-structural components was collected. Various cases were deepened in the art objects field as for non-structural elements of high importance included in strategic buildings.

An in-depth on-site survey realized within the MIBAC Ministry project named *Arcus* allowed to analyse a large sample of data related to the identification of the seismic vulnerability of art objects and museum displaying systems. Various notes were taken in the attempt of understanding and prioritizing the troubles which affect such components when interested by seismic events. Some applicative cases of intervention with anchoring systems operating in both ordinary components fastening and additional restraint fastening are presented in §0.

Also some practical activities concerning the application of anchorage to the seismic protection of high importance equipment, such as fire suppression systems, are described in §5.3.1 of this document.

All the proposed applicative cases share a common generic scope, improve the level of resilience that a society can show when affected by a natural disaster. So far communities stricken by earthquakes always suffered serious tangible effects, in terms of both life

safety issues and inestimable economic losses. In the way of making the built environment a safer place that can function continuously, a huge step forward can be accomplished by addressing the issue of non-structural elements included in strategic buildings. In a good design management the professionals should take into account the current available provisions and recommendations. The scientific community by its side, and with a multidisciplinary approach, is increasing the efforts in studying this challenging subject.

6.4. FUTURE DEVELOPMENTS

The work included in this research project can represent a starting point for some topics of anchorage theory and practice. Indeed it mainly consists in a basic study which aims at describing several generic aspects of anchors behaviour under seismic conditions. The work allowed to cover different applicative fields, which are commonly present in constructions and may be not considered by standards or guidelines.

As a consequence of that various works can be undertook in order to continue the research topic here presented.

6.4.1. Scientific Developments

A substantial part of the work was dedicated to achieve the extended research on the behaviour of post-installed anchors under seismic actions. Applicative cases were studied after the experimental achievements. Therefore more attention in the future can be given to the development of specific applicative cases of interest.

Further analyses can be developed to deepen the knowledge of the dynamic and mechanical performance of the tested anchors. The hysteretic behaviour could be investigated relating the slip and load values in each instant, thus allowing to study the dissipation capacity of the fasteners.

The investigation could be also completed deepening the comparison of the obtained results in terms of both failure modes and load-slip curves with the static and quasi-static qualification (according to EOTA procedures) of each anchor in order to compare the different loading conditions. Among all a reliable reducing factor to compute the dynamic strength of each anchor starting from the static mechanical characterization can be evaluated.

The development of expressly designed FE models would allow to widely increase the knowledge of the mechanical behaviour of fasteners. The obtained results would permit to define a modification of product with the aim to improve the overall performances, especially in terms of maximum slip and failure load.

A deeper analysis of data collected from real applications tested under this experimental campaign would permit to obtain an in-depth study that could be used for the design of the connection on real cases.

All the obtained results and the additional analyses should lead to draft technical documents, guidelines and support tools for each tested anchor. These will allow an in-depth knowledge of the seismic behaviour of the product and thus to support professionals on the design of applications in seismic regions. These tools will allow to provide fundamental information and data in the fields not covered by the normative, such as the use of plastic anchors or the application in masonry supports.

6.4.2. Industrial Developments

The research started as a part of a wider industrial project which aims at achieving an in-depth knowledge on the critical applications of technical solutions used widely in the civil constructions as well as at identifying and facing through innovation the technical challenges brought by natural disasters such as earthquakes. The most critical issues for such connection systems were evidenced by a preliminary research included in chapter §1 of this document.

For the future it will be possible to investigate further on specific anchoring systems and related configuration of interest, on the basis of what already discovered. These further studies can lead to an assessment of innovative technical solutions which can be developed in the meanwhile according to what observed during this experimental testing and the outcomes noted after the test data analyses.

REFERENCES

(Agbabian et al. 1988) Agbabian MS, Masri SF, Nigbor RL, and Ginell WS. "Seismic Damage Mitigation Concepts for Art Objects in Museums". *Proceedings of Ninth World Conference (Vol. VII)*, August 2-9, Tokyo-Kyoto, Japan, 1988.

(Algin 2007) Algin HM. "Investigation of Masonry Wall Fixings Subject to Pullout Load and Torque". *Construction and Building Materials*, No 21, pp.2041–2046, Elsevier, 2007.

(AON Benfield 2010) AON Benfield. "Update on Chile's Earthquake and Its Potential Impact to the Insurance Industry". May 12, Chicago, Illinois, 2010.

(Augusti and Ciampoli 1996) Augusti G and Ciampoli M. "Guidelines for Seismic Protection of Museum Contents". *Proceedings of Eleventh World Conference (Paper No. 1668)*, June 23-28, Acapulco, Mexico, 1996.

(Badillo-Almaraz 2003) Badillo-Almaraz H. "Seismic Fragility Testing Of Suspended Ceiling Siystems". *Seismic design and analysis of nonstructural building components*, 67-72, University of Buffalo, 2003.

(Berto et al. 2011) Berto L, Favaretto T, Saetta A. "Seismic Vulnerability Of Art Objects The Statues Of The Galleria Dei Prigioni - Galleria Dell'accademia Of Firenze". *Proceedings of XIV Convegno Nazionale di Ingegneria Sismica, ANIDIS*. September 18-22, Bari, Italy, 2011.

(Chauduri and Hutchinson 2004) Chaudhuri SR, Hutchinson TC. "Distribution Of Peak Horizontal Floor Acceleration For Estimating Non-Structural Element Vulnerability". *Proceedings of the 13th World Conference on Earthquake Engineering*, paper n. 1721, Vancouver, B.C., Canada, August 1-6, 2004.

(Collins et al. 1989) Collins DM. "Load-Deflection Behaviour Of Cast-In-Place And Retrofit Concrete Anchors Subjected To Static, Fatigue, And Impact Tensile Loads". *MSc Thesis, The University of Texas at Austin*, May, Texas, 1988.

(Comerio 2005) Comerio MC. “PEER Testbed Study On A Laboratory Building Exercising Seismic Performance Assessment”. Pacific Earthquake Engineering Research Center, Berkeley, California, 2005.

(Di Sarno et al. 2014) Di Sarno L, Petrone C, Magliulo G, Maddaloni G, Prota A. “Shake Table Tests To Evaluate The Seismic Demand, Capacity And Dynamic Properties Of Hospital Contents”, *2ECEES - 15th European Conference on Earthquake Engineering*, August 24-29, Istanbul, Turkey, 2014.

(Eligehausen et al. 2006) Eligehausen R, Malleé R, Silva J. “Anchorage in Concrete Construction”. Wilhelm Ernst & Sohn GmbH & Co.KG, Berlin, 2006.

(Retamales et al. 2011) Retamales R, Mosqueda G, Filiatrault A, and Reinhorn AM. “Testing Protocol For Experimental Seismic Qualification Of Distributed Nonstructural Systems”. *Earthquake Spectra*, 27(3):835-856, 2011.

(Fuchs et al. 1995) Fuchs W, Eligehausen R, Breen JE. “Concrete Capacity Design (CCD) Approach For Fastening To Concrete”. *ACI Structural Journal*, 73-94, 1995.

(Ghobarah and Aziz 2004) Ghobarah A, and Aziz TS. “Seismic Qualification Of Expansion Anchors To Canadian Nuclear Standards”. *Nuclear Engineering and Design* 228, 377–392, Elsevier 2004.

(Hoehler 2006) Hoehler M. “Behavior and Testing of Fastenings to Concrete for Use in Seismic Applications”. *Ph.D. Thesis, IWB, Universität Stuttgart*, Germany, 2006.

(Hoehler et al. 2009) Hoehler M, Panagiotou M, Restrepo JI, Silva JF, Floriani L, Bourgund U, and Gassner H. “Performance Of Suspended Pipes And Their Anchorages During Shake Table Testing Of A Seven-Story Building”. *Earthquake spectra* (Earthquake Engineering Research Institute) 25, n. 1 (2009): 71-91, 2009.

(Hoehler et al. 2011) Hoehler M, Mahrenholtz P, Eligehausen R. “Behavior of Anchors in Concrete at Seismic-Relevant Loading Rates”. *Structural Journal*, 108(2), pp.238-247, 2011.

(Housner 1963) Housner GW. “The Behavior Of Inverted Pendulum Structures During Earthquakes”. *Bulletin of Seismological Society of America*, Vol.53 No.2, pp.403-417, February, 1963.

(Ishiyama 1983) Ishiyama Y. “Motions Of Rigid Bodies And Criteria For Overturning By Earthquake Excitations”. Presented at *Third South Pacific Regional Conference on Earthquake Engineering*, May 1983, Wellington, Bulletin of the New Zealand Society for Earthquake Engineering, Vol.17, No.1, March 1984.

(ITW Construction 2013) ITW Construction Products Italy srl. “Product General Catalogue”. Padova, Italy, 2013

(Klingner and Mendonca 1982) Klingner RE, and Mendonca JA. “Shear Capacity of Short Anchor Bolts and Welded Studs: A Literature Review”. ACI Journal, Vol.79, No.5, Sept.-Oct., 1982.

(Liberatore 2000) Gruppo Nazionale per la Difesa dai Terremoti (edited by Liberatore D). “Vulnerabilità dei Beni Archeologici e degli Oggetti Esibiti nei Musei”. Esagrafica, Roma, Italy, 2000.

(Lowry et al. 2007) Lowry . “Protecting Collections in the J. Paul Getty Museum from Earthquake Damage”. *WAAC Newsletter*, Vol.29, No.3, September 2007.

(Makris and Black 2001) Makris N, and Black CJ. “Rocking Response of Equipment Anchored to a Base Foundation, Final Report”. *PEER, Department of Civil and Environmental Engineering, University of California*, Berkeley, California, 2001.

(Mahrenholtz et al. 2012) Mahrenholtz P, Hutchinson TC, Eligehausen R, and Hofmann J. “Shake Table Tests: Seismic Performance of Anchors Connecting Suspended Nonstructural Components to Concrete”. *Proceedings of XV World Conference on Earthquake Engineering, WCEE.* September 24-28, Lisboa, Portugal, 2012.

(Mazzon et al. 2013a) Mazzon N, Abate M, da Porto F, Modena C. “Design of Seismic Tests on Post-installed Anchors for Concrete and Masonry Applications”. *Proceedings of XV Convegno Nazionale di Ingegneria Sismica, ANIDIS*. June 30- July 4, Padova, Italy, 2013.

(Mazzon et al. 2013b) Mazzon N, Tecchio G, Abate M, Santoro DA, Gualano D, Modena C. “Design and Verification of a Dynamic Experimental Campaign on Anchoring Systems through Macro and Micro Numerical Models”. *Proceedings of International Conference on Computational Methods in Structural Dynamics and Earthquake Engineering, COMPDYN 2013*. 12th – 14th June, Kos, Greece, 2013.

(Meyer and Pregartner 2001) Meyer A, and Pregartner T. “Fastening in Masonry”. *International Symposium on Connections between Steel and Concrete,* R. Eligehausen. Stuttgart, Germany, 2001.

(Miranda et al. 2003) Miranda E, and Taghavi S. “Estimation of Seismic Demands on Acceleration-Sensitive Nonstructural Components in Critical Facilities”. *Proceedings of the Seminar on Seismic Design, Performance, and Retrofit of Nonstructural Components in Critical Facilities*, ATC 29-2, 347-360, Newport Beach, California, 2003.

(Miranda et al. 2012) Miranda E, Mosqueda G, Retamales R, Pekcan G. “Performance of Nonstructural Components during the 27 February 2010 Chile Earthquake”, *Earthquake Spectra*, June 2012, 28(S1), pp. S453-

S471, 2012.

(Naumoski et al. 2002) Naumoski N, Foo S, Saatcioglu M. “Seismic Hazard Assessment and Mitigation for Buildings’ Functional and Operational Components”, *Office of Critical Infrastructure Protection and Emergency Preparedness*, University of Ottawa, Canada, 2002.

(Neurohr 2007) Neurohr T. “The Seismic Vulnerability Of Art Objects”, MSc Thesis, *Department of Civil Engineering and Applied Mechanics, McGill University Montréal*, Québec, Canada, January, 2007.

(Neuhrohr and McClure 2008) Neurohr T, and McClure G. “Shake Table Testing Of Museum Display Cases”. *Department of Civil Engineering and Applied Mechanics, McGill University Montréal*, Québec, Canada, 2008.

(NISEE 1976) NISEE Software Library. “SIMQKE User Manual”. University of California, Berkeley, California, 1976.

(Nuti 2008) Nuti C, and Santini S. “Fastening Technique In Seismic Areas: A Critical Review”. *Tailor Made Concrete Structures – Walraven & Stoelhorst (eds)*, Taylor & Francis Group, London, 2008.

(Pregartner and Eligehausen 2007) Pregartner T, and Eligehausen R. “Load Bearing Behaviour Of Plastic Anchors In Cracked Concrete”. Beton- und Stahlbetonbau, n. 102 (2007): 22-30, 2007.

(Rieder 2009) Rieder A. “Seismic Response of Post-installed Anchors in Concrete”, *Ph.D. Thesis, Institut für Konstruktiven Ingenieurbau*, Wien, Austria, 2009.

(Scheidel 2011) Scheidel JT. “Shear Behavior Of Anchors For Squat Attached Building Components Under Severe Earthquake Loading”. MSc. Thesis, *San Diego State University*, San Diego, California, 2011.

(Sinica et al. 2010) Sinica M, Sezemanas G, Mikulskis D, and Kligys M. “Determination of Fixing Loads for Plastic Anchors Subject to Structure and Voidage of Masonry Units”. *Modern Building Materials, Structures and Techniques*, The 10th International Conference, Vilnius, Lithuania, 2010.

(Solomos and Berra 2006) Solomos G and Berra M. “Testing of Anchorages in Concrete under Dynamic Tensile Loading,” Materials and Structures, 39(7), pp. 695-706, 2006.

(Spyrakos et al. 2008) Spyrakos CC, Maniatakis ChA, and Taflampas IM. “Assessment of Seismic Risk for Museum Artifacts”. *Proceedings of XIV World Conference on Earthquake Engineering, WCEE,* October 12-17, Beijing, China, 2008.

(Taghavi and Miranda 2002) Taghavi S and Miranda E. “Seismic Performance and Loss Assessment of Nonstructural Building Components”. *Proceedings of 7th National Conference on Earthquake Engineering*, Boston, Massachussetts, 2002.

(Taghavi and Miranda 2003) Taghavi S and Miranda E. “Response Assessment of Nonstructural Building Elements”. *Research Report PEER* 2003/05, 96p, University of California, Berkeley, California, 2003.

(Usami et al. 1980) Usami S, Abe U, and Matsuzaki Y. “Experimental Study On The Strength Of Headed Anchor Bolts Under Alternate Shear Load And Combined Load (Shear And Axial).” *Proceedings of the Annual Meeting of the Kantou Branch of the Architectural Institute of Japan*, 1980.

(Vanmarcke et al. 1997) Vanmarcke EH, Zavoni EH, Fenton EA. "SIMQKE II Conditioned Earthquake Ground Motion Simulator: User's Manual, Version 2", Princeton University Press, 1997.

(Villaverde 1996) Villaverde R. “Earthquake Resistant Design Of Secondary Structures: A Report On The State Of The Art”, *Proceedings of the 11th World Conference on Earthquake Engineering*, paper n. 643, Elsevier Science Ltd., Oxford, England, 1996.

(Watkins 2011) Watkins DA. “Seismic Behavior and Modeling of Anchored Nonstructural Components Considering the Influence of Cyclic Cracks”. Ph.D. Thesis, University of California, San Diego, California, 2011.

(Zienkievicz and Taylor 1989) Zienkiewicz OC, and Taylor RC. “The Finite Element Method”, Vol. I, 4th Edition. McGraw Hill, 1989.

CODES AND STANDARDS

(AC 156 2010) AC156. Acceptance Criteria For Seismic Certification By Shake-Table Testing Of Nonstructural Components, Whittier, California, ICC-ES, 2010.

(AC 60) AC60. Acceptance Criteria For Anchors In Unreinforced Masonry Elements. Whittier, California, ICC-ES, 2005.

(AC 193) AC193. Acceptance Criteria For Mechanical Anchors In Concrete Elements. Whittier, California. ICC-ES, 2005.

(ACI 318 2005) American Concrete Institute. ACI 318 Appendix D - Anchoring to Concrete. In ACI 318 Building Code and Commentary, 379-405, Farmington Hills, Michigan, ACI 2005.

(ACI 355.2 2007) American Concrete Institute. ACI 355.2-07. Qualification Of Post-Installed Mechanical Anchors In Concrete. Farmington Hills, Michigan, ACI, 2007.

(ACI 355.4 2010) American Concrete Institute. ACI 355.4-10. Acceptance Criteria for Qualification of Post-Installed Adhesive Anchors in Concrete. Farmington Hills, Michigan, ACI, 2010.

(ASCE 7-10 2010) American Society of Civil Engineers. ASCE 7-10 Minimum Design Loads for Building and other Structures. Reston, Virginia, Virginia, ASCE, 2010.

(ASTM E488 2003) ASTM E488. Standard Test Methods for Strength of Anchors in Concrete and Masonry Elements. ASTM International, West Conshohocken, Pennsylvania, 2003.

(ATC 69 2008) ATC 69. Reducing the Risks of Nonstructural Earthquake Damage: State-of-the-Art and Practice Report. Applied Technology Council, California, 2008.

(CSA N287.2 1998) CSA N287.2. Material Requirements for Concrete Containment Structures for CANDU Nuclear Power Plants. Canadian Standards Association, Rexdale, Ontario, 1998.

(ETAG 001 2013) ETAG 001. Metal Anchors for Use in Concrete. European Organization for Technical Approvals, Brussels, 2013.

(ETAG 020 2012) ETAG 020. Plastic anchors for multiple use in concrete and masonry for non-structural applications. European Organization for Technical Approvals, Brussels, 2012.

(ETAG 029 2013) ETAG 029. Metal injection anchors for use in masonry", European Organization for Technical Approvals, Brussels, 2013.

(EN 1992-4) EN 1992-4. Eurocode 2 - part4: Design of Fastenings for Use in Concrete. European Comittee of Standardization CEN, Brussels, in preparation.

(Eurocode 2) EN 1992-1. Eurocode 2 - part1: Design of Concrete Structures. European Comittee of Standardization CEN, Brussels, 2004.

(Eurocode 8) EN 1998-1. Eurocode 8 - part1: General Rules Seismic Actions And Rules For Buildings. European Comittee of Standardization CEN, Brussels, 2003.

(FEMA E-74 2011) FEMA E-74. Reducing The Risks Of Nonstructural Earthquake Damage - A Practical Guide. Applied Technology Council. Washington, D.C., FEMA, 2011.

(FM 2-8 2010) FM 2-8. Earthquake Protection For Water-Based Fire Protection Systems. Factory Mutual Global. Property Loss Prevention Data Sheets, 2010.

(NFPA 13 2013) NFPA 13. Standard for the Installation of Sprinkler Systems. National Fire Protection Association, Quincy, Massachusetts, 2013.

(NTC 2008) D. M. 14/01/2008. NTC 2008 - Norme Tecniche Per Le Costruzioni. Ministerial Decree, Italy, 2008.

(Protezione civile 2009) Protezione Civile. Linee Guida Per La Riduzione Della Vulnerabilità Di Elementi Non Strutturali, Arredi E Impianti. Presidenza del Consiglio dei Ministri Dipartimento della Protezione Civile, June, Italy, 2009.

(TR 045 2013) Technical Report 045 - ETAG 001. Design of Metal Anchors For Use In Concrete Under Seismic Actions. European Organization for Technical Approvals, Brussels, 2013

ANNEX A. STRUCTURAL UNITS DESIGN DRAWINGS

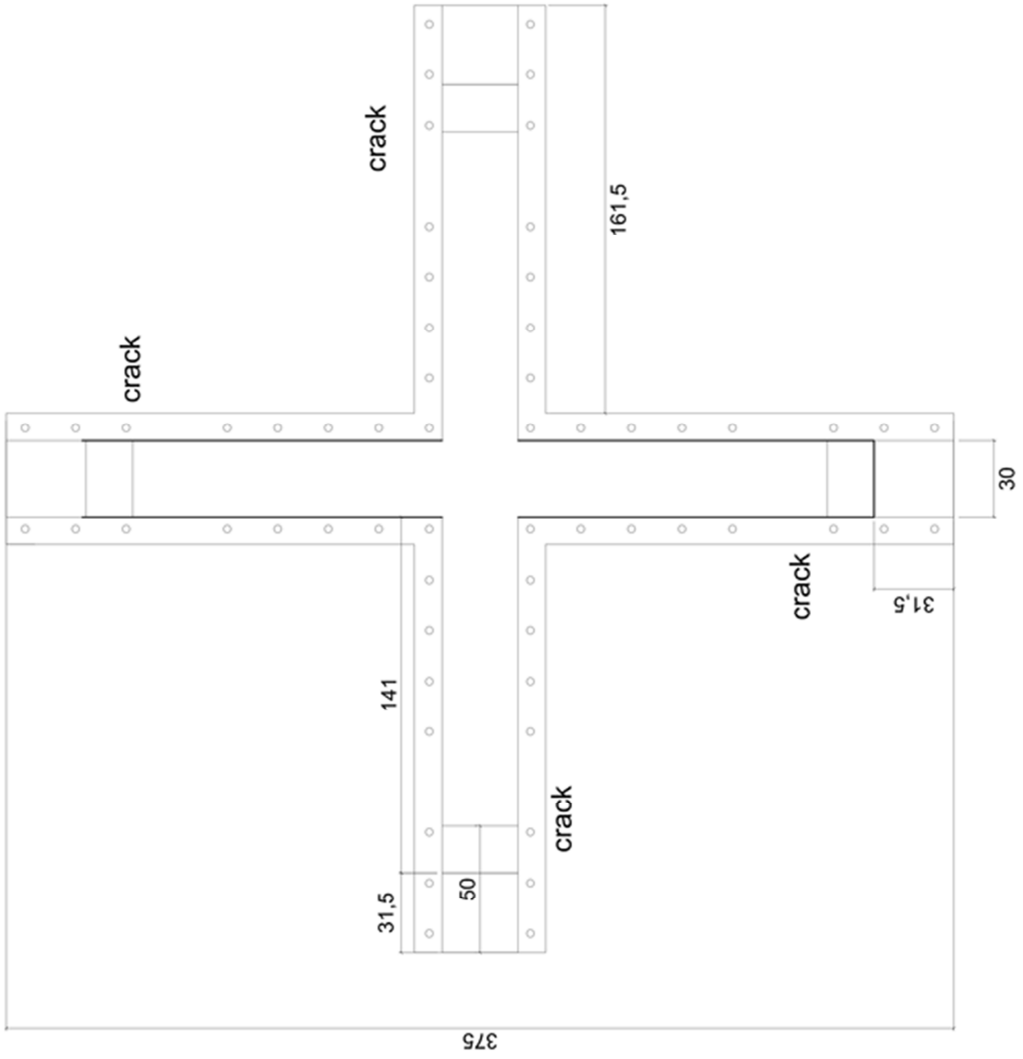

Plan view of the Concrete structure

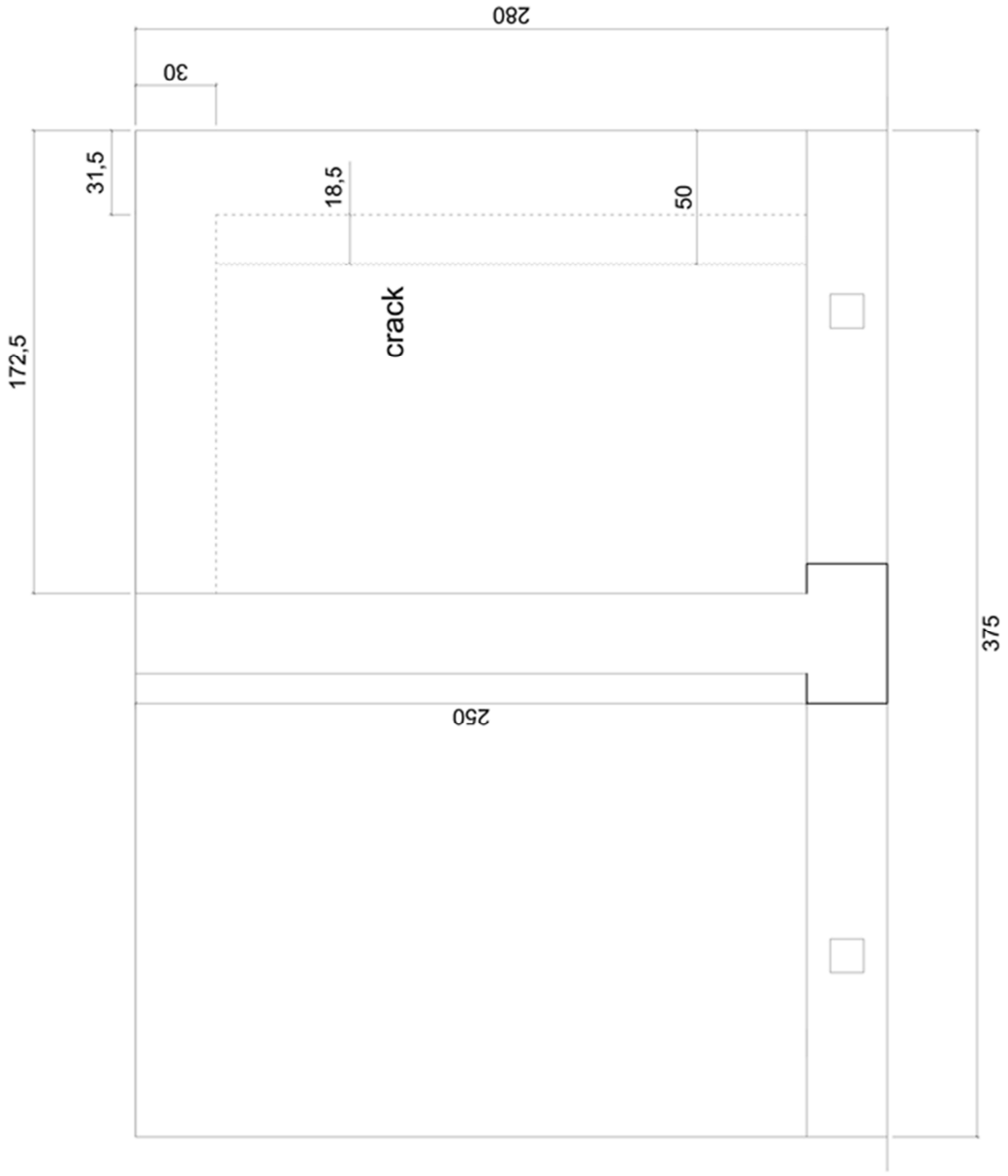

Lateral view of the Concrete structure

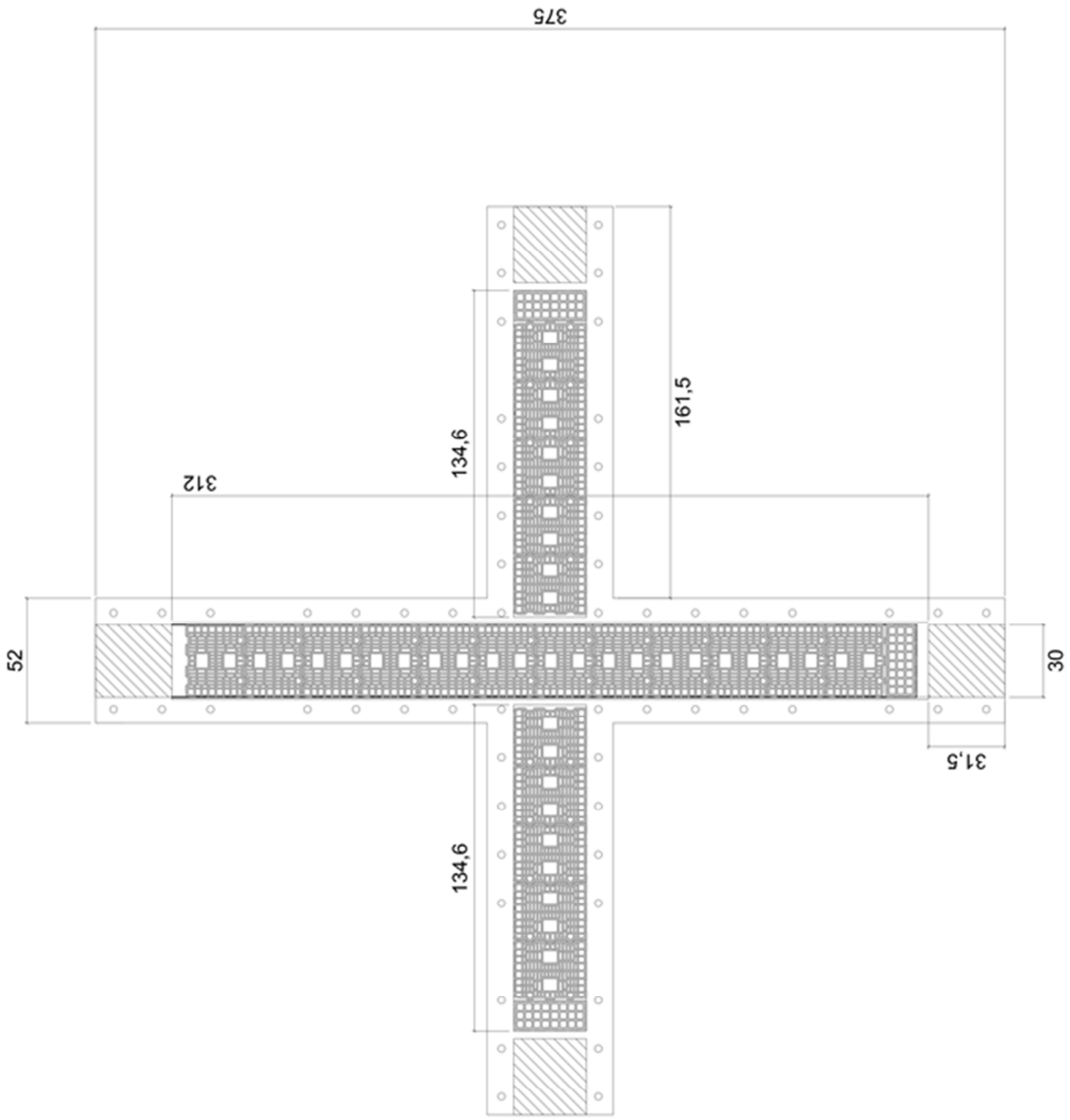

Plan view of the Masonry structure

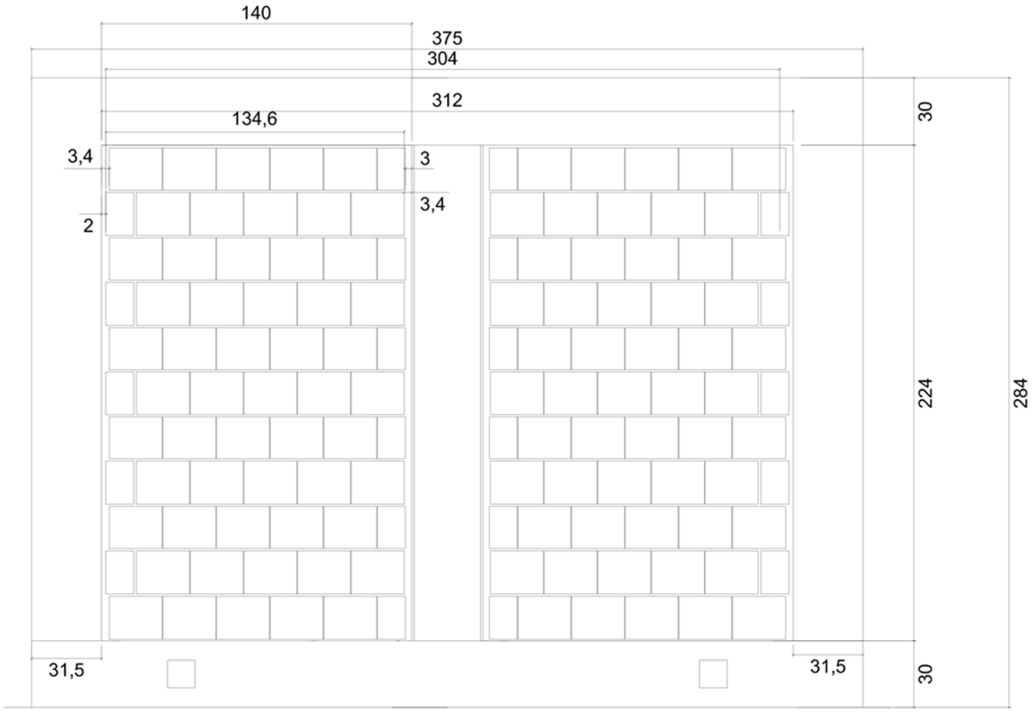

Lateral view 1 of the Masonry structure

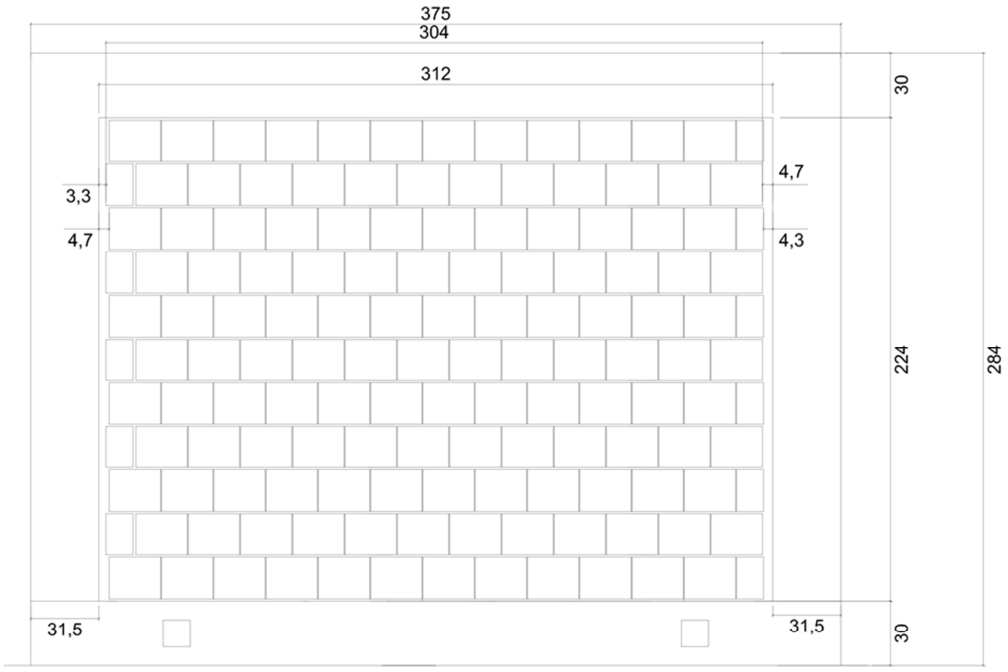

Lateral view 2 of the Masonry structure

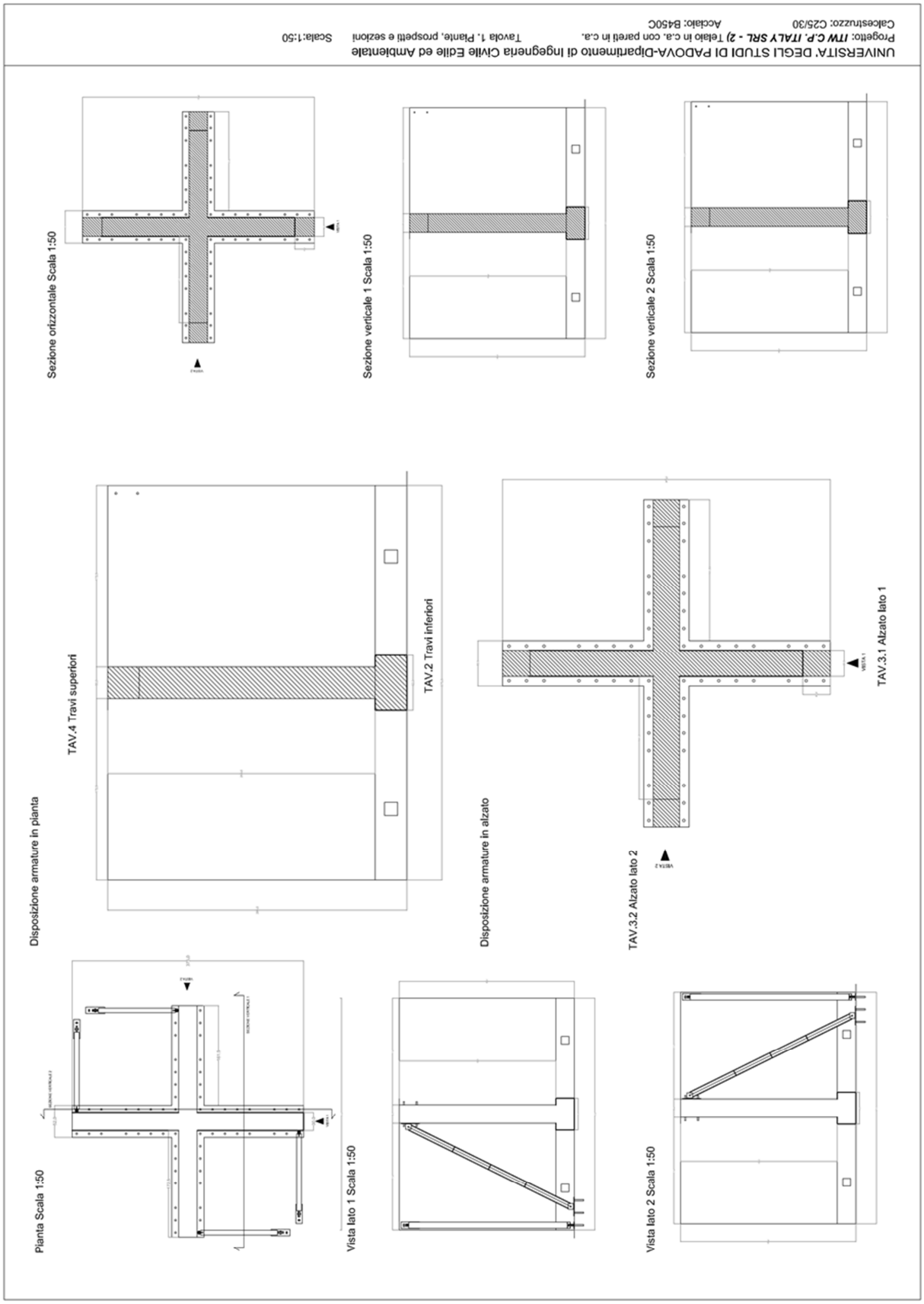
UNIVERSITA' DEGLI STUDI DI PADOVA-Dipartimento di Ingegneria Civile Edile ed Ambientale
Progetto: ITW C.P. ITALY SRL - 2) Telaio in c.a. con pareti in c.a.
Acciaio: B450C
Calcestruzzo: C25/30
Tavola 1. Piante, prospetti e sezioni
Scala:1:50
Sezione orizzontale Scala 1:50
Sezione verticale 1 Scala 1:50
Sezione verticale 2 Scala 1:50
TAV.4 Travi superiori
TAV.2 Travi inferiori
Disposizione armature in planta
Disposizione armature in alzato
TAV.3.1 Alzato lato 1
TAV.3.2 Alzato lato 2
Pianta Scala 1:50
Vista lato 1 Scala 1:50
Vista lato 2 Scala 1:50

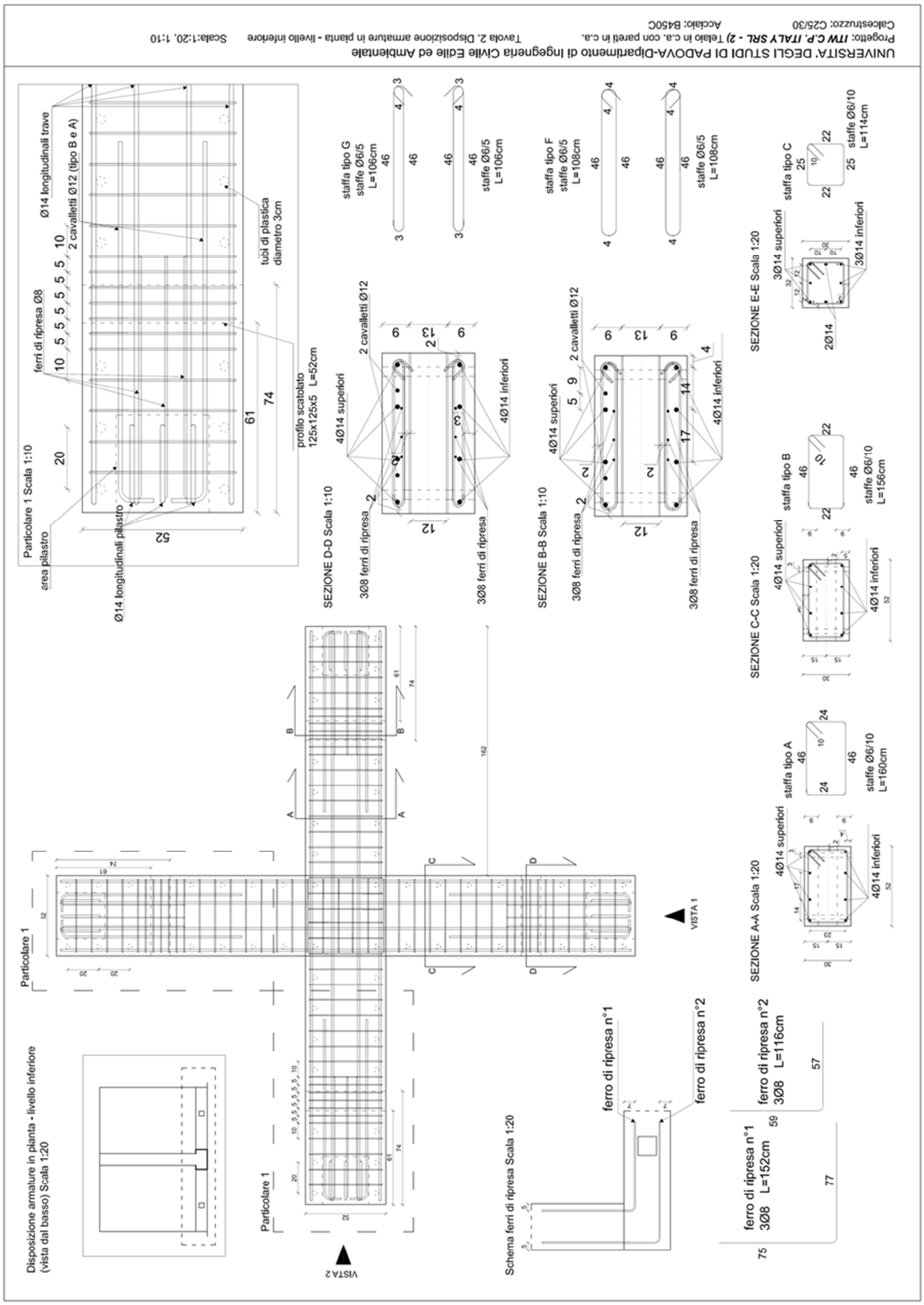
UNIVERSITA' DEGLI STUDI DI PADOVA-Dipartimento di Ingegneria Civile Edile ed Ambientale
Progetto: ITW C.P. ITALY SRL - 2) Telaio in c.a. con pareti in c.a.
Tavola 2. Disposizione armature in pianta - livello inferiore
Scala:1:20, 1:10
Calcestruzzo: C25/30 Acciaio: B450C
Particolare 1 Scala 1:10
area pilastro
ferri di ripresa Ø8
Ø14 longitudinali trave
2 cavalletti Ø12 (tipo B e A)
tubi di plastica diametro 3cm
Ø14 longitudinali pilastro
profilo scatolato 125x125x5 L=52cm
SEZIONE D-D Scala 1:10
SEZIONE B-B Scala 1:10
SEZIONE E-E Scala 1:20
SEZIONE C-C Scala 1:20
SEZIONE A-A Scala 1:20
staffa tipo G staffe Ø6/5 L=106cm
staffa tipo F staffe Ø6/5 L=108cm
staffa tipo A
staffa tipo B
staffa tipo C
staffe Ø6/10 L=160cm
staffe Ø6/10 L=156cm
staffe Ø6/10 L=114cm
4Ø14 superiori
4Ø14 inferiori
3Ø14 inferiori
2Ø14
3Ø8 ferri di ripresa
Disposizione armature in pianta - livello inferiore (vista dal basso) Scala 1:20
Particolare 1
VISTA 1
VISTA 2
Schema ferri di ripresa Scala 1:20
ferro di ripresa n°1 3Ø8 L=152cm
ferro di ripresa n°2 3Ø8 L=116cm
ferro di ripresa n°1
ferro di ripresa n°2

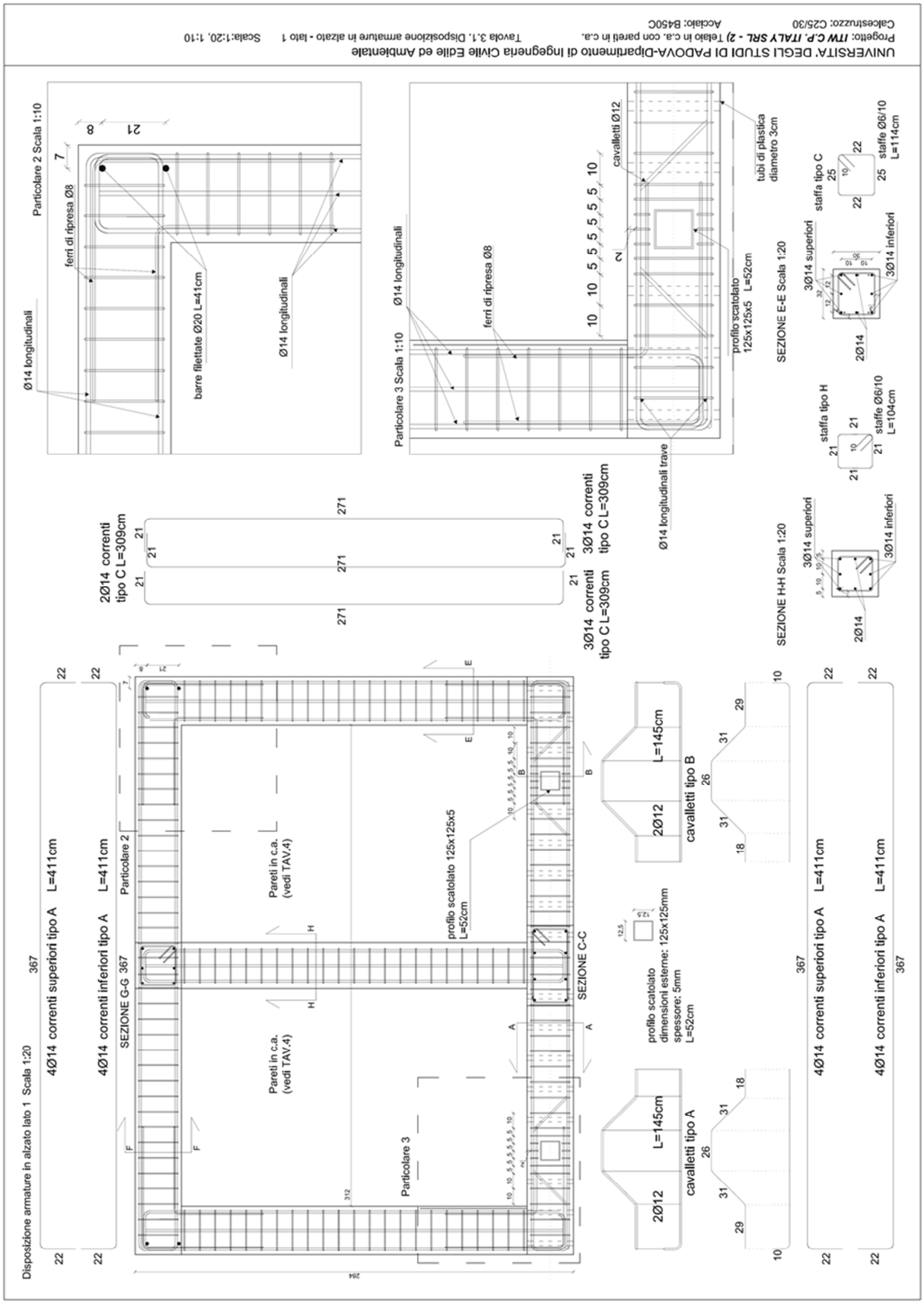
UNIVERSITA' DEGLI STUDI DI PADOVA-Dipartimento di Ingegneria Civile Edile ed Ambientale
Progetto: ITW C.P. ITALY SRL - 2) Telaio in c.a. con pareti in c.a.
Tavola 3.1. Disposizione armature in alzato - lato 1
Scala:1:20, 1:10
Calcestruzzo: C25/30
Acciaio: B450C
Disposizione armature in alzato lato 1 Scala 1:20
4Ø14 correnti superiori tipo A L=411cm
4Ø14 correnti inferiori tipo A L=411cm
SEZIONE G-G
Particolare 2
Particolare 3
Pareti in c.a. (vedi TAV.4)
profilo scatolato 125x125x5 L=52cm
SEZIONE C-C
profilo scatolato dimensioni esterne: 125x125mm spessore: 5mm L=52cm
cavalletti tipo A
cavalletti tipo B
2Ø12
L=145cm
Particolare 2 Scala 1:10
ferri di ripresa Ø8
barre filettate Ø20 L=41cm
Ø14 longitudinali
Particolare 3 Scala 1:10
cavalletti Ø12
tubi di plastica diametro 3cm
Ø14 longitudinali trave
2Ø14 correnti tipo C L=309cm
3Ø14 correnti tipo C L=309cm
SEZIONE E-E Scala 1:20
3Ø14 superiori
3Ø14 inferiori
staffa tipo C
staffe Ø6/10 L=114cm
SEZIONE H-H Scala 1:20
staffa tipo H
staffe Ø6/10 L=104cm

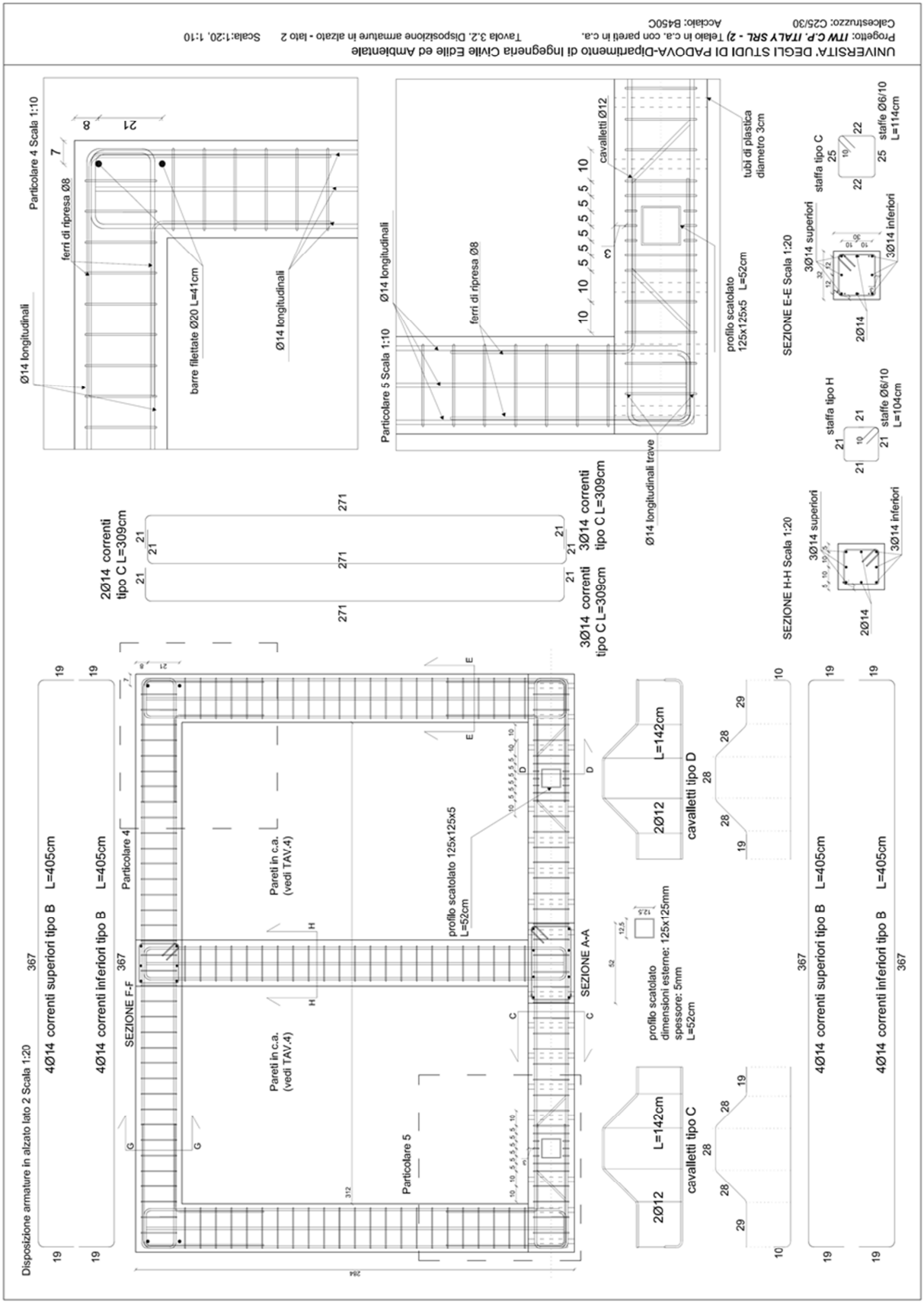
UNIVERSITA' DEGLI STUDI DI PADOVA-Dipartimento di Ingegneria Civile Edile ed Ambientale
Progetto: ITW C.P. ITALY SRL - 2) Telaio in c.a. con pareti in c.a.
Tavola 3.2. Disposizione armature in alzato - lato 2
Scala:1:20, 1:10
Calcestruzzo: C25/30
Acciaio: B450C
Disposizione armature in alzato lato 2 Scala 1:20
4Ø14 correnti superiori tipo B L=405cm
4Ø14 correnti inferiori tipo B L=405cm
SEZIONE F-F
Particolare 4
Particolare 5
Pareti in c.a. (vedi TAV.4)
profilo scatolato 125x125x5 L=52cm
SEZIONE A-A
profilo scatolato dimensioni esterne: 125x125mm spessore: 5mm L=52cm
2Ø12
L=142cm
cavalletti tipo D
cavalletti tipo C
2Ø14 correnti tipo C L=309cm
3Ø14 correnti tipo C L=309cm
Particolare 4 Scala 1:10
Ø14 longitudinali
ferri di ripresa Ø8
barre filettate Ø20 L=41cm
Particolare 5 Scala 1:10
cavalletti Ø12
profilo scatolato 125x125x5 L=52cm
tubi di plastica diametro 3cm
Ø14 longitudinali trave
SEZIONE E-E Scala 1:20
3Ø14 superiori
3Ø14 inferiori
2Ø14
staffa tipo C
staffe Ø6/10 L=114cm
staffa tipo H
staffe Ø6/10 L=104cm
SEZIONE H-H Scala 1:20

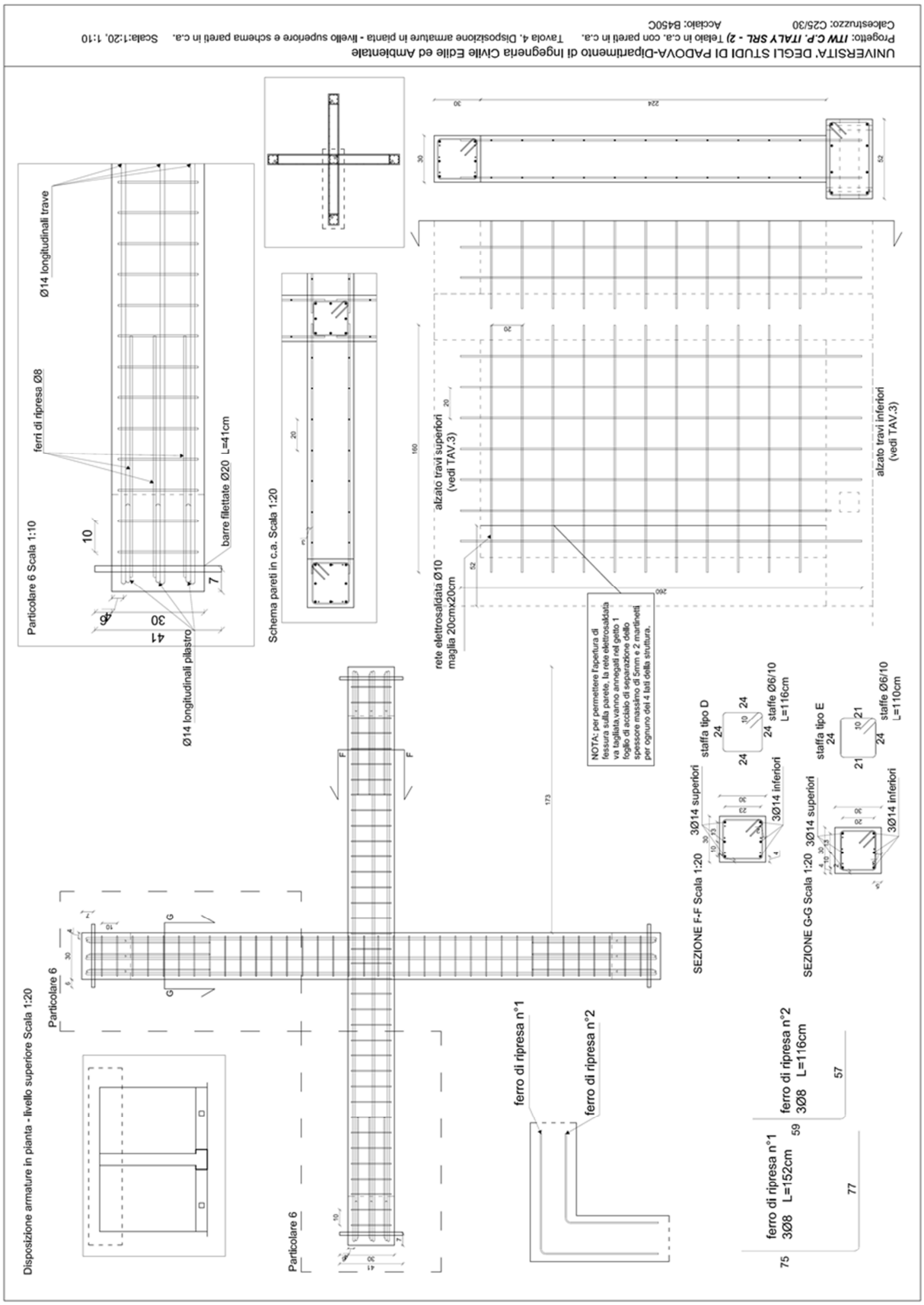
UNIVERSITA' DEGLI STUDI DI PADOVA-Dipartimento di Ingegneria Civile Edile ed Ambientale
Progetto: ITW C.P. ITALY SRL - 2) Telaio in c.a. con pareti in c.a. Tavola 4. Disposizione armature in pianta - livello superiore e schema pareti in c.a. Scala:1:20, 1:10
Calcestruzzo: C25/30 Acciaio: B450C
Disposizione armature in pianta - livello superiore Scala 1:20
Particolare 6
Particolare 6
Particolare 6 Scala 1:10
ferri di ripresa Ø8
Ø14 longitudinali trave
barre filettate Ø20 L=41cm
Ø14 longitudinali pilastro
Schema pareti in c.a. Scala 1:20
alzato travi superiori (vedi TAV.3)
alzato travi inferiori (vedi TAV.3)
rete elettrosaldata Ø10 maglia 20cmx20cm
NOTA: per permettere l'apertura di fessura sulla parete, la rete elettrosaldata va tagliata,vanno annegati nel getto 1 foglio di acciaio di separazione dello spessore massimo di 5mm e 2 martinetti per ognuno dei 4 lati della struttura.
SEZIONE F-F Scala 1:20
staffa tipo D
staffa Ø6/10 L=116cm
3Ø14 superiori
3Ø14 inferiori
SEZIONE G-G Scala 1:20
staffa tipo E
staffa Ø6/10 L=110cm
3Ø14 superiori
3Ø14 inferiori
ferro di ripresa n°1
ferro di ripresa n°2
ferro di ripresa n°1 3Ø8 L=152cm
ferro di ripresa n°2 3Ø8 L=116cm

Tabella riassuntiva della carpenteria necessaria

Pezzo	Ø [mm]	Quantità	Schema [non in scala]	Lunghezza di ogni singolo pezzo
Staffa tipo A	6	36		160cm
Staffa tipo B	6	36		156cm
Staffa tipo C	6	88		114cm
Staffa tipo D	6	36		116cm
Staffa tipo E	6	36		110cm
Staffa tipo F	6	12		108cm
Staffa tipo G	6	12		106cm
Staffa tipo H	6	22		104cm
Barra filettata DIN 975-Ø20 x 2.5	20	8		41cm
Cavalletto tipo A	12	2		145cm
Cavalletto tipo B	12	2		145cm

Tabella riassuntiva della carpenteria necessaria

Pezzo	Ø [mm]	Quantità	Schema [non in scala]	Lunghezza di ogni singolo pezzo
Cavalletto tipo C	12	2		142cm
Cavalletto tipo D	12	2		142cm
Ferro di ripresa n°1	8	24		152cm
Ferro di ripresa n°2	8	24		116cm
Corrente tipo A TRAVE	14	14		411cm
Corrente tipo B TRAVE	14	14		405cm
Corrente tipo C PILASTRO	14	32		309cm
Rete elettrosaldata PARETI	10 (maglia 20cmx20cm)	8		260cmx160cm
Profilo scatolato in acciaio a sezione quadrata Tubi di plastica a sezione circolare			Dimensioni esterne: 125mmx125mm Quantità: 4 Spessore: 5mm Lunghezza: 52cm Diametro: 30mm Quantità: 60 Altezza: 30cm	

UNIVERSITA' DEGLI STUDI DI PADOVA-Dipartimento di Ingegneria Civile Edile ed Ambientale
Progetto: ***ITW C.P. ITALY SRL - 2)*** Telaio in c.a. con pareti in c.a. Tavola 5. Tabella carpenteria
Calcestruzzo: C25/30 Acciaio: B450C

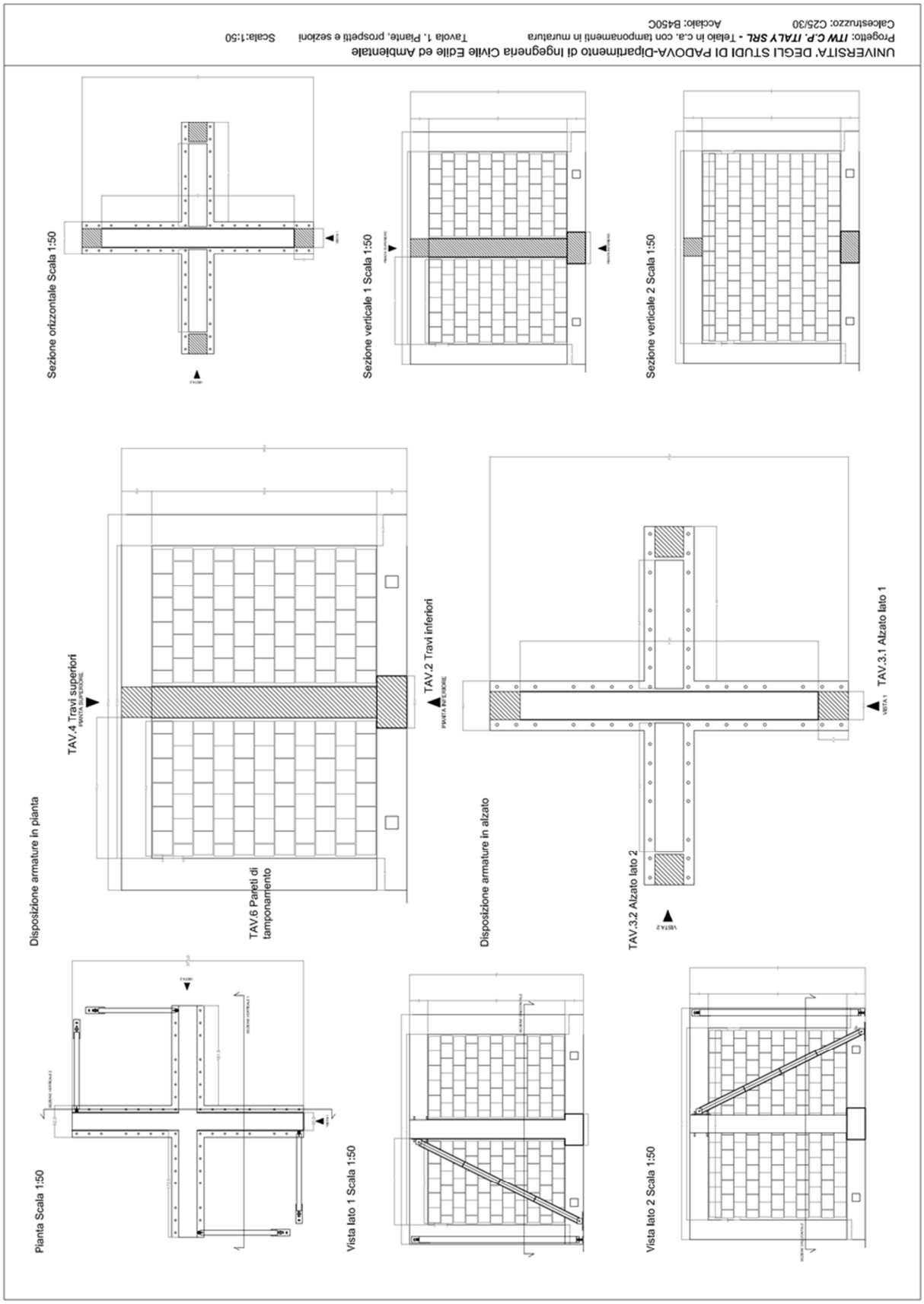
UNIVERSITA' DEGLI STUDI DI PADOVA-Dipartimento di Ingegneria Civile Edile ed Ambientale
Progetto: ITW C.P. ITALY SRL - Telaio in c.a. con tamponamenti in muratura
Calcestruzzo: C25/30 Acciaio: B450C
Tavola 1, Piante, prospetti e sezioni
Scala:1:50
Sezione orizzontale Scala 1:50
Sezione verticale 1 Scala 1:50
Sezione verticale 2 Scala 1:50
TAV.4 Travi superiori
TAV.2 Travi inferiori
TAV.6 Pareti di tamponamento
TAV.3.1 Alzato lato 1
TAV.3.2 Alzato lato 2
Disposizione armature in planta
Disposizione armature in alzato
Pianta Scala 1:50
Vista lato 1 Scala 1:50
Vista lato 2 Scala 1:50

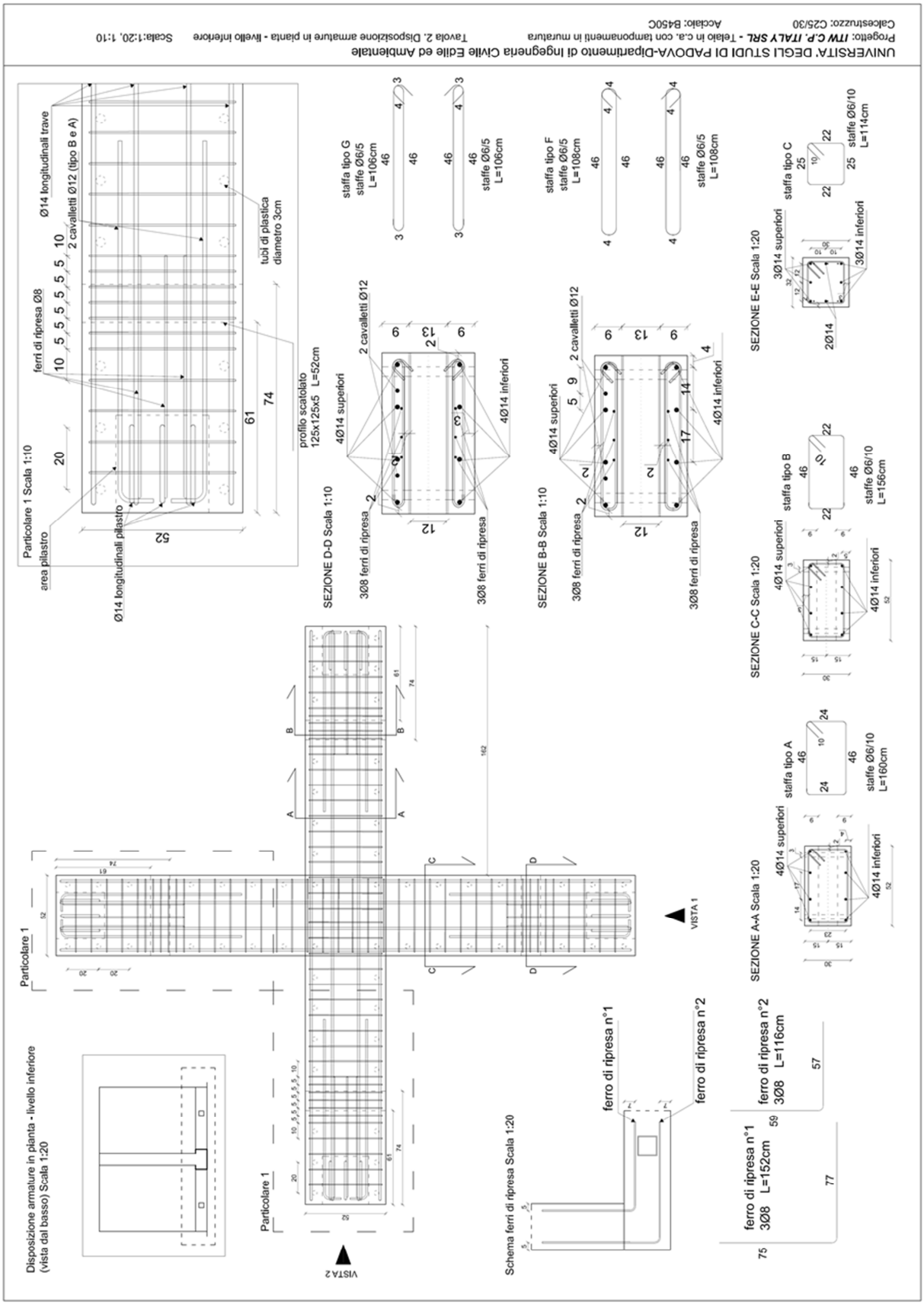
UNIVERSITA' DEGLI STUDI DI PADOVA-Dipartimento di Ingegneria Civile Edile ed Ambientale
Progetto: ITW C.P. ITALY SRL - Telaio in c.a. con tamponamenti in muratura
Calcestruzzo: C25/30 Acciaio: B450C
Tavola 2. Disposizione armature in pianta - livello inferiore Scala:1:20, 1:10
Particolare 1 Scala 1:10
area pilastro
ferri di ripresa Ø8
Ø14 longitudinali trave
2 cavalletti Ø12 (tipo B e A)
tubi di plastica diametro 3cm
profilo scatolato 125x125x5 L=52cm
Ø14 longitudinali pilastro
SEZIONE D-D Scala 1:10
4Ø14 superiori
2 cavalletti Ø12
3Ø8 ferri di ripresa
4Ø14 inferiori
staffa tipo G
staffe Ø6/5
L=106cm
staffa tipo F
staffe Ø6/5
L=108cm
SEZIONE B-B Scala 1:10
SEZIONE E-E Scala 1:20
3Ø14 superiori
3Ø14 inferiori
2Ø14
staffa tipo C
staffe Ø6/10
L=114cm
SEZIONE C-C Scala 1:20
staffa tipo B
staffe Ø6/10
L=156cm
SEZIONE A-A Scala 1:20
staffa tipo A
staffe Ø6/10
L=160cm
Particolare 1
VISTA 1
VISTA 2
Disposizione armature in pianta - livello inferiore
(vista dal basso) Scala 1:20
Schema ferri di ripresa Scala 1:20
ferro di ripresa n°1
ferro di ripresa n°2
3Ø8 L=116cm
3Ø8 L=152cm

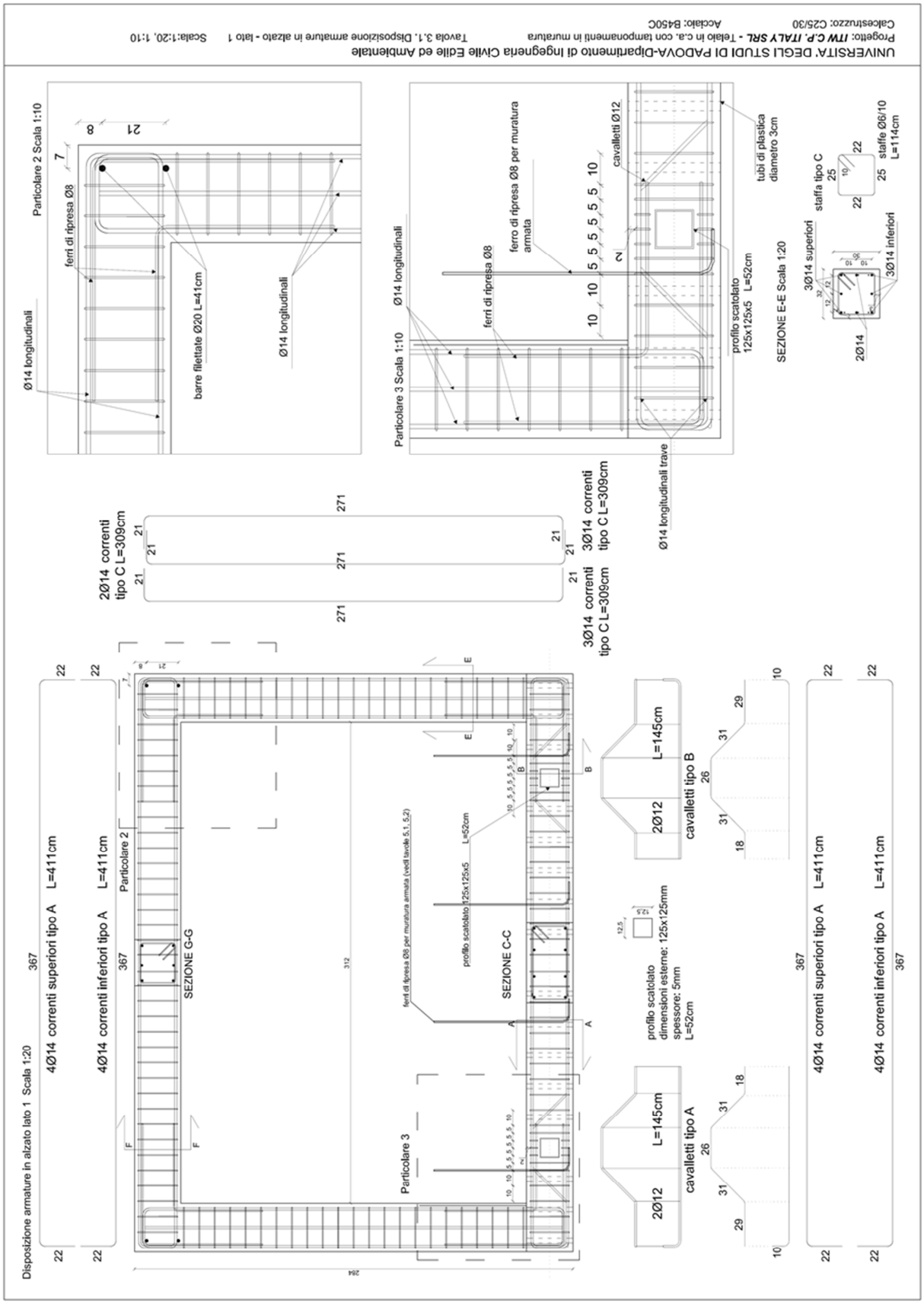
UNIVERSITA' DEGLI STUDI DI PADOVA-Dipartimento di Ingegneria Civile Edile ed Ambientale
Progetto: ITW C.P. ITALY SRL - Telaio in c.a. con tamponamenti in muratura
Calcestruzzo: C25/30 Acciaio: B450C
Tavola 3.1, Disposizione armature in alzato - lato 1 Scala:1:20, 1:10
Disposizione armature in alzato lato 1 Scala 1:20
4Ø14 correnti superiori tipo A L=411cm
4Ø14 correnti inferiori tipo A L=411cm
Particolare 2
SEZIONE G-G
SEZIONE C-C
Particolare 3
ferri di ripresa Ø8 per muratura armata (vedi tavole 5.1, 5.2)
profilo scatolato 125x125x5 L=52cm
profilo scatolato dimensioni esterne: 125x125mm spessore: 5mm L=52cm
2Ø12 L=145cm
cavalletti tipo A
cavalletti tipo B
2Ø14 correnti tipo C L=309cm
3Ø14 correnti tipo C L=309cm
Particolare 2 Scala 1:10
Ø14 longitudinali
ferri di ripresa Ø8
barre filettate Ø20 L=41cm
Particolare 3 Scala 1:10
ferro di ripresa Ø8 per muratura armata
cavalletti Ø12
profilo scatolato 125x125x5 L=52cm
Ø14 longitudinali trave
tubi di plastica diametro 3cm
SEZIONE E-E Scala 1:20
3Ø14 superiori
3Ø14 inferiori
2Ø14
staffa tipo C
staffe Ø6/10 L=114cm

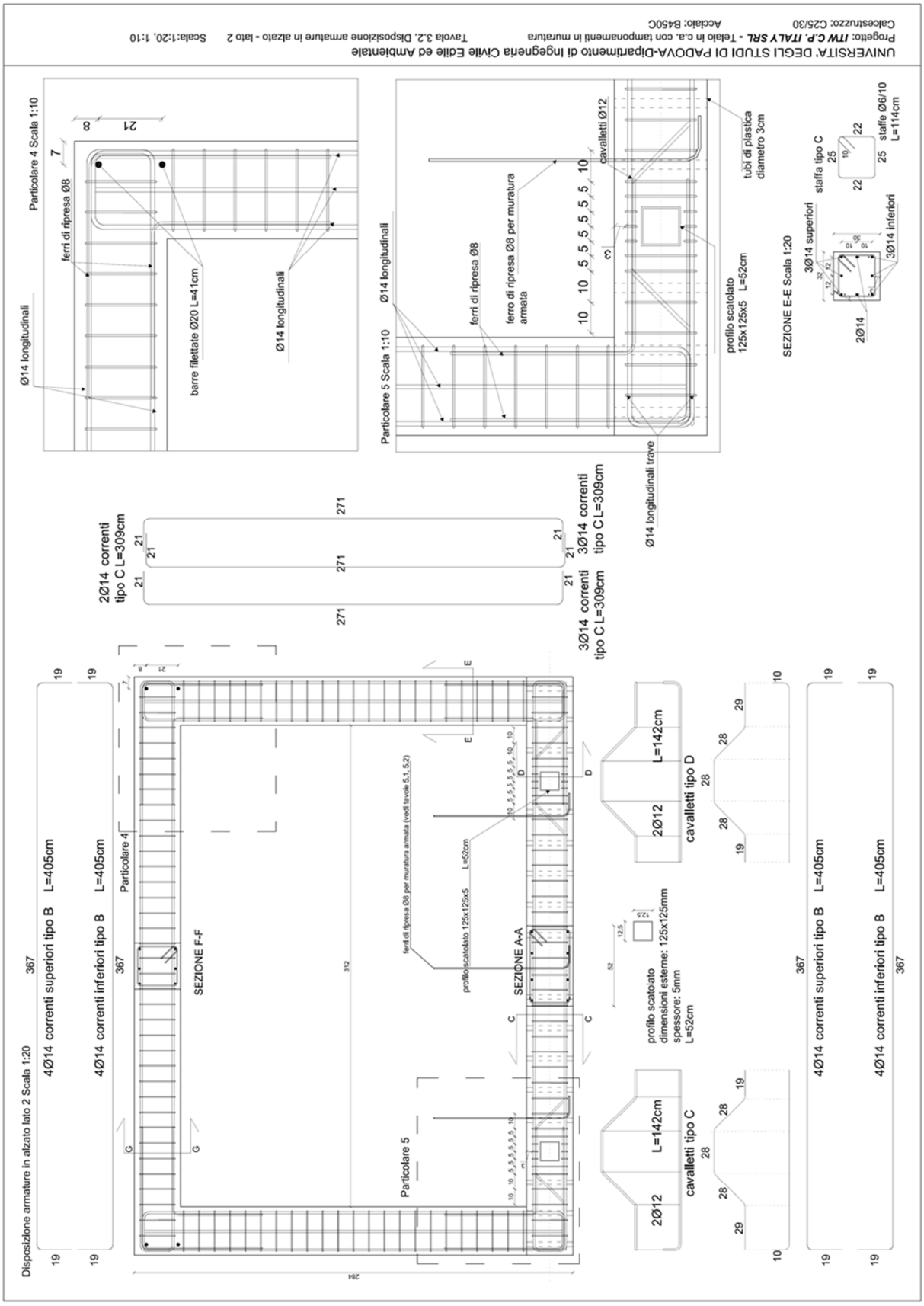
UNIVERSITA' DEGLI STUDI DI PADOVA-Dipartimento di Ingegneria Civile Edile ed Ambientale
Progetto: ITW C.P. ITALY SRL - Telaio in c.a. con tamponamenti in muratura
Calcestruzzo: C25/30 Acciaio: B450C
Tavola 3.2, Disposizione armature in alzato - lato 2 Scala:1:20, 1:10
Disposizione armature in alzato lato 2 Scala 1:20
4Ø14 correnti superiori tipo B L=405cm
4Ø14 correnti inferiori tipo B L=405cm
SEZIONE F-F
SEZIONE A-A
Particolare 4
Particolare 5
2Ø14 correnti tipo C L=309cm
3Ø14 correnti tipo C L=309cm
Particolare 4 Scala 1:10
Ø14 longitudinali
ferri di ripresa Ø8
barre filettate Ø20 L=41cm
Particolare 5 Scala 1:10
ferro di ripresa Ø8 per muratura armata
cavalletti Ø12
tubi di plastica diametro 3cm
profilo scatolato 125x125x5 L=52cm
Ø14 longitudinali trave
SEZIONE E-E Scala 1:20
3Ø14 superiori
staffa tipo C
staffe Ø6/10 L=114cm
3Ø14 inferiori
2Ø14
cavalletti tipo C
cavalletti tipo D
2Ø12
L=142cm
profilo scatolato dimensioni esterne: 125x125mm spessore: 5mm L=52cm

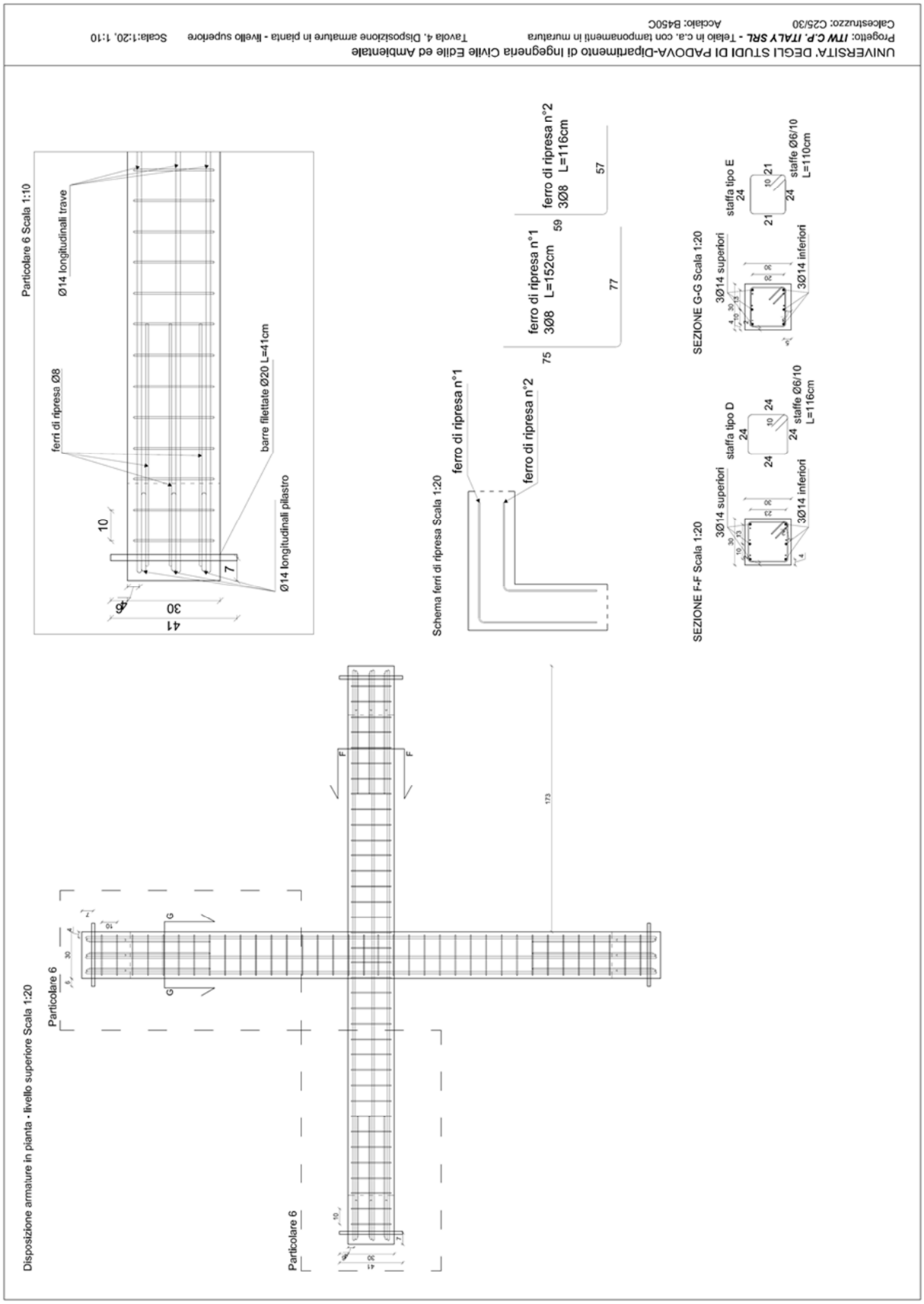
UNIVERSITA' DEGLI STUDI DI PADOVA-Dipartimento di Ingegneria Civile Edile ed Ambientale
Progetto: ITW C.P. ITALY SRL - Telaio in c.a. con tamponamenti in muratura
Calcestruzzo: C25/30 Acciaio: B450C
Tavola 4, Disposizione armature in pianta - livello superiore
Scala:1:20, 1:10
Particolare 6 Scala 1:10
Ø14 longitudinali trave
ferri di ripresa Ø8
barre filettate Ø20 L=41cm
Ø14 longitudinali pilastro
10
7
30
41
Schema ferri di ripresa Scala 1:20
ferro di ripresa n°1
ferro di ripresa n°2
ferro di ripresa n°1
3Ø8 L=152cm
59
75
77
ferro di ripresa n°2
3Ø8 L=116cm
57
SEZIONE G-G Scala 1:20
3Ø14 superiori
staffa tipo E
staffe Ø6/10
L=110cm
3Ø14 inferiori
SEZIONE F-F Scala 1:20
3Ø14 superiori
staffa tipo D
staffe Ø6/10
L=116cm
3Ø14 inferiori
Disposizione armature in pianta - livello superiore Scala 1:20
Particolare 6
Particolare 6
173

Tabella riassuntiva della carpenteria necessaria

Pezzo	Ø [mm]	Quantità	Schema [non in scala]	Lunghezza di ogni singolo pezzo
Staffa tipo A	6	36	46, 24, 24, 46	160cm
Staffa tipo B	6	36	46, 22, 22, 46	156cm
Staffa tipo C	6	88	25, 10, 22, 22, 25	114cm
Staffa tipo D	6	36	24, 10, 24, 24, 24	116cm
Staffa tipo E	6	36	24, 10, 21, 21, 24	110cm
Staffa tipo F	6	12	46, 4, 4, 46	108cm
Staffa tipo G	6	12	46, 3, 4, 3, 46	106cm
Cavalletto tipo A	12	2	vista frontale: 26, 31, 18, 31, 29, 10; vista in pianta	145cm
Cavalletto tipo B	12	2	vista frontale: 26, 31, 29, 18, 31, 10; vista in pianta	145cm
Cavalletto tipo C	12	2	vista frontale: 26, 28, 19, 28, 29, 10; vista in pianta	142cm
Cavalletto tipo D	12	2	vista frontale: 28, 28, 29, 19, 28, 10; vista in pianta	142cm

Tabella riassuntiva della carpenteria necessaria

Pezzo	Ø [mm]	Quantità	Schema [non in scala]	Lunghezza di ogni singolo pezzo
Ferro di ripresa n°1	8	24	75, 77	152cm
Ferro di ripresa n°2	8	24	59, 57	116cm
Corrente tipo A TRAVE	14	14	365, 22, 22	411cm
Corrente tipo B TRAVE	14	14	365, 19, 19	405cm
Corrente tipo C PILASTRO	14	32	271, 21, 21	309cm
Barra filettata DIN 975 - Ø20 x 2.5	20	8	41	41cm
Ferro di ripresa per muratura armata	8	7	83.5, 10.5	100cm
Barre verticali muratura	7	8	221	221cm
Staffe orizzontali muratura lato 1	12	6	71, 18	160cm
Staffe orizzontali muratura lato 2	6	6	160, 18	338cm
Profilo scatolato in acciaio a sezione quadrata			Dimensioni esterne: 125mmx125mm Quantità: 4 Spessore: 5mm Lunghezza: 52cm	
Tubi di plastica a sezione circolare			Diametro: 30mm Quantità: 60 Altezza: 30cm	

UNIVERSITA' DEGLI STUDI DI PADOVA-Dipartimento di Ingegneria Civile Edile ed Ambientale

Progetto: *ITW C.P. ITALY SRL* - Telaio in c.a. con tamponamenti in muratura Tavola 6. Tabella carpenteria

Calcestruzzo: C25/30 Acciaio: B450C

UNIVERSITA' DEGLI STUDI DI PADOVA-Dipartimento di Ingegneria Civile Edile ed Ambientale
Progetto: ITW C.P. ITALY SRL - Telaio in c.a. con tamponamenti in muratura
Calcestruzzo: C25/30 Acciaio: B450C
Tavola 5.1. Pareti di tamponamento in muratura armata - lato 1 Scala:1:20, 1:10
Schema blocchi di laterizio Scala 1:10
Blocchi tipo:
P69TA
Pieno 71129
Vuoti 35472
Perc foratura 49.87%
MA124
Pieno 37303
Vuoti 17988
Perc foratura 48.25%
30
24
5
5
9
13
LATO 1
NOTE: n° 2 pannelli
11 corsi per 5 blocchi+ 1/2 a corso ogni pannello
110 blocchi P69TA e 22 tipo MA124 in totale;
Giunti orizzontali da 10 mm e riempimento con malta cementizia M10 (malta tipo Tassullo T300).
Giunti verticali esterni di tutti i lati dei pannelli non riempiti con malta ma lasciati vuoti. Giunti verticali ad incastro, realizzati a secco.
E' mostrato lo schema di posa dei blocchi. Intonaco di 10mm sulle facce dei pannelli che guardano i quadranti senza controventi.
Barre verticali Ø8 collegate solamente al cordolo inferiore;
Staffatura orizzontale Ø6 ad U (L=1600mm) posizionate secondo lo schema nel disegno.
Schema pareti di tamponamento in muratura armata Scala 1:20
Vista lato 1
barre verticali Ø8
barre verticali Ø8
staffatura orizzontale Ø6
staffatura orizzontale Ø6
corso 2 campione sinistra
corso 5 campione destra

UNIVERSITA' DEGLI STUDI DI PADOVA-Dipartimento di Ingegneria Civile Edile ed Ambientale
Progetto: ITW C.P. ITALY SRL - Telaio in c.a. con tamponamenti in muratura
Calcestruzzo: C25/30 Acciaio: B450C
Tavola 5.2. Pareti di tamponamento in muratura armata - lato 2 Scala:1:20, 1:10
Schema blocchi di laterizio Scala 1:10
Blocchi tipo:
P69TA
Pieno 71129
Vuoti 35472
Perc foratura 49.87%
MA124
Pieno 37303
Vuoti 17988
Perc foratura 48.25%
30
24
5
5
5
30
13
LATO 2
NOTE: n° 1 pannello
11 corsi per 12 blocchi+1/2 a corso
132 blocchi P69TA e 11 tipo MA124 in totale;
Giunti orizzontali da 10 mm e riempimento con malta cementizia M10 (malta tipo Tassullo T300).
In questo caso la parete è vincolata anche nei giunti verticali laterali con riempimento degli stessi con malta M10. Giunti verticali ad incastro, realizzati a secco.
E' mostrato lo schema di posa dei blocchi. Intonaco di 10mm sulle facce dei pannelli che guardano i quadranti senza controventi.
Barre verticali Ø8 collegate solamente al cordolo inferiore;
Staffatura orizzontale Ø6 ad U (L=3380mm) posizionate secondo lo schema nel disegno.
Schema pareti di tamponamento in muratura armata Scala 1:20
Vista lato 2
11
10
9
8
7
6
5
4
3
2
1
barre verticali Ø8
staffatura orizzontale Ø6
corso 2

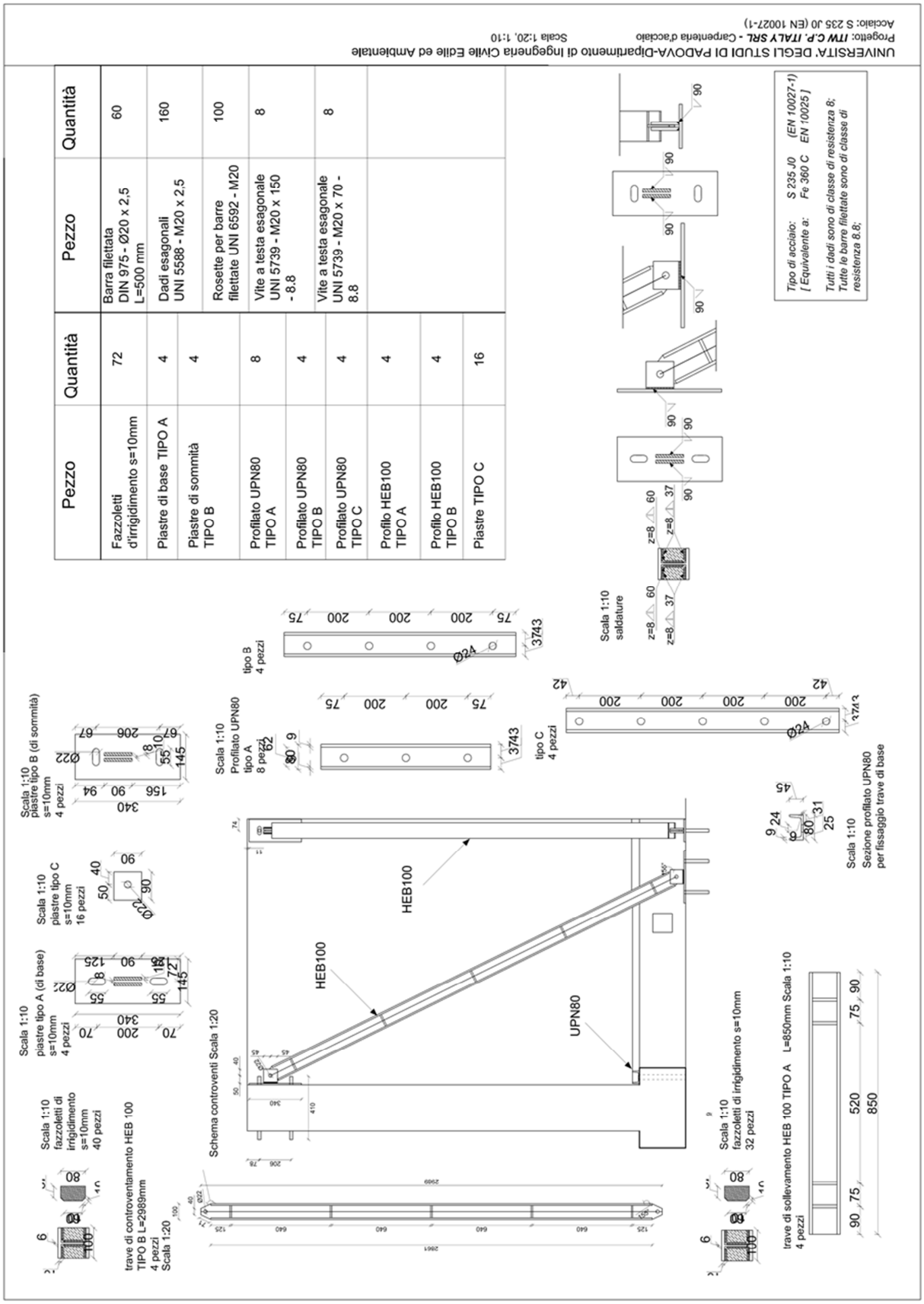
UNIVERSITA' DEGLI STUDI DI PADOVA-Dipartimento di Ingegneria Civile Edile ed Ambientale
Progetto: ITW C.P. ITALY SRL - Carpenteria d'acciaio
Acciaio: S 235 J0 (EN 10027-1)
Scala 1:20, 1:10
Pezzo | Quantità
Fazzoletti d'irrigidimento s=10mm | 72
Piastre di base TIPO A | 4
Piastre di sommità TIPO B | 4
Profilato UPN80 TIPO A | 8
Profilato UPN80 TIPO B | 4
Profilato UPN80 TIPO C | 4
Profilo HEB100 TIPO A | 4
Profilo HEB100 TIPO B | 4
Piastre TIPO C | 16
Pezzo | Quantità
Barra filettata DIN 975 - Ø20 x 2,5 L=500 mm | 60
Dadi esagonali UNI 5588 - M20 x 2,5 | 160
Rosette per barre filettate UNI 6592 - M20 | 100
Vite a testa esagonale UNI 5739 - M20 x 150 - 8.8 | 8
Vite a testa esagonale UNI 5739 - M20 x 70 - 8.8 | 8
Tipo di acciaio: S 235 J0 (EN 10027-1) / Equivalente a: Fe 360 C EN 10025
Tutti i dadi sono di classe di resistenza 8; Tutte le barre filettate sono di classe di resistenza 8.8;
Scala 1:10 saldature
Scala 1:10 piastre tipo B (di sommità) s=10mm 4 pezzi
Scala 1:10 piastre tipo A (di base) s=10mm 4 pezzi
Scala 1:10 piastre tipo C s=10mm 16 pezzi
Scala 1:10 fazzoletti di irrigidimento s=10mm 40 pezzi
Scala 1:10 Profilato UPN80 tipo A 8 pezzi
tipo B 4 pezzi
tipo C 4 pezzi
Scala 1:10 fazzoletti di irrigidimento s=10mm 32 pezzi
Scala 1:10 Sezione profilato UPN80 per fissaggio trave di base
Schema controventi Scala 1:20
HEB100
HEB100
UPN80
trave di controventamento HEB 100 TIPO B L=2989mm 4 pezzi Scala 1:20
trave di sollevamento HEB 100 TIPO A L=850mm Scala 1:10 4 pezzi

ANNEX B. TESTING PLAN

List of performed steps for each tests

No.	Test 1	Test 2	Test 3	Test 4	Test 5
1	0.05g	0.05g	0.05g	0.05g	0.70g
2	0.10g	0.10g	0.10g	0.10g	0.90g
3	0.15g	0.15g	0.15g	0.15g	1.00g
4	0.20g	0.20g	0.20g	0.20g	1.10g
5	0.25g	0.25g	0.25g	0.25g	1.20g
6	0.30g	0.30g	0.30g	0.30g	-
7	0.35g	0.35g	0.35g	0.35g	-
8	0.40g	0.40g	0.40g	0.40g	-
9	0.45g	0.45g	0.45g	0.45g	-
10	0.50g	0.50g	0.50g	0.50g	-
11	0.55g	0.55g	0.55g	0.55g	-
12	0.60g	0.60g	0.60g	0.60g	-
13	0.65g	0.60g	0.65g	0.65g	-
14	0.70g	0.65g	0.70g	0.70g	
15	0.75g	0.70g	0.75g	0.75g	-
16	0.80g	0.75g	0.80g	0.80g	-
17	0.40g	0.80g	0.90g	0.85g	-
18	0.45g	0.80g	0.90g	0.90g	-
19	0.50g	0.90g	1.00g	1.00g	-
20	0.55g	1.00g	1.10g	-	-
21	0.60g	-	-	-	-
22	0.65g	-	-	-	-
23	0.70g	-	-	-	
24	0.75g	-	-	-	-
25	0.80g	-	-	-	-
26	0.90g	-	-	-	-
27	1.00g	-	-	-	-
28	1.10g	-	-	-	-

ANNEX C. INSTRUMENTATION

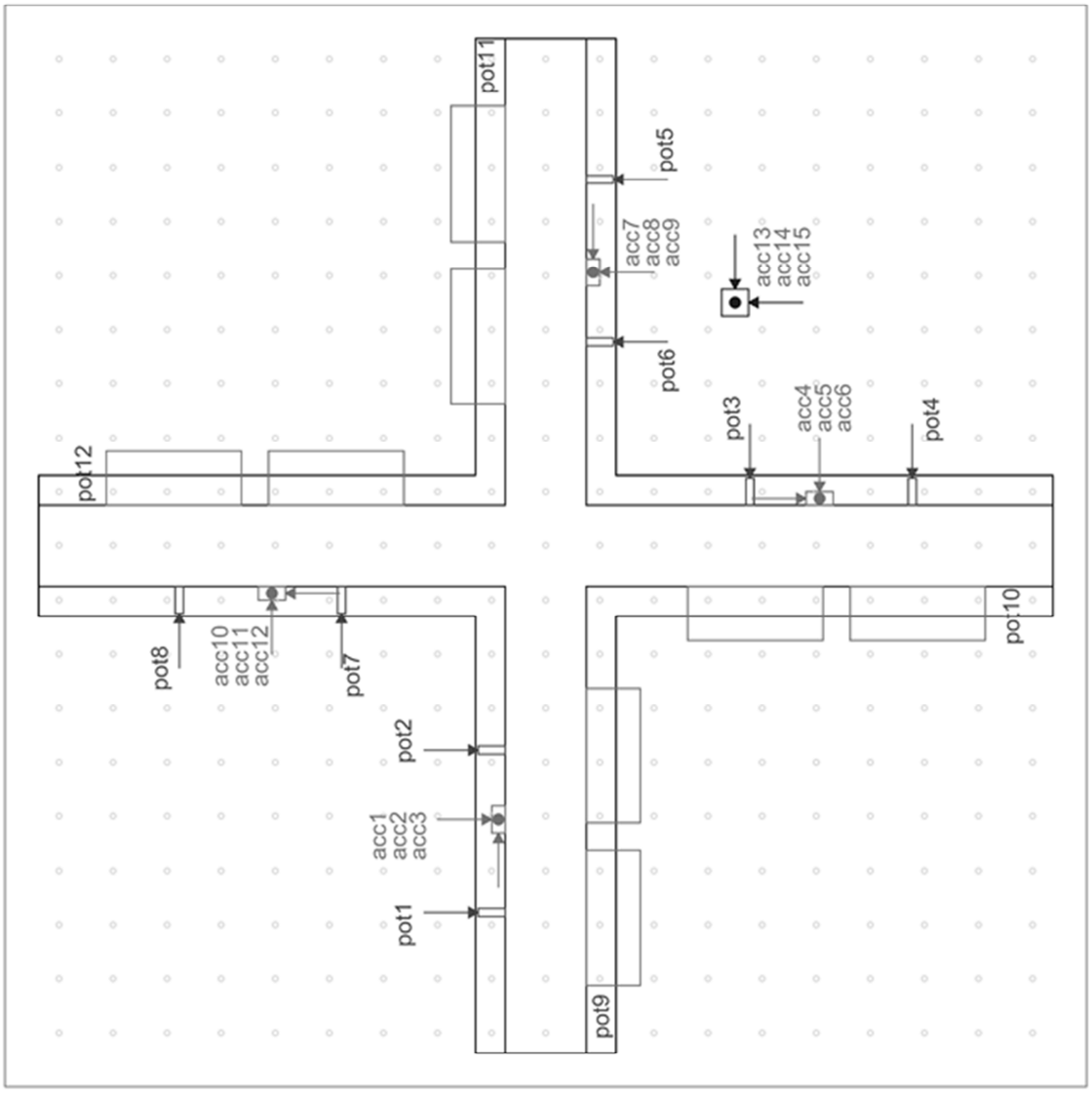

Setup instrumentation for TS1; system 1.

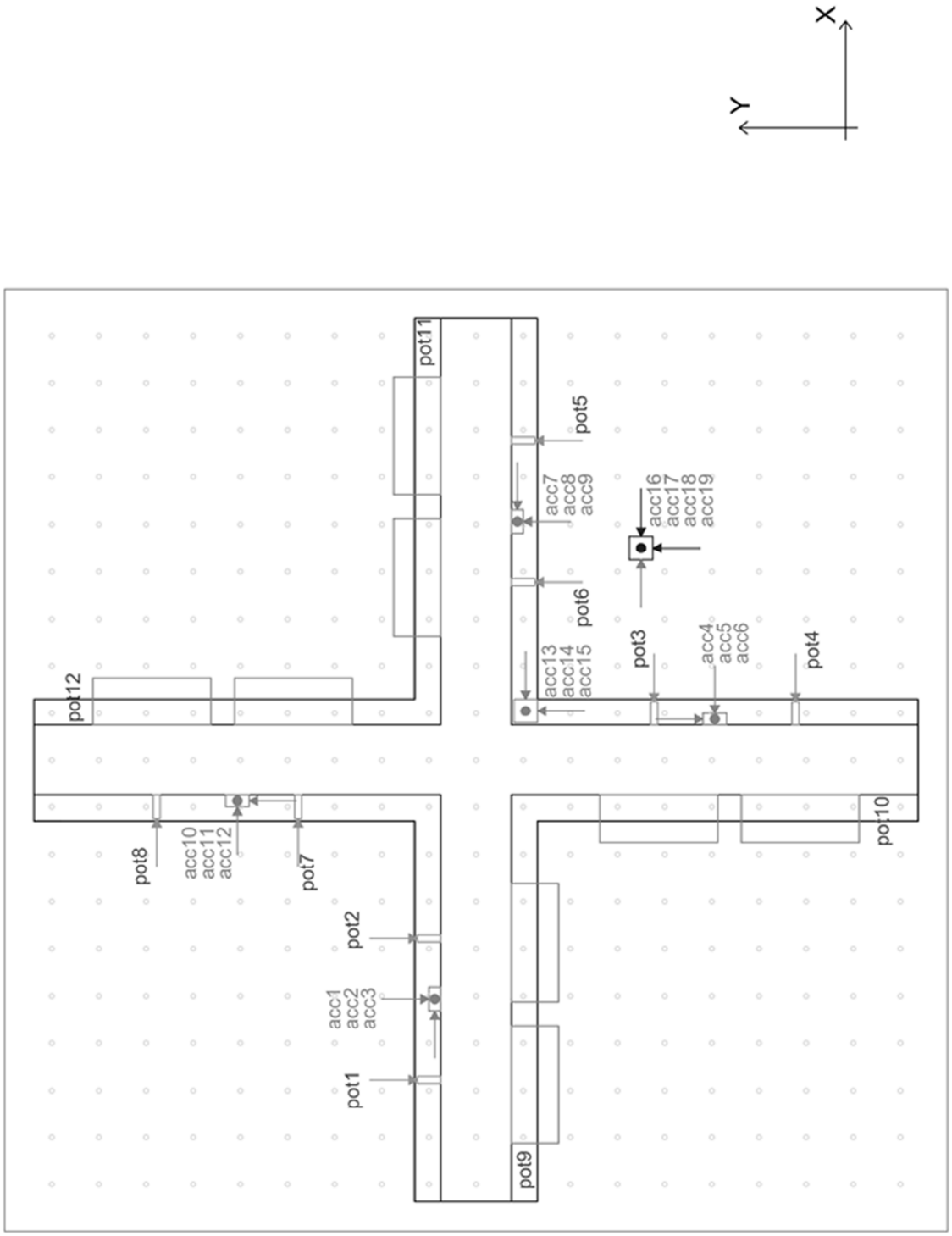

Setup instrumentation for TS2; system 1.

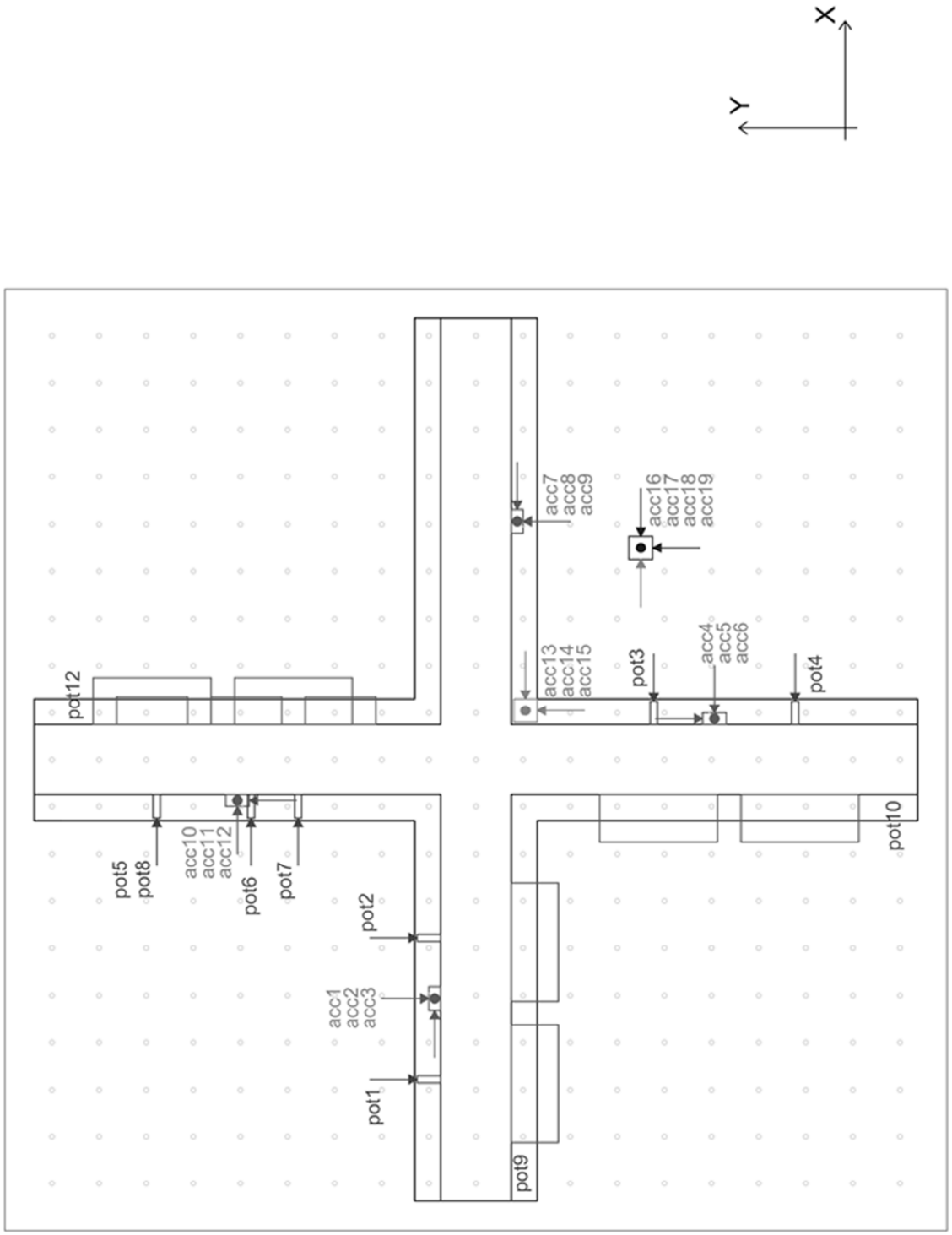

Setup instrumentation for TS3; system 1.

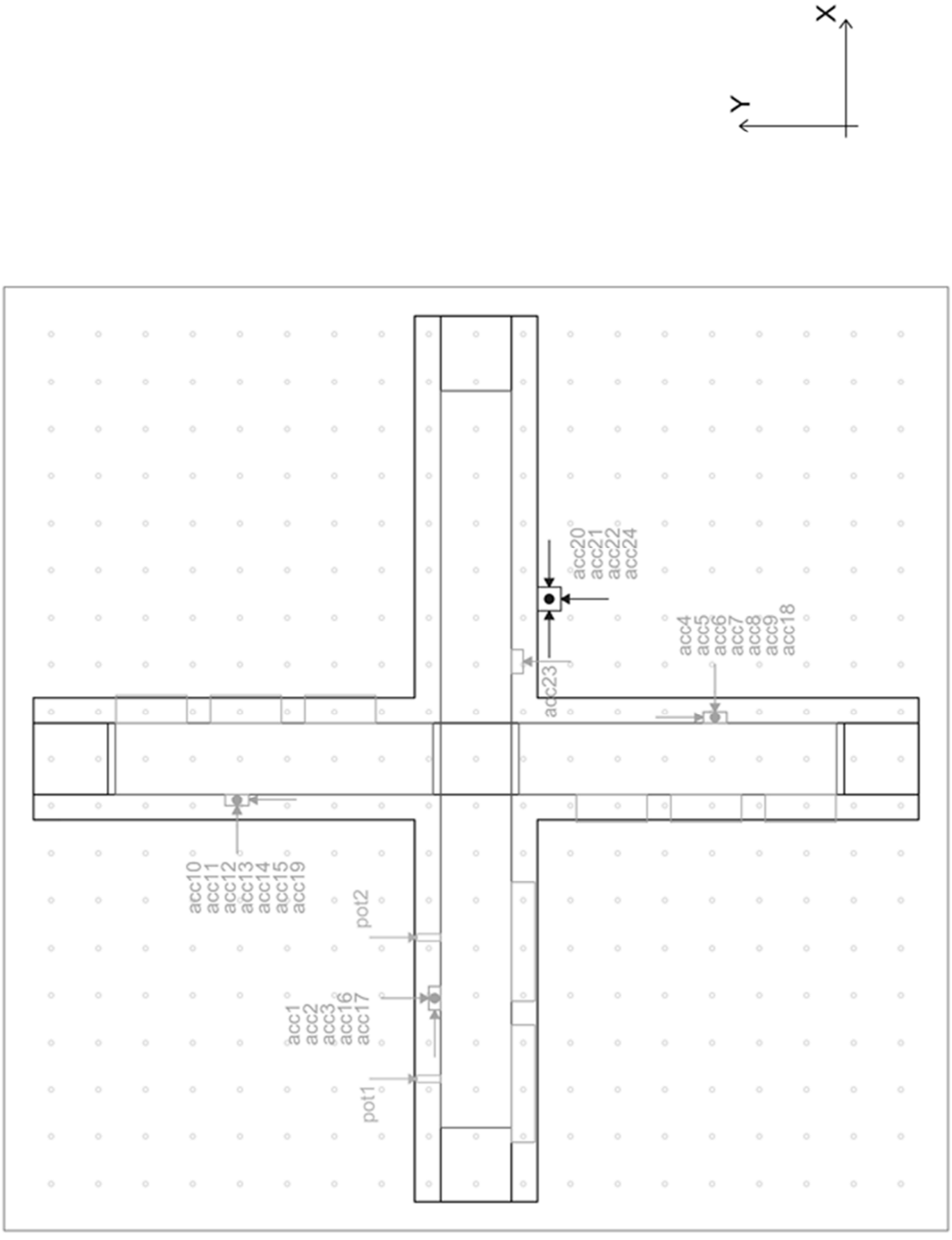

Setup instrumentation for TS4; system 1.

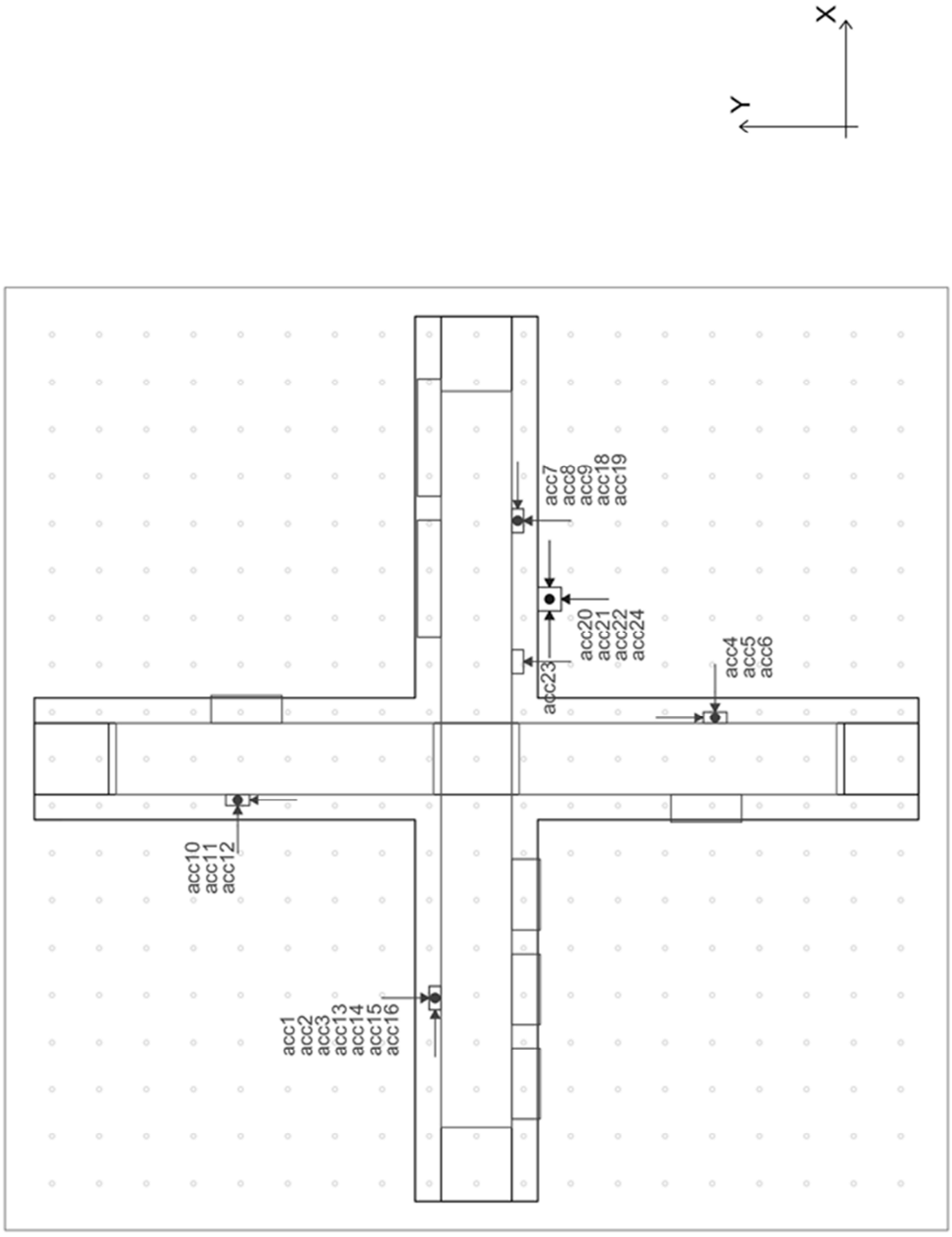

Setup instrumentation for TS5; system 1.

ANNEX D. ART OBJECTS SEISMIC EVALUATION SHEET

Progetto ARCUS "Verifica della sicurezza sismica dei musei statali"
Università degli Studi di Padova
Dipartimento di Ingegneria Civile, Edile ed Ambientale

SCHEDA PER IL RILIEVO DELLA VULNERABILITA' SISMICA DEI BENI MOBILI ESPOSTI NEI MUSEI

1 CONTESTO

1.1 Anagrafica scheda

N° scheda: _____
Compilatore: Cognome _____ Nome _____
Data: _____

1.2 Edificio e struttura

Nome Museo:
Proprietà: Regione:
Provincia: Località:
Comune: Indirizzo:
CAP:
Tipologia costruttiva:
Numero piani (compresi interrati):
Altezza struttura (compresi interrati): [m]

2 RACCOLTA DATI

2.1 ID oggetto d'arte

Elemento singolo ◯ Gruppo di elementi ◯ Numero elementi _____
In esposizione si ◯ no ◯
Sala: _____ Piano: _____
Oggetto: _____ Codice ID museo: _____
Autore: _____ Datazione: _____

2.2 Geometria e composizione

Altezza _____ [cm] Altezza G _____ [cm]
Larghezza _____ [cm] Dist G da O _____ [cm]
Profondità _____ [cm] Massa _____ [kg]
Diametro _____ [cm] Materiale _____
Oggetto solidale con appoggio: si ◯ no ◯ NR ◯
Base di appoggio: Base _____ X _____ [cm] Altezza _____ [cm] Massa _____ [kg]
Fissaggio alla struttura dell'appoggio sostegno: si ◯ no ◯

2.3 Classificazione

Tipologia				Supporto		
	T1 ◯	VASE		A1 ◯	PAV
	T2 ◯	BUST		A2 ◯	PIED
	T3 ◯	STAT		A3 ◯	VETR
	T4 ◯	QUAD		A4 ◯	MENS
	T5 ◯	LAMP		B ◯	PIANO
	T6 ◯	MISC		C1 ◯	PARE
				C2 ◯	SOFF

2.4 Supporto

Materiale superficie di appoggio:

		Supporto per fissaggio:	
Plexiglass/plexiglass ◯		Calcestruzzo ◯
Plexiglass/vetro ◯		Mattoni pieni ◯
Plexiglass/teflon ◯		Mattoni forati ◯
Alluminio/formica ◯		Cartongesso ◯
Alluminio/mosaico ◯		Legno ◯
Marmo/mosaico ◯		Altro _____
Teflon/vetro ◯		
Terracotta/plexiglass ◯		
Terracotta/vetro ◯		Braccio: _____ [m]
Alluminio/teflon ◯		
Altro _____		

Distanza da bordo/ostacolo più vicino: _____ [cm]
Interventi presenti di mitigazione del rischio sismico: si ◯ no ◯
Se si quali:

Clip di fissaggio ◯		Strato in appoggio ◯
Monofilamenti ◯		Isolamento ◯
Sostegni sagomati ◯		Altro _____

3 NOTE

3.1 Giudizio visivo dell'operatore

buono ◯ medio ◯ scarso ◯ Commenti .....

3.2 Disegni

Legenda:

Categoria	*Descrizione dell'oggetto*	*Sigla*
T1	piccoli oggetti a base piana	VASE
T2	piccoli oggetti privi di una base piana	BUST
T3	statue, sculture in genere e grandi vasi	STAT
T4	quadri e dipinti in genere	QUAD
T5	lampadari ed oggetti sospesi	LAMP
T6	altri	MISC

	A *Oggetti poggiati su di una superficie piana*				B *Oggetti fissati su di un piano o di un piedistallo*	C *Oggetti appesi o sospesi*	
	A1 *sul pavimento*	A2 *su di un piedistallo*	A3 *all'interno di vetrine*	A4 *su mensole o all'interno di bacheche*		C1 *appesi ad una parete*	C2 *sospesi al soffitto*
T1	*	*	*	*	*		
T2	*	*	*	*	*		
T3	*	*			*		
T4						*	
T5							*
T6	*	*	*	*	*	*	*